(12) INTERNATIONAL APPLICATION PUBLISHED UNDER THE PATENT COOPERATION TREATY (PCT)

(19) World Intellectual Property Organization
International Bureau

(43) International Publication Date
29 February 2024 (29.02.2024)

WIPO | PCT

(10) International Publication Number
WO 2024/041574 A1

(51) International Patent Classification:
A61K 39/395 (2006.01) *C12Q 1/6886* (2018.01)
C07K 16/30 (2006.01) *A61P 35/00* (2006.01)
A61K 47/50 (2017.01)

(21) International Application Number:
PCT/CN2023/114497

(22) International Filing Date:
23 August 2023 (23.08.2023)

(25) Filing Language: English

(26) Publication Language: English

(30) Priority Data:
PCT/CN2022/114520
24 August 2022 (24.08.2022) CN
PCT/CN2023/073257
19 January 2023 (19.01.2023) CN
PCT/CN2023/110046
28 July 2023 (28.07.2023) CN

(71) Applicants: **SUZHOU TRANSCENTA THERAPEUTICS CO., LTD.** [CN/CN]; B6-501, 218 Xinghu Street, Suzhou, Jiangsu 215123 (CN). **BEIJING CANCER HOSPITAL** [CN/CN]; No. 52 Fucheng Road, Haidian District, Beijing 100142 (CN).

(72) Inventors: **QIAN, Xueming**; B6-501, 218 Xinghu Street, Suzhou, Jiangsu 215123 (CN). **TENG, Fei**; B6-501, 218 Xinghu Street, Suzhou, Jiangsu 215123 (CN). **ZHU, Hua**; No. 52 Fucheng Road, Haidian District, Beijing 100142 (CN). **YANG, Zhi**; No. 52 Fucheng Road, Haidian District, Beijing 100142 (CN). **DING, Jin**; No. 52 Fucheng Road, Haidian District, Beijing 100142 (CN). **WANG, Feng**; No. 52 Fucheng Road, Haidian District, Beijing 100142 (CN). **LI, Hongjun**; B6-501, 218 Xinghu Street, Suzhou, Jiangsu 215123 (CN).

(74) Agent: **JUN HE LAW OFFICES**; 20/F, China Resources Building 8 Jianguomenbei Avenue, Dongcheng District, Beijing 100005 (CN).

(81) Designated States *(unless otherwise indicated, for every kind of national protection available)*: AE, AG, AL, AM, AO, AT, AU, AZ, BA, BB, BG, BH, BN, BR, BW, BY, BZ, CA, CH, CL, CN, CO, CR, CU, CV, CZ, DE, DJ, DK, DM, DO, DZ, EC, EE, EG, ES, FI, GB, GD, GE, GH, GM, GT, HN, HR, HU, ID, IL, IN, IQ, IR, IS, IT, JM, JO, JP, KE, KG, KH, KN, KP, KR, KW, KZ, LA, LC, LK, LR, LS, LU, LY, MA, MD, MG, MK, MN, MU, MW, MX, MY, MZ, NA, NG, NI, NO, NZ, OM, PA, PE, PG, PH, PL, PT, QA, RO, RS, RU, RW, SA, SC, SD, SE, SG, SK, SL, ST, SV, SY, TH, TJ, TM, TN, TR, TT, TZ, UA, UG, US, UZ, VC, VN, WS, ZA, ZM, ZW.

(84) Designated States *(unless otherwise indicated, for every kind of regional protection available)*: ARIPO (BW, CV, GH, GM, KE, LR, LS, MW, MZ, NA, RW, SC, SD, SL, ST, SZ, TZ, UG, ZM, ZW), Eurasian (AM, AZ, BY, KG, KZ, RU, TJ, TM), European (AL, AT, BE, BG, CH, CY, CZ, DE, DK, EE, ES, FI, FR, GB, GR, HR, HU, IE, IS, IT, LT, LU, LV, MC, ME, MK, MT, NL, NO, PL, PT, RO, RS, SE, SI, SK, SM, TR), OAPI (BF, BJ, CF, CG, CI, CM, GA, GN, GQ, GW, KM, ML, MR, NE, SN, TD, TG).

Published:
— *with international search report (Art. 21(3))*
— *with sequence listing part of description (Rule 5.2(a))*

(54) Title: NON-INVASIVE METHODS USING ANTI-CLDN18.2 ANTIBODY-RADIONUCLIDE CONJUGATES

(57) Abstract: Provided herein are uses of conjugates of anti-CLDN18.2 antibodies or antigen-binding fragments thereof with radionuclides in imaging, patient screening, treatment process monitoring and efficacy evaluation.

WO 2024/041574 A1

NON-INVASIVE METHODS USING ANTI-CLDN18.2 ANTIBODY–RADIONUCLIDE CONJUGATES

FIELD OF THE INVENTION

[0001] The present invention generally relates to non-invasive imaging methods.

BACKGROUND

[0002] Claudin 18.2 (CLDN18.2) is a member of the Claudins protein family, which was discovered by Shouchiro Tsukita and his colleagues in 1998 (1). Claudin is an important molecule constituting the cell tight junction, which can both determine the permeability of the epithelial cells and block the diffusion of proteins and lipids on the surface of the cell membrane (2, 3).

[0003] However, at present, there remains the huge limitations in the precise detection of CLDN18.2 in lesions (13). Since CLDN18.2 is only different from CLDN18.1 on its first exon, they share highly homologous amino acid sequences (91% of the amino acid sequences are the same, and there are only 69 differential amino acids) and most of the differential amino acids are neutral, which makes it difficult to develop the detection antibody specifically probing CLDN18.2.

[0004] Current detection antibodies of CLDN18.2 are only available for immunohistochemistry (IHC) of paraffin tissue sections and frozen tissue sections, which is invasive and cumbersome and need high requirements for the general situation of patients. Furthermore, it cannot reflect *in vivo* tumor heterogeneity and cannot detect repeatedly and dynamically. Therefore, exploring a noninvasive, real-time and dynamic detection technology is essential to achieve the comprehensive evaluation of all lesions.

SUMMARY OF INVENTION

[0005] In one aspect, the present disclosure provides methods of using such anti-CLDN18.2 radionuclide conjugates provided herein (in particular those conjugated to a diagnostic radionuclide, and preferably ^{124}I-18B10 or ^{89}Zr-18B10 or ^{177}Lu-18B10 or ^{124}I-SF106 or ^{177}Lu-DOTA-SF106), for detecting or visualizing CLDN18.2 protein, for diagnosing a subject as having a CLDN18.2 associated disease, for identifying a subject in need as likely to be responsive to a CLDN18.2 targeted therapy, for monitoring progression of a CLDN18.2 associated disease in a subject during a monitoring time period, and for monitoring therapeutic efficacy in a subject having a CLDN18.2 associated disease and

having been treated with a therapy for a therapeutic period, among others. The methods provided herein comprise administering to the subject a detectably effective amount of the anti-CLDN18.2 antibody-radionuclide conjugate provided herein. In certain embodiments, the methods provided herein further comprise conducting radionuclide imaging to the subject to obtain an image. In certain embodiments, the methods provided herein further comprise determining or visualizing presence of the CLDN18.2 protein in a site of interest of the subject from the image, wherein the presence and/or location of the radionuclide conjugate above background is indicative of the presence and/or location of the CLDN18.2 protein.

[0006] In one aspect, the present disclosure provides a method of detecting or visualizing CLDN18.2 protein at a site of interest in a subject, the method comprising:

a) administering to the subject a detectably effective amount of an anti-CLDN18.2 antibody-radionuclide conjugate provided herein; and

b) conducting radionuclide imaging to the subject at a subsequent time point after the administration of the anti-CLDN18.2 antibody-radionuclide conjugate to obtain an image; and

c) determining or visualizing presence of the CLDN18.2 protein in the site of interest of the subject from the image,

wherein the presence and/or location of radionuclide uptake above background is indicative of the presence and/or location of the CLDN18.2 protein, and wherein the anti-CLDN18.2 antibody-radionuclide conjugate comprises an anti-CLDN18.2 antibody-diagnostic radionuclide conjugate.

[0007] In some embodiments, the subject has not been treated with, or is not receiving CLDN18.2 targeted therapy.

[0008] In another aspect, the present disclosure provides a method of diagnosing a subject as having a CLDN18.2 associated disease, the method comprising:

a) administering to the subject a detectably effective amount of an anti-CLDN18.2 antibody-radionuclide conjugate provided herein; and

b) conducting radionuclide imaging to the subject at a subsequent time point after the administration of the anti-CLDN18.2 antibody-radionuclide conjugate to obtain an image;

c) diagnosing the CLDN18.2 associated disease in the subject based on presence and /or location of the CLDN18.2 protein in the site of interest of the subject as determined from the image;

wherein the presence and/or location of radionuclide uptake above background is indicative of the presence and/or location of the CLDN18.2 protein, and

wherein the anti-CLDN18.2 antibody-radionuclide conjugate comprises an anti-CLDN18.2 antibody-diagnostic radionuclide conjugate.

[0009] In some embodiment, the subject has not been treated with, or is not receiving CLDN18.2 targeted therapy.

[0010] In yet another aspect, the present disclosure provides a method of identifying a subject in need as likely to be responsive to a CLDN18.2 targeted therapy, the method comprising:

a) administering to the subject a detectably effective amount of an anti-CLDN18.2 antibody-radionuclide conjugate provided herein; and

b) conducting radionuclide imaging to the subject at a subsequent time point after the administration of the anti-CLDN18.2 antibody-radionuclide conjugate to obtain an image;

c) identifying the subject as likely to respond to the CLDN18.2 targeted therapy based on presence and/or location of the CLDN18.2 protein in the site of interest of the subject as determined from the image,

wherein the presence and/or location of the radionuclide uptake above background is indicative of the presence and/or location of the CLDN18.2 protein, and

wherein the anti-CLDN18.2 antibody-radionuclide conjugate comprises an anti-CLDN18.2 antibody-diagnostic radionuclide conjugate.

[0011] In some embodiment, the subject has not been treated with, or is not receiving CLDN18.2 targeted therapy.

[0012] In some embodiment, the diagnostic radionuclide is selected from the group consisting of: ^{18}F, ^{32}P, ^{33}P, ^{45}Ti, ^{47}Sc, ^{52}Fe, ^{59}Fe, ^{62}Cu, ^{64}Cu, ^{67}Cu, ^{67}Ga, ^{68}Ga, ^{75}Sc, ^{77}As, ^{86}Y, ^{90}Y, ^{89}Sr, ^{89}Zr, ^{94}Tc, ^{94}Tc, ^{99m}Tc, ^{99}Mo, ^{105}Pd, ^{105}Rh, ^{111}Ag, ^{111}In, ^{123}I, ^{124}I, ^{125}I, ^{131}I, ^{142}Pr, ^{143}Pr, ^{149}Pm, ^{153}Sm, $^{154"1581}Gd$, ^{161}Tb, ^{166}Dy, ^{166}Ho, ^{169}Er, ^{175}Lu, ^{177}Lu, ^{186}Re, ^{188}Re, ^{189}Re, ^{194}Ir, ^{198}Au, ^{199}Au, ^{211}At, ^{211}Pb, ^{212}Bi, ^{212}Pb, ^{213}Bi, ^{223}Ra and ^{225}Ac.

[0013] In some embodiment, the method further comprises:

d) administering a therapeutically effective amount of a CLDN18.2 targeted therapy to the subject identified as having presence of the CLDN18.2 protein in the site of interest, diagnosed as having a CLDN18.2 associated disease, and/or identified as likely to be responsive to a CLDN18.2 targeted therapy.

[0014] In some embodiment, the CLDN18.2 targeted therapy comprises a therapy selected from the group consisting of an anti-CLDN18.2 antibody therapy, a CLDN18.2 targeted compound, a CLDN18.2 targeted nucleic acid therapy, a CLDN18.2 targeted peptide, a CLDN18.2 targeted cell therapy, and a CLDN18.2 targeted gene therapy.

[0015] In some embodiment, the anti-CLDN18.2 antibody therapy comprises an anti-CLDN18.2 antibody-therapeutic radionuclide conjugate, wherein the therapeutic radionuclide is from the group consisting of: ^{111}In, ^{111m}In, ^{177}Lu, ^{212}Bi, ^{213}Bi, ^{211}At, ^{62}Cu, ^{64}Cu, ^{67}Cu, ^{90}Y, ^{125}I, ^{131}I, ^{32}P, ^{33}P, ^{47}Sc, ^{111}Ag, ^{67}Ga, ^{142}Pr, ^{153}Sm, ^{161}Tb, ^{166}Dy, ^{166}Ho, ^{186}Re, ^{188}Re, ^{189}Re, ^{212}Pb, ^{223}Ra, ^{225}Ac, ^{59}Fe, ^{75}Se, ^{77}As, ^{89}Sr, ^{99}Mo, ^{105}Rh, ^{109}Pd, ^{143}Pr, ^{149}Pm, ^{169}Er, ^{194}Ir, ^{198}Au, ^{199}Au, ^{199}Au, and ^{211}Pb.

[0016] In some embodiment, the therapeutic radionuclide is ^{177}Lu or ^{124}I.

[0017] In some embodiment, the therapeutic radionuclide is the same as the diagnostic radionuclide.

[0018] In some embodiment, both the therapeutic radionuclide and the diagnostic radionuclide are ^{177}Lu or ^{124}I.

[0019] In some embodiment, the anti-CLDN18.2 antibody-diagnostic radionuclide conjugate is identical to the anti-CLDN18.2 antibody-therapeutic radionuclide.

[0020] In some embodiment, the therapeutically effective amount is at least 100%, 150%, 200%, 300%, 400%, 500%, 600%, 700%, 800%, 900%, or 1000% of the detectably effective amount.

[0021] In yet another aspect, the present disclosure provides a method of monitoring progression of a CLDN18.2 associated disease in a subject during a monitoring time period, the method comprising:

a) administering to the subject a detectably effective amount of an anti-CLDN18.2 antibody-radionuclide conjugate provided herein after the monitoring time period;

b) conducting radionuclide imaging to the subject at a subsequent time point after the administration of the anti-CLDN18.2 antibody-radionuclide conjugate to obtain a post-monitor image; and

c) comparing the post-monitor image with a pre-monitor image, to determine change in the level of the CLDN18.2 protein during the monitoring time period from the image, wherein the level of the radionuclide conjugate above background is indicative of the level of the CLDN18.2 protein,

wherein the change is indicative of presence or absence of disease progression, wherein the anti-CLDN18.2 antibody-radionuclide conjugate comprises an anti-CLDN18.2 antibody-diagnostic radionuclide conjugate.

[0022] In some embodiments, the pre-monitor image is obtained from the subject before the monitoring time period by:

administering with the effective amount of the anti-CLDN18.2 antibody-radionuclide conjugate, followed by conducting radionuclide imaging to the subject at a subsequent time point after the administration of the anti-CLDN18.2 antibody-radionuclide conjugate to obtain the pre-monitor image.

[0023] In some embodiments, the change comprises an increase in the CLDN18.2 level or absence of the increase in the CLDN18.2 level. In some embodiments, increase in the CLDN18.2 level during the monitoring time period is indicative of disease progression, and absence of the increase in the CLDN18.2 level during the monitoring time period is indicative of absence of disease progression.

[0024] In some embodiments, the subject has not been treated with, or is not receiving CLDN18.2 targeted therapy.

[0025] In some embodiments, the disease is tumor.

[0026] In some embodiments, the progression is metastasis of the tumor.

[0027] In some embodiments, the level of the CLDN18.2 protein comprises amount, distribution and/or location of the CLDN18.2 protein.

[0028] In some embodiments, the subject is at risk of metastasis.

[0029] In yet another aspect, the present disclosure provides a method of monitoring therapeutic efficacy in a subject having a CLDN18.2 associated disease and having been treated with a therapy for a therapeutic period, the method comprising:

a) administering to the subject a detectably effective amount of an anti-CLDN18.2 antibody-radionuclide conjugate provided herein after the therapeutic period;

b) conducting radionuclide imaging to the subject at a subsequent time point after the administration of the anti-CLDN18.2 antibody-radionuclide conjugate to obtain a post-treatment image; and

c) comparing the post-treatment image with a pre-treatment image, to determine change in the level of the CLDN18.2 protein during the therapeutic period from the image, wherein the level of the radionuclide uptake above background is indicative of the level of the CLDN18.2 protein,

wherein the change is indicative of presence or absence of therapeutic efficacy, wherein the anti-CLDN18.2 antibody-radionuclide conjugate comprises an anti-CLDN18.2 antibody-diagnostic radionuclide conjugate.

[0030] In some embodiments, the pre-treatment image is obtained from the subject before the therapeutic period by:

administering with the effective amount of the anti-CLDN18.2 antibody-radionuclide conjugate, followed by conducting radionuclide imaging to the subject at a subsequent time point after the administration of the anti-CLDN18.2 antibody-radionuclide conjugate to obtain the pre-treatment image.

[0031] In some embodiments, the change comprises an increase in the CLDN18.2 level, decrease, or absence of the increase in the CLDN18.2 level. In some embodiments, increase in the CLDN18.2 level during the therapeutic period is indicative of absence of therapeutic efficacy or poor therapeutic efficacy, and/or wherein decrease or absence of the increase in the CLDN18.2 level during the therapeutic period is indicative of presence of therapeutic efficacy or positive therapeutic efficacy.

[0032] In some embodiments, the method further comprises:

a) increasing the dose of the therapy or discontinuing the therapy when poor therapeutic efficacy is determined; or

b) recommending the subject continuing the therapy when positive therapeutic efficacy is determined.

[0033] In some embodiments, the therapy comprises a CLDN18.2 targeted therapy.

[0034] In some embodiments, the CLDN18.2 targeted therapy comprises a therapy selected from the group consisting of an anti-CLDN18.2 antibody therapy, a CLDN18.2 targeted compound, a CLDN18.2 targeted nucleic acid therapy, a CLDN18.2 targeted peptide, a CLDN18.2 targeted cell therapy, and a CLDN18.2 targeted gene therapy.

[0035] In some embodiments, the method further comprises recommending the subject switching to a therapy other than a CLDN18.2 targeted therapy when post-treatment CLDN18.2 level is below a corresponding reference level. In certain embodiments, the method further comprises recommending the subject switching to a therapy other than a CLDN18.2 targeted therapy when post-treatment CLDN18.2 level decreased by at least 40% (or at least 50%, 60%, 70%, 80%, 90% or 95%) relative to the pre-treatment CLDN18.2 level.

[0036] In some embodiments, the therapy is not a CLDN18.2 targeted therapy.

[0037] In any of the above embodiments, the diagnostic radionuclide is selected from the group consisting of ^{18}F, ^{32}P, ^{33}P, ^{45}Ti, ^{47}Sc, ^{52}Fe, ^{59}Fe, ^{62}Cu, ^{64}Cu, ^{67}Cu, ^{67}Ga, ^{68}Ga, ^{75}Sc, ^{77}As, ^{86}Y, ^{90}Y, ^{89}Sr, ^{89}Zr, ^{94}Tc, ^{94}Tc, ^{99m}Tc, ^{99}Mo, ^{105}Pd, ^{105}Rh, ^{111}Ag, ^{111} In, ^{123}I, ^{124}I, ^{125}I, ^{131} I, ^{142}Pr, ^{143}Pr, ^{149}Pm, ^{153}Sm, $^{154"1581}Gd$, ^{161}Tb, ^{166}Dy, ^{166}Ho, ^{169}Er, ^{175}Lu, ^{177}Lu, ^{186}Re, ^{188}Re, ^{189}Re, ^{194}Ir, ^{198}Au, ^{199}Au, ^{211} At, ^{211} Pb, ^{212}Bi, ^{212}Pb, ^{213}Bi, ^{223}Ra and ^{225} Ac. In some of these embodiments, the diagnostic radionuclide is ^{124}I, ^{123}I, ^{131}I, ^{89}Zr or ^{177}Lu.

[0038] In any of the above embodiments, the anti-CLDN18.2 antibody-radionuclide conjugate comprises ^{124}I-labeled anti-CLDN18.2 antibody provided herein. In any of the above embodiments, the anti-CLDN18.2 antibody-radionuclide conjugate comprises ^{124}I-labeled 18B10.

[0039] In any of the above embodiments, the anti-CLDN18.2 antibody-radionuclide conjugate is administered at a dose ranging from 0.5 mCi to 10mCi (18.5 MBq to 370 MBq).

[0040] In any of the above embodiments, the radionuclide imaging is conducted 2 hours after the administration of the anti-CLDN18.2 antibody-radionuclide conjugate to the subject, or conducted at a time point between 2 hours and 144 hours, between 12 hours and 144 hours, or preferably between 24 hours and 144 hours, between 24 hours and 120 hours, or between 24 hours and 96 hours after the administration of the anti-CLDN18.2 antibody-radionuclide conjugate to the subject. In any of the above embodiments, the radionuclide imaging is conducted once, twice, three times or more at different time points between 2 hours and 144 hours, between 12 hours and 144 hours, or preferably between 24 hours and 144 hours, between 24 hours and 120 hours, or between 24 hours and 96 hours after the administration of the anti-CLDN18.2 antibody-radionuclide conjugate to the subject.

[0041] In any of the above embodiments, the anti-CLDN18.2 antibody-radionuclide conjugate comprises heavy chain HCDR1, HCDR2 and HCDR3 and/or light chain LCDR1, LCDR2 and LCDR3 sequences, wherein:

the HCDR1 sequence comprises GYNMN (SEQ ID NO: 1), or a homologue sequence of at least 80% sequence identity thereof;

the HCDR2 sequence comprises X1IDPYYX2X3TX4YNQKFX5G (SEQ ID NO: 32), or a homologue sequence of at least 80% sequence identity thereof;

the HCDR3 sequence comprises X6X7X8GNAFDY (SEQ ID NO: 33), or a homologue sequence of at least 80% sequence identity thereof;

the LCDR1 sequence comprises KSSQX9LX10NX11GNX12KNYLT (SEQ ID NO: 34) or a homologue sequence of at least 80% sequence identity thereof;

the LCDR2 sequence comprises WASTRX13S (SEQ ID NO: 35) or a homologue sequence of at least 80% sequence identity thereof;

the LCDR3 sequence comprises QNDYSX15PX16T (SEQ ID NO: 36) or a homologue sequence of at least 80% sequence identity thereof;

wherein X_1 is N or Y or H, X_2 is G or V, X_3 is A or G or T, X_4 is R or T or S, X_5 is K or R, X_6 is S or M, X_7 is Y or F, X_8 is Y or H, X_9 is S or N, X_{10} is L or F, X_{11} is S or N, X_{12} is Q or L, X_{13} is E or K, X_{15} is F or Y and X_{16} is F or L.

[0042] In any of the above embodiments, the CLDN18.2 associated disease is a CLDN18.2 positive tumor or a CLDN18.2 positive non-cancerous lesion (e.g., gastric lesion).

[0043] In any of the above embodiments, the tumor is gastric cancer, ovarian cancer, pancreatic cancer, cholangiocarcinoma, colorectal cancer, lung cancer, or esophageal adenocarcinoma.

[0044] In some embodiments, the gastric lesion is a gastric ulcer.

[0045] In any of the above embodiments, the CLDN18.2 targeted therapy comprises a therapy that specifically targets CLDN18.2 or CLDN18.2-expressing cells.

[0046] In some embodiments, the CLDN18.2 targeted therapy comprises a therapy selected from the group consisting of an anti-CLDN18.2 antibody therapy, a CLDN18.2 targeted compound, a CLDN18.2 targeted nucleic acid therapy, a CLDN18.2 targeted peptide, a CLDN18.2 targeted cell therapy, and a CLDN18.2 targeted gene therapy.

[0047] In some embodiments, the anti-CLDN18.2 antibody therapy comprises an anti-CLDN18.2 antibody–therapeutic radionuclide conjugate, wherein the therapeutic radionuclide is selected from the group consisting of: ^{111}In, ^{111m}In, ^{177}Lu, ^{212}Bi, ^{213}Bi, ^{211}At, ^{62}Cu, ^{64}Cu, ^{67}Cu, ^{90}Y, ^{125}I, ^{131}I, ^{32}P, ^{33}P, ^{47}Sc, ^{111}Ag, ^{67}Ga, ^{142}Pr, ^{153}Sm, ^{161}Tb, ^{166}Dy, ^{166}Ho, ^{186}Re, ^{188}Re, ^{189}Re, ^{212}Pb, ^{223}Ra, ^{225}Ac, ^{59}Fe, ^{75}Se, ^{77}As, ^{89}Sr, ^{99}Mo, ^{105}Rh, ^{109}Pd, ^{143}Pr, ^{149}Pm,

^{169}Er, ^{194}Ir, ^{198}Au, ^{199}Au, ^{199}Au, and ^{211}Pb. In certain embodiments, the therapeutic radionuclide is ^{177}Lu.

[0048] In some embodiments, the CLDN18.2 targeted cell therapy comprises a CAR T cell, TCR T cell, or CAR NK cell that targets CLDN18.2.

[0049] In any of the above embodiments, the site of interest has or is suspected of a tumor or a gastric lesion.

[0050] In some embodiments, the site of interest is whole body.

[0051] In any of the above embodiments, the radionuclide imaging comprises positron emission tomography (PET) or SPECT. In some embodiments, the radionuclide imaging is combined with CT, MR or ultrasound.

[0052] In yet another aspect, the present disclosure provides a kit comprising an anti-CLDN18.2 antibody-diagnostic radionuclide conjugate.

[0053] In yet another aspect, the present disclosure provides a kit for 1) diagnosing a subject as having a CLDN18.2 associated disease, 2) identifying a subject in need as likely be responsive to a CLDN18.2 targeted therapy, 3) monitoring progression of a CLDN18.2 associated disease in a subject during a monitoring time period, and/or 4) monitoring therapeutic efficacy in a subject having a CLDN18.2 associated disease and having been treated with a therapy for a therapeutic period, comprising an anti-CLDN18.2 antibody-diagnostic radionuclide conjugate.

[0054] In certain embodiments, the kit further comprises a therapeutically effective amount of an anti-CLDN18.2 antibody-therapeutic radionuclide conjugate.

[0055] In certain embodiments, the therapeutic radionuclide is ^{177}Lu or ^{124}I.

[0056] In certain embodiments, the therapeutic radionuclide is the same as the diagnostic radionuclide.

[0057] In certain embodiments, both the therapeutic radionuclide and the diagnostic radionuclide are ^{177}Lu or ^{124}I.

[0058] In certain embodiments, the kit further comprises an instruction providing a detectably effective amount of the anti-CLDN18.2 antibody-diagnostic radionuclide conjugate, and a therapeutically effective amount of the anti-CLDN18.2 antibody-therapeutic radionuclide conjugate.

[0059] In certain embodiments, the therapeutically effective amount is at least 100%, 150%, 200%, 300%, 400%, 500%, 600%, 700%, 800%, 900%, or 1000% of the detectably effective amount.

[0060] In any of the above embodiments, the anti-CLDN18.2 antibody-radionuclide conjugate comprises:

a heavy chain variable region comprises a HCDR1 comprising the sequence of SEQ ID NO: 1, a HCDR2 comprising the sequence of SEQ ID NO: 3, and a HCDR3 comprising the sequence of SEQ ID NO: 5; and a light chain variable region comprises a LCDR1 comprising the sequence of SEQ ID NO: 2, a LCDR2 comprising the sequence of SEQ ID NO: 4, and a LCDR3 comprising the sequence of SEQ ID NO: 6;

a heavy chain variable region comprises a HCDR1 comprising the sequence of SEQ ID NO: 1, a HCDR2 comprising the sequence of SEQ ID NO: 7, and a HCDR3 comprising the sequence of SEQ ID NO: 5; and a light chain variable region comprises a LCDR1 comprising the sequence of SEQ ID NO: 2, a LCDR2 comprising the sequence of SEQ ID NO: 4, and a LCDR3 comprising the sequence of SEQ ID NO: 8;

a heavy chain variable region comprises a HCDR1 comprising the sequence of SEQ ID NO: 1, a HCDR2 comprising the sequence of SEQ ID NO: 9, and a HCDR3 comprising the sequence of SEQ ID NO: 11; and a light chain variable region comprises a LCDR1 comprising the sequence of SEQ ID NO: 10, a LCDR2 comprising the sequence of SEQ ID NO: 4, and a LCDR3 comprising the sequence of SEQ ID NO: 6;

a heavy chain variable region comprises a HCDR1 comprising the sequence of SEQ ID NO: 1, a HCDR2 comprising the sequence of SEQ ID NO: 19, and a HCDR3 comprising the sequence of SEQ ID NO: 21; and a light chain variable region comprises a LCDR1 comprising the sequence of SEQ ID NO: 14, a LCDR2 comprising the sequence of SEQ ID NO: 16, and a LCDR3 comprising the sequence of SEQ ID NO: 18; or

a heavy chain variable region comprises a HCDR1 comprising the sequence of SEQ ID NO: 1, a HCDR2 comprising the sequence of SEQ ID NO: 22, and a HCDR3 comprising the sequence of SEQ ID NO: 5; and a light chain variable region comprises a LCDR1 comprising the sequence of SEQ ID NO: 20, a

LCDR2 comprising the sequence of SEQ ID NO: 4, and a LCDR3 comprising the sequence of SEQ ID NO: 6.

[0061] In some embodiments of the anti-CLDN18.2 antibody-radionuclide conjugate, the heavy chain variable region further comprises one or more of heavy chain HFR1, HFR2, HFR3 and HFR4, and/or the light chain variable region further comprises one or more of light chain LFR1, LFR2, LFR3 and LFR4, wherein:

the HFR1 comprises **QVQLVQSGAEVKKPGASVKVSCKASGYX$_{17}$FT** (SEQ ID NO: 54) or a homologous sequence of at least 80% sequence identity thereof,

the HFR2 comprises **WVX$_{18}$QAPGQGLEWX$_{19}$G** (SEQ ID NO: 55) or a homologous sequence of at least 80% sequence identity thereof,

the HFR3 sequence comprises **RVTX$_{20}$TIDKSTSTVYMELSSLRSEDTAVYYCAR** (SEQ ID NO: 56) or a homologous sequence of at least 80% sequence identity thereof,

the HFR4 comprises **WGQGTTVTVSS** (SEQ ID NO: 57) or a homologous sequence of at least 80% sequence identity thereof,

the LFR1 comprises **DIVMTQSPDSLAVSLGERATX$_{21}$NC** (SEQ ID NO: 58) or a homologous sequence of at least 80% sequence identity thereof,

the LFR2 comprises **WYQQKPGQPPKLLIY** (SEQ ID NO: 59) or a homologous sequence of at least 80% sequence identity thereof,

the LFR3 comprises **GVPDRFX$_{22}$GSGSGTDFTLTISSLQAEDVAVYYC** (SEQ ID NO: 60) or a homologous sequence of at least 80% sequence identity thereof, and

the LFR4 comprises **FGGGTKVEIK** (SEQ ID NO: 61) or a homologous sequence of at least 80% sequence identity thereof,

wherein X_{17} is T or S, X_{18} is R or K, X_{19} is M or I, X_{20} is M or L, X_{21} is I or M, and X_{22} is S or T.

[0062] In some embodiments of the anti-CLDN18.2 antibody-radionuclide conjugate, the HFR1 comprises a sequence selected from the group consisting of SEQ ID NOs: 62 and 63, the HFR2 comprises a sequence selected from the group consisting of SEQ ID NOs: 64 and

65, the HFR3 comprises the sequence selected from the group consisting of SEQ ID NOs: 66 and 67, the HFR4 comprises a sequence of SEQ ID NO: 57, the LFR1 comprises the sequence from the group consisting of SEQ ID NOs: 68 and 69, the LFR2 comprises a sequence of SEQ ID NO: 59, the LFR3 comprises a sequence selected from the group consisting of SEQ ID NOs: 70 and 71, and the LFR4 comprises a sequence of SEQ ID NO: 61.

[0063] In some embodiments of the anti-CLDN18.2 antibody-radionuclide conjugate, the heavy chain variable region comprises a sequence selected from the group consisting of SEQ ID NO: 25, SEQ ID NO: 27, SEQ ID NO: 29, SEQ ID NO: 37, SEQ ID NO: 39, SEQ ID NO: 41, SEQ ID NO: 45, and SEQ ID NO: 47, and a homologous sequence thereof having at least 80% sequence identity yet retaining specific binding affinity to CLDN18.2.

[0064] In some embodiments of the anti-CLDN18.2 antibody-radionuclide conjugate, the light chain variable region comprises a sequence selected from the group consisting of SEQ ID NO: 26, SEQ ID NO: 28, SEQ ID NO: 38, SEQ ID NO: 40, SEQ ID NO: 42, SEQ ID NO: 46, SEQ ID NO: 48, and a homologous sequence thereof having at least 80% sequence identity yet retaining specific binding affinity to CLDN18.2.

[0065] In some embodiments of the anti-CLDN18.2 antibody-radionuclide conjugate, the heavy chain variable region comprising the sequence of SEQ ID NO: 23 and a light chain variable region comprising the sequence of SEQ ID NO: 24;

the heavy chain variable region comprises a sequence of SEQ ID NO: 25 and the light chain variable region comprises a sequence of SEQ ID NO: 26;

the heavy chain variable region comprises a sequence of SEQ ID NO: 27 and the light chain variable region comprises a sequence of SEQ ID NO: 28;

the heavy chain variable region comprises a sequence of SEQ ID NO: 29 and the light chain variable region comprises a sequence of SEQ ID NO: 26, or 28;

the heavy chain variable region comprises a sequence of SEQ ID NO: 37 and the light chain variable region comprises a sequence of SEQ ID NO: 38;

the heavy chain variable region comprises a sequence of SEQ ID NO: 39 and the light chain variable region comprises a sequence of SEQ ID NO: 40;

the heavy chain variable region comprises a sequence of SEQ ID NO: 41 and the light chain variable region comprises a sequence of SEQ ID NO: 42;

the heavy chain variable region comprises a sequence of SEQ ID NO: 45 and the light chain variable region comprises a sequence of SEQ ID NO: 46; or

the heavy chain variable region comprises a sequence of SEQ ID NO: 47 and the light chain variable region comprises a sequence of SEQ ID NO: 48.

[0066] In some embodiments of the anti-CLDN18.2 antibody-radionuclide conjugate, the anti-CLDN18.2 antibody-radionuclide conjugate is humanized.

[0067] In some embodiments of the anti-CLDN18.2 antibody-radionuclide conjugate, the anti-CLDN18.2 antibody-radionuclide conjugate comprises a diabody, a Fab, a Fab', a $F(ab')_2$, a Fd, an Fv fragment, a disulfide stabilized Fv fragment (dsFv), a $(dsFv)_2$, a bispecific dsFv (dsFv-dsFv'), a disulfide stabilized diabody (ds diabody), a single-chain antibody molecule (scFv), an scFv dimer (bivalent diabody), a multispecific antibody, a camelized single domain antibody, a nanobody, a domain antibody, and a bivalent domain antibody.

[0068] In some embodiments of the anti-CLDN18.2 antibody-radionuclide conjugate is in a composition with a specific activity of 3.0-6.0 GBq/μmol.

[0069] In some embodiments of the anti-CLDN18.2 antibody-radionuclide conjugate is in a composition having at least 95% to at least 99% of ^{124}I-labled anti-CLDN18.2 antibody (e.g., ^{124}I-labled 18B10 or ^{124}I-SF106) or ^{89}Zr-labled anti-CLDN18.2 antibody (e.g., ^{89}Zr-18B10) or ^{177}Lu -labled anti-CLDN18.2 antibody (e.g., ^{177}Lu-18B10 or ^{177}Lu-DOTA-SF106) as measured by radio thin layer chromatography (TLC), or as measured by radio high performance liquid chromatography (HPLC).

[0070] In yet another aspect, the present disclosure provides a composition comprising an anti-CLDN18.2 antibody-radionuclide conjugate defined herein and one or more pharmaceutically acceptable carriers, wherein the anti-CLDN18.2 antibody-radionuclide conjugate has at least one of the following characteristics:

a) having a radiochemical purity of at least 90% (e.g., at least 91%, at least 92%, at least 93%, at least 94%, at least 95%, at least 96%, at least 97%, at least 98% or at least 99%);

b) having a radiolabeling rate of at least 70% (e.g., at least 75%, at least 80%, at least 85%, at least 90%, at least 92%, at least 94%, at least 95%, at least 96%, at least 97%, at least 98%, or at least 99%);

c) capable of specifically binding to CLDN18.2 at a Kd value of no more than 15nM (e.g., no more than 14nM, no more than 13nM, no more than 12nM, no more than 10nM, no more than 8nM, no more than 6nM, no more than 4nM, or no more than 2nM); and

d) capable of specifically binding to CLDN18.2 at an EC50 value of no more than 1.0 nM (e.g., no more than 0.8 nM, no more than 0.6 nM, no more than 0.5 nM, no more than 0.4 nM, or no more than 0.3 nM) as measured by ELISA.

[0071] In certain embodiments, the anti-CLDN18.2 antibody-radionuclide conjugate comprises a therapeutic radionuclide selected from the group consisting of: ^{111}In, ^{111m}In, ^{177}Lu, ^{212}Bi, ^{213}Bi, ^{211}At, ^{62}Cu, ^{64}Cu, ^{67}Cu, ^{90}Y, ^{125}I, ^{131}I, ^{32}P, ^{33}P, ^{47}Sc, ^{111}Ag, ^{67}Ga, ^{142}Pr, ^{153}Sm, ^{161}Tb, ^{166}Dy, ^{166}Ho, ^{186}Re, ^{188}Re, ^{189}Re, ^{212}Pb, ^{223}Ra, ^{225}Ac, ^{59}Fe, ^{75}Se, ^{77}As, ^{89}Sr, ^{99}Mo, ^{105}Rh, ^{109}Pd, ^{143}Pr, ^{149}Pm, ^{169}Er, ^{194}Ir, ^{198}Au, ^{199}Au, ^{199}Au, and ^{211}Pb, or a diagnostic radionuclide selected from the group consisting of: ^{18}F, ^{32}P, ^{33}P, ^{45}Ti, ^{47}Sc, ^{52}Fe, ^{59}Fe, ^{62}Cu, ^{64}Cu, ^{67}Cu, ^{67}Ga, ^{68}Ga, ^{75}Sc, ^{77}As, ^{86}Y, ^{90}Y, ^{89}Sr, ^{89}Zr, ^{94}Tc, ^{94}Tc, ^{99m}Tc, ^{99}Mo, ^{105}Pd, ^{105}Rh, ^{111}Ag, ^{111} In, ^{123}I, ^{124}I, ^{125}I, ^{131} I, ^{142}Pr, ^{143}Pr, ^{149}Pm, ^{153}Sm, $^{154"1581}$Gd, ^{161}Tb, ^{166}Dy, ^{166}Ho, ^{169}Er, ^{175}Lu, ^{177}Lu, ^{186}Re, ^{188}Re, ^{189}Re, ^{194}lr, ^{198}Au, ^{199}Au, ^{211} At, ^{211} Pb, ^{212}Bi, ^{212}Pb, ^{213}Bi, ^{223}Ra and ^{225} Ac.

[0072] In certain embodiments, the therapeutic radionuclide is ^{177}Lu or ^{124}I.

[0073] In certain embodiments, the diagnostic radionuclide is ^{124}I-18B10, ^{89}Zr or ^{177}Lu.

[0074] In certain embodiments, the anti-CLDN18.2 antibody-radionuclide conjugate further comprises a chelator.

[0075] In certain embodiments, the chelator is DFO or DOTA.

[0076] In certain embodiments, the chelator is DFO, and the radionuclide is ^{89}Zr.

[0077] In certain embodiments, the chelator is DOTA, and the radionuclide is ^{177}Lu.

[0078] In certain embodiments, the anti-CLDN18.2 antibody-radionuclide conjugate comprises a compound of Formula (I):

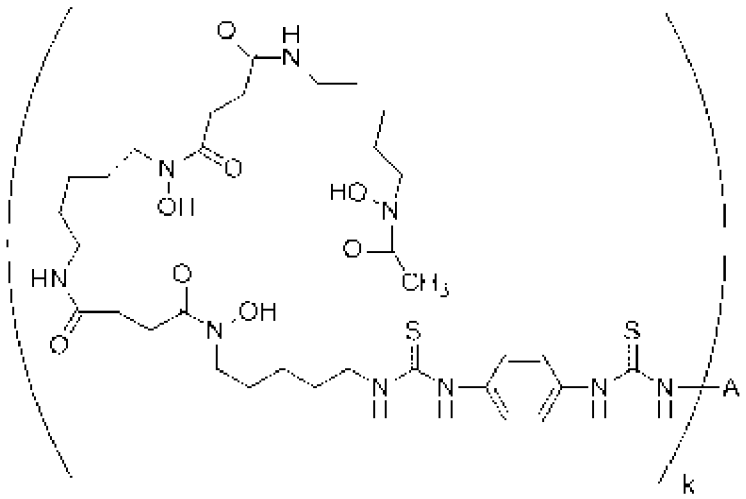

, wherein

[0079] A is an anti-CLDN18.2 antibody or antigen-binding fragment thereof defined in any of the preceding claims, k is from 1-40 (e.g., 3-5, 5-35, 10-30, 15-25, or 20).

[0080] In certain embodiments, the anti-CLDN18.2 antibody-radionuclide conjugate comprises compound portion of Formula (II):

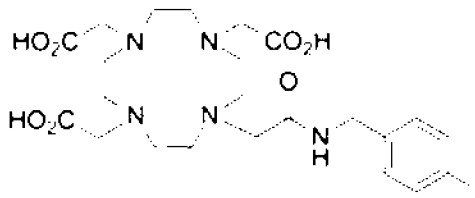

BRIEF DESCRIPTION OF THE DRAWINGS

[0081] The following drawings form part of the present specification and are included to further demonstrate certain aspects of the present disclosure. The disclosure may be better understood by reference to one or more of these drawings in combination with the detailed description of specific embodiments presented herein.

[0082] Figure 1 shows the study design of ^{124}I-18B10 PET/CT and PET/MR imaging.

[0083] Figure 2A shows the Quantification of PET data which was conducted by analyzing ROIs to demonstrate dynamic changes of the tracer in tumors at different post-injection time points. Figure 2B shows the paraffin-embedded tissues slides from mice which were subjected to IHC staining. Figure 2C shows the maximum intensity projection (MIP) images.

[0084] Figure 3A shows maximum intensity projection (MIP) images at 2 h, 24 h, 48 h, 72 h of patient 3. Figure 3B shows ^{124}I- biodistribution in human. Figure 3C shows that the ^{124}I-18B10 tumor uptake was significantly different between different lesion sites ($P < 0.0001$), the ovarian metastases showed the highest uptake with a mean SUVmax of 23.65 ± 2.05, and the lung metastases showed the lowest uptake with a SUVmax of 1.5. Figure 3D shows that the uptake in the lesions that had not been treated by the CLDN18.2 targeted therapy was significantly higher than the uptake in the lesions that had been treated (SUVmax 24h: 6.00 ± 7.38 vs 2.37 vs 1.43, $P = 0.042$).

[0085] Figure 4 shows the ^{124}I-18B10 PET/CT results, wherein panel A indicates that maximum intensity projection (MIP) images at 2 h, 24 h, 48 h, 120 h of patient 4 showed the two mass in the bilateral ovarian with abnormally high uptake. panels B-D indicates that the ^{124}I-18B10 PET/CT showed increased uptake of ^{124}I-18B10 in some liver and bone metastases with SUVmax of 3.2 and 4.4 respectively, and two soft tissue mass were observed in the bilateral ovarian with abnormally high uptake with SUVmax of 12.5 and 17.6 left and

right respectively. Figure 4 panel E shows the pathological examination results (IHC) of the primary lesion of the patient. Figure 4 panel F is the time-dependent curve of ^{124}I-18B10 uptake in each organ.

[0086] Figure 5 shows ^{124}I-18B10 PET results, where panels A-C indicate that the 18F-FDG PET/CT, the ^{124}I-18B10 PET/CT at 72 h and the ^{124}I-18B10 PET/MR at 96 h (Patient No.8) showed high uptake in the lymphoid node next to the left iliac vessel with SUVmax of 4, 6.1 and 6.6 respectively, panel D is the pathological examination results (IHC) of the primary lesion of the Patient No.8, which showed a CLDN18.2 expression level was 3+, 90%, panels E-G indicated that the 18F-FDG PET/CT, the ^{124}I-18B10 PET/CT at 72 h and the ^{124}I-18B10 PET/MR at 96 h (Patient No.10) showed high uptake in the retroperitoneal metastatic lymph node with SUVmax of 3.5, 8.1 and 2.5 respectively, and panel H is the pathological examination results of the primary lesion of the Patient No.10, which showed a CLDN18.2 expression level was also 3+, 90%.

[0087] Figure 6 shows ^{124}I-18B10 PET results, where panels A-C indicate that on the ^{124}I-18B10 PET before the treatment, there were several peritoneal metastases showing high uptake of ^{124}I-18B10 with SUVmax of 3.1, 3.2 and 4.2, panels D-F indicate that on the ^{124}I-18B10 PET after receiving CLDN18.2 targeted therapy, the original high uptake peritoneal metastases showed no obvious uptake, and panel G indicates the pathological examination results of the primary lesion of the patient.

[0088] Figure 7A shows the stability within 48 h of the ^{124}I-18B10 in PBS. Figure 7B shows that the uptake of positive cells was significantly higher than that of negative cells or blocking control at each selected time point ($p<0.0001$). Figure 7C shows the binding constant (Kd = 4.11 nM) of ^{124}I-18B10 to CLDN18.2 receptors determined by a cell saturation binding assay using MKN45CLDN18.2+ cells. Figure 7D shows the biodistribution study in normal mice (n = 4) which illustrated decreases with time in all tissues, showing no specific for the probe in normal organs.

[0089] Figure 8A shows that high gastric uptake was observed within 4 h after gavage (2.53±0.27 at 4 h and 2.98±0.24 at 24 h), and the uptake gradually decreased with the gradual healing of gastric injury. Figure 8B indicates that after autopsy, the gastric body showed local redness, there were different degrees of spotting bleeding, and the gastric body was congested. Figure 8C indicates the HE results showing that there was no obvious damage in the gastric tissue at all the time points except 4h after gavage. Figure 8D shows that much higher uptake ($p<0.05$) was observed in the nearly healed gastric tissue in the gastric ulcer model than in

normal mice at longer time points (1.81±0.20 vs 0.74±0.05 at 48 h and 1.01±0.10 vs 0.46±0.07 at 96 h).

[0090] Figure 9 shows detailed information about quality control of ^{124}I-18B10.

[0091] Figure 10 summarizes the characteristics of 17 patients with pathological results who were enrolled in the analysis, namely, 6 males and 11 females, with a median age of 51 (29–65) years, from May 2021 to April 2022. The CLDN18.2 expression was determined by IHC on the primary lesion which has been resected before PET imaging.

[0092] Figure 11 indicates that the dosimetry estimates from OLINDA show that three organs receiving the highest absorbed doses were spleen, kidney and liver with mean values of 1.20, 0.717 and 0.616 mGy/MBq respectively. The mean effective dose was 0.213 mSv/MBq (0.788 rem/mCi).

[0093] Figure 12 indicates amino acid sequences of certain proteins used in the present disclosure.

[0094] Figure 13 shows the study design of ^{89}Zr-18B10 micro-PET imaging.

[0095] Figure 14A shows MALDI-TOF-MS of 18B10. Figure 14B shows MALDI-TOF-MS of DFO-18B10. Figure 14C shows nonreducing SDS-PAGE characterization. Figure 14D shows binding of 18B10 and DFO-18B10 to human CLDN18.2 protein that was evaluated by ELISA.

[0096] Figure 15 shows synthesis and radiolabeling, purity and in vitro stability of [^{89}Zr]Zr-DFO-18B10, where panel A shows synthesis and radiolabeling of [^{89}Zr]Zr-DFO-18B10, panel B shows radio-TLC results of [^{89}Zr]Zr-DFO-18B10 before and after purification, and panel C shows in vitro stability of [^{89}Zr]Zr-DFO-18B10.

[0097] Figure 16 shows in vitro CLDN18.2 expression of cell lines, where panel A shows western blotting results of CLDN18.2 expression in the BGC823$^{CLDN18.2}$ and BGC823 cell lines, panel B shows relative expression of CLDN18.2 in BGC823$^{CLDN18.2}$ and BGC823 cells (results are shown as the mean ± SD, n = 3), panel C shows flow cytometry histogram of BGC823$^{CLDN18.2}$ and BGC823 cells, panel D shows cellular uptake of [^{89}Zr]Zr-DFO-18B10 in BGC823$^{CLDN18.2}$ and BGC823 cells. (*, $P < 0.05$; **, $P < 0.01$; ***, $P< 0.001$).

[0098] Figure 17A shows small-animal PET images of four different groups at 2, 24, 48, 72 and 96 h. Figure 17B shows SUVmean of [^{89}Zr]Zr-DFO-18B10 in the organs of BGC823$^{CLDN18.2}$ mice. Figure 17C shows SUVmean of [^{89}Zr]Zr-DFO-18B10 in organs of BGC823$^{CLDN18.2}$ mice with unlabelled 18B10 blockade. Figure 17D shows SUVmean [^{89}Zr]Zr-DFO-18B10 in the organs of BGC823 mice. Figure 17E shows SUVmean of [89Zr]Zr-DFO-IgG in organs of BGC823$^{CLDN18.2}$ mice.

[0099] Figure 18A shows section images of tumor uptake 48 h p.i. compared to section images of ^{18}F-FDG in BGC823$^{CLDN18.2}$ mice 1 h p.i. Figure 18B shows SUVmean in the organs of different experimental group mice in organs at 48h. Figure 18C shows T/H at each point p.i. Figure 18D shows T/M at each point p.i. Figure 18E shows IHC analysis of CLDN18.2 expression in BGC823$^{CLDN18.2}$ (++) (e1) and BGC823 (-) (e2) tumors.

[00100] Figure 19A shows biodistribution in the three different tumor models p.i. 48 h. Figure 19B shows T/L p.i. 48 h. Figure 19C shows T/S 48 h p.i.. Figure 19D shows T/B 48 h p.i.

[00101] Figure 20A shows the biodistribution of[^{89}Zr]Zr-DFO-18B10 in normal mice. Figure 20B shows micro-PET/CT imaging of [^{89}Zr]Zr-DFO-18B10 in normal mice at 2, 24, 48 ,72 h and 120 h after tail vein injection. Figure 20C shows SUVmean of vital organs at different time points.

[00102] Figures 21A-21E show SUVmean of different experimental group mice in organs at different time points.

[00103] Figure 22 shows immunohistochemistry result of stomach in BGC823$^{CLDN18.2}$ model mice (+++) (panel A)of stomach in BGC823 model mice (+++) (panel B), of spleen in BGC823$^{CLDN18.2}$ model mice (-) (panel C), of spleen in BGC823 model mice (-) (panel D), of liver in BGC823$^{CLDN18.2}$ model mice (-) (panel E), of liver in BGC823 model mice (-) (panel F).

[00104] Figure 23 shows steps and conditions for ^{177}Lu labeling.

[00105] Figure 24A shows small-animal PET images of BGC823$^{CLDN18.2}$ positive tumor bearing mice after being injected with 300 uCi of ^{177}Lu-DOTA-18B10. Figure 24B shows small-animal PET images of AGS$^{CLDN18.2}$ positive tumor bearing mice after being injected with 300 uCi of ^{177}Lu-DOTA-18B10.

[00106] Figure 25 shows small-animal PET images of a BGC823 CLDN18.2-positive tumor bearing mouse, a BGC823 CLDN18.2-negative tumor bearing mouse, and a blocked tumor bearing mouse after being injected with 300 uCi of ^{177}Lu-DOTA-18B10.

[00107] Figure 26 shows small-animal PET images of a AGS CLDN18.2-positive tumor bearing mouse, a AGS CLDN18.2-negative tumor bearing mouse, and a blocked tumor bearing mouse after being injected with 300 uCi of ^{177}Lu-DOTA-18B10.

[00108] Figure 27 shows CLDN18.2 immunohistochemical staining of BGC823 CLDN18.2-positive tumor bearing mouse, AGS CLDN18.2-positive tumor bearing mouse and BGC823 CLDN18.2-negative tumor bearing mouse.

[00109] Figure 28 shows ^{177}Lu-DOTA-18B10 uptake in gastric cancer cell lines BGC823 and AGS.

[00110] Figure 29A shows Kd constant in the saturated binding test of ^{177}Lu-DOTA-18B10 in AGS cells.

[00111] Figure 29B shows pharmacokinetics of ^{177}Lu-DOTA-18B10 on normal KM mice.

[00112] Figures 30-31 shows biodistribution of ^{177}Lu-DOTA-18B10 in BGC823 CLDN18.2-positive tumor bearing mouse.

[00113] Figure 32 shows therapeutic effects of ^{177}Lu-DOTA-18B10.

[00114] Figure 33 shows effects of ^{177}Lu-DOTA-18B10 on mouse weight.

[00115] Figure 34 shows HE staining of tumor tissues of mice injected with 300uCi or 150uCi of ^{177}Lu-DOTA-18B10 or in a control group.

[00116] Figure 35 shows HE staining of different organs of mice injected with 300uCi or 150uCi of ^{177}Lu-DOTA-18B10 or in a control group.

[00117] Figure 36 shows a novel scFv-Fc (SF106) antibody targeting CLDN18.2 was labeled with ^{124}I and ^{177}Lu. The uptake of ^{124}I-SF106 in targeted cells were analyzed. ^{124}I-SF106 micro-PET imaging was performed in CLDN18.2 positive tumor-bearing mice, and a preliminary treatment study was conducted through ^{177}Lu-DOTA-SF106.

[00118] Figure 37 shows construction process and biochemical characterization of scFv-Fc antibody. Figure 37A shows overview of scFv-Fc antibody generation. Figure 37B shows the mean molecular weight of SF106 antibody measured by MALDI-TOF-MS is 108303.124 Da. Figure 37C shows FACS analysis SF106 binding on HEK293-human CLDN18.2-hi cells, and the EC50 was 11.31nM.

[00119] Figure 38 shows construction of ^{124}I-SF106 and in vitro analysis, where panel A shows structure model of SF106 antibody and Isotopic Labeling abridged general view of SF106 antibody with [^{124}I] Iodine, panel B shows the stability of ^{124}I-SF106 in 0.01M PBS and 5% HSA solution, panel C shows the detection of CLDN18.2 expression in BGC823$^{CLDN18.2}$ and BGC823 cells by flow cytometry, and panel D shows cell uptake experiments of ^{124}I-SF106 in BGC823$^{CLDN18.2}$ and BGC823 cells (*** $P < 0.001$).

[00120] Figure 39 shows Micro-PET imaging of ^{124}I-SF106 in tumor-bearing mouse models (arrows point out tumor) after injection (4, 24, 48, 72, 96 and 120 h).

[00121] Figure 40 shows analysis of Micro-PET imaging, where panel A shows SUVmax trend of ^{124}I-SF106 in tumors of different groups from 4 to 120 h, panel B shows the tumor/muscle (T/M) of different groups at each point postinjection, panel C shows the tumor to liver (T/L) of different groups at each point postinjection, panel D shows the tumor/heart

(T/H) of different groups at each point postinjection, panel E shows IHC of BGC823$^{CLDN18.2}$ tumors was positive (++), and panel F shows IHC of BGC823 tumors was negative (-).

[00122] Figure 41 shows construction of ^{177}Lu-DOTA-SF106 and study on radioimmunoimaging and radionuclide therapy, where panel A shows stages of Synthesize ^{177}Lu-DOTA-SF106, panel B shows small-animal SPECT/CT imaging of ^{177}Lu-DOTA-SF106 in AGS$^{CLDN18.2}$ tumor-bearing mouse, panel C shows small-animal SPECT/CT imaging of ^{177}Lu-DOTA-SF106 in AGS tumor-bearing mouse, panel D shows tumor growth curves of mice after the treatment by ^{177}Lu-DOTA-SF106 and 0.01M PBS (*** $P < 0.001$), and panel E shows weight curves of mice after the treatment by ^{177}Lu-DOTA-SF106 and 0.01M PBS.

[00123] Figure 42 shows ^{nat}I-SF106 mass spectrometry detection and ^{124}I-SF106 in vitro studies. Figure 42 A shows MALDI-TOF-MS of ^{nat}I-SF106 (108963 Da). Figure 42B shows Micro-PET imaging and SDS-PAGE characterization SF106, ^{nat}I-SF106 and ^{124}I-SF106. Figure 42C shows Radio-TLC results of the experiment before purification. Figure 42D shows Radio-TLC results of ^{124}I-SF106 after purification. Figure 42E shows determination of the saturation binding constant (K_d) of ^{124}I-SF106 in BGC823$^{CLDN18.2}$ cells, the K_d value is 17.74 nmol/L. Figure 42F shows the pharmacokinetics of ^{124}I-SF106 in blood of KM mice (n = 5) after intravenous (tail vein) injection. The half-life (slow) was 27.68 h, and the half-life (fast) was 0.6354 h.

[00124] Figure 43 shows SUVmax analysis of Micro-PET/CT imaging and biodistribution study, where panel A shows SUVmax of tumor, muscle, heart, and liver on PET/CT imaging in BGC823$^{CLDN18.2}$ model, panel B shows SUVmax of tumor, muscle, heart, and liver on PET/CT imaging in BGC823 model, panel C shows SUVmax of tumor, muscle, heart, and liver on PET/CT imaging in BGC823 $^{CLDN18.2}$ model with SF106 co-injection, panel D shows biodistribution of ^{124}I-SF106 in KM mice at 4 h, 24 h, 48 h and 96 h after tail vein injection, and panel E shows biodistribution of ^{124}I-SF106 in BGC823$^{CLDN18.2}$ mice at 4 h, 24 h, 48 h, 96 h and 120 h after tail vein injection.

[00125] Figure 44 shows results of co-injection of the anti-CLDN18.2 monoclonal antibody Hu18B10HaLa, where panel A shows Micro-PET imaging of BGC823$^{CLDN18.2}$ tumor-bearing mouse after co-injection with ^{124}I-SF106 and Hu18B10HaLa, and injected with ^{124}I-IgG only, panel B shows SUVmax of tumor on PET/CT imaging in BGC823$^{CLDN18.2}$ tumor-bearing mouse.

[00126] Figure 45 shows DOTA-SF106 mass spectrometry detection and ^{177}Lu-DOTA-SF106 in vitro studies, where panel A shows MALDI-TOF-MS study of DOTA-SF106, panel

B shows the stability of ^{177}Lu-DOTA-SF106 in 0.01M PBS and 5% HSA solution, panel C shows Radio-TLC results of the experiment before purification, and panel D shows Radio-TLC results of ^{124}I-SF106 after purification.

[00127] Figure 46 shows radiolabeling, cell uptake assay and saturation binding experiment. Figure 46A shows flow chart of the radiolabeling of ^{177}Lu-DOTA-18B10. Figure 46B shows cell uptake assay of ^{177}Lu-DOTA-18B10 in BGC823$^{CLDN18.2}$/BGC823 and AGS$^{CLDN18.2}$/AGS cells. Figure 46C shows cell saturation binding experiment and K_d calculation of ^{177}Lu-DOTA-18B10.

[00128] Figures 47A-47E shows SPECT imaging, ROI analysis and histological verification. Figure 47A shows imaging of ^{177}Lu-DOTA-18B10 probe in BGC823$^{CLDN18.2}$/AGS$^{CLDN18.2}$ xenograft mouse models. Figure 47B shows ROI analysis of the SPECT imaging of BGC823$^{CLDN18.2}$/AGS$^{CLDN18.2}$ models. Figure 47C shows imaging compares of xenograft between BGC823$^{CLDN18.2}$ mouse model and its negative/block group, and the compare between AGS$^{CLDN18.2}$ mouse model and its block group. Figure 47D shows radioactive uptake compares of tumor or spleen between positive/negative/block groups in BGC823 and AGS xenograft models. Figure 47E shows CLDN18.2 IHC staining of tumor tissue dissected from BGC823$^{CLDN18.2}$/BGC823/AGS$^{CLDN18.2}$ mouse models. (Bar = 100 μm).

[00129] Figure 48 shows biodistribution experiments, where panel A shows biodistribution of ^{177}Lu-DOTA-18B10 in a BGC823$^{CLDN18.2}$ mouse model over time, and panel B shows comparison of the biodistribution between positive, negative and block groups of BGC823$^{CLDN18.2}$ model at 48 h after injection.

[00130] Figure 49 shows the therapeutic efficacy of ^{177}Lu-DOTA-18B10 in GC mouse models. Figure 49A shows the treatment curves of ^{177}Lu-DOTA-18B10 in BGC823$^{CLDN18.2}$/AGS$^{CLDN18.2}$ models. Figure 49B shows tumor volume compare between each treatment group of BGC823$^{CLDN18.2}$/AGS$^{CLDN18.2}$ models. Figure 49C shows Tumor H&E and Ki67 IHC staining compare between each treatment group. (H&E bar = 50 μm; IHC bar = 100 μm; ***: $p < 0.001$).

[00131] Figure 50 shows toxicity experiments results. The complete blood count analyses and liver function tests of male or female balb/c nude mice treated with 300 μCi ^{177}Lu-DOTA-18B10 or saline. The grey box represents the mean ± SD of the values collected from the entire cohort of toxicity experiment mouse queue on the day before treatment. The grey dotted line represents the normal range for female or male balb/c mice. (*: $p < 0.05$, ***: $p < 0.001$).

[00132] Figure 51shows stability tests. Stability tests results of ^{177}Lu-DOTA-18B10 production.

[00133] Figure 52 shows flow cytometry experiment, where panel A shows the CLDN18.2 expression level of AGS$^{CLDN18.2}$ and AGS cells, and panel B shows the CLDN18.2 expression level of BGC823$^{CLDN18.2}$ and BGC823 cells.

[00134] Figure 53 shows spleen CLDN18.2 IHC staining. The expression level of CLDN18.2 in the spleen tissue of the balb/c nude mouse model. (Bar = 100 μm).

[00135] Figure 54 shows T/NT value of biodistribution of vital organs in BGC823$^{CLDN18.2}$ mouse model over time.

[00136] Figure 55 shows pharmacokinetic experiments. Pharmacokinetic results of ^{177}Lu-DOTA-18B10 in normal healthy KM mice.

[00137] Figure 56 shows body weight monitoring of BGC823$^{CLDN18.2}$ and AGS$^{CLDN18.2}$ mice during the therapy experiment.

[00138] Figure 57 shows histological toxicity tests. H&E staining of various organs after the injection of 300 μCi ^{177}Lu-DOTA-18B10 probe or saline in balb/c nude mice. (Bar = 50 μm).

DETAILED DESCRIPTION OF THE INVENTION

[00139] Before the present disclosure is described in greater detail, it is to be understood that this disclosure is not limited to particular embodiments described, and as such may, of course, vary. It is also to be understood that the terminology used herein is for the purpose of describing particular embodiments only, and is not intended to be limiting, since the scope of the present disclosure will be limited only by the appended claims.

[00140] Unless defined otherwise, all technical and scientific terms used herein have the same meaning as commonly understood by one of ordinary skill in the art to which this disclosure belongs. Although any methods and materials similar or equivalent to those described herein can also be used in the practice or testing of the present disclosure, the preferred methods and materials are now described.

[00141] All publications and patents cited in this specification are herein incorporated by reference as if each individual publication or patent were specifically and individually indicated to be incorporated by reference and are incorporated herein by reference to disclose and describe the methods and/or materials in connection with which the publications are cited. The citation of any publication is for its disclosure prior to the filing date and should not be construed as an admission that the present disclosure is not entitled to antedate such

publication by virtue of prior disclosure. Further, the dates of publication provided could be different from the actual publication dates that may need to be independently confirmed.

[00142] As will be apparent to those of skill in the art upon reading this disclosure, each of the individual embodiments described and illustrated herein has discrete components and features which may be readily separated from or combined with the features of any of the other several embodiments without departing from the scope or spirit of the present disclosure. Any recited method can be carried out in the order of events recited or in any other order that is logically possible.

[00143] **Definitions**

[00144] The following definitions are provided to assist the reader. Unless otherwise defined, all terms of art, notations and other scientific or medical terms or terminology used herein are intended to have the meanings commonly understood by those of skill in the chemical and medical arts. In some cases, terms with commonly understood meanings are defined herein for clarity and/or for ready reference, and the inclusion of such definitions herein should not necessarily be construed to represent a substantial difference over the definition of the term as generally understood in the art.

[00145] As used herein, the singular forms "a", "an" and "the" include plural references unless the context clearly dictates otherwise.

[00146] The term "antibody" as used herein includes any immunoglobulin, monoclonal antibody, polyclonal antibody, multivalent antibody, bivalent antibody, monovalent antibody, multispecific antibody, or bispecific antibody that binds to a specific antigen. A native intact antibody comprises two heavy (H) chains and two light (L) chains. Mammalian heavy chains are classified as alpha, delta, epsilon, gamma, and mu, each heavy chain consists of a variable region (V_H) and a first, second, and third constant region (C_{H1}, C_{H2}, C_{H3}, respectively); mammalian light chains are classified as λ or κ, while each light chain consists of a variable region (V_L) and a constant region. The antibody has a "Y" shape, with the stem of the Y consisting of the second and third constant regions of two heavy chains bound together via disulfide bonding. Each arm of the Y includes the variable region and first constant region of a single heavy chain bound to the variable and constant regions of a single light chain. The variable regions of the light and heavy chains are responsible for antigen binding. The variable regions in both chains generally contain three highly variable loops called the complementarity determining regions (CDRs) (light chain CDRs including LCDR1, LCDR2, and LCDR3, heavy chain CDRs including HCDR1, HCDR2, HCDR3). CDR boundaries for the antibodies and antigen-binding domains disclosed herein may be defined or identified by

the conventions of Kabat, IMGT, AbM, Chothia, or Al-Lazikani (Al-Lazikani, B., Chothia, C., Lesk, A. M., J. Mol. Biol., 273(4), 927 (1997); Chothia, C. et al., J Mol Biol. Dec 5;186(3):651-63 (1985); Chothia, C. and Lesk, A.M., J.Mol.Biol., 196,901 (1987); N. R. Whitelegg et al, Protein Engineering, v13(12), 819-824 (2000); Chothia, C. et al., Nature. Dec 21-28;342(6252):877-83 (1989) ; Kabat E.A. et al., National Institutes of Health, Bethesda, Md. (1991); Marie-Paule Lefranc et al, Developmental and Comparative Immunology, 27: 55-77 (2003); Marie-Paule Lefranc et al, Immunome Research, 1(3), (2005); Marie-Paule Lefranc, Molecular Biology of B cells (second edition), chapter 26, 481-514, (2015)). The three CDRs are interposed between flanking stretches known as framework regions (FRs), which are more highly conserved than the CDRs and form a scaffold to support the hypervariable loops. The constant regions of the heavy and light chains are not involved in antigen-binding, but exhibit various effector functions. Antibodies are assigned to classes based on the amino acid sequence of the constant region of their heavy chain. The five major classes or isotypes of antibodies are IgA, IgD, IgE, IgG, and IgM, which are characterized by the presence of alpha, delta, epsilon, gamma, and mu heavy chains, respectively. Several of the major antibody classes are divided into subclasses such as IgG1 (gamma1 heavy chain), IgG2 (gamma2 heavy chain), IgG3 (gamma3 heavy chain), IgG4 (gamma4 heavy chain), IgA1 (alpha1 heavy chain), or IgA2 (alpha2 heavy chain). In certain embodiments, the antibody provided herein encompasses any antigen-binding fragments thereof.

[00147] As used herein, the term "antigen-binding fragment" refers to an antibody fragment formed from a fragment of an antibody comprising one or more CDRs, or any other antibody portion that binds to an antigen but does not comprise an intact native antibody structure. Examples of antigen-binding fragment include, without limitation, a diabody, a Fab, a Fab', a $F(ab')_2$, a Fd, an Fv fragment, a disulfide stabilized Fv fragment (dsFv), a $(dsFv)_2$, a bispecific dsFv (dsFv-dsFv'), a disulfide stabilized diabody (ds diabody), a single-chain antibody molecule (scFv), scFv-Fc, an scFv dimer (bivalent diabody), a multispecific antibody, a camelized single domain antibody, a nanobody, a domain antibody, and a bivalent domain antibody. An antigen-binding fragment is capable of binding to the same antigen to which the parent antibody binds. In certain embodiments, an antigen-binding fragment may comprise one or more CDRs from a particular human antibody.

[00148] "Fab" with regard to an antibody refers to a monovalent antigen-binding fragment of the antibody consisting of a single light chain (both variable and constant regions) bound

to the variable region and first constant region of a single heavy chain by a disulfide bond. Fab can be obtained by papain digestion of an antibody at the residues proximal to the N-terminus of the disulfide bond between the heavy chains of the hinge region.

[00149] "Fab'" refers to a Fab fragment that includes a portion of the hinge region, which can be obtained by pepsin digestion of an antibody at the residues proximal to the C-terminus of the disulfide bond between the heavy chains of the hinge region and thus is different from Fab in a small number of residues (including one or more cysteines) in the hinge region.

[00150] "$F(ab')_2$"refers to a dimer of Fab' that comprises two light chains and part of two heavy chains.

[00151] "Fc" with regard to an antibody refers to that portion of the antibody consisting of the second and third constant regions of a first heavy chain bound to the second and third constant regions of a second heavy chain via disulfide bond. IgG and IgM Fc regions contain three heavy chain constant regions (second, third and fourth heavy chain constant regions in each chain). It can be obtained by papain digestion of an antibody. The Fc portion of the antibody is responsible for various effector functions such as ADCC, ADCP and CDC, but does not function in antigen binding.

[00152] "Fv" with regard to an antibody refers to the smallest fragment of the antibody to bear the complete antigen binding site. A Fv fragment consists of the variable region of a single light chain bound to the variable region of a single heavy chain. A "dsFv" refers to a disulfide-stabilized Fv fragment that the linkage between the variable region of a single light chain and the variable region of a single heavy chain is a disulfide bond.

[00153] "Single-chain Fv antibody" or "scFv" refers to an engineered antibody consisting of a light chain variable region and a heavy chain variable region connected to one another directly or via a peptide linker sequence (Huston JS *et al. Proc Natl Acad Sci USA*, 85:5879(1988)). A "scFv dimer" refers to a single chain comprising two heavy chain variable regions and two light chain variable regions with a linker. In certain embodiments, an "scFv dimer" is a bivalent diabody or bivalent ScFv (BsFv) comprising V_H-V_L (linked by a peptide linker) dimerized with another V_H-V_L moiety such that V_H's of one moiety coordinate with the V_L's of the other moiety and form two binding sites which can target the same antigens (or eptipoes) or different antigens (or eptipoes). In other embodiments, a "scFv dimer" is a bispecific diabody comprising V_{H1}-V_{L2} (linked by a peptide linker)

associated with V_{L1}-V_{H2} (also linked by a peptide linker) such that V_{H1} and V_{L1} coordinate and V_{H2} and V_{L2} coordinate and each coordinated pair has a different antigen specificity.

[00154] "Single-chain Fv-Fc antibody" or "scFv-Fc" refers to an engineered antibody consisting of a scFv connected to the Fc region of an antibody.

[00155] "Camelized single domain antibody," "heavy chain antibody," "nanobody" or "HCAb" refers to an antibody that contains two V_H domains and no light chains (Riechmann L. and Muyldermans S., *J Immunol Methods.* Dec 10;231(1-2):25-38 (1999); Muyldermans S., *J Biotechnol.* Jun;74(4):277-302 (2001); WO94/04678; WO94/25591; U.S. Patent No. 6,005,079). Heavy chain antibodies were originally obtained from *Camelidae* (camels, dromedaries, and llamas). Although devoid of light chains, camelized antibodies have an authentic antigen-binding repertoire (Hamers-Casterman C. *et al.*, *Nature.* Jun 3;363(6428):446-8 (1993); Nguyen VK. *et al.* "Heavy-chain antibodies in Camelidae; a case of evolutionary innovation," Immunogenetics. Apr;54(1):39-47 (2002); Nguyen VK. *et al. Immunology.* May;109(1):93-101 (2003)). The variable domain of a heavy chain antibody (VHH domain) represents the smallest known antigen-binding unit generated by adaptive immune responses (Koch-Nolte F. *et al.*, *FASEB J.* Nov;21(13):3490-8. Epub 2007 Jun 15 (2007)). "Diabodies" include small antibody fragments with two antigen-binding sites, wherein the fragments comprise a V_H domain connected to a V_L domain in a single polypeptide chain (V_H-V_L or V_L-V_H) (see, *e.g.*, Holliger P. *et al.*, *Proc Natl Acad Sci U S A.* Jul 15;90(14):6444-8 (1993); EP404097; WO93/11161). The two domains on the same chain cannot be paired, because the linker is too short, thus, the domains are forced to pair with the complementary domains of another chain, thereby creating two antigen-binding sites. The antigen–binding sites may target the same of different antigens (or epitopes).

[00156] A "domain antibody" refers to an antibody fragment containing only the variable region of a heavy chain or the variable region of a light chain. In certain embodiments, two or more V_H domains are covalently joined with a peptide linker to form a bivalent or multivalent domain antibody. The two V_H domains of a bivalent domain antibody may target the same or different antigens.

[00157] In certain embodiments, a "$(dsFv)_2$" comprises three peptide chains: two V_H moieties linked by a peptide linker and bound by disulfide bridges to two V_L moieties.

[00158] In certain embodiments, a "bispecific ds diabody" comprises V_{H1}-V_{L2} (linked by a peptide linker) bound to V_{L1}-V_{H2} (also linked by a peptide linker) via a disulfide bridge between V_{H1} and V_{L1}.

[00159] In certain embodiments, a "bispecific dsFv" or "dsFv-dsFv'" comprises three peptide chains: a V_{H1}-V_{H2} moiety wherein the heavy chains are bound by a peptide linker (*e.g.*, a long flexible linker) and paired via disulfide bridges to V_{L1} and V_{L2} moieties, respectively. Each disulfide paired heavy and light chain has a different antigen specificity.

[00160] The term "humanized" as used herein means that the antibody or antigen-binding fragment comprises CDRs derived from non-human animals, FR regions derived from human, and when applicable, constant regions derived from human. In certain embodiments, the amino acid residues of the variable region framework of the humanized CLDN18.2 antibody are substituted for sequence optimization. In certain embodiments, the variable region framework sequences of the humanized CLDN18.2 antibody chain are at least 65%, 70%, 75%, 80%, 85%, 90%, 95% or 100% identical to the corresponding human variable region framework sequences.

[00161] The term "chimeric" as used herein refers to an antibody or antigen-binding fragment that has a portion of heavy and/or light chain derived from one species, and the rest of the heavy and/or light chain derived from a different species. In an illustrative example, a chimeric antibody may comprise a constant region derived from human and a variable region derived from a non-human species, such as from mouse.

[00162] The term "germline sequence" refers to the nucleic acid sequence encoding a variable region amino acid sequence or subsequence that shares the highest determined amino acid sequence identity with a reference variable region amino acid sequence or subsequence in comparison to all other known variable region amino acid sequences encoded by germline immunoglobulin variable region sequences. The germline sequence can also refer to the variable region amino acid sequence or subsequence with the highest amino acid sequence identity with a reference variable region amino acid sequence or subsequence in comparison to all other evaluated variable region amino acid sequences. The germline sequence can be framework regions only, complementarity determining regions only, framework and complementarity determining regions, a variable segment (as defined above), or other combinations of sequences or subsequences that comprise a variable region. Sequence identity can be determined using the methods described herein, for example, aligning two

sequences using BLAST, ALIGN, or another alignment algorithm known in the art. The germline nucleic acid or amino acid sequence can have at least about 90%, 91, 92%, 93%, 94%, 95%, 96%, 97%, 98%, 99%, or 100% sequence identity with the reference variable region nucleic acid or amino acid sequence. Germline sequences can be determined, for example, through the publicly available international ImMunoGeneTics database (IMGT) and V-base.

[00163] "Anti-CLDN18.2 antibody" or "an antibody against CLDN18.2" as used herein refers to an antibody that is capable of specific binding to CLDN18.2 (e.g. human or non-human CLDN18.2) with a sufficient affinity, for example, to provide for diagnostic and/or therapeutic use.

[00164] The term "affinity" as used herein refers to the strength of non-covalent interaction between an immunoglobulin molecule (i.e. antibody) or fragment thereof and an antigen.

[00165] The term "specific binding" or "specifically binds" as used herein refers to a non-random binding reaction between two molecules, such as for example between an antibody and an antigen. In certain embodiments, the antibodies or antigen-binding fragments provided herein specifically bind to human and/or non-human CLDN18.2 with a binding affinity (K_D) of $\leqslant 10^{-6}$ M (e.g., $\leqslant 5x10^{-7}$ M, $\leqslant 2x10^{-7}$ M, $\leqslant 10^{-7}$ M, $\leqslant 5x10^{-8}$ M, $\leqslant 2x10^{-8}$ M, $\leqslant 10^{-8}$ M, $\leqslant 5x10^{-9}$ M, $\leqslant 4x10^{-9}$M, $\leqslant 3x10^{-9}$M, $\leqslant 2x10^{-9}$ M, or $\leqslant 10^{-9}$ M. K_D used herein refers to the ratio of the dissociation rate to the association rate (k_{off}/k_{on}), which may be determined by using any conventional method known in the art, including but are not limited to surface plasmon resonance method, microscale thermophoresis method, HPLC-MS method and flow cytometry (such as FACS) method. In certain embodiments, the K_D value can be appropriately determined by using flow cytometry method. A variety of immunoassay formats may be used to select antibodies specifically immunoreactive with a particular protein. For example, solid-phase ELISA immunoassays are routinely used to select antibodies specifically immunoreactive with a protein (see, e.g., Harlow & Lane, Using Antibodies, A Laboratory Manual (1998), for a description of immunoassay formats and conditions that can be used to determine specific immunoreactivity). Typically a specific or selective binding reaction will produce a signal at least twice over the background signal and more typically at least 10 to 100 times over the background.

[00166] "Percent (%) sequence identity" with respect to amino acid sequence (or nucleic acid sequence) is defined as the percentage of amino acid (or nucleic acid) residues in a

candidate sequence that are identical to the amino acid (or nucleic acid) residues in a reference sequence, after aligning the sequences and, if necessary, introducing gaps, to achieve the maximum correspondence. Alignment for purposes of determining percent amino acid (or nucleic acid) sequence identity can be achieved, for example, using publicly available tools such as BLASTN, BLASTp (available on the website of U.S. National Center for Biotechnology Information (NCBI), see also, Altschul S.F. et al, J. Mol. Biol., 215:403–410 (1990); Stephen F. et al, Nucleic Acids Res., 25:3389–3402 (1997)), ClustalW2 (available on the website of European Bioinformatics Institute, see also, Higgins D.G. et al, Methods in Enzymology, 266:383-402 (1996); Larkin M.A. et al, Bioinformatics (Oxford, England), 23(21): 2947-8 (2007)), and ALIGN or Megalign (DNASTAR) software. Those skilled in the art may use the default parameters provided by the tool, or may customize the parameters as appropriate for the alignment, such as for example, by selecting a suitable algorithm. In certain embodiments, the non-identical residue positions may differ by conservative amino acid substitutions. A "conservative amino acid substitution" is one in which an amino acid residue is substituted by another amino acid residue having a side chain (R group) with similar chemical properties (e.g., charge or hydrophobicity). In general, a conservative amino acid substitution will not substantially change the functional properties of a protein. In cases where two or more amino acid sequences differ from each other by conservative substitutions, the percent or degree of similarity may be adjusted upwards to correct for the conservative nature of the substitution. Means for making this adjustment are well known to those of skill in the art. See, e.g., Pearson (1994) Methods Mol. Biol. 24: 307-331, which is herein incorporated by reference.

[00167] As used herein, a “homologue sequence” and “homologous sequence” are used interchangeable and refer to polynucleotide sequences (or its complementary strand) or amino acid sequences that have sequences identity of at least 80% (e.g. at least 85%, 88%, 90%, 91%, 92%, 93%, 94%, 95%, 96%, 97%, 98%, 99%) to another sequences when optionally aligned.

[00168] The term "antibody-radionuclide conjugate" as used herein refers to an antibody or an antigen binding fragment thereof conjugated with a radionuclide, e.g., a diagnostic radionuclide or a therapeutic radionuclide. Examples of diagnostic radionuclide suitable for conjugation with an antibody include, without limitation, ^{18}F, ^{32}P, ^{33}P, ^{45}Ti, ^{47}Sc, ^{52}Fe, ^{59}Fe, ^{62}Cu, ^{64}Cu, ^{67}Cu, ^{67}Ga, ^{68}Ga, ^{75}Sc, ^{77}As, ^{86}Y, ^{90}Y, ^{89}Sr, ^{89}Zr, ^{94}Tc, ^{94}Tc, ^{99m}Tc, ^{99}Mo, ^{105}Pd, ^{105}Rh, ^{111}Ag, ^{111} ln, ^{123}l, ^{124}l, ^{125}l, ^{131} l, ^{142}Pr, ^{143}Pr, ^{149}Pm, ^{153}Sm, $^{154"1581}Gd$, ^{161}Tb, ^{166}Dy, ^{166}Ho,

^{169}Er, ^{175}Lu, ^{177}Lu, ^{186}Re, ^{188}Re, ^{189}Re, ^{194}lr, ^{198}Au, ^{199}Au, ^{211} At, ^{211} Pb, ^{212}Bi, ^{212}Pb, ^{213}Bi, ^{223}Ra and ^{225}Ac. Examples of therapeutic radionuclide suitable for conjugation with an antibody include, without limitation, ^{111}In, ^{111m}In, ^{177}Lu, ^{212}Bi, ^{213}Bi, ^{211}At, ^{62}Cu, ^{64}Cu, ^{67}Cu, ^{90}Y, ^{125}I, ^{131}I, ^{32}P, ^{33}P, ^{47}Sc, ^{111}Ag, ^{67}Ga, ^{142}Pr, ^{153}Sm, ^{161}Tb, ^{166}Dy, ^{166}Ho, ^{186}Re, ^{188}Re, ^{189}Re, ^{212}Pb, ^{223}Ra, ^{225}Ac, ^{59}Fe, ^{75}Se, ^{77}As, ^{89}Sr, ^{99}Mo, ^{105}Rh, ^{109}Pd, ^{143}Pr, ^{149}Pm, ^{169}Er, ^{194}Ir, ^{198}Au, ^{199}Au, ^{199}Au, and ^{211}Pb.

[00169] It is noted that in this disclosure, terms such as "comprises", "comprised", "comprising", "contains", "containing" and the like are intended to be inclusive or open-ended, and do not exclude additional, un-recited elements or method steps.

[00170] The terms "determining/determine", "measuring" and "detecting/detect" can be used interchangeably and refer to both quantitative and semi-quantitative determinations.

[00171] As used herein, "likelihood" and "likely" with respect to response of a subject to a treatment is a measurement of how probable the therapeutic response is to occur in the subject. It may be used interchangeably with "probability". Likelihood refers to a probability that is more than speculation, but less than certainty. Thus, a therapeutic response is likely if a reasonable person using common sense, training or experience concludes that, given the circumstances, a therapeutic response is probable. In one embodiment, the term "likelihood" and "likely" denotes a chance in percent of how probable a therapeutic response is to occur. In some embodiments, a subject with cancer identified as "likely to respond" refers to a subject with cancer who has more than 30% chance, more than 40% chance, more than 50% chance, more than 60% chance, more than 70% chance, more than 80% chance, more than 90% chance of responding to a CLDN18.2 targeted therapy.

[00172] The term "responsive" or "responsiveness" as used in the context of a subject's therapeutic response to a therapy, are used interchangeably and refer to a beneficial response of a subject to a treatment as opposed to unfavorable responses, i.e. adverse events. In a subject having tumor, beneficial response can be expressed in terms of a number of clinical parameters, including complete response (e.g. loss of detectable tumor), or partial response (e.g. decrease in tumor size and/or cancer cell number). , tumor growth rate reduction which prolongs overall survival, enhancement of anti-tumor immune response, possibly resulting in regression or rejection of the tumor; relief, to some extent, of one or more symptoms associated with the tumor; increase in the length of survival following treatment; and/or decreased mortality at a given point of time following treatment. Continued increase in tumor size and/or cancer cell number (without any growth rate reduction that benefits overall

survival), and/or tumor metastasis is indicative of lack of beneficial response to treatment, and therefore decreased responsiveness.

[00173] As used herein, "cancer" is a generic name for a wide range of cellular malignancies characterized by unregulated growth, lack of differentiation, and the potential or ability to invade local tissues and metastasize. These neoplastic malignancies affect, with various degrees of prevalence, every tissue and organ in the body. Cancer involves presence of cells possessing characteristics typical of cancer-causing cells, such as uncontrolled proliferation, immortality, metastatic potential, rapid growth and proliferation rate, and certain characteristic morphological features. Often, cancer cells will be in the form of a tumor, but such cells may exist alone or may circulate in the blood stream as independent cells, such as leukemic cells. The term cancer and tumor can be used interchangeably herein. The term includes all known cancers and neoplastic conditions, whether characterized as malignant, benign, hematologic or solid, and cancers of all stages and grades including pre- and post-metastatic cancers.

[00174] As used herein, the term "subject" refers to a human or any non-human animal (e.g., mouse, rat, rabbit, dog, cat, cattle, swine, sheep, horse or primate). In many embodiments, a subject is a human being. A subject can be a patient, which refers to a human presenting to a medical provider for diagnosis or treatment of a disease. The term "subject" is used herein interchangeably with "individual" or "patient." A subject can be afflicted with or is susceptible to a disease or disorder but may or may not display symptoms of the disease or disorder.

[00175] The term "treating", or "treatment" of CLDN18.2 associated disease as used herein, unless otherwise indicated, means reversing, alleviating, inhibiting the progress of, or preventing, either partially or completely, the progression of the CLDN18.2 associated disease in a subject.

[00176] The term "prognose" or "prognosing" as used herein refers to the prediction or forecast of the future course or outcome of a disease or condition.

[00177] The term "CLDN18.2" refers to Claudin-18 splice variant 2 derived from mammals, such as primates (e.g. humans, monkeys) and rodents (e.g. mice). In certain embodiments, CLDN18.2 is human CLDN18.2. Exemplary sequence of human CLDN18.2 includes human CLDN18.2 protein (NCBI Ref Seq No. NP_001002026.1, or SEQ ID NO: 30). Exemplary sequence of CLDN18.2 includes mous) CLDN18.2 protein (NCBI Ref Seq No. NP_001181852.1), Macaca fascicularis (crab-eating macaque) CLDN18.2 protein (NCBI Ref

Seq No. XP_015300615.1). CLDN18.2 is expressed in a cancer cell. In one embodiment said CLDN18.2 is expressed on the surface of a cancer cell.

[00178] Reference to "about" a value or parameter herein includes (and describes) embodiments that are directed to that value or parameter per se. For example, description referring to "about X" includes description of "X." Numeric ranges are inclusive of the numbers defining the range. Generally speaking, the term "about" refers to the indicated value of the variable and to all values of the variable that are within the experimental error of the indicated value (e.g. within the 95% confidence interval for the mean) or within 10 percent of the indicated value, whichever is greater. Where the term "about" is used within the context of a time period (years, months, weeks, days etc.), the term "about" means that period of time plus or minus one amount of the next subordinate time period (e.g. about 1 year means 11-13 months; about 6 months means 6 months plus or minus 1 week; about 1 week means 6-8 days; etc.), or within 10 percent of the indicated value, whichever is greater.

[00179] **CLDN18.2 as a Biomarker**

[00180] Claudin-18 (CLDN18) molecule (Genbank accession number: splice variant 1 (CLDN18A1 or CLDN18.1): NP_057453, NM_016369, and splice variant 2 (CLDN18A2 or CLDN18.2): NM_001002026, NP_001002026) is an integral transmembrane protein with a molecular weight of approximately 27.9/27.72kD. CLDN18 proteins are located within the tight junctions of epithelia and endothelia that organize a network of interconnected strands of intramembranous particles between adjacent cells. CLDN18 and occludin are the most prominent transmembrane protein components in the tight junctions. Due to their strong intercellular adhesion properties, these tight junction proteins create a primary barrier to prevent and control the paracellular transport of solutes, and also restrict the lateral diffusion of membrane lipids and proteins to maintain cellular polarity.

[00181] CLDN18 displays several different conformations, which may be selectively addressed by antibodies (see Sahin U, Koslowski M, Dhaene K, et al. Claudin-18 splice variant 2 is a pan-cancer target suitable for therapeutic antibody development[J]. Clinical Cancer Research, 2008, 14(23): 7624-7634). CLDN18-Conformation-1 has all four hydrophobic regions serving as the transmembrane domains (TM), and two extracellular loops (loop1 embraced by hydrophobic region 1 and hydrophobic region 2; loop2 embraced by hydrophobic region 3 and 4) are formed, as described for the vast majority of CLDN family members. A second conformation (CLDN18-Conformation-2) implies that, as described for PMP22, the second and third hydrophobic domains do not fully cross the

plasma membrane so that portion (loop D3) between the first and fourth transmembrane domains is extracellular. A third conformation (CLDN18-Conformation-3) shows a large extracellular domain with two internal hydrophobic regions embraced by the first and fourth hydrophobic regions. Because of a classical N-glycosylation site in the loop D3, the CLDN-18 topology variants CLDN18 topology-2 and CLDN18 topology-3 harbor an additional extracellular N-glycosylation site.

[00182] CLDN18 has two different splice variants, which are present in both mouse and human. The splice variants CLDN18.1 and CLDN18.2 differ in the first 21 amino acids at the N-terminus that comprises the first TM and the loop1, whereas the protein sequences in the C-terminus are identical (see Niimi T, Nagashima K, Ward J M, et al. Claudin-18, a novel downstream target gene for the T/EBP/NKX2. 1 homeodomain transcription factor, encodes lung-and stomach-specific isoforms through alternative splicing[J]. Molecular and cellular biology, 2001, 21(21): 7380-7390.).

[00183] CLDN18.1 is selectively expressed on normal lung and stomach epithelia, whereas CLDN18.2 is only expressed on gastric cells. Most importantly, CLDN18.2 expression is restricted to the differentiated short-lived cells of stomach epithelium, but devoid from the gastric stem cell region. Using sensitive RT-PCR, both variants are not detectable in any other normal human organ. However, they are highly expressed in several cancer types including stomach, esophageal, pancreatic and lung tumors as well as human cancer cell lines (see Matsuda Y, Semba S, Ueda J, et al. Gastric and intestinal claudin expression at the invasive front of gastric carcinoma[J]. Cancer science, 2007, 98(7): 1014-1019.).

[00184] Due to CLDN18.2 is highly specific to normal tissues and expressing in a variety of cancers, CLDN18.2 become a potential target for epithelial tumors. Anti- CLDN18.2 antibodies showed their antitumor effect in patients with advanced gastric adenocarcinoma in clinical trials (7-10). The FAST research showed that therapy of CLDN18.2 antibody drug IMAB362 (dose 800mg/m2) combined with chemotherapy (EOX: epirubicin + oxaliplatin + capecitabine) could significantly prolong the survival of patients with advanced gastric and gastroesophageal junction tumors (PFS: 5.7 months vs 7.9 months; OS: 8.7 months vs 12.5 months) (11). And the curative effect was more significant in the population with strong expression degree of CLDN18.2 (IHC: CLDN18.2 expression intensity $\geq$ 2 +, and the proportion of expression cells $\geq$ 70%) (PFS: 6.1 months vs 9.1 months; OS: 9.3 months vs

16.6 months). Therefore, it is crucial to comprehensively evaluate CLDN18.2 expression of patients in this new targeted treatment.

[00185] Without wishing to be bound to any theories, it is believed that the molecular and functional characteristics of CLDN18.2 make it a highly interesting target for antibody-based cancer diagnosis and therapy. These include (i) absence of CLDN18 from the majority of toxicity relevant normal tissues, (ii) restriction of CLDN18.2 variant expression to a dispensable cell population as differentiated gastric cells that can be replenished by target-negative stem cells of the stomach, (iii) potential differential glycosylation between normal and neoplastic cells, and (iv) the presence of different conformational topologies.

[00186] It has been found that the molecular weight of the CLDN18 protein differs between tumors and adjacent normal tissues. The higher molecular weight CLDN18 protein is observed in healthy tissues, which can be decreased to the same molecular weight as observed in tumor by treatment of the normal tissue lysates with deglycosylating compound PNGase F. This suggests that CLDN18 is less N-glycosylated in tumor as compared to its normal tissue counterpart. A classical N-glycosylation motif is in amino acid residue 116 within the loop D3 domain of the CLDN18 molecule. The molecular weight difference and the inferred structural difference may represent an altered epitope for antibody binding.

[00187] In addition, CLDN18 as a tight junction protein may also contribute to a good specificity for diagnosis, and a good therapeutic window for treatment. Since tumor cells express CLDNs but often do not form the classical tight junctions by homotypic and heterotypic association of CLDNs as found in normal epithelial tissue, they likely have a considerable pool of free CLDNs that are amenable to extracellular antibody binding and immunotherapy. It is possible that binding epitopes of CLDNs in healthy epithelium are shielded within the tight junctions from being accessed to antibody binding.

[00171] **<u>Anti-CLDN18.2 Antibody-Radionuclide Conjugates</u>**

[00172] In one aspect, the present disclosure provides anti-CLDN18.2 antibody radionuclide conjugates, comprising anti-CLDN18.2 antibody or an antigen-binding fragment thereof conjugated to a radionuclide.

[00173] Radionuclide are agents characterized by an unstable nucleus that is capable of undergoing radioactive decay. Radionuclides useful within the present disclosure include gamma-emitters, positron-emitters, Auger electron-emitters, X-ray emitters and fluorescence-emitters. In certain embodiments, the radionuclides are diagnostic.

[00174] Diagnostic radionuclide can be used as an imaging agent. An imaging agent can indicate position of radionuclide and adherents thereto, in a cell or tissue of an animal or human subject, or a cell or tissue under in vitro conditions. In certain embodiments, the radionuclides are those which can be detected externally in a non-invasive manner following administration in vivo. Radionuclides for diagnostic use such as imaging agents are preferably with relatively low cytotoxicity but decay with emissions suitable for imaging. Radionuclides having diagnostic uses can include, for example, ^{18}F, ^{32}P, ^{33}P, ^{45}Ti, ^{47}Sc, ^{52}Fe, ^{59}Fe, ^{62}Cu, ^{64}Cu, ^{67}Cu, ^{67}Ga, ^{68}Ga, ^{75}Sc, ^{77}As, ^{86}Y, ^{90}Y, ^{89}Sr, ^{89}Zr, ^{94}Tc, ^{94}Tc, ^{99m}Tc, ^{99}Mo, ^{105}Pd, ^{105}Rh, ^{111}Ag, ^{111} ln, ^{123}I, ^{124}I, ^{125}I, ^{131} I, ^{142}Pr, ^{143}Pr, ^{149}Pm, ^{153}Sm, $^{154"1581}Gd$, ^{161}Tb, ^{166}Dy, ^{166}Ho, ^{169}Er, ^{175}Lu, ^{177}Lu, ^{186}Re, ^{188}Re, ^{189}Re, ^{194}lr, ^{198}Au, ^{199}Au, ^{211} At, ^{211} Pb, ^{212}Bi, ^{212}Pb, ^{213}Bi, ^{223}Ra and ^{225} Ac. Paramagnetic ions that may be used as diagnostic agents in accordance with the embodiments of the disclosure include, but are not limited to, ions of transition and lanthanide metals (e.g. metals having atomic numbers of 6 to 9, 21 -29, 42, 43, 44, or 57-71). These metals include ions of Cr, V, Mn, Fe, Co, Ni, Cu, La, Ce, Pr, Nd, Pm, Sm, Eu, Gd, Tb, Dy, Ho, Er, Tm, Yb and Lu.

[00175] In certain embodiments, the radionuclides are radioactive metal ions, gamma-emitting radioactive halogens and positron-emitting radioactive non-metals. In certain embodiments, the radionuclide is detectable by positron emission tomography (PET) or single-photon emission computerized tomography (SPECT). For example, radionuclides that decay with gamma emissions are suitable for planar and Single Photon Computerized Emission Tomography (SPECT) imaging, while radionuclides that decay with positron (beta) emission and annihilation photons are suitable for Positron Emission Tomography (PET). Diagnostic Radionuclides label detectable by such as PET or SPECT imaging technology include, for example, without limitation, ^{64}Cu, ^{67}Cu, ^{89}Zr, ^{124}I, ^{86}Y, ^{90}Y, ^{111}In, $^{123/124/131}I$, ^{177}Lu, ^{11}C, ^{14}C, ^{41}Ca, ^{67}Ga, ^{68}Ga, ^{13}N, ^{15}O, ^{44}Sc, ^{18}F, ^{99m}Tc, ^{90m}Tc and the like.

[00176] In some embodiments, the radionuclide is non-metallic. In some embodiments, the radionuclide comprises a radioactive halogen. In some embodiments, the radionuclide is ^{124}I or ^{123}I or ^{131}I. In some embodiments, the anti-CLDN18.2 antibody radionuclide conjugates provided herein comprises anti-CLDN18.2 antibody or an antigen-binding fragment thereof provided herein conjugated to ^{124}I or ^{123}I or ^{131}I.

[00177] Methods of preparing radioiodinated antibodies are known in the art, see, e.g., Grassi, J. et al. (1987). Radioiodination and Other Labeling Techniques. Handbook of

Experimental Pharmacology, 91–141, Eclelman, W.C. et al, Cancer Research, 40, 3036-3042, 1998, which are incorporated herein by reference in its entirety.

[00178] In some embodiments, the ^{124}I or ^{123}I or ^{131}I is labeled to at least one phenyl hydroxyl group of the antibody or an antigen-binding fragment thereof.

[00179] In certain embodiments, the antibody or an antigen-binding fragment thereof is directly iodinated by electrophilic substitution into tyrosine residues, in the presence of a radioiodine such as $Na^{124}I$. In certain embodiments, the antibody or an antigen-binding fragment thereof is indirectly iodinated by covalent linkage of a pre-labelled compound or a compound capable of post linkage labelling, for example, Bolton and Hunter reagent for peptides.

[00180] In some embodiments, the ^{124}I or ^{123}I or ^{131}I is labeled to the antibody or an antigen-binding fragment thereof in the presence of an oxidant. Any suitable oxidants can be used, including chemical oxidant and enzymatic oxidant. Exemplary oxidant includes, without limitation, N-Bromosuccinimide, chloramine T, chlorine gas, or lactoperoxidase.

[00181] In some embodiments, the ^{124}I or ^{123}I or ^{131}I is labeled to the antibody or an antigen-binding fragment thereof by N-bromosuccinimide (NBS) reaction.

[00182] Methods of making radionuclide conjugated antibodies and antigen-binding fragments are known in the art. In general, methods are different for metallic radionuclides, and non-metallic radionuclides. Conjugation of metallic radionuclide typically require a chelator for the conjugation, which may not be necessary for non-metallic radionuclides. Methods of conjugation of a metallic radionuclide to an antibody is known in the art, for example, via a suitable chelator (see, e.g., WO94/11026; Current Protocols in Immunology, Volumes 1 and 2, Coligen et al, Ed. Wiley-Interscience, New York, N.Y., Pubs. (1991)).

[00183] The term "chelator" as used herein refers to a chemical structure capable of binding a metal with two or more bonds. A chelator can have one or more chelating groups that can bind to a metal ion. For example, a chelator can comprise at least one heteroatom suitable for coordination to a metal ion, and sequester a metal ion from aqueous solution.

[00184] In some embodiments, the chelator comprises three or more atoms for chelation, wherein each atom is selected from the group consisting of nitrogen, sulfur, oxygen, and phosphorus.

[00185] Examples of chelators that may be used according to the disclosure include, but are not limited to, DFO (desferoxamine), DOTA (1, 4, 7, 10-tetraazacyclododecane-1, 4, 7, 10-tetracetic acid), DTPA (NR-diethylenetriaminepentacetic acid), NOTA (1, 4, 7-triazacyclononane-1, 4, 7-acetic acid), TRITA (1,4,7,10-tetraazacyclotridecane-N,N',N",N'"-tetraacetic acid); TETA (1,4,8,11-tetraazacyclotetradecane-N,N',N",N'"-tetraacetic acid); and HETA (1,5,9,13-tetraazacyclohexadecane-N,N',N",N'"-tetraacetic acid), EDTA (ethylenediaminetetraacetic acid), NETA({4-[2-(bis-carboxymethylamino)-ethyl]-7-carboxymethyl-[1,4,7]triazonan-1-yl}-acetic acid), TACN-TM (N,N′,N″, tris(2-mercaptoethyl)1,4,7-triazacyclononane), TRAP (1,4,7-triazacyclononane-1,4,7-tris[methyl(2-carboxyethyl)phosphinic acid]), CP256,PCTA (3,6,9,15-tetraazabicyclo[9.3.1]pentadeca-1(15),11,13-triene-3,6,9,-triacetic acid), porphyrins, polyamines, crown ethers, bis-thiosemicarbazones, polyoximes, and derivatives thereof.

[00186] In some embodiments, the anti-CLDN18.2 radionuclide conjugates provided herein comprise a metallic radionuclide conjugated to the anti-CLDN18.2 antibody or antigen-binding fragment thereof provided herein via a chelator. A person skilled in the art can select a suitable chelator for a radionuclide based on knowledge known in the art, for example, as described by Price E. W et al, Chem. Soc. Rev., 2014, **43**, 260-290.

[00187] In some embodiments, the metallic radionuclide can be ^{64}Cu, ^{67}Cu, ^{89}Zr, ^{86}Y, ^{90}Y, ^{111}In, ^{177}Lu, ^{67}Ga, ^{44}Sc, or ^{99m}Tc. In some embodiments, the radionuclide is ^{177}Lu, ^{64}Cu, ^{67}Cu, or ^{89}Zr. In some embodiments, the ^{177}Lu, ^{64}Cu, ^{67}Cu or ^{89}Zr is labeled to the antibody or an antigen-binding fragment thereof via a chelator.

[00188] In some embodiments, the chelator further comprises a reactive functional group for conjugation to the antibody. Chelates may be directly linked to antibodies or peptides, for example as disclosed in U.S. Pat. No. 4,824,659, incorporated herein in its entirety by reference. Such a reactive group allows the chelator to react with a functional group in one or more amino acid residues of the antibody, for example, free cysteine, lysine, and the like. Such amino acid residues (i.e., conjugation sites) to be reacted with (either directly or indirectly) the chelator can be, for example, native or engineered, and can be, for example, present on the heavy or light chain of an antibody. Cysteine conjugation sites can be obtained by insertion, mutation, or reduction of antibody disulfide bonds. Methods for making cysteine engineered antibodies have been disclosed in, for example, WO2011/056983. Site-specific conjugation methods can also be used to direct the conjugation reaction to specific sites of an antibody, achieve desirable stoichiometry, and/or achieve desirable chelator-to-antibody

ratios. Such conjugation methods are known to the art, such as cysteine engineering and enzymatic and chemo-enzymatic methods, including, but not limited to, Q295 conjugation, glutamine conjugation, and trasnglutamiinase-mediated conjugation, as well as those described in J. Clin. Immunol., 36: 100 (2016), incorporated herein by reference in its entirety. Suitable reactive functional group generally enable efficient and facile coupling of the anti-CLDN18.2 antibodies or antigen-binding fragments thereof. Reactive functional groups reactive to lysine and cysteine sites include electrophilic groups, which are known in the art. In certain embodiments, when the desired conjugation site is lysine, the reactive moiety is an isothiocyanate, e.g., p-isothiocyanatobenyl group or reactive ester. In certain embodiments, when the desired conjugation site is cysteine, the reactive moiety is a maleimide.

[00189] Examples of reactive group include Maleimide, aminobenzyl, N-hydroxysuccinimide ester, and so on.

[00190] In certain embodiments, the chelator is conjugated to the antibody or antigen-binding fragment thereof provided herein by a bifunctional linker reagent. Examples of such bifunctional linkers include, without limitation, N-succinimidyl-3-(2-pyridyldithio) propionate (SPDP), succinimidyl-4-(N-maleimidomethyl) cyclohexane-1-carboxylate (SMCC), N-succinimidyl-4-(2-pyridylthio)pentanoate (SPP), iminothiolane (IT), bifunctional derivatives of imidoesters (such as dimethyl adipimidate HCl), active esters (such as disuccinimidyl suberate), aldehydes (such as glutaraldehyde), bis-azido compounds (such as bis (p-azidobenzoyl) hexanediamine), methyltetrazine-amine, *p*−isothiocyanatobenze, bis-diazonium derivatives (such as bis-(p-diazoniumbenzoyl)-ethylenediamine), diisocyanates (such as toluene 2,6-diisocyanate), bis-active fluorine compounds (such as 1,5-difluom-2,4-dinitrobenzene), BMPS, EMCS, GMBS, HBVS, LC-SMCC, MBS, MPRH, SBAP, SIA, SIAB, SMPB, SMPH, sulfo-EMCS, sulfo-GMBS, sulfo -KMUS, sulfo-MBS, sulfo-SIAB, sulfo-SMCC, and sulfo-SMPB, and SVSG (succinimidyl-(4-vinylsulfone)benzoate). Those linker reagents are commercially available (e.g., from Pierce Biotechnology, Inc., Rockford, Ill., U.S.A, see pages 467-498, 2003-2004 Applications Handbook and Catalog).

[00191] In some embodiments, the radionuclide is ^{64}Cu or ^{67}Cu, and the chelator comprises TETA, NOTA, NODA, or NODGA. In some embodiments, the radionuclide is ^{89}Zr and the chelator comprises DFO. When the chelator is DFO, suitable bifunctional linker reagents include, but are not limited to, an isothiocyantatobenzyl group, an n-hydroxysuccinimide ester,2,3,5,6 tetrafluorophenol ester, n-succinimidyl-S-acetylthioacetate,

and those described in *BioMed Research International*, Vol 2014, Article ID 203601, incorporated herein by reference in its entirety. In certain embodiments, the chelator comprising a reactive functional group reactive to the conjugation site is *p*–isothiocyanatobenzyl-desferrioxamine (p-NCS-Bz-DFO):

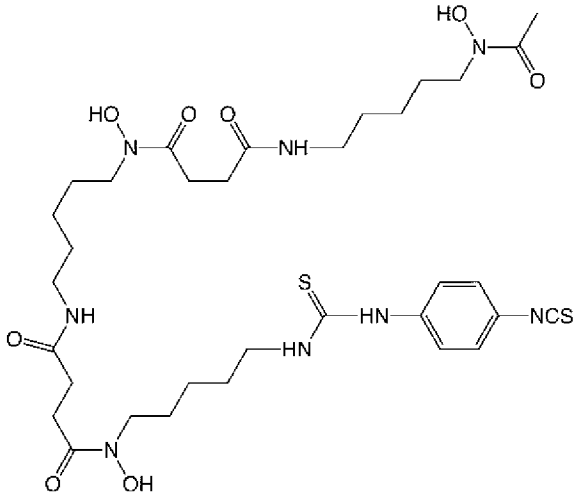

[00192]

[00193] In some embodiments, the radionuclide is ^{177}Lu and the chelator comprises DOTA. When the chelator is DOTA, suitable bifunctional linker reagent may be methyltetrazine-amine or absent. In certain embodiments, the chelator conjugated to the bifunctional linker reagent is methyltetrazine-DOTA:

[00194]

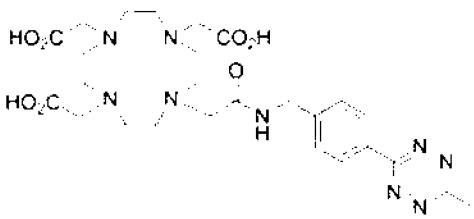

[00195]

[00196] In some embodiments, the anti-CLDN18.2 radionuclide conjugates provided herein can be further conjugated to a nanoparticle. For example, nanoparticles can be used in therapeutic applications as drug carriers that, when conjugated to a CLDN18.2-specific antibody or fragment of the present invention, deliver chemotherapeutic agents, radiotherapeutic agents, toxins, or any other cytotoxic or anti-cancer agent known in the art to cancerous cells that overexpress CLDN18.2 on the cell surface.

[00197] In some embodiments, the anti-CLDN18.2 radionuclide conjugates provided herein can be further conjugated to a drug (e.g., at the epsilon amino group of a lysine residue), and the carrier may incorporate an additional therapeutic or diagnostic agent.

[00198] **i. Antibody sequences**

[00199] In certain embodiments, the anti-CLDN18.2 radionuclide conjugates provided herein comprises an anti-CLDN18.2 antibody or an antigen-binding fragment thereof comprising heavy chain HCDR1, HCDR2 and HCDR3 and/or light chain LCDR1, LCDR2 and LCDR3 sequences, wherein

the HCDR1 sequence comprises GYNMN (SEQ ID NO: 1), or a homologue sequence of at least 80% sequence identity thereof;

the HCDR2 sequence comprises **X_1IDPYYX_2X_3TX_4YNQKFX_5G** (SEQ ID NO: 32), or a homologue sequence of at least 80% (or at least 85%, 90%, 95%) sequence identity thereof;

the HCDR3 sequence comprises **$X_6X_7X_8$GNAFDY** (SEQ ID NO: 33), or a homologue sequence of at least 80% sequence identity thereof;

the LCDR1 sequence comprises **KSSQX_9LX_{10}NX_{11}GNX_{12}KNYLT** (SEQ ID NO: 34) or a homologue sequence of at least 80% (or at least 85%, 90%, 95%) sequence identity thereof;

the LCDR2 sequence comprises **WASTRX_{13}S** (SEQ ID NO: 35) or a homologue sequence of at least 80% sequence identity thereof; and

the LCDR3 sequence comprises **QNDYSX_{15}PX_{16}T** (SEQ ID NO: 36) or a homologue sequence of at least 80% sequence identity thereof;

wherein X_1 is N or Y or H, X_2 is G or V, X_3 is A or G or T, X_4 is R or T or S, X_5 is K or R, X_6 is S or M, X_7 is Y or F, X_8 is Y or H, X_9 is S or N, X_{10} is L or F, X_{11} is S or N, X_{12} is Q or L, X_{13} is E or K, X_{15} is F or Y and X_{16} is F or L.

[00200] In certain embodiments, the anti-CLDN18.2 radionuclide conjugates provided herein comprises an anti-CLDN18.2 antibody or an antigen-binding fragment thereof, wherein the heavy chain variable region comprises:

a) a HCDR1 comprises a sequence selected from SEQ ID NO: 1,

b) a HCDR2 comprises a sequence selected from SEQ ID NO: 3, SEQ ID NO: 7, SEQ ID NO: 9, SEQ ID NO: 19, and SEQ ID NO: 22, and

c) a HCDR3 comprises a sequence selected from SEQ ID NO: 5, SEQ ID NO: 11, and SEQ ID NO: 21, and/or

a light chain variable region comprising:

d) a LCDR1 comprises a sequence of SEQ ID NO: 2, SEQ ID NO: 10, SEQ ID NO: 14, and SEQ ID NO: 20,

e) a LCDR2 comprises a sequence of SEQ ID NO: 4, and SEQ ID NO: 16, and

f) a LCDR3 comprises a sequence selected from SEQ ID NO: 6, SEQ ID NO: 8, and SEQ ID NO: 18.

[00201] In certain embodiments, the heavy chain variable region is selected from the group consisting of:

a) a heavy chain variable region comprising a HCDR1 comprising the sequence of SEQ ID NO: 1, a HCDR2 comprising the sequence of SEQ ID NO: 3, and a HCDR3 comprising the sequence of SEQ ID NO: 5;

b) a heavy chain variable region comprising a HCDR1 comprising the sequence of SEQ ID NO: 1, a HCDR2 comprising the sequence of SEQ ID NO: 7, and a HCDR3 comprising the sequence of SEQ ID NO: 5;

c) a heavy chain variable region comprising a HCDR1 comprising the sequence of SEQ ID NO: 1, a HCDR2 comprising the sequence of SEQ ID NO: 9, and a HCDR3 comprising the sequence of SEQ ID NO: 11;

d) a heavy chain variable region comprising a HCDR1 comprising the sequence of SEQ ID NO: 1, a HCDR2 comprising the sequence of SEQ ID NO: 19, and a HCDR3 comprising the sequence of SEQ ID NO: 21; and

e) a heavy chain variable region comprising a HCDR1 comprising the sequence of SEQ ID NO: 1, a HCDR2 comprising the sequence of SEQ ID NO: 22, and a HCDR3 comprising the sequence of SEQ ID NO: 5.

[00202] In certain embodiments, the light chain variable region is selected from the group consisting of:

a) a light chain variable region comprising a LCDR1 comprising the sequence of SEQ ID NO: 2, a LCDR2 comprising the sequence of SEQ ID NO: 4, and a LCDR3 comprising the sequence of SEQ ID NO: 6;

b) a light chain variable region comprising a LCDR1 comprising the sequence of SEQ ID NO: 2, a LCDR2 comprising the sequence of SEQ ID NO: 4, and a LCDR3 comprising the sequence of SEQ ID NO: 8;

c) a light chain variable region comprising a LCDR1 comprising the sequence of SEQ ID NO: 10, a LCDR2 comprising the sequence of SEQ ID NO: 4, and a LCDR3 comprising the sequence of SEQ ID NO: 6;

d) a light chain variable region comprising a LCDR1 comprising the sequence of SEQ ID NO: 14, a LCDR2 comprising the sequence of SEQ ID NO: 16, and a LCDR3 comprising the sequence of SEQ ID NO: 18; and

e) a light chain variable region comprising a LCDR1 comprising the sequence of SEQ ID NO: 20, a LCDR2 comprising the sequence of SEQ ID NO: 4, and a LCDR3 comprising the sequence of SEQ ID NO: 6.

[00203] In certain embodiments, in the anti-CLDN18.2 radionuclide conjugates provided herein:

a) the heavy chain variable region comprises a HCDR1 comprising the sequence of SEQ ID NO: 1, a HCDR2 comprising the sequence of SEQ ID NO: 3, and a HCDR3 comprising the sequence of SEQ ID NO: 5; and the light chain variable region comprises a LCDR1 comprising the sequence of SEQ ID NO: 2, a LCDR2 comprising the sequence of SEQ ID NO: 4, and a LCDR3 comprising the sequence of SEQ ID NO: 6 (referred to as antibody "7C12");

b) the heavy chain variable region comprises a HCDR1 comprising the sequence of SEQ ID NO: 1, a HCDR2 comprising the sequence of SEQ ID NO: 7, and a HCDR3 comprising the sequence of SEQ ID NO: 5; and the light chain variable region comprises a LCDR1 comprising the sequence of SEQ ID NO: 2, a LCDR2 comprising the sequence of SEQ ID NO: 4, and a LCDR3 comprising the sequence of SEQ ID NO: 8 (referred to as antibody "11F12");

c) the heavy chain variable region comprises a HCDR1 comprising the sequence of SEQ ID NO: 1, a HCDR2 comprising the sequence of SEQ ID NO: 9, and a HCDR3 comprising the sequence of SEQ ID NO: 11; and the light chain variable region comprises a LCDR1 comprising the sequence of SEQ ID NO: 10, a LCDR2 comprising the sequence of SEQ ID NO: 4, and a LCDR3 comprising the sequence of SEQ ID NO: 6 (referred to as antibody "22G6");

d) the heavy chain variable region comprises a HCDR1 comprising the sequence of SEQ ID NO: 1, a HCDR2 comprising the sequence of SEQ ID NO: 19, and a HCDR3 comprising the sequence of SEQ ID NO: 21; and the light chain variable region comprises a LCDR1 comprising the sequence of SEQ ID NO: 14, a LCDR2 comprising the sequence of SEQ ID NO: 16, and a LCDR3 comprising the sequence of SEQ ID NO: 18 (referred to as antibody "18B10"); or

e) the heavy chain variable region comprises a HCDR1 comprising the sequence of SEQ ID NO: 1, a HCDR2 comprising the sequence of SEQ ID NO: 22, and a HCDR3 comprising the sequence of SEQ ID NO: 5; and the light chain variable region comprises a LCDR1 comprising the sequence of SEQ ID NO: 20, a LCDR2 comprising the sequence of SEQ ID NO: 4, and a LCDR3 comprising the sequence of SEQ ID NO: 6 (referred to as antibody "12E9").

[00204] In certain embodiments, the anti-CLDN18.2 radionuclide conjugates provided herein comprises an anti-CLDN18.2 antibody or an antigen-binding fragment thereof comprising heavy chain HCDR1, HCDR2 and HCDR3 and/or light chain LCDR1, LCDR2 and LCDR3 sequences, wherein the HCDR1, HCDR2 and HCDR3 are the same as the HCDR1, HCDR2 and HCDR3 of the heavy chain variable region comprising the sequence of SEQ ID NO: 37, 39, 41, 45 or 47, the LCDR1, LCDR2 and LCDR3 are the same as the LCDR1, LCDR2 and LCDR3 of the light chain variable region comprising the sequence of SEQ ID NO: 38, 40, 42, 46 or 48.

[00205] In certain embodiments, the anti-CLDN18.2 radionuclide conjugates provided herein comprise one or more (e.g. 1, 2, 3, 4, 5, or 6) CDR sequences of a CLDN18.2 antibodies 7C12, 11F12, 26G6, 18B10 and 12E9.

[00206] **Table 1. Sequences of CLDN18.2 antibodies' CDR region**

Antibody	**Region**	**CDR1**	**CDR2**	**CDR3**
7C12	**HCDR**	SEQ ID NO: 1 GYNMN	SEQ ID NO: 3 NIDPYYGATRYNQKFKG	SEQ ID NO: 5 SYYGNAFDY
	LCDR	SEQ ID NO: 2 KSSQSLLNSGNQKNYLT	SEQ ID NO: 4 WASTRES	SEQ ID NO: 6 QNDYSFPFT
11F12	**HCD**	SEQ ID NO: 1	SEQ ID NO: 7	SEQ ID NO:

	R	GYNMN	YIDPYYGGTRYNQKFKG	5 SYYGNAFDY
	LCDR	SEQ ID NO: 2 KSSQSLLNSGNQKNYLT	SEQ ID NO: 4 WASTRES	SEQ ID NO: 8 QNDYSYPFT
26G6	**HCDR**	SEQ ID NO: 1 GYNMN	SEQ ID NO: 9 HIDPYYVTTTYNQKFRG	SEQ ID NO: 11 SFYGNAFDY
	LCDR	SEQ ID NO: 10 KSSQSLFNSGNQKNYLT	SEQ ID NO: 4 WASTRES	SEQ ID NO: 6 QNDYSFPFT
18B10	**HCDR**	SEQ ID NO: 1 GYNMN	SEQ ID NO: 19 NIDPYYGGTSYNQKFKG	SEQ ID NO: 21 MYHGNAFDY
	LCDR	SEQ ID NO: 14 KSSQSLLNSGNLKNYLT	SEQ ID NO: 16 WASTRKS	SEQ ID NO: 18 QNDYSYPLT
12E9	**HCDR**	SEQ ID NO: 1 GYNMN	SEQ ID NO: 22 NIDPYYGGTRYNQKFKG	SEQ ID NO: 5 SYYGNAFDY
	LCDR	SEQ ID NO: 20 KSSQNLLNNGNQKNYLT	SEQ ID NO: 4 WASTRES	SEQ ID NO: 6 QNDYSFPFT

[00207] Table 2. Sequences of mouse/chimeric antibody VH/VL

	VH	**VL**
7C12	SEQ ID NO: 37 EFQLQQSGPELEKPGASVRISC KTSGYSFTGYNMNWVKQSNG ESLEWIGNIDPYYGATRYNQKF KGKATLTVDKSSSTAYMQLKS LTSEDSAVYYCARSYYGNAFD YWGQGTTLTVSS	SEQ ID NO: 38 DIVMTQSPSSLTVTAGEKVTM SCKSSQSLLNSGNQKNYLTW YQQKPGQPPKLLIYWASTRES GVPDRFTGSGSGTDFTLTISSV QAEDLAVYYCQNDYSFPFTFG SGTKLEIK
11F12	SEQ ID NO: 39	SEQ ID NO: 40

	EFQLQQSGPELEKPGASVRISC KTSGYSFTGYNMNWVKQSNG ESLEWIGYIDPYYGGTRYNQKF KGKATLTVDKSSSTAYMQLKS LTSEDSAVYYCARSYYGNAFD YWGQGTTLTVSS	DIVMTQSPSSLTVTAGEKVTM SCKSSQSLLNSGNQKNYLTW YQQKPGQPPKLLIYWASTRES GVPDRFTGSGSGTDFTLTISSV QAEDLAVYYCQNDYSYPFTF GSGTKLEIK
26G6	SEQ ID NO:41 EFQLQQSGPELEKPGASVKISC KTSGYSFTGYNMNWVKQSNG QSLEWIGHIDPYYVTTTYNQKF RGKATLTVDKSSSTAYMQLKS LTSEDSAVYYCARSFYGNAFD YWGQGTTLTVSS	SEQ ID NO: 42 DIVMTQSPSSLTVTAGEKVTM SCKSSQSLFNSGNQKNYLTW YQQKPGQPPKLLIYWASTRES GVPDRFTGSGSGTDFTLTISSV QAEDLAVYYCQNDYSFPFTFG SGTKLEIK
18B10	SEQ ID NO:45 EFQLQQSGPELEKPGASVRISC KTSGYSFTGYNMNWVKQSNG ESLEWIGNIDPYYGGTSYNQKF KGKATLTVDKSSSTAYMQLKS LTSEDSAVYYCARMYHGNAF DYWGQGTTLTVSS	SEQ ID NO: 46 DIVMTQSPSSLTVTAGEKVTM SCKSSQSLLNSGNLKNYLTWY QQKPGQPPKLLIYWASTRKSG VPDRFTGSGSGTDFTLTLSSV QAEDLAVYYCQNDYSYPLTF GAGTKLELK
12E9	SEQ ID NO:47 EFQLQQSGPELEKPGASVRISC KTSGYSFTGYNMNWVKQSNG ESLEWIGNIDPYYGGTRYNQKF KGKATLTVDKSSSTAYMQLKS LTSEDSAVYYCARSYYGNAFD YWGQGTTLTVSS	SEQ ID NO: 48 DIVMTQSPSSLTVTAGEKVTM SCKSSQNLLNNGNQKNYLTW YQQKPGQPPKLLIYWASTRES GVPDRFTGSGSGTDFILTISSV QAEDLAVYYCQNDYSFPFTFG AGTKLELK

[00208] In certain embodiments, the anti-CLDN18.2 antibody conjugates provided herein comprise suitable framework region (FR) sequences, as long as the antibodies and antigen-binding fragments thereof can specifically bind to CLDN18.2. The CDR sequences provided in Table 1 are obtained from mouse antibodies, but they can be grafted to any suitable FR sequences of any suitable species such as mouse, human, rat, rabbit, among others, using suitable methods known in the art such as recombinant techniques.

[00209] In certain embodiments, the anti-CLDN18.2 radionuclide conjugates provided herein are humanized. A humanized antibody or antigen-binding fragment is desirable in its reduced immunogenicity in human. A humanized antibody is chimeric in its variable regions, as non-human CDR sequences are grafted to human or substantially human FR sequences. Humanization of an antibody or antigen-binding fragment can be essentially performed by substituting the non-human (such as murine) CDR genes for the corresponding human CDR genes in a human immunoglobulin gene (see, for example, Jones et al. (1986) Nature

321:522-525; Riechmann et al. (1988) Nature 332:323-327; Verhoeyen et al. (1988) Science 239:1534-1536).

[00210] Suitable human heavy chain and light chain variable domains can be selected to achieve this purpose using methods known in the art. In an illustrative example, "best-fit" approach can be used, where a non-human (e.g., rodent) antibody variable domain sequence is screened or BLASTed against a database of known human variable domain germline sequences, and the human sequence closest to the non-human query sequence is identified and used as the human scaffold for grafting the non-human CDR sequences (see, for example, Sims et al, (1993) J. Immunol. 151:2296; Chothia et al. (1987) J. Mot. Biol. 196:901). Alternatively, a framework derived from the consensus sequence of all human antibodies may be used for the grafting of the non-human CDRs (see, for example, Carter et al. (1992) Proc. Natl. Acad. Sci. USA, 89:4285; Presta et al. (1993) J. Immunol.,151:2623).

[00211] In certain embodiments, the humanized antibody conjugates provided herein are composed of substantially all human sequences except for the CDR sequences which are non-human. In some embodiments, the variable region FRs, and constant regions if present, are entirely or substantially from human immunoglobulin sequences. The human FR sequences and human constant region sequences may be derived different human immunoglobulin genes, for example, FR sequences derived from one human antibody and constant region from another human antibody. In some embodiments, the humanized antibody or antigen-binding fragment comprise human heavy/light chain FR1-4.

[00212] In some embodiments, the FR regions derived from human may comprise the same amino acid sequence as the human immunoglobulin from which it is derived. In some embodiments, one or more amino acid residues of the human FR are substituted with the corresponding residues from the parent non-human antibody. This may be desirable in certain embodiments to make the humanized antibody or its fragment closely approximate the non-human parent antibody structure to reduce or avoid immunogenicity and/or improve or retain the binding activity or binding affinity.

[00213] In certain embodiments, the humanized antibody conjugates provided herein comprises no more than 10, 9, 8, 7, 6, 5, 4, 3, 2, or 1 amino acid residue substitutions in each of the human FR sequences, or no more than 10, 9, 8, 7, 6, 5, 4, 3, 2, or 1 amino acid residue substitutions in all the FRs of a heavy or a light chain variable domain. In some embodiments, such change in amino acid residue could be present in heavy chain FR regions

only, in light chain FR regions only, or in both chains. In certain embodiments, the one or more amino acid residues are mutated, for example, back-mutated to the corresponding residue found in the non-human parent antibody (e.g. in the mouse framework region) from which the CDR sequences are derived. Suitable positions for mutations can be selected by a skilled person following principles known in the art. For example, a position for mutation can be selected where: 1) the residue in the framework of the human germline sequence is rare (e.g. in less than 20% or less than 10% in human variable region sequence); 2) the position is immediately adjacent to one or more of the 3 CDR's in the primary sequence of the human germline chain, as it is likely to interact with residues in the CDRs; or 3) the position is close to CDRs in a 3-dimensional model, and therefore can have a good probability of interacting with amino acids in the CDR. The residue at the selected position can be mutated back to the corresponding residue in the parent antibody, or to a residue which is neither the corresponding residue in human germline sequence nor in parent antibody, but to a residue typical of human sequences, i.e. that occurs more frequently at that position in the known human sequences belonging to the same subgroup as the human germline sequence (see U.S. Pat. No. 5,693,762).

[00214] In certain embodiments, the humanized light and heavy chains of the present disclosure are substantially non-immunogenic in humans and retain substantially the same affinity as or even higher affinity than the parent antibody to CLDN18.2.

[00215] In certain embodiments, the humanized antibody conjugates thereof provided herein comprise one or more light chain FR sequences of human germline framework sequence VK/4-1, and/or one or more heavy chain FR sequences of human germline framework sequence VH/1-46, without or without back mutations. Back mutations can be introducted in to the human germline framework sequence, if needed. In certain embodiments, the humanized antibody 18B10 may contain one or more back mutations selected from the group consisting of: R71I, T73K, T28S, M69L, R38K, and M48I, all based on Kabat numbering, in heavy chain framework sequence VH/1-46. The humanized antibody 18B10 may contain one or more back mutations selected from the group consisting of: S63T, and I21M, all based on Kabat numbering, in light chain framework sequence VK/4-1.

[00216] In certain embodiments, in anti-CLDN18.2 antibody conjugates provided herein, the anti-CLDN18.2 antibody or an antigen-binding fragment thereof comprises a heavy chain variable region comprising the sequence selected from the group consisting of SEQ ID NO: 25, SEQ ID NO: 27, SEQ ID NO: 29, SEQ ID NO: 37, SEQ ID NO: 39, SEQ ID NO: 41,

SEQ ID NO: 45, and SEQ ID NO: 47, and a homologous sequence thereof having at least 80% (e.g. at least 85%, 90%, 95%, 96%, 97%, 98%, or 99%) sequence identity yet retaining specific binding affinity to CLDN18.2, in particular human CLDN18.2.

[00217] In certain embodiments, in anti-CLDN18.2 antibody conjugates provided herein, the anti-CLDN18.2 antibody or an antigen-binding fragment thereof comprises a light chain variable region comprising the sequence selected from the group consisting of SEQ ID NO: 26, SEQ ID NO: 28, SEQ ID NO: 38, SEQ ID NO: 40, SEQ ID NO: 42, SEQ ID NO: 46, SEQ ID NO: 48, and a homologous sequence thereof having at least 80% (e.g. at least 85%, 90%, 95%, 96%, 97%, 98%, or 99%) sequence identity yet retaining specific binding affinity to CLDN18.2, in particular human CLDN18.2.

[00218] In certain embodiments, the anti-CLDN18.2 radionuclide conjugates provided herein comprises:

a heavy chain variable region comprising the sequence of SEQ ID NO: 25 and a light chain variable region comprising the sequence of SEQ ID NO: 26;
a heavy chain variable region comprising the sequence of SEQ ID NO: 27 and a light chain variable region comprising the sequence of SEQ ID NO: 28;
a heavy chain variable region comprising the sequence of SEQ ID NO: 29 and a light chain variable region comprising the sequence of SEQ ID NO: 26, or 28;
a heavy chain variable region comprising the sequence of SEQ ID NO: 37 and a light chain variable region comprising the sequence of SEQ ID NO: 38;
a heavy chain variable region comprising the sequence of SEQ ID NO: 39 and a light chain variable region comprising the sequence of SEQ ID NO: 40;
a heavy chain variable region comprising the sequence of SEQ ID NO: 41 and a light chain variable region comprising the sequence of SEQ ID NO: 42;
a heavy chain variable region comprising the sequence of SEQ ID NO: 45 and a light chain variable region comprising the sequence of SEQ ID NO: 46; or
a heavy chain variable region comprising the sequence of SEQ ID NO: 47 and a light chain variable region comprising the sequence of SEQ ID NO: 48.

[00219] In certain embodiments, the anti-CLDN18.2 radionuclide conjugates provided herein further comprises one or more of heavy chain HFR1, HFR2, HFR3 and HFR4, and/or one or more of light chain LFR1, LFR2, LFR3 and LFR4, wherein:

the HFR1 comprises **QVQLVQSGAEVKKPGASVKVSCKASGYX$_{17}$FT** (SEQ ID NO: 54) or a homologous sequence of at least 80% (or at least 85%, 90%, 95%) sequence identity thereof,

the HFR2 comprises **WVX$_{18}$QAPGQGLEWX$_{19}$G** (SEQ ID NO: 55) or a homologous sequence of at least 80% (or at least 90%) sequence identity thereof,

the HFR3 sequence comprises **RVTX$_{20}$TIDKSTSTVYMELSSLRSEDTAVYYCAR** (SEQ ID NO: 56) or a homologous sequence of at least 80% (or at least 85%, 90%, 95%) sequence identity thereof,

the HFR4 comprises **WGQGTTVTVSS** (SEQ ID NO: 57) or a homologous sequence of at least 80% sequence identity thereof,

the LFR1 comprises **DIVMTQSPDSLAVSLGERATX$_{21}$NC** (SEQ ID NO: 58) or a homologous sequence of at least 80% (or at least 85%, 90%, 95%) sequence identity thereof,

the LFR2 comprises **WYQQKPGQPPKLLIY** (SEQ ID NO: 59) or a homologous sequence of at least 80% (or at least 85%, 90%) sequence identity thereof,

the LFR3 comprises **GVPDRFX$_{22}$GSGSGTDFTLTISSLQAEDVAVYYC** (SEQ ID NO: 60) or a homologous sequence of at least 80% (or at least 85%, 90%, 95%) sequence identity thereof, and

the LFR4 comprises **FGGGTKVEIK** (SEQ ID NO: 61) or a homologous sequence of at least 80% (or at least 90%) sequence identity thereof,

wherein X_{17} is T or S, X_{18} is R or K, X_{19} is M or I, X_{20} is M or L, X_{21} is I or M, and X_{22} is S or T.

[00220] In certain embodiments, the HFR1 comprises a sequence selected from the group consisting of SEQ ID NOs: 62 and 63, the HFR2 comprises a sequence selected from the group consisting of SEQ ID NOs: 64 and 65, the HFR3 comprises the sequence selected from the group consisting of SEQ ID NOs: 66 and 67, the HFR4 comprises a sequence of SEQ ID NOs: 57, the LFR1 comprises the sequence from the group consisting of SEQ ID NOs: 68 and 69, the LFR2 comprises a sequence of SEQ ID NO: 59, the LFR3 comprises a sequence selected from the group consisting of SEQ ID NOs: 70 and 71, and the LFR4 comprises a sequence of SEQ ID NO: 61.

[00221] Table 3-1. Framework (FR) sequences of humanized CLDN18.2 antibodies 18B10

Antibody chain	FR1	FR2	FR3	FR4
Hu18B10-Ha	SEQ ID NO: 62	SEQ ID NO: 64	SEQ ID NO: 66	SEQ ID NO: 57
	QVQLVQSGAEVKKPGASVKVSCKASGYTFT	WVRQAPGQGLEWMG	RVTMTIDKSTSTVYMELSSLRSEDTAVYYCAR	WGQGTTVTVSS
Hu18B10-Hb	SEQ ID NO: 63	SEQ ID NO: 64	SEQ ID NO: 67	SEQ ID NO: 57
	QVQLVQSGAEVKKPGASVKVSCKASGYSFT	WVRQAPGQGLEWMG	RVTLTIDKSTSTVYMELSSLRSEDTAVYYCAR	WGQGTTVTVSS
Hu18B10-Hc	SEQ ID NO:63	SEQ ID NO: 65	SEQ ID NO: 67	SEQ ID NO: 57
	QVQLVQSGAEVKKPGASVKVSCKASGYSFT	WVKQAPGQGLEWIG	RVTLTIDKSTSTVYMELSSLRSEDTAVYYCAR	WGQGTTVTVSS
Hu18B10_La	SEQ ID NO: 68	SEQ ID NO: 59	SEQ ID NO: 70	SEQ ID NO: 61
	DIVMTQSPDSLAVSLGERATINC	WYQQKPGQPPKLLIY	GVPDRFSGSGSGTDFTLTISSLQAEDVAVYYC	FGGGTKVEIK
Hu18B10_Lb	SEQ ID NO: 69	SEQ ID NO: 59	SEQ ID NO: 71	SEQ ID NO: 61
	DIVMTQSPDSLAVSLGERATMNC	WYQQKPGQPPKLLIY	GVPDRFSGSGSGTDFTLTISSLQAEDVAVYYC	FGGGTKVEIK

[00222] Table 3-2 illustrates sequences of the variable regions of humanized 18B10 antibodies.

[00223] **Table 3-2. Sequences of humanized 18B10**

Antibody chain	Sequences
18B10 HC germline	QVQLVQSGAEVKKPGASVKVSCKASGYTFTSYYMH WVRQAPGQGLEWMGIINPSGGSTSYAQKFQGRVTM TRDTSTSTVYMELSSLRSEDTAVYYCAR **(SEQ ID NO: 23)**

Hu18B10-Ha	QVQLVQSGAEVKKPGASVKVSCKASGYTFTGYNMN WVRQAPGQGLEWMGNIDPYYGGTSYNQKFKGRVT MTIDKSTSTVYMELSSLRSEDTAVYYCARMYHGNAF DYWGQGTTVTVSS **(SEQ ID NO: 25)**
Hu18B10-Hb	QVQLVQSGAEVKKPGASVKVSCKASGYSFTGYNMN WVRQAPGQGLEWMGNIDPYYGGTSYNQKFKGRVTL TIDKSTSTVYMELSSLRSEDTAVYYCARMYHGNAFD YWGQGTTVTVSS **(SEQ ID NO: 27)**
Hu18B10-Hc	QVQLVQSGAEVKKPGASVKVSCKASGYSFTGYNMN WVKQAPGQGLEWIGNIDPYYGGTSYNQKFKGRVTL TIDKSTSTVYMELSSLRSEDTAVYYCARMYHGNAFD YWGQGTTVTVSS **(SEQ ID NO: 29)**
18B10-LC germline	DIVMTQSPDSLAVSLGERATINCKSSQNNKNYLAWY QQKPGQPPKLLIYWASTRESGVPDRFSGSGSGTDFTL TISSLQAEDVAVYYCQQYYSTP **(SEQ ID NO: 24)**
Hu18B10_La	DIVMTQSPDSLAVSLGERATINCKSSQSLLNSGNLKN YLTWYQQKPGQPPKLLIYWASTRKSGVPDRFSGSGS GTDFTLTISSLQAEDVAVYYCQNDYSYPLTFGGGTK VEIK **(SEQ ID NO: 26)**
Hu18B10_Lb	DIVMTQSPDSLAVSLGERATMNCKSSQSLLNSGNLK NYLTWYQQKPGQPPKLLIYWASTRKSGVPDRFTGSG SGTDFTLTISSLQAEDVAVYYCQNDYSYPLTFGGGTK VEIK **(SEQ ID NO: 28)**

[00224] In certain embodiments, the anti-CLDN18.2 radionuclide conjugates provided herein comprises ^{124}I- or ^{123}I- or ^{131}I or ^{89}Zr or ^{177}Lu-labeled 18B10, for example, ^{124}I or ^{89}Zr or ^{177}Lu -labeled humanized 18B10 (for example, as listed in Table 3-2). In certain embodiments, the ^{124}I or ^{89}Zr or ^{177}Lu -labeled humanized 18B10 radionuclide conjugates provided herein comprises: the heavy chain variable region comprises a HCDR1 comprising the sequence of SEQ ID NO: 1, a HCDR2 comprising the sequence of SEQ ID NO: 19, and a

HCDR3 comprising the sequence of SEQ ID NO: 21; and the light chain variable region comprises a LCDR1 comprising the sequence of SEQ ID NO: 14, a LCDR2 comprising the sequence of SEQ ID NO: 16, and a LCDR3 comprising the sequence of SEQ ID NO: 18.

[00225] In certain embodiments, the ^{124}I or ^{89}Zr or ^{177}Lu -labeled humanized 18B10 radionuclide conjugates provided herein comprises:

a heavy chain variable region comprising the sequence of SEQ ID NO: 25 and a light chain variable region comprising the sequence of SEQ ID NO: 26 ("Hu18B10HaLa");
a heavy chain variable region comprising the sequence of SEQ ID NO: 27 and a light chain variable region comprising the sequence of SEQ ID NO: 28 ("Hu18B10HbLb"); or
a heavy chain variable region comprising the sequence of SEQ ID NO: 29 and a light chain variable region comprising the sequence of SEQ ID NO: 26, or 28.

[00226] In certain embodiments, the humanized anti-CLDN18.2 radionuclide conjugates provided herein may comprise the heavy chain variable region fused to the constant region of human IgG1 isotype and the light chain variable region fused to the constant region of human kappa chain.

[00227] In certain embodiments, the anti-CLDN18.2 radionuclide conjugates provided herein further comprise an immunoglobulin constant region, optionally a constant region of human Ig, or optionally a constant region of human IgG. In some embodiments, an immunoglobulin constant region comprises a heavy chain and/or a light chain constant region. The heavy chain constant region comprises CH1, hinge, and/or CH2-CH3 regions. In certain embodiments, the heavy chain constant region comprises an Fc region. In certain embodiments, the light chain constant region comprises Cκ or Cλ.

[00228] In certain embodiments, the anti-CLDN18.2 radionuclide conjugates provided herein comprises a full-length antibody (e.g. humanized 18B10) conjugated to the radionuclide provided herein. In certain embodiments, the anti-CLDN18.2 radionuclide conjugates provided herein comprises an scFv-Fc antibody derived from the humanized 18B10 provided herein(e.g. Hu18B10HaLa), conjugated to the radionuclide provided herein.

[00229] In certain embodiments, the anti-CLDN18.2 radionuclide conjugate is conjugated to ^{89}Zr (for example via a chelator comprising DFO), and such CLDN18.2 radionuclide conjugate does not bind to FcγR. For example, the anti-CLDN18.2 ^{89}Zr conjugate lacks an Fc domain, or comprises an engineered Fc domain that lacks binding to

FcγR. In certain embodiments, the anti-CLDN18.2 radionuclide conjugate is conjugated to ^{177}Lu (for example via a chelator comprising DOTA).

[00230] In certain embodiments, the anti-CLDN18.2 radionuclide conjugates provided herein further comprise a constant region of human IgG1, IgG2, IgG3, or IgG4. In certain embodiments, the anti-CLDN18.2 antibodies and antigen-binding fragments thereof provided herein comprises a constant region of IgG1 isotype. In certain embodiments, the constant region of human IgG1 comprises SEQ ID NO: 49, or a homologous sequence having at least 80% (e.g. at least 85%, 90%, 95%, 96%, 97%, 98%, or 99%) sequence identity thereof.

[00231] The anti-CLDN18.2 antibodies and antigen-binding fragment thereof have been disclosed in a published PCT application WO2021/032157, which is incorporated herein to its entirety. These anti-CLDN18.2 antibodies and antigen-binding fragment thereof have been shown to have strong binding affinity and specificity to human CLDN18.2, and have been shown to bind to a unique epitope on human CLDN18.2. All the binding properties and experimental data for these anti-CLDN18.2 antibodies as disclosed in WO2021/032157 are incorporated herein by reference.

[00232] In certain embodiments, the anti-CLDN18.2 antibodies, antigen-binding fragment thereof, and the anti-CLDN18.2 radionuclide conjugates provided herein has an EC50 value for binding to a human CLDN18.2 (or a mouse CLDN18.2) expressing cell of no more than 70 μg/ml (or no more than 65, 60, 55, 50, 45, 40, 35, 30, 25, 20, 15, 12, or 10, 9, 8, 7, 6, 5, 4, 3, 2, or 1 μg/ml), as measured by flow cytometry assay. In certain embodiments, the anti-CLDN18.2 antibodies, antigen-binding fragment thereof, and the anti-CLDN18.2 radionuclide conjugates provided herein has an EC50 value for binding to a human CLDN18.2 (or a mouse CLDN18.2) expressing cell of no more than 500 nM (or no more than 250, 200, 100, 50, 45, 40, 35, 30, 25, 20, 15, 12, or 10, 9, 8, 7, 6, 5, 4, 3, 2, 1 nM), as measured by flow cytometry assay. In certain embodiments, the anti-CLDN18.2 antibodies, antigen-binding fragment thereof, and the anti-CLDN18.2 radionuclide conjugates provided herein has an EC50 value for binding to a human CLDN18.2 (or a mouse CLDN18.2) expressing cell of no more than 1.0 nM (e.g., no more than 0.8 nM, no more than 0.6 nM, no more than 0.5 nM, no more than 0.4 nM, or no more than 0.3 nM) as measured by ELISA. In certain embodiments, the anti-CLDN18.2 antibodies, antigen-binding fragment thereof, and the anti-CLDN18.2 radionuclide conjugates provided herein specifically bind to a human CLDN18.2 expressing cell at an EC50 value no more than 80%, 70%, 60%, 50%, 40%, 30%, 20%, 15%, 10%, 1%, or 0.1% of that of IMAB362, as measured by flow cytometry assay. In

certain embodiments, the EC50 is determined with NUGC4 cell line, KATOIII cell line, SNU-601 cell line, SNU-620 cell line, or a comparable cell thereof having a human CLDN18.2 protein expression level comparable to or no more than that of NUGC4 cell line, KATOIII cell line, SNU-601 cell line, or SNU-620 cell line, for example, a human CLDN18.2 low-expressing cell line, or a human CLDN18.2 medium-expressing cell line.. In certain embodiments, the EC50 is determined with a human CLDN18.2 high-expressing cell line.

[00233] In certain embodiments, the anti-CLDN18.2 antibodies, antigen-binding fragment thereof, and the anti-CLDN18.2 radionuclide conjugates provided herein has an EC50 value of no more than 5, 4, 3 or 2 μg/ml for binding to a human CLDN18.2 high-expressing cell line or human CLDN18.2 medium-expressing cell line.

[00234] In certain embodiments, the anti-CLDN18.2 antibodies, antigen-binding fragment thereof, and anti-CLDN18.2 antibody conjugates provided herein has an EC50 value for binding to NUGC4 cells of no more than 70 μg/ml (or no more than 65, 60, 55, 50, 45, 40, 35, 30, 25, 20, 15, 12, or 10, 9, 8, 7, 6, 5, 4, 3, 2, or 1 μg/ml), as measured by flow cytometry assay.

[00235] In certain embodiments, the anti-CLDN18.2 radionuclide conjugates provided herein do not bind to CLDN18.1 (e.g. human CLDN18.1 or mouse CLDN18.1).

[00236] In certain embodiments, the anti-CLDN18.2 antibodies, antigen-binding fragment thereof, and anti-CLDN18.2 antibody conjugates provided herein are capable of specifically binding to mouse CLDN18.2 (e.g. a cell expressing mouse CLDN18.2) at an EC50 value no more than 1.5μg/ml as measured by Flow Cytometry. In certain embodiments, the anti-CLDN18.2 radionuclide conjugates provided herein bind to mouse CLDN18.2 at an EC50 of 0.1μg/ml-1.5μg/ml (e.g. 0.1μg/ml-1.2μg/ml, 0.2μg/ml-1μg/ml, 0.5μg/ml-1μg/ml, 0.6μg/ml-1μg/ml, 0.6μg/ml-0.8μg/ml, or 0.67μg/ml) as measured by Flow Cytometry.

[00237] In certain embodiments, the anti-CLDN18.2 antibodies, antigen-binding fragment thereof, and the anti-CLDN18.2 radionuclide conjugates provided herein binds to an epitope comprising at least one or more (e.g. one, two, three or more) of amino acid residues at positions D28, W30, V43, N45, Y46, L49, W50, R51, R55, E56, F60, E62, Y66, L72, L76, V79 and R80 of human CLDN18.2 having the amino acid sequence of SEQ ID NO: 30.

[00238] The term "epitope" as used herein refers to the specific group of atoms or amino acids on an antigen to which an antibody binds. An epitope can include specific amino acids, sugar side chains, phosphoryl or sulfonyl groups that directly contact an antibody. Those skilled in the art will recognize that it is possible to determine, without undue experimentation, if an antibody binds to the same or overlapping or adjacent epitope as the antibody of present disclosure (e.g., hybridoma/chimeric or humanized antibodies 7C12, 11F12, 26G6, 18B10 and any of the chimeric and humanized variant thereof provided herein) by ascertaining whether the two competes for binding to a CLDN18.2 antigen polypeptide.

[00239] The term "compete for binding" as used herein with respect to two antigen-binding proteins (e.g. antibodies), means that one antigen-binding protein blocks or reduces binding of the other to the antigen (e.g., human/mouse CLDN18.2), as determined by a competitive binding assay. Competitive binding assays are well known in the art, include, for example, direct or indirect radioimmunoassay (RIA), direct or indirect enzyme immunoassay (EIA), and sandwich competition assay (see, e.g., Stahli et al., 1983, *Methods in Enzymology* 9:242-253). Typically, such an assay involves the use of purified antigen bound to a solid surface or cells bearing the antigen, an unlabelled test antibody and a labeled reference antibody. Competitive inhibition is measured by determining the amount of label bound to the solid surface or cells in the presence of the test antibody. Usually the test antibody is present in excess. If two antibodies competes for binding to the CLDN18.2, then the two antibodies bind to the same or overlapping epitope, or an adjacent epitope sufficiently proximal to the epitope bound by the other antibody for steric hindrance to occur. Usually, when a competing antibody is present in excess, it will inhibit (e.g., reduce) specific binding of a test antibody to a common antigen by at least 50-55%, 55-60%, 60-65%, 65-70%, 70-75% 75-80%, 80-85%, 85-90% or more.

[00240] In certain embodiments, the epitope or the amino acid residue in the epitope bound by an antibody can be determined by mutating specific residues in the antigen, i.e., CLDN18.2. If an antibody binds to a mutant CLDN18.2 having an amino acid residue mutated, for example to alanine, at significantly reduced level relative to its binding to wild-type CLDN18.2, then this would indicate that the mutated residue is directly involved in the binding of the antibody to CLDN18.2 antigen, or is in close proximity to the antibody when it is bound to the antigen. Such a mutated residue is considered to be within the epitope, and the antibody is considered to specifically bind to an epitope comprising the residue. A significantly reduced level in binding as used herein, means that the binding affinity (e.g.

EC50, Kd, or binding capacity) between the antibody and the mutant CLDN18.2 is reduced by greater than 10%, 20%, 30%, 40%, 50%, 60%, 70%, 80%, 90%, or more, relative to the binding between the antibody and a wild type CLDN18.2. Such a binding measurement can be conducted using any suitable methods known in the art and disclosed herein, for example, without limitation, KinExA assay, and flow cytometry.

[00241] In certain embodiments, the anti-CLDN18.2 antibodies, antigen-binding fragment thereof, and the anti-CLDN18.2 radionuclide conjugates provided herein exhibit significantly lower binding for a mutant CLDN18.2 in which a residue in a wild-type CLDN18.2 is substituted with alanine, and the residue is selected from the group consisting of: D28, W30, V43, N45, Y46, L49, W50, R51, R55, E56, F60, E62, Y66, L72, L76, V79 and R80 of human CLDN18.2 (SEQ ID NO: 30). In certain embodiments, the residue is E56. In certain embodiments, the residue is selected from the group consisting of: W30, L49, W50, R55, and E56. In certain embodiments, the residue is selected from the group consisting of: T41, N45, Y46, R51, F60, E62, and R80. In certain embodiments, the residue is selected from the group consisting of: D28, V43, N45, Y46, Y66, L72, L76, and V79.

[00242] In certain embodiments, the anti-CLDN18.2 antibodies, antigen-binding fragment thereof, and the anti-CLDN18.2 radionuclide conjugates provided herein exhibit at least 80%, 90%, 95% or 99% or more reduction in binding for a mutant CLDN18.2 comprising E56A of human CLDN18.2, relative to the binding between the antibody and a wild type CLDN18.2.

[00243] In certain embodiments, the anti-CLDN18.2 antibodies, antigen-binding fragment thereof, and the anti-CLDN18.2 radionuclide conjugates provided herein exhibit at least 50%, 60%, 70%, 80%, or 90% reduction in binding for a mutant CLDN18.2 comprising one or more mutated residue selected from the group consisting of: W30A, L49A, W50A, R55A, and E56A of human CLDN18.2, relative to the binding between the antibody and a wild type CLDN18.2.

[00244] In certain embodiments, the anti-CLDN18.2 antibodies, antigen-binding fragment thereof, and the anti-CLDN18.2 radionuclide conjugates provided herein exhibit at least 30%, 35%, 40%, 45%, or 50% reduction in binding for a mutant CLDN18.2 comprising one or more mutated residue selected from the group consisting of: D28, V43, N45, Y46, Y66, L72, L76, and V79 of human CLDN18.2, relative to the binding between the antibody and a wild type CLDN18.2.

[00245] In certain embodiments, the anti-CLDN18.2 antibodies, antigen-binding fragment thereof, and the anti-CLDN18.2 radionuclide conjugates provided herein exhibit at least 10%, 15%, 20%, 25%, or 30% reduction in binding for a mutant CLDN18.2 comprising one or more mutated residue selected from the group consisting of: T41A, N45A, Y46A, R51A, F60A, E62A, and R80A of human CLDN18.2, relative to the binding between the antibody and a wild type CLDN18.2.

[00246] In certain embodiments, the anti-CLDN18.2 antibodies, antigen-binding fragment thereof, and the anti-CLDN18.2 radionuclide conjugates provided herein do not bind to A42, and/or N45.

[00247] **ii. Antibody Variants**

[00248] The anti-CLDN18.2 antibodies and antigen-binding fragments thereof in the anti-CLDN18.2 antibody conjugates provided herein also encompass various types of variants of the antibody sequences provided herein.

[00249] In certain embodiments, the variants comprise one or more modification(s) or substitution(s) in 1, 2, or 3 CDR sequences as provided in Table 1, in one or more FR sequences, in the heavy or light chain variable region sequences provided herein, and/or in the constant region (e.g., Fc region). Such antibody variants retain specific binding affinity to CLDN18.2 of their parent antibodies, but have one or more desirable properties conferred by the modification(s) or substitution(s). For example, the antibody variants may have improved antigen-binding affinity, improved glycosylation pattern, reduced risk of glycosylation, reduced deamination, reduced or increased effector function(s), improved FcRn receptor binding, increased pharmacokinetic half-life, pH sensitivity, and/or compatibility to conjugation (e.g., one or more introduced cysteine residues), to name a few.

[00250] **a). Affinity variant**

[00251] An affinity variant retain specific binding affinity to CLDN18.2 of the parent antibody, or even have improved CLDN18.2 specific binding affinity over the parent antibody. Various methods known in the art can be used to achieve this purpose. For example, a library of antibody variants (such as Fab or scFv variants) can be generated and expressed with phage display technology, and then screened for the binding affinity to human CLDN18.2. For another example, computer software can be used to virtually simulate the binding of the antibodies to human CLDN18.2, and identify the amino acid residues on the antibodies which form the binding interface. Such residues may be either avoided in the

substitution so as to prevent reduction in binding affinity, or targeted for substitution to provide for a stronger binding.

[00252] **b). Glycosylation variant**

[00253] The anti-CLDN18.2 antibodies and antigen-binding fragments in the anti-CLDN18.2 antibody conjugates provided herein also encompass a glycosylation variant, which can be obtained to either increase or decrease the extent of glycosylation of the antibody or antigen binding fragment. The term "glycosylation" as used herein, refers to enzymatic process that attaches glycans such as fucose, xylose, mannose, or GlcNAc phosphoserine glycan to proteins, lipids, or other organic molecules. Depending on the carbon linked to the glycan, glycosylation can be divided into five classes including: N-linked glycosylation, O-linked glycosylation, phospho-glycosylation, C-linked glycosylation, and glypiation.

[00254] **c). Cysteine-engineered variant**

[00255] The anti-CLDN18.2 antibodies and antigen-binding fragments in the anti-CLDN18.2 antibody conjugates provided herein also encompass a cysteine-engineered variant, which comprises one or more introduced free cysteine amino acid residues.

[00256] **d). Fc variants**

[00257] The anti-CLDN18.2 antibodies and antigen-binding fragments in the anti-CLDN18.2 antibody conjugates provided herein also encompass an Fc variant, which comprises one or more amino acid residue modifications or substitutions at its Fc region and/or hinge region.

[00258] The humanized variants of the heavy chain and light chain of 18B10 are linked to human IgG1 heavy chain constant region and kappa light chain constant region as shown below:

[00259] Human IgG1 heavy chain constant region (SEQ ID NO: 49):

[00260] ASTKGPSVFPLAPSSKSTSGGTAALGCLVKDYFPEPVTVSWNSGALTSGV HTFPAVLQSSGLYSLSSVVTVPSSSLGTQTYICNVNHKPSNTKVDKKVEPKSCDKTHT CPPCPAPELLGGPSVFLFPPKPKDTLMISRTPEVTCVVVDVSHEDPEVKFNWYVDGV EVHNAKTKPREEQYNSTYRVVSVLTVLHQDWLNGKEYKCKVSNKALPAPIEKTISK AKGQPREPQVYTLPPSRDELTKNQVSLTCLVKGFYPSDIAVEWESNGQPENNYKTTP PVLDSDGSFFLYSKLTVDKSRWQQGNVFSCSVMHEALHNHYTQKSLSLSPGK

[00261] Human Kappa light chain constant region (SEQ ID NO: 50):

[00262] RTVAAPSVFIFPPSDEQLKSGTASVVCLLNNFYPREAKVQWKVDNALQS GNSQESVTEQDSKDSTYSLSSTLTLSKADYEKHKVYACEVTHQGLSSPVTKSFNRGE C

[00263] In certain embodiments, the constant region of the antibodies or antigen-binding fragments thereof provided herein comprises one or more amino acid residue substitutions relative to SEQ ID NO: 49 (i.e. the wild-type sequence), selected from the group consisting of: L235V, F243L, R292P, Y300L, P396L, or any combination thereof.

[00264] **iii. Antigen-binding fragments**

[00265] The anti-CLDN18.2 antibody conjugates provided herein may also comprise anti-CLDN18.2 antigen-binding fragments. Various types of antigen-binding fragments are known in the art and can be developed based on the anti-CLDN18.2 antibodies provided herein, including for example, the exemplary antibodies whose CDR sequences are shown in Tables 1, and their different variants (such as affinity variants, glycosylation variants, Fc variants, cysteine-engineered variants and so on).

[00266] In certain embodiments, an anti-CLDN18.2 antigen-binding fragment provided herein is a diabody, a Fab, a Fab', a F(ab')2, a Fd, an Fv fragment, a disulfide stabilized Fv fragment (dsFv), a (dsFv)2, a bispecific dsFv (dsFv-dsFv'), a disulfide stabilized diabody (ds diabody), a single-chain antibody molecule (scFv), a scFv-Fc antibody, an scFv dimer (bivalent diabody), a multispecific antibody, a camelized single domain antibody, a nanobody, a domain antibody, or a bivalent domain antibody.

[00267] Various techniques can be used for the production of such antigen-binding fragments. Illustrative methods include, enzymatic digestion of intact antibodies (see, e.g., Morimoto et al., Journal of Biochemical and Biophysical Methods 24:107-117 (1992); and Brennan et al., Science, 229:81 (1985)), recombinant expression by host cells such as E. Coli (e.g., for Fab, Fv and ScFv antibody fragments), screening from a phage display library as discussed above (e.g., for ScFv), and chemical coupling of two Fab'-SH fragments to form F(ab')2 fragments (Carter et al., Bio/Technology 10:163-167 (1992)). Other techniques for the production of antibody fragments will be apparent to a skilled practitioner.

[00268] In certain embodiments, the antigen-binding fragment is a scFv. Generation of scFv is described in, for example, WO 93/16185; U.S. Pat. Nos. 5,571,894; and 5,587,458.

scFv may be fused to an effector protein at either the amino or the carboxyl terminus to provide for a fusion protein (see, for example, Antibody Engineering, ed. Borrebaeck).

[00269] In certain embodiments, the anti-CLDN18.2 antibodies and antigen-binding fragments thereof in the anti-CLDN18.2 antibody conjugates provided herein are bivalent, tetravalent, hexavalent, or multivalent. The term "valent" as used herein refers to the presence of a specified number of antigen binding sites in a given molecule. As such, the terms "bivalent", "tetravalent", and "hexavalent" denote the presence of two binding site, four binding sites, and six binding sites, respectively, in an antigen-binding molecule. Any molecule being more than bivalent is considered multivalent, encompassing for example, trivalent, tetravalent, hexavalent, and so on.

[00270] A bivalent molecule can be monospecific if the two binding sites are both specific for binding to the same antigen or the same epitope. This, in certain embodiments, provides for stronger binding to the antigen or the epitope than a monovalent counterpart. Similar, a multivalent molecule may also be monospecific. In certain embodiments, in a bivalent or multivalent antigen-binding moiety, the first valent of binding site and the second valent of binding site are structurally identical (i.e. having the same sequences), or structurally different (i.e. having different sequences albeit with the same specificity).

[00271] A bivalent can also be bispecific, if the two binding sites are specific for different antigens or epitopes. This also applies to a multivalent molecule. For example, a trivalent molecule can be bispecific when two binding sites are monospecific for a first antigen (or epitope) and the third binding site is specific for a second antigen (or epitope).

[00272] **Methods of Using the Anti-CLDN18.2 Radionuclide Conjugates**

[00273] In another aspect, the present disclosure provides methods of using such anti-CLDN18.2 radionuclide conjugates provided herein (in particular those conjugated to a diagnostic radionuclide, and preferably ^{124}I-18B10), for detecting or visualizing CLDN18.2 protein, for diagnosing a subject as having a CLDN18.2 associated disease, for identifying a subject in need as likely to be responsive to a CLDN18.2 targeted therapy, for monitoring progression of a CLDN18.2 associated disease in a subject during a monitoring time period, and for monitoring therapeutic efficacy in a subject having a CLDN18.2 associated disease and having been treated with a therapy for a therapeutic period, among others. In certain embodiments, the anti-CLDN18.2 antibody-radionuclide conjugate comprises an anti-CLDN18.2 antibody-diagnostic radionuclide conjugate.

[00274] The anti- CLDN18.2 antibody radionuclide conjugate provided herein can be used *in vivo* to provide information about (i) presence or expression level of CLDN18.2 protein, (ii) location and/or distribution of CLDN18.2, and (iii) change in expression level or location/distribution of CLDN18.2. Compared with currently available diagnostic methods for CLDN18.2 such as immunohistochemistry (IHC), the antibody radionuclide conjugates provided herein are advantageous in non-invasive treatment, quantifiable, whole body assessment, and repetitive dosing and assessment at multiple time points.

[00275] A "CLDN18.2-associated disease" as used herein refers to any disease or condition caused by, exacerbated by, or otherwise linked to increased or decreased expression or activities of CLDN18.2. In certain embodiments, the CLDN18.2 associated disease is a CLDN18.2 positive tumor or a CLDN18.2 positive non-cancerous lesion (e.g., gastric lesion).

[00276] In certain embodiments, the CLDN18.2 associated condition is cancer. In certain embodiments, the CLDN18.2 associated condition is CLDN18.2-expressing cancer.

[00277] In certain embodiments, the cancer is selected from gastric cancer, pancreatic cancer, cholangiocarcinoma, lung cancer, bronchial cancer, bone cancer, liver and bile duct cancer, breast cancer, liver cancer, ovarian cancer, testicle cancer, kidney cancer, bladder cancer, head and neck cancer, spine cancer, brain cancer, cervix cancer, uterine cancer, endometrial cancer, colon cancer, colorectal cancer, rectal cancer, anal cancer, esophageal cancer, esophageal adenocarcinoma, gastrointestinal cancer, skin cancer, prostate cancer, pituitary cancer, stomach cancer, vagina cancer, thyroid cancer, glioblastoma, astrocytoma, melanoma, myelodysplastic syndrome, sarcoma, teratoma, and adenocarcinoma.

[00278] Other examples of cancers include but are not limited to, non-small cell lung cancer (squamous/nonsquamous), small cell lung cancer, renal cell cancer, colorectal cancer, colon cancer, ovarian cancer, breast cancer (including basal breast carcinoma, ductal carcinoma and lobular breast carcinoma), pancreatic cancer, gastric carcinoma, bladder cancer, esophageal cancer, mesothelioma, melanoma, head and neck cancer, thyroid cancer, sarcoma, prostate cancer, glioblastoma, cervical cancer, thymic carcinoma, melanoma, myelomas, mycoses fungoids, merkel cell cancer, hepatocellular carcinoma (HCC), fibrosarcoma, myxosarcoma, liposarcoma, chondrosarcoma, osteogenic sarcoma, and other sarcomas, synovioma, mesothelioma, Ewing's tumor, leiomyosarcoma, rhabdomyosarcoma, lymphoid malignancy, basal cell carcinoma, adenocarcinoma, sweat gland carcinoma, medullary thyroid carcinoma, papillary thyroid carcinoma, pheochromocytomas sebaceous gland carcinoma, papillary carcinoma, papillary adenocarcinomas, medullary carcinoma,

bronchogenic carcinoma, hepatoma, bile duct carcinoma, choriocarcinoma, Wilms' tumor, cervical cancer, testicular tumor, seminoma, classical Hodgkin lymphoma (CHL), primary mediastinal large B-cell lymphoma, T-cell/histiocyte-rich B-cell lymphoma, acute lymphocytic leukemia, acute myelocytic leukemia, acute myelogenous leukemia, chronic myelocytic (granulocytic) leukemia, chronic myelogenous leukemia, chronic lymphocytic leukemia, polycythemia vera, mast cell derived tumors, EBV-positive and -negative PTLD, and diffuse large B-cell lymphoma (DLBCL), plasmablastic lymphoma, extranodal NK/T-cell lymphoma, nasopharyngeal carcinoma, HHV8-associated primary effusion lymphoma, non-Hodgkin's lymphoma, multiple myeloma, Waldenstrom's macroglobulinemia, heavy chain disease, myelodysplastic syndrome, hairy cell leukemia and myelodysplasia, primary CNS lymphoma, spinal axis tumor, brain stem glioma, astrocytoma, medulloblastoma, craniopharyogioma, ependymoma, pinealoma, hemangioblastoma, acoustic neuroma, oligodendroglioma, menangioma, melanoma, neuroblastoma and retinoblastoma.

[00279] In certain embodiments, the cancer is a CLDN18.2-expressing cancer. "CLDN18.2-expressing cancer" as used herein refers to any cancer or tumor involving cancer cells expressing CLDN18.2 that do not substantively form the classical tight junctions as found in normal epithelial tissue. Such CLDN18.2-expressing cells are amenable to extracellular antibody binding, and therefore can be detected as CLDN18.2-positive. Examples of CLDN18.2-expressing cancer include gastric cancer, esophageal cancer, pancreatic cancer, cholangiocarcinoma, lung cancer such as non-small cell lung cancer (NSCLC) and small cell lung cancer (SCLC), ovarian cancer, colon cancer, colorectal cancer, gastrointestinal stromal tumors (GIST), gastrointestinal carcinoid tumors, rectal cancer, anal cancer, bile duct cancer, small intestine cancer, appendix cancer; prostate cancer, renal cancer (*e.g.*, renal cell carcinoma), hepatic cancer, head-neck cancer, and cancer of the gallbladder and metastases thereof, for example, gastric cancer metastasis such as Krukenberg tumors, peritoneal metastasis and lymph node metastasis.

[00280] In certain embodiments, the CLDN18.2-expressing cancer can be an adenocarcinoma, for example, an advanced adenocarcinoma. In certain embodiments, the cancer is selected from adenocarcinomas of the stomach, the esophagus, the pancreatic duct, the bile ducts, the lung and the ovary. In certain embodiments, the CLDN18.2-expressing cancer comprises a cancer of the stomach, a cancer of the esophagus, in particular the lower esophagus, a cancer of the esogastric junction and gastroesophageal cancer.

[00281] In certain embodiments, the cancer is gastric cancer, ovarian cancer, pancreatic cancer, cholangiocarcinoma, colorectal cancer, lung cancer, or esophageal adenocarcinoma.

[00282] In certain embodiments, the CLDN18.2 associated disease involves a non-cancerous lesion, such as gastric lesion. In certain embodiments, the CLDN18.2 associated disease is gastric ulcer.

[00283] The anti-CLDN18.2 antibody radionuclide conjugates provided herein provided herein may be used with an *in vivo* nuclear imaging modality to visualize the CLDN18.2 protein within the topography of a subject's body. In addition to diagnosing a condition or disease (e.g. cancer) associated with CLDN18.2 expression, the anti-CLDN18.2 antibody radionuclide conjugates provided herein may also be used to diagnose, predict responsiveness to a CLDN18.2 targeted therapy, monitor disease progression, monitor therapeutic efficacy, and so on, in a subject, according to methods provided herein.

[00284] In certain embodiments, the subject is a human. In certain embodiments, the subject is non-human animal. In certain embodiments, the subject has or is suspected of having a CLDN18.2 associated disease. In certain embodiment, the subject has been diagnosed as having a CLDN18.2 associated disease.

[00285] In certain embodiments, the subject has or is suspected of having a CLDN18.2-expressing cancer. In certain embodiments, the subject is at risk of or is suspected of having cancer metastasis.

[00286] In certain embodiments, the subject has not received any CLDN18.2 targeted therapy. Without wishing to be bound by any theory, it is believed that subject having not received any CLDN18.2 targeted therapy is likely to have higher CLDN18.2 expression than those who have been treated with CLDN18.2 targeted therapy. Accordingly, subject having not received any CLDN18.2 targeted therapy is likely to have higher detection signal, for example, in the radionuclide imaging.

[00287] In certain embodiments, the subject has received a CLDN18.2 targeted therapy.

[00288] **Administration of the Anti-CLDN18.2 Radionuclide Conjugate**

[00289] The methods provided herein comprise administering to the subject a detectably effective amount of the anti-CLDN18.2 antibody-radionuclide conjugate provided herein. In certain embodiments, the anti-CLDN18.2 antibody-radionuclide conjugate comprises an anti-CLDN18.2 antibody-diagnostic radionuclide conjugate.

[00290] As described herein, the term "detectably effective amount" with respect to an anti-CLDN18.2 antibody-radionuclide conjugate refers to an amount sufficient to uptake into the CLDN18.2 expressing tissue in the subject, and produce a detectable signal in the subject to yield an acceptable image using a suitable equipment for radionuclide imaging, such as positron emission tomography (PET), single photon emission computed tomography

(SPECT). The term "detectable" with respect to radionuclide imaging, means that the radionuclide signal derived from the imaging equipment can be detected and can be distinguished from the background signal generated by the imaging equipment. In certain embodiments, a detectable signal is significantly different from the background signal, for example, at least about 0.1%, 1%, 3%, 5%, 10%, 15%, 20%, 25%, 30%, or more difference. In certain embodiments, the ratio of a specific signal to background signal is at least 1.5, 2, 2.5, 3, 4, 5 or more.

[00291] A detectably effective amount of anti-CLDN18.2 antibody-radionuclide conjugate can be administered in one injection or alternatively in more than one injection, and may vary according to factors, such as the degree of susceptibility of the individual, the sex, age, and weight of the individual, idiosyncratic responses of the subject. The detectably effective amount may also vary according to instrument and the imaging methodologies used. Optimization of these factors is well known in the art.

[00292] The anti-CLDN18.2 antibody-radionuclide conjugate provided herein can be administered to the subject in any suitable route known in the art, such as for example parenteral (e.g., subcutaneous, intraperitoneal, intravenous, including intravenous infusion, intramuscular, or intradermal injection). Other routes of administration can also be useful, for example, oral, topical, subcutaneous, peritoneal, intra-arterial, inhalation, vaginal, rectal, nasal, intrathecal, or inhalation. In certain embodiments, the anti-CLDN18.2 antibody-radionuclide conjugate provided herein is administered via a venous catheter inserted into the contralateral ulnar vein.

[00293] The anti-CLDN18.2 antibody-radionuclide conjugate provided herein can be administered at a suitable amount of antibody protein, for example, from about 0.1 mg to about 30 mg, from about 0.1 mg to about 20 mg, from about 0.1 mg to about 10 mg, from about 0.1 mg to about 5 mg, from about 0.1 mg to about 3 mg, from about 0.1 mg to about 2 mg of the antibody protein. In certain embodiments, such amount of the antibody protein is administered intravenously, for example, in a single injection or infusion.

[00294] In certain embodiments, the anti-CLDN18.2 antibody-radionuclide conjugate (e.g. ^{124}I-18B10 or ^{89}Zr-18B10 or ^{177}Lu-18B10, or ^{124}I-SF106 or ^{177}Lu-DOTA-SF106) provided herein can be administered to a human in the range from about 0.1 mg to 10 mg per square meter of body surface area of the anti-CLDN18.2 antibody-radionuclide conjugate for the typical adult, for example, as a single bolus injection, although a lower or higher dosage also may be administered as circumstances dictate.

[00295] In certain embodiments, the anti-CLDN18.2 antibody-radionuclide conjugate (e.g. ^{124}I-18B10 or ^{89}Zr-18B10 or ^{177}Lu-18B10, or ^{124}I-SF106 or ^{177}Lu-DOTA-SF106) provided herein can be administered to a human in the range from 0.01 mg to 10 mg, 0.05 mg to 10 mg, 0.1 mg to 5 mg, 0.5 mg to 5 mg, and 0.5 mg to 2mg, for example, as a single bolus injection.

[00296] In certain embodiments, the anti-CLDN18.2 antibody-radionuclide conjugate (e.g. ^{124}I-18B10 or ^{89}Zr-18B10 or ^{177}Lu-18B10 or ^{124}I-SF106 or ^{177}Lu-DOTA-SF106) provided herein can be administered to a human between 0.015 mg/kg of body weight to 1 mg/kg of body weight per day, e.g., between 0.015 mg/kg of body weight to 0.5 mg/kg, e.g., per day, between 0.015 mg/kg of body weight to 0.1 mg/kg of body weight, e.g., per day, between 0.015 mg/kg of body weight to 0.075 mg/kg of body weight, e.g., per day, or between 0.015 mg/kg of body weight to 0.05 mg/kg of body weight, for example, as a single bolus injection.

[00297] Dosage regimens can be adjusted to provide the desired detectable amount for obtaining a clear image of the tissue or cells which uptake the anti-CLDN18.2 antibody-radionuclide conjugate (e.g. ^{124}I-18B10 or ^{89}Zr-18B10 or ^{177}Lu-18B10 or ^{124}I-SF106 or ^{177}Lu-DOTA-SF106) provided herein. In certain embodiments, the amount of anti-CLDN18.2 antibody-radionuclide conjugate (e.g. ^{124}I-18B10 or ^{89}Zr-18B10 or ^{177}Lu-18B10 or ^{124}I-SF106 or ^{177}Lu-DOTA-SF106) provided herein administered into a human subject required for imaging will be determined by the prescribing physician with the dosage generally varying according to the quantity of emission from the radionuclide, so as to obtain an amount which is effective to achieve the desired uptake of the anti-CLDN18.2 antibody-radionuclide conjugate (e.g. ^{124}I-18B10 or ^{89}Zr-18B10 or ^{177}Lu-18B10 or ^{124}I-SF106 or ^{177}Lu-DOTA-SF106) in the cells or tissues of a particular subject, without being toxic to the subject.

[00298] In particular, sufficient care has to be taken about exposure doses to a subject. A saturating dose of anti-CLDN18.2 antibody-radionuclide conjugate (e.g. ^{124}I-18B10 or ^{89}Zr-18B10 or ^{177}Lu-18B10 or ^{124}I-SF106 or ^{177}Lu-DOTA-SF106) may be administered to the patient. For example, the amount of radioactivity of anti-CLDN18.2 antibody-radionuclide conjugate to be administered to a subject may range from 18.5 megabecquerels (MBq) to 370 MBq, from 18.5 MBq to 350 MBq, from 18.5 MBq to 300 MBq, from 18.5 MBq to 250 MBq, from 18.5 MBq to 200 MBq, from 18.5 MBq to 150 MBq, from 18.5 MBq to 125 MBq, or from 18.5 MBq to 100 MBq. Alternatively, the dosage may be measured in millicuries (mCi). In some embodiments, the amount of ^{124}I or ^{89}Zr or ^{177}Lu imaging agent administered for imaging studies in a subject is from 0.1 to 10 mCi, 0.2 to 10 mCi, 0.3 to 10 mCi, 0.4 to 10 mCi, 0.5 to 10 mCi, 0.5 to 7.5 mCi, 0.5 to 5 mCi, 0.5 to 2.5 mCi or 0.5 to 2 mCi. In some embodiments, the detectably effective amount will be the amount of compound sufficient to

produce emissions in the range of from 0.5 to 10 mCi, 0.5 to 7.5 mCi, 0.5 to 5 mCi, 0.5 to 2.5 mCi or 0.5 to 2 mCi. In certain embodiments, an anti-CLDN18.2 antibody-radionuclide conjugate is administered to a human subject in an amount of 0.5 to 10 mCi, 0.5 to 7.5 mCi, 0.5 to 5 mCi, 0.5 to 2.5 mCi or 0.5 to 2 mCi.

[00299] In some embodiments of the anti-CLDN18.2 antibody-radionuclide conjugate is in a composition with a specific activity of 3.0-6.0 GBq/μmol, for example, of 3.0-5.0 GBq/μmol, 3.5-5.0 GBq/μmol, 3.0-4.5 GBq/μmol, or 4.0-4.5 GBq/μmol.

[00300] In certain embodiments, an ^{124}I or ^{89}Zr or ^{177}Lu labeled anti-CLDN18.2 antibody-radionuclide conjugate (e.g. ^{124}I-18B10 or ^{89}Zr-18B10 or ^{177}Lu-18B10 or ^{124}I-SF106 or ^{177}Lu-DOTA-SF106) is administered as a composition comprising 95-99% of the ^{124}I or ^{89}Zr or ^{177}Lu labeled anti-CLDN18.2 antibody-radionuclide conjugate (e.g. ^{124}I-18B10 or ^{89}Zr-18B10 or ^{177}Lu-18B10 or ^{124}I-SF106 or ^{177}Lu-DOTA-SF106), and 1-5%, respectively, of the non-radiolabeled anti-CLDN18.2 antibody-radionuclide conjugate. In certain embodiments, the ratio is 98% of the ^{124}I or ^{89}Zr or ^{177}Lu labeled anti-CLDN18.2 antibody-radionuclide conjugate and 2% of the non-radiolabeled anti-CLDN18.2 antibody-radionuclide conjugate. The purity of the ^{124}I labeled anti-CLDN18.2 antibody-radionuclide can be measured by radio thin layer chromatography (TLC), or radio high performance liquid chromatography (HPLC).

[00301] **<u>Detecting or visualizing CLDN18.2 protein</u>**

[00302] The methods provided herein further comprise conducting radionuclide imaging to the subject to obtain an image.

[00303] Suitable methods of in vivo radionuclide imaging that may be used in accordance with the methods described herein include, but are not limited to, positron emission tomography (PET), and single photon emission computed tomography (SPECT).

[00304] The term "Positron Emission Tomography (PET)" as used herein refers to a nuclear imaging technique used in the medical field to visualize a target tissue or organ or activities. PET measures the two annihilation photons that are produced back-to-back after positron emission from a radionuclide conjugated tracer molecule, which is chosen to mark a specific function in the body on a biochemistry level. PET provides molecular imaging of biological function instead of anatomy. PET allows examination of the patient by producing pictures of many functions of the human body unobtainable by other imaging techniques. After a short-lived positron-emitting radioactive tracer is injected into the subject, it can distribute within the body according to the physiologic pathways associated with the stable

counterparts. When the tracer is a targeting molecule specifically directed to a target of interest, the tracer allows visualization of tissues or organs expressing such a target.

[00305] The term "SPECT" as used herein refers to "Single-Photon Emission Computed Tomography, which is a nuclear medicine tomographic imaging technique using gamma rays. It is similar to conventional nuclear medicine planar imaging using a gamma camera and able to provide true 3D information. This information is typically presented as cross-sectional slices through the patient, but can be freely reformatted or manipulated as required. Injection of a gamma-emitting radionuclide or its conjugate into the subject is needed for the imaging.

[00306] PET may be accompanied by other scanning or imaging techniques for anatomic reference purposes. In certain embodiments, the radionuclide imaging is combined with CT, MRI, ultrasound. In certain embodiments, the radionuclide imaging is combined with a low-dose or diagnostic CT-scan.

[00307] The term "CT" as used herein refers to "Computerized Tomography", which is a noninvasive medical examination or procedure that uses specialized X-ray equipment to produce cross-sectional images of the body. These cross-sectional images are used for a variety of diagnostic and therapeutic purposes. The CT images of internal organs, bones, soft tissue, and blood vessels provide greater clarity and more details than conventional X-ray images, such as a chest X-Ray. Thus, CT is a valuable medical tool that can help to diagnose disease, trauma or abnormality, plan and guide interventional or therapeutic procedures, and monitor the effectiveness of therapy (e.g., cancer treatment). PET/CT combination imager can be used to conduct PET and CT in combination.

[00308] The term "MRI" as used herein refers to "Magnetic Resonance Imaging", which is a medical imaging procedure for making images of the internal structures of the body. MRI scanners use strong magnetic fields and radio waves (radiofrequency energy) to make images. The signal in an MR image comes mainly from the protons in fat and water molecules in the body. MRI is a noninvasive way for a doctor to examine your organs, tissues and skeletal system. It produces high-resolution images of the inside of the body that help diagnose a variety of problems including the abnormalities of the brain and spinal cord, heart and blood vessels, bones and joints, other internal organs and the like.

[00309] Ultrasound imaging uses high-frequency sound waves to view inside the body. Because ultrasound images are captured in real-time, they can also show movement of the body's internal organs as well as blood flowing through the blood vessels. In an ultrasound

exam, a transducer (probe) is placed directly on the skin or inside a body opening. A thin layer of gel is applied to the skin so that the ultrasound waves are transmitted from the transducer through the gel into the body. The strength (amplitude) of the sound signal and the time it takes for the wave to travel through the body provide the information necessary to produce an image. Ultrasound imaging is an ideal medical tool that can help to visualize abdominal tissues and organs, assess bone fragility, view the heart and the like.

[00310] The subject is scanned by a radionuclide imaging system to obtain an image. In general, the subject can be positioned in the PET camera, and images can be acquired by scanning the subject for an amount of time appropriate for the particular radionuclide being used.

[00311] The subject is exposed to radionuclide imaging at a subsequent time point after the administration of the anti-CLDN18.2 antibody-radionuclide conjugate.

[00312] In certain embodiments, the radionuclide imaging is conducted at least 2 hours after the administration of the anti-CLDN18.2 antibody-radionuclide conjugate (e.g. ^{124}I-18B10 or ^{89}Zr-18B10 or ^{177}Lu-18B10 or ^{124}I-SF106 or ^{177}Lu-DOTA-SF106) to the subject. In certain embodiments, the radionuclide imaging is conducted at a time point between 2 hours and 144 hours, between 12 hours and 144 hours, or preferably between 24 hours and 144 hours, between 24 hours and 120 hours, or between 24 hours and 96 hours after the administration of the anti-CLDN18.2 antibody-radionuclide conjugate (e.g. ^{124}I-18B10 or ^{89}Zr-18B10 or ^{177}Lu-18B10 or ^{124}I-SF106 or ^{177}Lu-DOTA-SF106) to the subject. In any of the above embodiments, the radionuclide imaging is conducted once, twice, three times or more at different time points between 2 hours and 144 hours, between 12 hours and 144 hours, or preferably between 24 hours and 144 hours, between 24 hours and 120 hours, or between 24 hours and 96 hours after the administration of the anti-CLDN18.2 antibody-radionuclide conjugate to the subject. For example, the radionuclide imaging may be conducted one or more times at the 2nd hour, the 24th hour, the 48th four, and/or the 96th hour, respectively, after the administration of the anti-CLDN18.2 antibody-radionuclide conjugate to the subject. The subject can rest from 24 hours to 96 hours (e.g., 36 hours, 48 hours, 60 hours, 72 hours, 84 hours, or 96 hours) after the administration of the anti-CLDN18.2 antibody-radionuclide conjugate, before being subject to a radionuclide detection.

[00313] In certain embodiments, the radionuclide imaging is conducted to a site of interest of the subject. In some embodiments, the site of interest is a site expressing or suspected of expressing claudin 18.2.

[00314] In some embodiments, the site of interest has or is suspected of having tumor. In some embodiments, the site of interest can be whole body, torso, head, or limbs.

[00315] **Determining or Visualizing Presence of the Claudin18.2 Protein**

[00316] In certain embodiments, methods provided herein further comprise determining or visualizing presence of the CLDN18.2 protein in a site of interest of the subject from the image, wherein the presence and/or location of the radionuclide conjugate above background is indicative of the presence and/or location of the CLDN18.2 protein.

[00317] The anti-CLDN18.2 antibody-radionuclide conjugate provided herein can bind to CLDN18.2-expressing tissues and cells, thereby allowing detection or visualization of such CLDN18.2-expressing tissues and cells based on the bound radionuclide signal, or in other words, radionuclide uptake.

[00318] Radionuclide imaging (such as PET imaging) with the anti-CLDN18.2 antibody-radionuclide conjugate provided herein can be used to qualitatively or quantitatively detect CLDN18.2 protein.

[00319] For quantification of radionuclide uptake, the clinician may visually identify one or more lesion of interest (e.g. a tumor lesion or a gastric lesion or a suspected metastatic lesion) on a PET or CT scan and determine a region-of-interest (ROI) around these lesions. Uptake of the anti-CLDN18.2 antibody-radionuclide conjugate (e.g. ^{124}I-18B10 or ^{89}Zr-18B10 or ^{177}Lu-18B10, or ^{124}I-SF106 or ^{177}Lu-DOTA-SF106, the radio tracer) in these ROI's may be corrected for body weight and injected dose and quantified as standardized uptake value (SUV). SUV refers to the ratio of the concentration of radionuclide in a volume of tissue in microcuries of injected agent per volume to concentration in the body if uniformly distributed (determined by a standard body phantom). The SUV has no units. An SUV of 1.0 is achieved in any tissue volume when the count rate is equal to the count rate of the uniformly distributed activity in the body phantom. The results are usually normalized to body weight. For calculation of the SUV, circular regions of interest can be drawn around areas of interest (e.g. tumor primary site or metastatic lesions) in transaxial slices and adapted to a three-dimensional volume of interest (VOI).

[00320] In certain embodiments, the maximum standardized uptake value (SUVmax) is measured for the suspected lesions. In certain embodiments, the SUVmax can be the SUV with the highest value within a volume of interest.

[00321] In certain embodiments, the mean standardized uptake value (SUVmean) is measured for certain tissues or organs, for example, normal tissues or organs.

[00322] The presence and/or location of the radionuclide uptake above background is indicative of the presence and/or location of the CLDN18.2 protein.

[00323] Tomographic images are obtained through image reconstruction. For determining the distribution of radiotracer, ROIs may be drawn on the reconstructed image including, but not limited to, the stomach, peritoneum, lungs, liver, heart, kidney, lymph nodes, ovary, bone, pancreas, intestines, skin, or other organs and tissue (e.g., cancer tissue). Radiotracer uptakes over time in these regions are used to generate time activity curves (TAC) at the various dosing paradigms examined. Data may be expressed as radioactivity per unit time per unit volume (μci/cc/mCi injected dose).

[00324] There are two types of PET procedures, involving static tracer imaging or dynamic tracer imaging. Static tracer imaging involves obtaining single time point estimates of tracer uptake or static imaging that provides a spatial map of regional tracer concentration. With static imaging, only an average value is measured (e.g. Standardized Uptake Value, SUV). Dynamic tracer imaging, on the other hand, can provide considerably more information about in vivo biology by delineating both the temporal and spatial pattern of tracer uptake. See, e.g., Muzi et al. Magn Reson Imaging. 2012 30(9): 1203-1215. The anti-CLDN18.2 antibody-radionuclide conjugate, such as ^{124}I-18B10, may be used in either static tracer imaging or dynamic tracer imaging.

[00325] The methods provided herein have a wide range of uses in preclinical settings and also in clinical settings, including without limitation, detecting or visualizing CLDN18.2 protein (e.g. direct visualization of in vivo saturation of CLDN18.2 protein), diagnosing a condition or disease (e.g. cancer) associated with CLDN18.2 expression, quantifying CLDN18.2 expressing tissue or diseased tissue; predicting responsiveness to a CLDN18.2 targeted therapy, monitoring disease progression or tumor metastasis, or monitoring therapeutic efficacy over time, monitoring resistance over time, or monitoring uptake in normal tissues to anticipate toxicity or patient to patient variation and so on, in a subject, according to methods provided herein.

[00326] **<u>Methods for Detection or Visualization</u>**

[00327] Described herein are methods of detecting or visualizing CLDN18.2 protein at a site of interest in a subject, comprising:

a) administering to the subject a detectably effective amount of an anti-CLDN18.2 antibody-radionuclide conjugate; and

b) conducting radionuclide imaging to the subject at a subsequent time point after the administration of the anti-CLDN18.2 antibody-radionuclide conjugate to obtain an image; and

c) determining or visualizing presence of the claudin18.2 protein in the site of interest of the subject from the image,

wherein the presence and/or location of the radionuclide conjugate above background is indicative of the presence and/or location of the CLDN18.2 protein.

[00328] In certain embodiments, the anti-CLDN18.2 antibody-radionuclide conjugate comprises an anti-CLDN18.2 antibody-diagnostic radionuclide conjugate.

[00329] In certain embodiments, the subject has not been treated with, or is not receiving CLDN18.2 targeted therapy.

[00330] In certain embodiments, the method further comprises administering a therapeutically effective amount of CLDN18.2 targeted therapy to the subject identified as having presence of the CLDN18.2 protein in the site of interest.

[00331] In certain embodiments, the CLDN18.2 targeted therapy comprises a therapy that specifically targets CLDN18.2 or CLDN18.2-expressing cells (i.e. cells that abnormally expressing CLDN18.2 in a manner that do not substantively form the classical tight junctions as found in normal epithelial tissue). The CLDN18.2 targeted therapy comprises a therapy selected from the group consisting of: an anti-CLDN18.2 antibody therapy, a CLDN18.2 targeted compound, a CLDN18.2 targeted nucleic acid therapy, a CLDN18.2 targeted peptide, a CLDN18.2 targeted cell therapy, and a CLDN18.2 targeted gene therapy. In certain embodiments, the anti-CLDN18.2 antibody therapy comprises a monoclonal anti-CLDN18.2 antibody, a multi-specific antibody targeting CLDN18.2 and a second antigen, and/or an antibody drug conjugate (ADC) targeting CLDN18.2. In certain embodiments, the anti-CLDN18.2 antibody therapy comprises a therapeutic radionuclide-conjugated anti-CLDN18.2 antibody conjugate, comprising an anti-CLDN18.2 antibody provided herein, conjugated to a therapeutic radionuclide, such as for example, ^{111}In, ^{111m}In, ^{177}Lu, ^{212}Bi, ^{213}Bi, ^{211}At, ^{62}Cu, ^{64}Cu, ^{67}Cu, ^{90}Y, ^{125}I, ^{131}I, ^{32}P, ^{33}P, ^{47}Sc, ^{111}Ag, ^{67}Ga, ^{142}Pr, ^{153}Sm, ^{161}Tb, ^{166}Dy, ^{166}Ho, ^{186}Re, ^{188}Re, ^{189}Re, ^{212}Pb, ^{223}Ra, ^{225}Ac, ^{59}Fe, ^{75}Se, ^{77}As, ^{89}Sr, ^{99}Mo, ^{105}Rh, ^{109}Pd, ^{143}Pr, ^{149}Pm, ^{169}Er, ^{194}Ir, ^{198}Au, ^{199}Au, ^{199}Au, and ^{211}Pb. In certain embodiments, the anti-CLDN18.2 antibody therapy comprises a therapeutic radionuclide-conjugated anti-CLDN18.2 antibody conjugate, comprising an anti-CLDN18.2 antibody provided herein, conjugated to ^{177}Lu.

[00332] In certain embodiments, the therapeutic radionuclide is the same as the diagnostic radionuclide. In certain embodiments, both the therapeutic radionuclide and the diagnostic radionuclide are ^{177}Lu. In certain embodiments, the anti-CLDN18.2 antibody-diagnostic radionuclide conjugate is identical to the anti-CLDN18.2 antibody-therapeutic radionuclide (for example, the radionuclides are identical, the sequences of the anti-CLDN18.2 antibodies or antigen-binding fragments thereof are identical, and/or the conjugation sites are identical). In certain embodiments, the therapeutically effective amount is at least 100%, 150%, 200%, 300%, 400%, 500%, 600%, 700%, 800%, 900%, or 1000% of the detectably effective amount.

[00333] **Methods for Diagnosis**

[00334] Described herein are methods of diagnosing a subject as having a CLDN18.2 associated disease, methods of identifying a subject in need as likely be responsive to a CLDN18.2 targeted therapy, methods of monitoring progression of a CLDN18.2 associated disease in a subject during a monitoring time period, methods of monitoring therapeutic efficacy in a subject having a CLDN18.2 associated disease and having been treated with a therapy for a therapeutic period, and kits for use in the above-mentioned methods. In certain embodiments, the anti-CLDN18.2 antibody-radionuclide conjugate comprises an anti-CLDN18.2 antibody-diagnostic radionuclide conjugate.

[00335] In one aspect, provided herein is a method of diagnosing a subject as having a CLDN18.2 associated disease. In certain embodiments, the method comprising: administering to the subject an effective amount of the anti-CLDN18.2 antibody-radionuclide conjugate provided herein; conducting radionuclide imaging to the subject at a subsequent time point after the administration of the anti-CLDN18.2 antibody-radionuclide conjugate to obtain an image; diagnosing the CLDN18.2 associated disease in the subject based on presence/or location of the CLDN18.2 protein in the site of interest of the subject as determined from the image; wherein the presence and/or location of the radionuclide uptake above background is indicative of the presence and/or location of the CLDN18.2 protein. In certain embodiments, the anti-CLDN18.2 antibody-radionuclide conjugate comprises an anti-CLDN18.2 antibody-diagnostic radionuclide conjugate.

[00336] Presence and/or location of the radionuclide uptake above background can be determined qualitatively or quantitatively. As described in preceding sections, radionuclide uptake can be quantified using SUVmax or SUVmean.

[00337] In certain embodiments, the level of the radionuclide uptake at the site of interest is compared with a corresponding a reference level to determine difference from the reference level.

[00338] In certain embodiments, the reference level can be the radionuclide uptake level at a non-diseased tissue or a normal tissue, for example, a muscle tissue. In some other embodiments, the reference level can be the radionuclide uptake level at same type of tissue but is non-diseased (and therefore does not known to express CLDN18.2). Such a reference level can be empirical or arbitrary.

[00339] In certain embodiments, if the difference is statistically significant, or if the difference reaches a predetermined threshold, then the subject can be diagnosed as having the CLDN18.2 associated disease.

[00340] In certain embodiments, the reference level can be the radionuclide uptake level at a standard confirmed lesion. A standard confirmed lesion can be a lesion that has been confirmed to have CLDN18.2 expression by other methods such immunohistochemistry (IHC) methods. In certain embodiments, the standard confirmed lesion is of the same type of tissue as the tissue of interest. By comparing with such a reference level of radionuclide uptake level at a standard confirmed lesion, it is possible to estimate the level (i.e. high, medium, or low) of CLDN18.2 protein at the site of interest in the subject.

[00341] In certain embodiments, the subject has not been treated with, or is not receiving CLDN18.2 targeted therapy. Without wishing to be bound by any theory, it is surprisingly found that in comparison with a subject having received a CLDN18.2 targeted therapy, the subject not yet received a CLDN18.2 targeted therapy shows much higher signal (e.g. SUV) in the radionuclide imaging. Therefore, the radionuclide imaging methods provided herein can be particularly useful for diagnosing CLDN18.2 associated disease in a subject that has not been treated with, or is not receiving CLDN18.2 targeted therapy.

[00342] In certain embodiments, the method further comprises administering a therapeutically effective amount of CLDN18.2 targeted therapy to the subject diagnosed as having a CLDN18.2 associated disease.

[00343] In certain embodiments, the CLDN18.2 targeted therapy comprises a therapy that specifically targets CLDN18.2 or CLDN18.2-expressing cells (i.e. cells that abnormally expressing CLDN18.2 in a manner that do not substantively form the classical tight junctions as found in normal epithelial tissue). The CLDN18.2 targeted therapy comprises a therapy selected from the group consisting of: an anti-CLDN18.2 antibody therapy, a CLDN18.2 targeted compound, a CLDN18.2 targeted nucleic acid therapy, a CLDN18.2 targeted peptide,

a CLDN18.2 targeted cell therapy, and a CLDN18.2 targeted gene therapy. In certain embodiments, the anti-CLDN18.2 antibody therapy comprises a monoclonal anti-CLDN18.2 antibody, a multi-specific antibody targeting CLDN18.2 and a second antigen, and/or an antibody drug conjugate (ADC) targeting CLDN18.2. In certain embodiments, the anti-CLDN18.2 antibody therapy comprises a therapeutic radionuclide-conjugated anti-CLDN18.2 antibody conjugate, comprising an anti-CLDN18.2 antibody provided herein, conjugated to a therapeutic radionuclide, such as for example, ^{111}In, ^{111m}In, ^{177}Lu, ^{212}Bi, ^{213}Bi, ^{211}At, ^{62}Cu, ^{64}Cu, ^{67}Cu, ^{90}Y, ^{125}I, ^{131}I, ^{32}P, ^{33}P, ^{47}Sc, ^{111}Ag, ^{67}Ga, ^{142}Pr, ^{153}Sm, ^{161}Tb, ^{166}Dy, ^{166}Ho, ^{186}Re, ^{188}Re, ^{189}Re, ^{212}Pb, ^{223}Ra, ^{225}Ac, ^{59}Fe, ^{75}Se, ^{77}As, ^{89}Sr, ^{99}Mo, ^{105}Rh, ^{109}Pd, ^{143}Pr, ^{149}Pm, ^{169}Er, ^{194}Ir, ^{198}Au, ^{199}Au, ^{199}Au, and ^{211}Pb. In certain embodiments, the anti-CLDN18.2 antibody therapy comprises a therapeutic radionuclide-conjugated anti-CLDN18.2 antibody conjugate, comprising an anti-CLDN18.2 antibody provided herein, conjugated to ^{177}Lu.

[00344] In certain embodiments, the therapeutic radionuclide is the same as the diagnostic radionuclide. In certain embodiments, both the therapeutic radionuclide and the diagnostic radionuclide are ^{177}Lu. In certain embodiments, the anti-CLDN18.2 antibody-diagnostic radionuclide conjugate is identical to the anti-CLDN18.2 antibody-therapeutic radionuclide (for example, the radionuclides are identical, the sequences of the anti-CLDN18.2 antibodies or antigen-binding fragments thereof are identical, and/or the conjugation sites are identical). In certain embodiments, the therapeutically effective amount is at least 100%, 150%, 200%, 300%, 400%, 500%, 600%, 700%, 800%, 900%, or 1000% of the detectably effective amount.

[00345] In certain embodiments, the anti-CLDN18.2 antibody-diagnostic radionuclide conjugate and the anti-CLDN18.2 antibody-t radionuclide conjugate

[00346] **Methods for Prognosis**

[00347] In another aspect, provided herein is a method of identifying a subject in need as likely be responsive to a CLDN18.2 targeted therapy. In certain embodiments, the method comprising: administering to the subject an effective amount of an anti-CLDN18.2 antibody-radionuclide conjugate; conducting radionuclide imaging to the subject at a subsequent time point after the administration of the anti-CLDN18.2 antibody-radionuclide conjugate to obtain an image; identifying the subject as likely to respond to the CLDN18.2 targeted therapy based on presence/or location of the CLDN18.2 protein in the site of interest of the subject as determined from the image, wherein the presence and/or location of the radionuclide conjugate above background is indicative of the presence and/or location of the

CLDN18.2 protein. In certain embodiments, the anti-CLDN18.2 antibody-radionuclide conjugate comprises an anti-CLDN18.2 antibody-diagnostic radionuclide conjugate.

[00348] Presence and/or location of the radionuclide uptake above background can be determined qualitatively or quantitatively. As described in preceding sections, radionuclide uptake can be quantified using SUVmax or SUVmean.

[00349] In certain embodiments, the level of the radionuclide conjugate at the site of interest is compared with a corresponding reference level to determine difference from the reference level. In certain embodiments, the methods further comprise identifying the subject as likely to respond to the CLDN18.2 targeted therapy when the difference is statistically significant, or when the different reaches a predetermined threshold.

[00350] These identified subjects may be recommended to take additional tests to confirm the conclusion.

[00351] In certain embodiments, the method further comprises administering a therapeutically effective amount of CLDN18.2 targeted therapy to the subject identified as likely to be responsive.

[00352] In certain embodiments, when the subject is identified as not likely to respond to the CLDN18.2 targeted therapy, the method further comprises recommending not to be treated with the CLDN18.2 targeted therapy.

[00353] In certain embodiments, the CLDN18.2 targeted therapy comprises a therapy that specifically targets CLDN18.2 or CLDN18.2-expressing cells (i.e. cells that abnormally expressing CLDN18.2 in a manner that do not substantively form the classical tight junctions as found in normal epithelial tissue). The CLDN18.2 targeted therapy comprises a therapy selected from the group consisting of: an anti-CLDN18.2 antibody therapy, a CLDN18.2 targeted compound, a CLDN18.2 targeted nucleic acid therapy, a CLDN18.2 targeted peptide, a CLDN18.2 targeted cell therapy, and a CLDN18.2 targeted gene therapy. In certain embodiments, the anti-CLDN18.2 antibody therapy comprises a monoclonal anti-CLDN18.2 antibody, a multi-specific antibody targeting CLDN18.2 and a second antigen, and/or an antibody drug conjugate (ADC) targeting CLDN18.2. In certain embodiments, the anti-CLDN18.2 antibody therapy comprises a therapeutic radionuclide-conjugated anti-CLDN18.2 antibody conjugate, comprising an anti-CLDN18.2 antibody provided herein, conjugated to a therapeutic radionuclide, such as for example, ^{111}In, ^{111m}In, ^{177}Lu, ^{212}Bi, ^{213}Bi, ^{211}At, ^{62}Cu, ^{64}Cu, ^{67}Cu, ^{90}Y, ^{125}I, ^{131}I, ^{32}P, ^{33}P, ^{47}Sc, ^{111}Ag, ^{67}Ga, ^{142}Pr, ^{153}Sm, ^{161}Tb, ^{166}Dy, ^{166}Ho, ^{186}Re, ^{188}Re, ^{189}Re, ^{212}Pb, ^{223}Ra, ^{225}Ac, ^{59}Fe, ^{75}Se, ^{77}As, ^{89}Sr, ^{99}Mo, ^{105}Rh, ^{109}Pd, ^{143}Pr, ^{149}Pm, ^{169}Er, ^{194}Ir, ^{198}Au, ^{199}Au, ^{199}Au, and ^{211}Pb. In certain embodiments, the anti-CLDN18.2

antibody therapy comprises a therapeutic radionuclide-conjugated anti-CLDN18.2 antibody conjugate, comprising an anti-CLDN18.2 antibody provided herein, conjugated to ^{177}Lu. In certain embodiments, the therapeutic radionuclide is the same as the diagnostic radionuclide. In certain embodiments, both the therapeutic radionuclide and the diagnostic radionuclide are ^{177}Lu. In certain embodiments, the anti-CLDN18.2 antibody-diagnostic radionuclide conjugate is identical to the anti-CLDN18.2 antibody-therapeutic radionuclide. In certain embodiments, the therapeutically effective amount is at least 100%, 150%, 200%, 300%, 400%, 500%, 600%, 700%, 800%, 900%, or 1000% of the detectably effective amount.

[00354] In certain embodiments, the CLDN18.2 targeted cell therapy comprises a chimeric antigen receptor (CAR) T cell, TCR T cell, or CAR NK cell that targets CLDN18.2. Chimeric antigen receptors (CARs) are engineered chimeric receptors that combine an antigen-binding domain (for example of an antibody) with one or more signaling domains for immune cell activation. Immune cells such as T cells and Nature Killer (NK) cells can be genetically engineered to express CARs. T cells expressing a CAR are referred to as CAR-T cells. CAR can mediate antigen-specific cellular immune activity in the T cells, enabling the CAR-T cells to eliminate cells (e.g. tumor cells) expressing the targeted antigen (e.g. CLDN18.2).

[00355] The CLDN18.2 targeted therapy can specifically bind to CLDN18.2 and exert therapeutic actions on the CLDN18.2-expressing cells such as cancer cells. In certain embodiments, the CLDN18.2 targeted therapy can specifically kill CLDN18.2-expressing cells.

[00356] **Methods of Monitoring Disease Progression**

[00357] In another aspect, provided herein is a method of monitoring progression of a CLDN18.2 associated disease in a subject during a monitoring time period. In certain embodiments, the method comprises: administering to the subject a detectably effective amount of an anti-CLDN18.2 antibody-radionuclide conjugate after the monitoring time period; conducting radionuclide imaging to the subject at a subsequent time point after the administration of the anti-CLDN18.2 antibody-radionuclide conjugate to obtain a post-monitor image; and comparing the post-monitor image with a pre-monitor image, to determine change in the level of the CLDN18.2 protein during the monitoring time period from the image, wherein the level of the radionuclide conjugate above background is indicative of the level of the CLDN18.2 protein, wherein the change is indicative of presence or absence of disease progression. In certain embodiments, the anti-CLDN18.2 antibody-

radionuclide conjugate comprises an anti-CLDN18.2 antibody-diagnostic radionuclide conjugate.

[00358] In certain embodiments, the pre-monitor image is obtained from the subject before the monitoring time period by: administering with the effective amount of the anti-CLDN18.2 antibody-radionuclide conjugate, followed by conducting radionuclide imaging to the subject at a subsequent time point after the administration of the anti-CLDN18.2 antibody-radionuclide conjugate to obtain the pre-monitor image.

[00359] In certain embodiments, increase in the CLDN18.2 level during the monitoring time period is indicative of disease progression, and absence of the increase in the CLDN18.2 level during the monitoring time period is indicative of absence of disease progression.

[00360] In certain embodiments, the subject has not been treated with, or is not receiving CLDN18.2 targeted therapy. In certain embodiments, the subject has been treated with, or is receiving CLDN18.2 targeted therapy.

[00361] In certain embodiments, the disease is tumor.

[00362] In certain embodiments, the progression is metastasis of the tumor. In certain embodiments, the presence of metastasis is indicated by spread of CLDN18.2 expression to a site where CLDN18.2 expression is previously not detectable.

[00363] In certain embodiments, the level of the CLDN18.2 protein comprises amount, distribution and/or location of the CLDN18.2 protein.

[00364] In certain embodiments, the subject is at risk of metastasis.

[00365] **Methods of Monitoring Therapeutic Efficacy**

[00366] In another aspect, provided herein is a method of monitoring therapeutic efficacy in a subject having a CLDN18.2 associated disease and having been treated with a therapy for a therapeutic period. In certain embodiments, the method comprises:

a) administering to the subject a detectably effective amount of an anti-CLDN18.2 antibody-radionuclide conjugate after the therapeutic period;

b) conducting radionuclide imaging to the subject at a subsequent time point after the administration of the anti-CLDN18.2 antibody-radionuclide conjugate to obtain a post-treatment image; and

c) comparing the post-treatment image with a pre-treatment image, to determine change in the level of the CLDN18.2 protein during the therapeutic period from the image, wherein the level of the radionuclide conjugate above background is indicative of the level of the CLDN18.2 protein,

wherein the change is indicative of presence or absence of therapeutic efficacy.

[00367] In certain embodiments, the anti-CLDN18.2 antibody-radionuclide conjugate comprises an anti-CLDN18.2 antibody-diagnostic radionuclide conjugate.

[00368] In certain embodiments, the pre-treatment image is obtained from the subject before the therapeutic period by: administering with the effective amount of the anti-CLDN18.2 antibody-radionuclide conjugate, followed by conducting radionuclide imaging to the subject at a subsequent time point after the administration of the anti-CLDN18.2 antibody-radionuclide conjugate to obtain the pre-treatment image.

[00369] In certain embodiments, increase in the CLDN18.2 level during the therapeutic period is indicative of absence of therapeutic efficacy or poor therapeutic efficacy, and/or wherein absence of the increase in the CLDN18.2 level during the therapeutic period is indicative of presence of therapeutic efficacy or positive therapeutic efficacy.

[00370] In certain embodiments, the therapy can be any therapeutic agent useful for treating the CLND18.2 associated disease. In certain embodiments, the CLDN18.2 associated disease is cancer. In certain embodiments, the CLDN18.2 associated disease is gastric cancer, ovarian cancer, pancreatic cancer, or cholangiocarcinoma.

[00371] For example, the therapy can be an anti-cancer drug, or a drug that treats gastric diseases such as gastric ulcer.

[00372] Examples of anti-cancer drug include, without limitation, a chemotherapeutic agent, an anti-cancer drug, radiation therapy, an immunotherapy agent, anti-angiogenesis agent, a targeted therapy agent, a cellular therapy agent, a gene therapy agent, a hormonal therapy agent, or cytokines.

[00366] The term "immunotherapy" as used herein, refers to a type of that stimulates immune system to fight against disease such as cancer or that boosts immune system in a general way. Immunotherapy includes passive immunotherapy by delivering agents with established tumor-immune reactivity (such as effector cells) that can directly or indirectly mediate anti-tumor effects and does not necessarily depend on an intact host immune system (such as an antibody therapy or CAR-T cell therapy). Immunotherapy can further include active immunotherapy, in which treatment relies on the *in vivo* stimulation of the endogenous host immune system to react against diseased cells with the administration of immune response-modifying agents.

[00367] Examples of immunotherapy include, without limitation, checkpoint modulators, adoptive cell transfer, cytokines, oncolytic virus and therapeutic vaccines.

[00368] Checkpoint modulators can interfere with the ability of cancer cells to avoid immune system attack, and help the immune system respond more strongly to a tumor. Immune checkpoint molecule can mediate co-stimulatory signal to augment immune response, or can mediate co-inhibitory signals to suppress immune response. Examples of checkpoint modulators include, without limitation, modulators of PD-1, PD-L1, PD-L2, CLTA-4, TIM-3, LAG3, A2AR, CD160, 2B4, TGF β, VISTA, BTLA, TIGIT, LAIR1, OX40, CD2, CD27, CD28, CD30, CD40, CD122, ICAM-1, IDO, NKG2C, SLAMF7, SIGLEC7, NKp80, CD160, B7-H3, LFA-1, 1COS, 4-1BB, GITR, BAFFR, HVEM, CD7, LIGHT, IL-2, IL-15, CD3, CD16 and CD83.

[00369] Adoptive cell transfer, which is a treatment that attempts to boost the natural ability of the T cells to fight cancer. In this treatment, T cells are taken from the patient, and are expanded and activated in vitro. In certain embodiments, the T cells are modified *in vitro* to CAR-T cells. T cells or CAR-T cells that are most active against the cancer are cultured in large batches *in vitro* for 2 to 8 weeks. During this period, the patients will receive treatments such as chemotherapy and radiation therapy to reduce the body's immunity. After these treatments, the *in vitro* cultured T cells or CAR-T cells will be given back to the patient. In certain embodiments, the immunotherapy is CAR-T therapy.

[00370] Cytokine therapy can also be used to enhance tumor antigen presentation to the immune system. The two main types of cytokines used to treat cancer are interferons and interleukins. Examples of cytokine therapy include, without limitation, interferons such as interferon-α, -β, and –γ, colony stimulating factors such as macrophage-CSF, granulocyte macrophage CSF, and granulocyte-CSF, insulin growth factor (IGF-1), vascular endothelial growth factor (VEGF), transforming growth factor (TGF), fibroblast growth factor (FGF), interleukins such as IL-1, IL-1α, IL-2, IL-3, IL-4, IL-5, IL-6, IL-7, IL-8, IL-9, IL-10, IL-11, and IL-12, tumor necrosis factors such as TNF-α and TNF-β or any combination thereof.

[00371] Oncolytic virus are genetically modified virus that can kill cancer cells. Oncolytic virus can specifically infect tumor cells, thereby leading to tumor cell lysis followed by release of large amount of tumor antigens that trigger the immune system to target and eliminate cancer cells having such tumor antigens. Examples of oncolytic virus include, without limitation, talimogene laherparepvec.

[00372] Therapeutic vaccines work against cancer by boosting the immune system's response to cancer cells. Therapeutic vaccines can comprise non-pathogenic microorganism

(e.g. *Mycobacterium bovis* Bacillus Calmette-Guérin, BCG), genetically modified virus targeting a tumor cell, or one or more immunogenic components. For example, BCG can be inserted directly into the bladder with a catheter and can cause an immune response against bladder cancer cells.

[00373] Anti-angiogenesis agent can block the growth of blood vessels that support tumor growth. Some of the anti-angiogenesis agent target VEGF or its receptor VEGFR. Examples of Anti-angiogenesis agent include, without limitation, Axitinib, Bevacizumab, Cabozantinib, Everolimus, Lenalidomide, Lenvatinib mesylate, Pazopanib, Ramucirumab, Regorafenib, Sorafenib, Sunitinib, Thalidomide, Vandetanib, and Ziv-aflibercept.

[00374] "Targeted therapy" is a type of therapy that acts on specific molecules associated with cancer, such as specific proteins that are present in cancer cells but not normal cells or that are more abundant in cancer cells, or the target molecules in the cancer microenvironment that contributes to cancer growth and survival. Targeted therapy targets a therapeutic agent to a tumor, thereby sparing of normal tissue from the effects of the therapeutic agent.

[00375] Targeted therapy can target, for example, tyrosine kinase receptors and nuclear receptors. Examples of such receptors include, erbB1 (EGFR or HER1), erbB2 (HER2), erbB3, erbB4, FGFR, platelet-derived growth factor receptor (PDGFR), and insulin-like growth factor-1 receptor (IGF-1R), estrogen receptors (ERs), nuclear receptors (NR) and PRs.

[00376] Targeted therapy can target molecules in tyrosine kinase or nuclear receptors signaling cascade, such as, Erk and PI3K/Akt, AP-2α, AP-2β, AP-2γ, mitogen-activated protein kinase (MAPK), PTEN, p53, p19ARF, Rb, Apaf-1, CD-95/Fas, TRAIL-R1/R2, Caspase-8, Forkhead, Box 03A, MDM2, IAPs, NF-kB, Myc, P13K, Ras, FLIP, heregulin (HRG) (also known as gp30), Bcl-2, Bcl-xL, Bax, Bak, Bad, Bok, Bik, Blk, Hrk, BNIP3, BimL, Bid, and EGL-1.

[00377] Targeted therapy can also target tumor-associated ligands such estrogen, estradiol (E2), progesterone, oestrogen, androgen, glucocorticoid, prolactin, thyroid hormone, insulin, P70 S6 kinase protein (PS6), Survivin, fibroblast growth factors (FGFs), EGF, Neu Differentiation Factor (NDF), transforming growth factor alpha (TGF-α), IL-1A, TGF-beta, IGF-1, IGF-II, IGFBPs, IGFBP proteases, and IL-10.

[00378] In certain embodiments, the therapy can be a CLDN18.2 targeted therapy as provided herein. In certain embodiments, the CLDN18.2 targeted therapy comprises a

therapy selected from the group consisting of: an anti-CLDN18.2 antibody therapy, a CLDN18.2 targeted compound, a CLDN18.2 targeted nucleic acid therapy, a CLDN18.2 targeted peptide, a CLDN18.2 targeted cell therapy, and a CLDN18.2 targeted gene therapy.

[00379] In certain embodiments, the method further comprises increasing the dose of the therapy or discontinuing the therapy when poor therapeutic efficacy is determined.

[00380] In certain embodiments, the method further comprises recommending the subject continuing the therapy when positive therapeutic efficacy is determined.

[00381] In certain embodiments, the therapy comprises a CLDN18.2 targeted therapy.

[00382] In certain embodiments, the method further comprises recommending the subject switching to a therapy other than a CLDN18.2 targeted therapy when post-treatment CLDN18.2 level is below a corresponding reference level. In certain embodiments, the method further comprises recommending the subject switching to a therapy other than a CLDN18.2 targeted therapy when post-treatment CLDN18.2 level decreased by at least 40% (or at least 50%, 60%, 70%, 80%, 90% or 95%) relative to the pre-treatment CLDN18.2 level.

[00383] In certain embodiments, the therapy is not a CLDN18.2 targeted therapy.

[00384] In certain embodiments, the site of interest has or is suspected of a tumor or a gastric lesion. In certain embodiments, the site of interest is whole body. In certain embodiments, the tumor comprises metastasis originated therefrom.

[00385] In certain embodiments, the subject is at risk of metastasis.

[00386] **Pharmaceutical Composition**

[00387] The present disclosure further provides pharmaceutical compositions comprising an anti-CLDN18.2 antibody conjugate provided herein and one or more pharmaceutically acceptable carriers. In certain embodiments, the anti-CLDN18.2 antibody-radionuclide conjugate has at least one of the following characteristics: a) having a radiochemical purity of at least 90% (e.g., at least 91%, at least 92%, at least 93%, at least 94%, at least 95%, at least 96%, at least 97%, at least 98% or at least 99%); b) having a radiolabeling rate of at least 70% (e.g., at least 75%, at least 80%, at least 85%, at least 90%, at least 92%, at least 94%, at least 95%, at least 96%, at least 97%, at least 98%, or at least 99%,); and c) capable of specifically binding to CLDN18.2 at a Kd value of no more than 15nM (e.g., no more than 14nM, no more than 13nM, no more than 12nM, no more than 10nM, no more than 8nM, no more than 6nM, no more than 4nM, or no more than 4nM); and d) capable of specifically binding to CLDN18.2 at an EC50 value of no more than 1.0 nM (e.g., no more than 0.8 nM, no more than 0.6 nM, no more than 0.5 nM, no more than 0.4 nM, or no more than 0.3 nM) as measured by ELISA.

[00388] In certain embodiments, the anti-CLDN18.2 antibody-radionuclide conjugate comprises a therapeutic radionuclide selected from the group consisting of: ^{111}In, ^{111m}In, ^{177}Lu, ^{212}Bi, ^{213}Bi, ^{211}At, ^{62}Cu, ^{64}Cu, ^{67}Cu, ^{90}Y, ^{125}I, ^{131}I, ^{32}P, ^{33}P, ^{47}Sc, ^{111}Ag, ^{67}Ga, ^{142}Pr, ^{153}Sm, ^{161}Tb, ^{166}Dy, ^{166}Ho, ^{186}Re, ^{188}Re, ^{189}Re, ^{212}Pb, ^{223}Ra, ^{225}Ac, ^{59}Fe, ^{75}Se, ^{77}As, ^{89}Sr, ^{99}Mo, ^{105}Rh, ^{109}Pd, ^{143}Pr, ^{149}Pm, ^{169}Er, ^{194}Ir, ^{198}Au, ^{199}Au, ^{199}Au, and ^{211}Pb, or a diagnostic radionuclide selected from the group consisting of: ^{18}F, ^{32}P, ^{33}P, ^{45}Ti, ^{47}Sc, ^{52}Fe, ^{59}Fe, ^{62}Cu, ^{64}Cu, ^{67}Cu, ^{67}Ga, ^{68}Ga, ^{75}Sc, ^{77}As, ^{86}Y, ^{90}Y, ^{89}Sr, ^{89}Zr, ^{94}Tc, ^{94}Tc, ^{99m}Tc, ^{99}Mo, ^{105}Pd, ^{105}Rh, ^{111}Ag, ^{111} ln, ^{123}l, ^{124}l, ^{125}l, ^{131} l, ^{142}Pr, ^{143}Pr, ^{149}Pm, ^{153}Sm, $^{154"1581}$Gd, ^{161}Tb, ^{166}Dy, ^{166}Ho, ^{169}Er, ^{175}Lu, ^{177}Lu, ^{186}Re, ^{188}Re, ^{189}Re, ^{194}lr, ^{198}Au, ^{199}Au, ^{211} At, ^{211} Pb, ^{212}Bi, ^{212}Pb, ^{213}Bi, ^{223}Ra and ^{225} Ac.

[00389] In certain embodiments, the therapeutic radionuclide is ^{177}Lu or ^{124}I. In certain embodiments, the diagnostic radionuclide is ^{124}I, ^{89}Zr or ^{177}Lu. In certain embodiments, the anti-CLDN18.2 antibody-radionuclide conjugate further comprises a chelator. In certain embodiments, the chelator is DFO or DOTA. In certain embodiments, the chelator is DFO, and the radionuclide is ^{89}Zr. In certain embodiments, the chelator is DOTA, and the radionuclide is ^{177}Lu. In certain embodiments, when the radionuclide is ^{89}Zr, the chelator conjugated to a bifunctional linker reagent is *p*–isothiocyanatobenzyl-desferrioxamine (p-NCS-Bz-DFO):

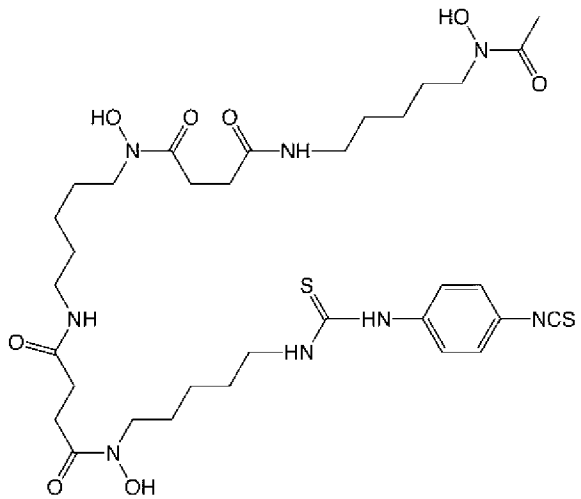

[00390]

[00391] In certain embodiments, when the radionuclide is ^{177}Lu, the anti-CLDN18.2 antibody-radionuclide conjugate comprises a compound portion of Formula (II):

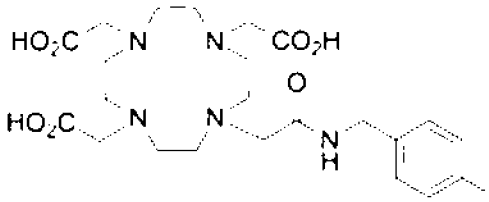

[00392]

[00393] In certain embodiments, the composition comprises ^{89}Zr and a compound of Formula (I):

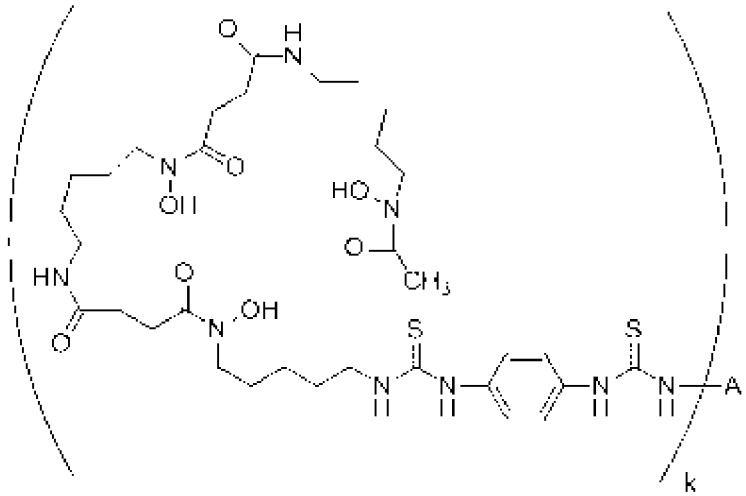

[00394] , wherein A is an anti-CLDN18.2 antibody or antigen-binding fragment thereof provided herein, k is from 1-40 (e.g., 3-5, 5-35, 10-30, 15-25, or 20).

[00395] In certain embodiments, the pharmaceutical compositions provided herein are suitable for parenteral administration, for example, suitable for bolus, intravenous, or intra-tumor injection. In certain embodiments, the pharmaceutical compositions are in a unit dosage injectable form.

[00396] Pharmaceutical acceptable carriers for use in the pharmaceutical compositions disclosed herein may include, for example, pharmaceutically acceptable liquid, gel, or solid carriers, aqueous vehicles, nonaqueous vehicles, antimicrobial agents, isotonic agents, buffers, antioxidants, anesthetics, suspending/dispending agents, sequestering or chelating agents, diluents, adjuvants, excipients, or non-toxic auxiliary substances, other components known in the art, or various combinations thereof.

[00397] Suitable components may include, for example, antioxidants, fillers, binders, disintegrants, buffers, preservatives, lubricants, flavorings, thickeners, coloring agents,

emulsifiers or stabilizers such as sugars and cyclodextrins. Suitable antioxidants may include, for example, methionine, ascorbic acid, EDTA, sodium thiosulfate, platinum, catalase, citric acid, cysteine, thioglycerol, thioglycolic acid, thiosorbitol, butylated hydroxanisol, butylated hydroxytoluene, and/or propyl gallate. As disclosed herein, inclusion of one or more antioxidants such as methionine in a composition comprising an antibody or antigen-binding fragment and conjugates as provided herein decreases oxidation of the antibody or antigen-binding fragment. This reduction in oxidation prevents or reduces loss of binding affinity, thereby improving antibody stability and maximizing shelf-life. Therefore, in certain embodiments compositions are provided that comprise one or more antibody conjugates as disclosed herein and one or more antioxidants such as methionine.

[00398] To further illustrate, pharmaceutical acceptable carriers may include, for example, aqueous vehicles such as sodium chloride injection, Ringer's injection, isotonic dextrose injection, sterile water injection, or dextrose and lactated Ringer's injection, nonaqueous vehicles such as fixed oils of vegetable origin, cottonseed oil, corn oil, sesame oil, or peanut oil, antimicrobial agents at bacteriostatic or fungistatic concentrations, isotonic agents such as sodium chloride or dextrose, buffers such as phosphate or citrate buffers, antioxidants such as sodium bisulfate, local anesthetics such as procaine hydrochloride, suspending and dispersing agents such as sodium carboxymethylcelluose, hydroxypropyl methylcellulose, or polyvinylpyrrolidone, emulsifying agents such as Polysorbate 80 (TWEEN-80), sequestering or chelating agents such as EDTA (ethylenediaminetetraacetic acid) or EGTA (ethylene glycol tetraacetic acid), ethyl alcohol, polyethylene glycol, propylene glycol, sodium hydroxide, hydrochloric acid, citric acid, or lactic acid. Antimicrobial agents utilized as carriers may be added to pharmaceutical compositions in multiple-dose containers that include phenols or cresols, mercurials, benzyl alcohol, chlorobutanol, methyl and propyl p-hydroxybenzoic acid esters, thimerosal, benzalkonium chloride and benzethonium chloride. Suitable excipients may include, for example, water, saline, dextrose, glycerol, or ethanol. Suitable non-toxic auxiliary substances may include, for example, wetting or emulsifying agents, pH buffering agents, stabilizers, solubility enhancers, or agents such as sodium acetate, sorbitan monolaurate, triethanolamine oleate, or cyclodextrin.

[00399] In certain embodiments, the pharmaceutical compositions are formulated into an injectable composition. The injectable pharmaceutical compositions may be prepared in any conventional form, such as for example liquid solution, suspension, emulsion, or solid forms suitable for generating liquid solution, suspension, or emulsion. Preparations for injection may include sterile and/or non-pyretic solutions ready for injection, sterile dry soluble

products, such as lyophilized powders, ready to be combined with a solvent just prior to use, including hypodermic tablets, sterile suspensions ready for injection, sterile dry insoluble products ready to be combined with a vehicle just prior to use, and sterile and/or non-pyretic emulsions. The solutions may be either aqueous or nonaqueous.

[00400] In certain embodiments, unit-dose parenteral preparations are packaged in an ampoule, a vial or a syringe with a needle. All preparations for parenteral administration should be sterile and not pyretic, as is known and practiced in the art.

[00401] In certain embodiments, the anti-CLDN18.2 antibody-radionuclide conjugates is formulated into parenteral compositions in dosage unit form for ease of administration and uniformity of dosage. Dosage unit form as used herein refers to physically discrete units suited as unitary dosages for the subjects to which the anti-CLDN18.2 antibody-radionuclide conjugate is to be administered. The specification for the dosage unit forms described herein are dictated by and directly dependent on (a) the unique characteristics of the anti-CLDN18.2 antibody in the antibody-radionuclide conjugate; (b) the tissue or cells to be targeted; (c) the limitations inherent in the imaging technology used.

[00402] In certain embodiments, a sterile, lyophilized powder is prepared by dissolving an antibody or antigen-binding fragment as disclosed herein in a suitable solvent. The solvent may contain an excipient which improves the stability or other pharmacological components of the powder or reconstituted solution, prepared from the powder. Excipients that may be used include, but are not limited to, water, dextrose, sorbital, fructose, corn syrup, xylitol, glycerin, glucose, sucrose or other suitable agent. The solvent may contain a buffer, such as citrate, sodium or potassium phosphate or other such buffer known to those of skill in the art at, in one embodiment, about neutral pH. Subsequent sterile filtration of the solution followed by lyophilization under standard conditions known to those of skill in the art provides a desirable formulation. In one embodiment, the resulting solution will be apportioned into vials for lyophilization. Each vial can contain a single dosage or multiple dosages of the anti-CLDN18.2 antibody conjugate or composition thereof. Overfilling vials with a small amount above that needed for a dose or set of doses (e.g., about 10%) is acceptable so as to facilitate accurate sample withdrawal and accurate dosing. The lyophilized powder can be stored under appropriate conditions, such as at about 4 °C to room temperature.

[00403] Reconstitution of a lyophilized powder with water for injection provides a formulation for use in parenteral administration. In one embodiment, for reconstitution the sterile and/or non-pyretic water or other liquid suitable carrier is added to lyophilized powder.

The precise amount depends upon the selected therapy being given and can be empirically determined.

[00404] **Kits**

[00405] In another aspect, the present disclosure further provides one or more reagents useful in any of the methods as described herein. The reagents can include the anti-CLDN18.2 antibody-radionuclide conjugates.

[00406] In another aspect, the present disclosure provides kits for use in the methods described above. Typically, the kit contain reagents useful in any of the methods provided herein in a carrier or compartmentalized container. The carrier can be a container or support, in the form of, e.g., bag, box, tube, rack, and is optionally compartmentalized.

[00407] In certain embodiments, the kits can further comprise a standard negative control, and/or a standard positive control.

[00408] In addition, the kits may include instructional materials containing directions (i.e., protocols) for the practice of the methods provided herein. While the instructional materials typically comprise written or printed materials they are not limited to such.

[00409] The following examples are provided to better illustrate the claimed invention and are not to be interpreted as limiting the scope of the invention. All specific compositions, materials, and methods described below, in whole or in part, fall within the scope of the present invention. These specific compositions, materials, and methods are not intended to limit the invention, but merely to illustrate specific embodiments falling within the scope of the invention. One skilled in the art may develop equivalent compositions, materials, and methods without the exercise of inventive capacity and without departing from the scope of the invention. It will be understood that many variations can be made in the procedures herein described while still remaining within the bounds of the present invention. It is the intention of the inventors that such variations are included within the scope of the invention.

EXAMPLES

[00410] While the disclosure has been particularly shown and described with reference to specific embodiments (some of which are preferred embodiments), it should be understood by those having skill in the art that various changes in form and detail may be made therein without departing from the spirit and scope of the present disclosure as disclosed herein.

[00411] **Example 1**

[00412] *Example 1.1 Background*

[00413] Claudin 18.2 (CLDN18.2) is specifically expressed in differentiated gastric mucosal epithelial cells but not expressed in the gastric stem cell region, and the loose structure of the interstitial space of cancer cells makes it possible for CLDN18.2 to be exposed to protein macromolecular drugs, which support it as a reliable target for lesion detecting and clinical implications in epithelial tumors, especially in digestive system neoplasms. However, there is no predicting technology for accurately whole body mapping the CLDN18.2 expression in patient till now.

[00414] Preclinical experiments of murine antibody 5C9 illustrated that novel CLDN18.2-targeted probes may be used as a supplement in clinical routine helping locate tumors, and guide surgery of CLDN18.2-positive tumors via various means (14). Our previous study also indicates that the ^{124}I-labeled antibody ^{124}I-18B10 has good radio-chemical characteristics and stability and was cumulated in CLDN18.2-positive tumors specifically (15). Most recently, we conducted phase 1 trial interim results using Claudin18.2-specific CAR T cells in gastrointestinal cancer patients (12), interim results indicate heavily pretreated, CLDN18.2-positive digestive system cancer patients receive promising efficacy.

[00415] Therefore, an open-label, single center, single-arm, first in human, phase 0 trial was sponsored to investigate the safety, whole-body distributions/dosimetry and CLDN18.2 targeting ability in patient and explore its primary relationship with patient outcome before and after anti-CLDN18.2 therapy.

[00416] Here the present invention reports the outcomes from a non-prespecified interim results of this ongoing trails (NCT04883970). We established a detectable CLDN18.2 targeting radioactive probe (^{124}I-18B10) with high specificity and sensitivity, which performed in the first-in-human study of ^{124}I-18B10 PET/CT and PET/MR in patients with gastric cancer, pancreatic cancer or cholangiocarcinoma. ^{124}I-18B10 is safe and feasible to indicates CLDN18.2 overexpression tumor lesions using PET functional imaging.

[00417] The primary goal of the study was to assess safety of ^{124}I-18B10 tracer and feasibility of map a whole body CLDN18.2 expression using PET functional imaging.

[00418] The secondary goal of the study was to detect lesion using 18F-FDG and novel ^{124}I-18B10 PET molecular imaging technology.

[00419] The study of ^{124}I-18B10 PET imaging was performed in cancer patients that have received or would receive CLDN18.2 targeted treatment. We hypothesis that patients with strong expression degree of CLDN18.2 may achieve more clinical benefits.

[00420] *Example 1.2 Preclinical and Patients*

[00421] The ^{124}I-18B10 probe was synthesized manually using the Hu18B10-Ha and Hu18B10-La (i.e. SEQ ID NOs: 25 and SEQ ID NO: 26), and preclinical experiments including binding affinity and specific targeting ability were conducted after testing in vitro and in vivo model cells and/or mice.

[00422] Digestive system neoplasms patients with pathologically confirmed were enrolled as in an ongoing, open-label, single-arm, first in human (FiH) Phase 0 trial (NCT04883970). ^{124}I-18B10 PET/CT or PET/MR and ^{18}F-FDG PET were undertaken within one week.

[00423] Uptake of ^{124}I-18B10 and ^{18}F-FDG in lesions were calculated as maximum standardized uptake value (SUVmax) and compared with the tumor lesion's CLDN immunohistochemistry and normal organ uptake was calculated as SUVmean. Tumor response was assessed according to (i)RECIST v1.1.

[00424] *Example 1.3 Results*

[00425] ^{124}I-18B10 was successfully constructed over 95% radiochemical yield. The results of preclinical experiments showed its high stability in saline and remains high affinity in CLDN18.2 over-expressing cells (Kd = 4.11 nM), and specific uptake in tumors of the model mice.

[00426] 17 patients including 12 gastric cancers, 4 pancreatic cancers, and 1 cholangiocarcinoma (phase 0) were enrolled. And the optimal time-point for PET scanning was selected to 48h-96h. As indicated by semi-quantifications of PET, ^{124}I-18B10 displayed high uptake in spleen and liver with mean SUVmean of 2.52±1.38 and 1.85±0.65 respectively, slight uptake in bone marrow, lung, gastric and pancreas with SUVmean of 0.83±0.41, 0.48±0.20, 1.2±0.80 and 0.77±0.12 respectively.

[00427] A total of 65 lesions in 17 patients were analyzed. The tracer uptake in tumor lesions of SUVmax ranged from 0.4 to 19.5. Compared with lesions treated by CLDN18.2 targeted therapy, the ^{124}I-18B10 uptake was significantly higher in the lesions that had not been treated by the CLDN18.2 targeted therapy (SUVmax 24h: 6.00 ± 7.38 vs 2.37 vs 1.43, P = 0.042). After undertaking regional ^{124}I-18B10 PET/MR in two patients with gastric cancers, the metastatic lymph nodes showed high signal on T2WI sequence and high tracer uptake.

[00428] *Example 1.4 Conclusions*

[00429] 1.^{124}I-18B10 was successfully prepared and remains high binding affinity and CLDN18.2 target specific in pre-clinical studies.

[00430] 2. ^{124}I-18B10 is the FiH CLDN18.2 PET tracer which remains safety with acceptable dosimetry and clearly indicates the most CLDN18.2 over-expression lesions.

[00431] 3. The tumor lesions showed different levels of uptake of the tracer.

[00432] Example 2 Study Design

[00433] The objective of the present invention is to evaluate the biodistribution, the safety and dosimetry of a single-dose injection of ^{124}I-18B10 for PET/CT or PET/MR imaging patients.

[00434] To investigate the uptake of ^{124}I-18B10 in tumor lesions and its relationship with patient outcome. The clinical study was approved by the Ethics Committee of Peking University Cancer Hospital (2021KT57) and was registered on ClinicalTrial.gov (NCT04883970).

[00435] (1) The primary goal of the study is to map a whole body CLDN18.2 expression.

[00436] (2) The secondary goal is to detect lesion using ^{18}F-FDG and novel ^{124}I-18B10 PET molecular imaging technology.

[00437] (3) The study of ^{124}I-18B10 PET imaging were performed in cancer patients that have received or will receive CLDN18.2 targeting treatment.

[00438] Example 3 Construction of ^{124}I-18B10 and Preclinical Study

[00439] ***Example 3.1 Production, quality control and in vitro experiments of ^{124}I-18B10***

[00440] *Example 3.1.1 Production and Quality Control of ^{124}I-18B10*

[00441] The CLDN18.2 antibody used in the study was provided by Suzhou Transcenta Therapeutics co., LTD (SuZhou, China). ^{124}I was produced and purified by the Cyclotron team of Nuclear Medicine Department of Peking University Cancer Hospital. The radiolabeling and quality control methods of ^{124}I-18B10 were indicated as follows.

[00442] ^{124}I-18B10 was prepared by NBS reaction: 0.8 mL 0.1M pH7.2 PB buffer, 0.1 mL (29.2mg/mL)Hu18B10HaLa monoclonal antibody solution (prepared with H_2O) and 36 μg NBS were added to 1.0 mL 59.2 KBq/μL Na^{124}I solution in turn, and cultured at 37℃ for 60 s, then 0.1 mL 10% human serum albumin was added to terminate the reaction; the final reaction solution was purified by PD-10 column to obtain the target product.

[00443] Before use, the PD-10 column was first equilibrated with 0.01 M pH 7.4 PBS solution, 5 mL PBS was added each time, the column was dried at the gravity flow rate, repeating 5 times; then the target product was purified with 0.01 M pH 7.4 PBS solution.

[00444] Radio-TLC and Radio-HPLC were used to determine the radiolabeling rate and radiochemical purity. Radio-TLC detection: 2 μL free Na^{124}I with radioactivity of 37-74 kBq (1-2 μCi) and purified ^{124}I-18B10 were added to 20 μL of saturated EDTA. 2 μL above solution was dropped 1 cm from the bottom of Xinhua No.1 filter paper and placed in the normal saline development system. After complete development, the filter paper was taken

out and dried for Radio-TLC detection. Radio-HPLC detection: 2 μL free $Na^{124}I$ with radioactivity of 37-74 kBq (1-2 μCi) and purified ^{124}I-18B10 were diluted into 50 μL 0.01M pH 7.4 PBS for Radio-HPLC analysis. Analysis conditions: Agilent Bio SEC-3 gel filtration/volume exclusion chromatography column, flow rate 1 mL/min, mobile phase 0.01 M pH 7.4 PBS.

[00445] The ^{124}I-18B10 was synthesized with radiochemical purity and yield over 95%. Detailed information about quality control of ^{124}I-18B10 can be found in Figure 9. The stability within 48 h of the ^{124}I-18B10 in PBS was evidenced (Figure 7A).

[00446] *Example 3.1.2 Cellular Uptake and Saturation Binding Studies of ^{124}I-18B10*

[00447] The cells uptake experiment was performed by adding ^{124}I-18B10 (20 μL, 37 kBq, 1.37×10-7 M) to wells (n=4) containing MKN45CLDN18.2+ and MKN45 cells as experiment group and negative control, respectively. And 124I-IgG (immunoglobulin G) was added in MKN45CLDN18.2+ as a control. The mixture was incubated in a 5% CO2 incubator at 37°C for 10, 30, 60 and 120 min, collected in 2-mL tubes, centrifuged at 2000 rpm for 3 min and washed with 1 mL of cold PBS (pH 7.4, 0.01 M) twice (the supernatant was removed after each centrifugation). For the blocking control, 60 μg of 18B10 in 10 μL of PBS (pH 7.4, 0.01 M) was added to wells (n=4) containing MKN45CLDN18.2+ cells, and the mixture was incubated in a 5% CO2 incubator at 37°C for 2 h, followed by the steps described above.

[00448] A saturation binding experiment was conducted to determine the binding potency between ^{124}I-18B10 and CLDN18.2. ^{124}I-18B10 was added to wells (n = 4) containing MKN45CLDN18.2+ cells with six concentration gradients, 0 kBq, 0.037 kBq, 0.37 kBq, 3.7 kBq, 37 kBq and 370 kBq, in 50 μL per well. The mixture was treated as mentioned above after incubation in a 5% CO_2 incubator at 37°C for 4 h. The value of the binding constant Kd was calculated according to the fitting curve of the summarized data.

[00449] The radioactivity of the cells and the total added radioactivity were counted using the γ-counter. The percentage of cell uptake was calculated as cell counts/total added counts. The final results of four independent parallel experiments are expressed as the mean ± standard deviation (SD).

[00450] The results of cellular uptake experiments showed that the uptake of ^{124}I-18B10 in MKN45CLDN18.2+ cells increased with time (from 20.08 ± 0.83% at 10 min to 23.51 ± 0.47% at 120 min). As a comparison, a significant down was observed in the MKN45 group (from 3.31 ± 0.54% at 10 min to 8.69 ± 0.35% at 120 min). The uptake of positive cells was

significantly higher than that of negative cells or blocking control at each selected time point ($p<0.0001$) (Figure 7B).

[00451] The binding constant (Kd = 4.11 nM) of ^{124}I-18B10 to CLDN18.2 receptors was also determined by a cell saturation binding assay using MKN45CLDN18.2+ cells (Figure 7C). These results demonstrated the targeting and specific binding of ^{124}I-18B10 to CLDN18.2-positive cells.

[00452] **Example 3.2 ^{124}I-18B10 Micro-PET/CT Functional Imaging and IHC Analysis**

[00453] *Example 3.2.1 Model Mice Construction and Biodistribution*

[00454] All of the animal experiments were performed in compliance with the guidelines established by the Peking University Cancer Hospital Animal Care and Use Committee.

[00455] *Gastric Ulcer Mice Model:*

[00456] Fifteen female KM mice (18-22g) were fasted for 24 hours, 10 of them were given 0.15 ml/mice with absolute ethanol by gavage, and the other 5 mice as blank control.

[00457] *PDX (patient-derived xenograft) Mice Models:*

[00458] PDX mice models were established by engrafting biopsied human gastric cancer tissue subcutaneously into flanks of 6-week-old female NOD/SCID mice (Vital River, China). When the tumor volume reaches over 150 mm^3, mice were randomized into groups (5-6 mice per group) for further experiments. The tumor volume and mice body weight were measured every 3 days. Tumor volume (length × width2)/2 was used to calculate tumor growth inhibition rate (TGI%).

[00459] *Biodistribution Study of ^{124}I-18B10:*

[00460] BALB/c female nude mice (20 g, four weeks old) purchased from Vital River (China) were intravenously injected with 200 μL of ^{124}I-18B10 (0.37-0.74 MBq) via the tail vein. The mice were sacrificed after isoflurane anesthesia at 2, 24, 60 h and 120 h post-injection. The main organs, including the heart, liver, spleen, lung, kidneys, stomach, intestines, muscle, bone, brain and blood, were collected, weighed and measured for radioactivity using the γ-counter. As a standard, ten samples of 1% injected dose were removed and measured. The results are expressed as the percent of injected dose per gram (%ID/g).

[00461] The biodistribution study in normal mice (n = 4) illustrated decreases with time in all tissues, which showed no specific for the probe in normal organs (Figure 7D). Blood occupied the top place and fall fast among all tested tissues (from 22.45 ± 6.24 %ID/g at 2 h to 8.89 ± 0.18 %ID/g at 120 h).

[00462] *Example 3.2.2 Micro-PET/CT imaging and IHC*

[00463] Small-animal PET imaging was performed with micro-PET/CT (Super Nova PET/CT, PINGSENG, Shanghai, China).

[00464] ^{124}I-18B10 Micro-PET/CT imaging was performed on gastric ulcer and normal (n = 5 per group) at 0, 4, 24, 48, and 96 h after gavage. At each imaging time point, a mouse in parallel group was sacrificed by cervical dislocation, the whole stomach was removed, the gastric ulcer was observed with the naked eye after the contents were removed. The samples were sectioned for IHC and HE staining to detect the changes of CLDN18.2 expression and the degree of gastric injury before and after gavage.

[00465] When the tumor volumes were estimated to be 400-900 mm^3, the mice were used for small-animal PET imaging. Under isoflurane inhalation, CLDN18.2 positive or negative PDX mice (n=4 per group) were injected intravenously with 200 μL of 5.55 MBq ^{124}I-18B10 for Micro-PET imaging. Scans were performed at 2, 60, and 120 h after administration. And 5.55 MBq ^{124}I-IgG was injected into as control (n=4), also, ^{124}I-18B10 was injected into CLDN18.2 low expression PDX mice as a negative control. And the milicounts/second values of regions of interest (ROIs) over the tumor were collected.

[00466] *Micro-PET Scan of Gastric Ulcer Models:*

[00467] Since no specific uptake was found in the normal stomach (whether mouse or human) with high CLDN18.2 expression in previous imaging, we used ethanol gavage to construct an acute gastric ulcer model to verify whether the gastric ulcer lesions may uptake more ^{124}I-18B10 tracer.

[00468] Imaging showed that high gastric uptake was observed within 4 h after gavage (2.53±0.27 at 4 h and 2.98±0.24 at 24 h), and the uptake gradually decreased with the gradual healing of gastric injury (Figure 8A). No death was found in the gavage mice, and the feeding and defecation were normal.

[00469] After autopsy, it was found that the gastric body showed local redness, there were different degrees of spotting bleeding, and the gastric body was congested (Figure 8B).

[00470] IHC data indicated that CLDN18.2 was expressed at the same level in gastric mucosa before and after injury (++ for normal stomach vs ++ at 0 h, ++ at 4 h, ++ at 24 h, ++ at 48 h, + at 96 h). In addition, it can be seen from the HE results that there was no obvious damage in the gastric tissue at all the time points except 4h after gavage (Figure 8C).

[00471] It can be seen that the gradual recovery of acute gastric ulcer after 24 hours did not affect the continuous accumulation of antibody probes in the stomach. And as illustrated in Figure 8D, more critically, much higher uptake ($p<0.05$) was observed in the nearly healed

gastric tissue in the gastric ulcer model than in normal mice at longer time points (1.81±0.20 vs 0.74±0.05 at 48 h and 1.01±0.10 vs 0.46±0.07 at 96 h). This simulation experiment seems to provide partial support for our hypothesis that the spatial structure of gastric mucosal cells limits their uptake of mAb probes.

[00472] *Micro-PET Scan of PDX Models:*

[00473] The in vivo distribution and metabolic characteristics of ^{124}I-18B10 were evaluated in real time and noninvasively via small-animal PET/CT imaging at 2, 60, and 120 h post-injection of the radiotracer (Figure 1). Quantification of PET data was conducted by analyzing ROIs to demonstrate dynamic changes of the tracer in tumors at different post-injection time points (Figure 2A).

[00474] The ^{124}I-18B10 accumulated in positive tumor beginning at 2 h, following a stable trend along to 120 h. The tumor uptake values in negative control were lower than those in the experimental group at each time point (0.85±0.10 vs 1.22±0.21 at 2 h, 0.64±0.10 vs 1.32±0.12 at 60 h, 0.45±0.06 vs 1.02±0.05 at 120 h, $p < 0.05$), so it is with that in blank control (0.53±0.07 at 2 h, 0.56±0.08 at 60 h, 0.55±0.10 at 120 h) as well.

[00475] To verify the in vivo specific of ^{124}I-18B10, the tumor/muscle ratio of probe uptake in the three experimental groups were calculated to be compared. It was found that the tumor/muscle ratio in the positive group increased with time (from 4.52±0.02 at 2 h to 5.37±0.02 at 120 h), while that in the negative control was the opposite (from 3.70±0.02 at 2 h to 2.14±0.01 at 120 h), and the blank control showed no obvious trend of change with time (3.12±0.01 at 2 h, 3.11±0.01 at 60 h, 3.06±0.01 at 120 h).

[00476] Additionally, paraffin-embedded tissues slides from mice were subjected to IHC staining (Figure 2B). CLDN18.2 was widely stained in the tumor of positive group (++), while no positive signal was observed in the negative group, which demonstrated the usefulness of these two xenograft models to evaluate radiotracer ^{124}I-18B10 binding specificity in vivo. It is worthy to note that CLDN18.2 also showed high expressing in heart (++) and gastric (+++/++) of both two groups.

[00477] From the maximum intensity projection (MIP) images shown in Figure 2C, although ^{124}I-18B10 showed accumulation in the heart and blood pool at the early time points (2 h), which was considered normal, PET imaging specifically and clearly delineated PDX tumors since 2 h. Uptake in the other two control groups was similar to that in the experimental group, except for low uptake in the tumor area because of non-specific of ^{124}I-IgG or because of negative CLDN18.2 expression in negative PDX model. These results were in accordance with the quantification of tumor uptake conducted by analyzing ROIs.

[00478] Example 4 First in Human Clinical Translational Study

[00479] *Example 4.1 Patients Eligibility Criteria and Characteristics*

[00480] Patients with pathologically confirmed with gastric cancer or pancreatic cancer or cholangiocarcinoma by using an Eastern Cooperative Oncology Group performance (status $\leqslant$ 2) were eligible. Other inclusion criteria include an age older than18 years old; a life expectancy of at least 3 months; and adequate liver and renal function. Written informed consent from all patients were obtained.

[00481] From May 2021 to April 2022, 17 patients with pathological results were enrolled in the analysis, namely, 6 males and 11 females, with a median age of 51 (29–65) years. Patient characteristics are summarized in Figure 10.

[00482] *Example 4.2 ^{18}F-FDG PET/CT and ^{124}I-18B10 PET/CT and/or PET/MR*

[00483] All patients underwent ^{124}I-18B10 PET/CT and 18F-FDG PET/CT within 1 week before or after ^{124}I-18B10 PET/CT imaging (Figure 1).

[00484] For ^{124}I-18B10 PET imaging, the thyroid glands of patients were blocked by taking Lugol's potassium iodide (ten drops each time, 3 times a day) 3 days before and 7 days after the administration of ^{124}I-18B10. ^{124}I-18B10 PET/CT scans were obtained with the Siemens Biograph mCT Flow 64 scanner (Erlangen, Germany) at 2 h, 24h, 72h, 96 h following administration of ^{124}I-18B10.

[00485] ^{124}I-18B10 PET/MR was performed using an integrated TOF PET/MR system (uPMR 790 PET/MR, United Imaging, Shanghai, China).

[00486] Images were read by two experienced nuclear medicine physicians who were familiar with the patient's medical history. The maximum standardized uptake value (SUVmax) of the tumor primary and metastatic lesions were measured, and the SUVmean of main organs in patients were measured at meantime.

[00487] *Example 4.3 Statistical Analysis*

[00488] Descriptive statistics include median, mean and the standard deviation (SD). Comparison between groups was analyzed using the independent sample t-test. The relationship between two groups was analyzed using Spearman correlation analysis. Statistical analysis was performed with SPSS 20.0. $P < 0.05$ was considered significant.

[00489] *Example 4.4 ^{124}I-18B10 whole body CLDN18.2 expression mapping*

[00490] The CLDN18.2 expression level was zero in the tumor tissue of one patient, while the CLDN18.2 expression levels in other 16 patients were positive. Among the enrolled patients, 10 patients have received CLDN18.2 targeted therapy before the ^{124}I-18B10 PET

imaging, and 7 patients had not receive CLDN18.2 targeted therapy. The first patient in this trail underwent twice ^{124}I-18B10 PET scans before and after receiving CLDN18.2 targeted therapy respectively. Patient characteristics are shown in Figure 10.

[00491] The biodistribution of ^{124}I-18B10 in patients were derived from the first five patients' images (Figure 3A, B). The thyroid glands were sufficiently blocked in the patients. The tracer was concentrated in the blood after injection and decreased over time, and the tracer concentration in the spleen and liver was increased over time. The spleen has the highest activity at 24, 48 and 72 h among all the organs. There was also tracer uptake in the kidneys, whereas, the uptake in the brain, lung and bone was low. No clear tracer uptake was seen in the normal gastric wall.

[00492] *Example 4.5 ^{124}I-18B10 functional PET imaging in tumor lesions*

[00493] A total of 65 tumor lesions in 17 patients were analyzed, of which 25 lesions had not been treated by the CLDN18.2 targeted therapy and 40 lesions had been treated by the CLDN18.2 targeted therapy before the imaging. Tracer uptake in tumor lesions ranged from 0.4 to 19.5 SUVmax. Tumor uptake did not differ between patients with gastric cancer, pancreatic cancer and cholangiocarcinoma (SUVmax 24h : 2.24±1.51 vs 2.42± 1.18 vs 10.00±10.66, $P > 0.05$; 48h : 2.14± 1.71 vs 2.95± 0.87 vs 6.86±6.63, $P > 0.05$). Compared with lesions treated by the CLDN18.2 targeted therapy, the uptake was significantly higher in the lesions that had not been treated by the CLDN18.2 targeted therapy (SUVmax 24h : 6.00 ± 7.38 vs 2.37 vs 1.43, $P = 0.042$) (Figure 3D).

[00494] Uptake of ^{124}I-18B10 in tumors was significantly different between different lesion sites ($P < 0.0001$) (Figure 3C). The ovarian metastases showed the highest uptake with a mean SUVmax of 23.65 ± 2.05, and the lung metastases showed the lowest uptake with a SUVmax of 1.5.

[00495] Of the seven patients that had not receive CLDN18.2 targeted therapy, one 57-years-old female patient (No.4) had bile duct derived moderately differentiated adenocarcinoma and liver, peritoneal, bone metastases and suspected metastasis of the right ovary. The primary lesion of the patient had been removed, and the expression level of CLDN18.2 was 3+ 30% by pathological examination. The ^{124}I-18B10 PET/CT showed increased uptake of ^{124}I-18B10 in some liver and bone metastases with SUVmax of 3.2 and 4.4 respectively, and two soft tissue mass were observed in the bilateral ovarian with abnormally high uptake with SUVmax of 12.5 and 17.6 left and right respectively (Figure 4).

[00496] After the injection of ^{124}I-18B10, two patients with gastric cancers undertook regional ^{124}I-18B10 PET/MR at 96 h. A 36-years-old female patient (No.8) with gastric

cancer and lymphoid node metastases, suspected metastasis of left ovary have received CLDN18.2 targeted therapy before, and the CLDN18.2 expression level was 3+, 90% (Figure 5 panel D). The ^{124}I-18B10 PET/MR showed high uptake in the lymphoid node next to the left iliac vessel with SUVmax of 6.6 (Figure 5 panels A-C) and slight uptake in the left ovarian metastasis with SUVmax of 1.3, which showed high signal on T2WI sequence. Another patient was a 43-years-old female with gastric cancer and lymphoid node matastases and also received CLDN18.2 targeted therapy before. The CLDN18.2 expression level was also 3+, 90%. The two retroperitoneal metastatic lymph nodes showed high signal on T2WI sequence and high uptake with SUVmax of 2.6 and 2.5 respectively on ^{124}I-18B10 PET/MR (Figure 5 panels E-G).

[00497] *Example 4.6 ^{124}I-18B10 PET uptake and response to therapy*

[00498] One patient with gastric cancer who has failed after two-line treatment including Capecitabin, Oxaliplatin and Paclitaxel underwent ^{124}I-18B10 PET/CT and 18F-FDG PET/CT. On the ^{124}I-18B10 PET before the treatment, there were several peritoneal metastases showing high uptake of ^{124}I-18B10 with SUVmax of 3.1, 3.2 and 4.2. Then the patient received CT041 infusion one time, a CLDN18.2 targeted CAR T cell therapy, and underwent ^{124}I-18B10 PET/CT and 18F-FDG PET/CT again 4 months later, on which the original high uptake peritoneal metastases showed no obvious uptake. And this patient continued to survive as long as 40 weeks without disease progression.

[00499] *Example 4.7 ^{124}I-18B10 Dosimetry Evaluation in Human*

[00500] Volume of interests (VOIs) were drawn on the major organs, including the brain, lung, heart, liver, spleen, kidneys, muscle, and bone, with the PET/CT images for measuring their activity concentration with the IntelliSpace Portal workstations (Philips, Netherlands). Values of standard male/female organ masses were taken from the OLINDA/EXM software (Ver 2.2, HERMES Medical Solutions, Inc, Canada) to estimate the human dosimetry.

[00501] No adverse events related with ^{124}I-18B10 were reported in patients during the whole examination. The dosimetry estimates from OLINDA show that three organs receiving the highest absorbed doses were spleen, kidney and liver with mean values of 1.20, 0.717 and 0.616 mGy/MBq respectively (Figure 11). The mean effective dose was 0.213 mSv/MBq (0.788 rem/mCi).

[00502] **Example 5 Discussion**

[00503] Targeted radionuclide labeling technology can realize real-time diagnosis and treatment through in vivo imaging, thus comprehensively reflect the spatial distribution and expression intensity of all focus targets. It provides a non-invasive and effective molecular

imaging method that can realize patients' screening, monitor the expression heterogeneity, predict the curative effect and evaluate the curative effect for precision medicine.

[00504] The first-in-human study of ^{124}I-18B10 PET/CT and PET/MR targeting CLDN18.2 in cancer patients was demonstrated. The result showed that ^{124}I-18B10 PET was a safe and invasive imaging for detection of CLDN18.2 in patients receiving CLDN18.2 targeting treatment.

[00505] The biodistribution of ^{124}I-18B10 in human is mainly concentrated in the liver, spleen and kidney, and gradually decreases with time. The uptake in brain, muscle and other tissues is very low, which is consistent with the distribution characteristic of ^{124}I labeled monoclonal antibody in human(16). Previous studies have shown that CLDN18.2 can also be highly expressed in normal gastric wall tissues(5), but no obvious uptake was observed in normal gastric wall tissues of the enrolled patients. it might because that CLDN18.2 is typically limited to inside the tight junction and largely inaccessible to monoclonal antibodies in normal mucosal cells(17). There are two possible mechanisms that explicate this phenomenon, which have not been confirmed and need further investigation. One is that the CLDN18.2 on the apical membrane is further from the microvasculature and is more difficult to reach than that on the basolateral membrane, and the other is that it is difficult for IgG antibodies to bind to the target which is surrounded by several tight junction components(11).

[00506] In order to prove whether the low uptake observed in normal gastric tissue stems from the above conjecture, we simply constructed gastric ulcer models, trying to change the external environment and spatial relationship of normal gastric mucosal cells, to interpret negative imaging of the stomach from the perspective of the structure-activity relationship of the monoclonal antibody probe. The high uptake observed in mice with unhealed/healed gastric ulcers suggested that the binding of the mAb probe to the gastric mucosa was inversely associated with inflammation, more human results are needed for validation though.

[00507] Several clinical trials had revealed that CLDN18.2 targeted therapy had achieved the highlighting development to CLDN18.2 positive patients. However, these studies also indicated the limitations in testing of CLDN18.2, and had the differences in cutoff used(18). It is highly need to develop unified detection means to reduce the impact of using different detection methods and different positivity threshold in trials. PET imaging with radiolabeled antibody is a noninvasive molecular imaging method, which can avoid the sampling errors and the influence of the tumor heterogeneity(19). Till now, several studies have showed that PET imaging might possess the potential to screen patients that might benefit from in PD-

1/L1 blockade immunotherapy(20-22). Hence, PET imaging targeting CLDN18.2 may also become an effective method in the investigation of the CLDN18.2 targeted therapy.

[00508] Both patients that have or have not received CLDN18.2 targeted therapy before the ^{124}I-18B10 PET imaging were enrolled. Compared with lesions treated by the CLDN18.2 targeted therapy, the uptake was significantly higher in the lesions that had not been treated by the CLDN18.2 targeted therapy. The tumor uptake did not relate with the CLDN18.2 expression levels whether in any group of patients or in all patients. Among the patients who have not received CLDN18.2 targeting treatment, the expression level of CLDN18.2 in one patient with cholangiocarcinoma was only 3+ 30%. But on ^{124}I-18B10 PET, there was significant high uptake in the multiple bone metastases, liver metastases and ovarian metastases, especially the abnormal concentration in the ovarian metastases, suggesting that the expression of CLDN18.2 in different lesions in the same patient might have significant heterogeneity.

[00509] After receiving CLDN18.2 targeting treatment, the tumor cells with high expression of CLDN18.2 in the patient's tumor lesions might be induced to apoptosis through the action of antibody-dependent cell-mediated cytotoxicity (ADCC) and complement dependent cytotoxicity (CDC) caused by anti-18B10-18.2 antibodes(23, 24). Therefore, although the expression level of CLDN18.2 was high in previous pathological tests, the lesion uptake was negative on CLDN18.2 PET. The negative uptake of lesions on CLDN18.2 PET indicates that there are no tumor cells with high expression of CLDN18.2 in the lesions, and the effect of CLDN18.2 targeted therapy may not reach the expectation, suggesting that the treatment scheme should be changed. After receiving CLDN18.2 targeting treatment, the tumor lesions in the patients still showed significantly high uptake in CLDN18.2 PET, suggesting that there are still tumor cells with high expression of CLDN18.2 in the lesions and CLDN18.2 targeted therapy may still have obvious curative effect.

[00510] A female gastric cancer patient (No.1) in the age of thirty with ovarian and peritoneal metastases who had undergone the resection of gastric cancer and ovarian metastases underwent twice ^{124}I-18B10 PET before and after receiving CLDN18.2 targeted therapy. The CLDN18.2 expression level of the patient was 90%, 3+. On the ^{124}I-18B10 PET before the treatment, there were several peritoneal metastases showing high uptake of ^{124}I-18B10 with SUVmax of 3.1, 3.2 and 4.2 (Figure 6 panels A-C). After receiving CLDN18.2 targeted therapy for almost 4 months, the patient undertook the ^{124}I-18B10 PET again, on which the original high uptake peritoneal metastases showed no obvious uptake (Figure 6 panels D-E). Thus, ^{124}I-18B10 PET can monitor CLDN18.2 expression levels in of the tumor

lesions dynamically and may play an important role in guiding the CLDN18.2 targeting treatment strategy.

[00511] In summary, the present invention showed that ^{124}I-18B10 PET imaging was safe with acceptable dosimetry and reveals a favorable biodistribution in human. Tumor lesions showed different levels of uptake of the tracer, and the uptake might correlate with the treatment response.

[00512] References for background, detailed description of the invention and Examples 1-5 can be seen in Table 7.

[00513] **Example 6**

[00514] *Example 6.1 Abstract*

[00515] In this study, we constructed a solid target radionuclide zirconium-89 (^{89}Zr) labled-18B10 to detect the expression of in the human stomach cancer BGC823$^{CLDN18.2}$ cell lines. The [^{89}Zr]Zr-DFO-18B10 showed high radiochemical purity (RCP, >99%) and specific activity (24.15 ± 1.34 GBq/μmol), and was stable in 5% HSA, and PBS (>85% radiochemical purity at 96 h). The concentration of 50% maximal effect (EC_{50}) values of 18B10 and DFO-18B10 were as high as 0.413 ± 0.055 nM and 0.361 ± 0.058 nM ($P > 0.05$), respectively. The radiotracer had a significantly higher uptake in CLDN18.2-positive tumors than in CLDN18.2-negative tumors (1.11 ± 0.02 vs. 0.49 ± 0.03, $P = 0.0016$) 2 days post injection (p.i.). BGC823$^{CLDN18.2}$ mice models showed high T/M values 96 h p.i. with [^{89}Zr]Zr-DFO-18B10 was much higher than those of the other imaging groups. Immunohistochemistry results showed that BGC823$^{CLDN18.2}$ tumors were highly positive (+++) for CLDN18.2, while those in the BGC823 group did not express CLDN18.2 (-). The results of ex vivo biodistribution studies showed that there was a higher distribution in the BGC823$^{CLDN18.2}$ tumor bearing mice (2.05 ± 0.16 %ID/g) than BGC823 mice (0.69 ± 0.02 %ID/g) and blocking group (0.72 ± 0.02 %ID/g). A dosimetry estimation study showed that the effective dose of [^{89}Zr]Zr-DFO-18B10 was 0.0705 mSv/MBq, which is within the range of acceptable doses for nuclear medicine research. Taken together, these results suggest that GMPs produced by this immune-PET probe can detect CLDN18.2-overexpressing tumors.

[00516] *Example 6.2 Introduction*

[00517] According to the cancer epidemiology report released in 2022, lung cancer is the primary cause of cancer death, followed by digestive tract tumors (such as stomach cancer, colorectal cancer, liver cancer, oesophageal cancer, etc.). In China, gastrointestinal cancers

account for 45% of cancer-related deaths, likely because gastrointestinal cancers are mostly diagnosed in the advanced stage and patients often have a poor prognosis[1–3]. Gastrointestinal cancers have become the primary medical and economic burden for people in China. In addition to traditional chemotherapy, and immunotherapy, little progress has been made with novel chemotherapies and targeted therapies for gastrointestinal tumors[4–7]. Among the 70 novel first-line agents approved for cancer treatment, only 5 drugs have been approved for advanced gastrointestinal cancer and the survival rates are still low based on data from the last five years[8]. Therefore, strategies to improve the survival of patients with advanced gastrointestinal cancer remain an unmet medical necessity.

[00518] CLDN18.2 is a tight junction protein belonging to the CLDN protein family (CLDNs) that is involved in the formation of intercellular adhesion structures, and controls cell polarity and the exchange of substances between cells[9–11]. Its expression is strictly limited to normal gastric mucosal cells, but is overexpressed in the process of proliferation, division and metastasis of tumor cells, making it an emerging therapeutic target for digestive tract tumor therapy[12,13]. Zolbetuximab (IMAB362) is the first targeted CLDN18.2 antibody that kills tumor cells through antibody-dependent cytotoxicity(ADCC) and complement-dependent cytotoxicity(CDC), and in combination with first-line epirubicin, oxaliplatin and capecitabine (EOX) to provide longer progression-free and overall survival[14]. 18B10 is an anti-CLDN18.2 monoclonal antibody developed worldwide after IMAB362. Compared to IMAB362, 18B10 has a higher affinity and stronger NK cell-mediated ADCC tumor killing activity. In a phase I clinical study of 18B10 (NCT04396821) in combination with capecitabine and oxaliplatin (CAPOX) as a first-line agent for advanced gastric/gastroesophageal junction adenocarcinoma, 73.3% achieved partial response, and 26.7% achieved stable disease[15]. A phase I study (NCT03874897) of CLDN18.2 CAR-T therapy conducted by Shen et al. showed that after receiving CLDN18.2 CAR-T infusion, the overall response rate (ORR) and disease control rate (DCR) reached 48.6% and 73.0%, respectively[16]. Interestingly, both clinical studies indicate that the CLDN18.2 expression level was correlated with drug efficacy, showing more clinical benefit in patients with high CLDN18.2 expression in tumors. Therefore, patient selection based on CLDN18.2 expression level becomes critical for CLDN18.2-targeted therapy. At present, the major detection method of CLDN18.2 protein is immunohistochemistry (IHC), and other methods include molecular beacons and RT–PCR[17]. IHC is invasive, and requires endoscopic biopsy, and the sampling site and number are limited. Due to the heterogeneous nature of tumor, the

CLDN18.2 distribution and dynamic changes in expression levels in patients cannot be fully reflected in real-time. Molecular imaging can be used as a noninvasive diagnostic tool to detect the expression and distribution of CLDN18.2 in the lesion using the radioactive signal emitted by the radiotracer, thereby helping to clinically screen patients with potential benefit, evaluate the efficacy of CLDN18.2 targeted therapy, and guide the accurate diagnosis and treatment of tumors. A recent study showed that ^{18}F-FDG PET/CT parameters including SUVmax, MTV and TLG did not predict CLDN18.2 expression status in diffuse-type gastric cancer[18]. Hu et al. developed three antibodies (anti-CLDN18.2 VHH, anti-CLDN18.2 VHH-ABD and anti-CLDN18.2 VHH-Fc) of different molecular weight sizes for PET/CT imaging, and identified [^{89}Zr]-anti-CLDN18.2 VHH-ABD as the most appropriate imaging agent (high tumor uptake and low uptake in the liver) in preclinical studies[19]. However, in a subsequent clinical study, [^{89}Zr]-VHH-Fc was found to be more specific and persistent than [^{89}Zr]-anti-CLDN18.2 VHH-ABD, and was also considered to be a molecular imaging tracer with potential value for cancer diagnosis, as it contains CLDN18.2[20]. More recently, we explored a CLDN18.2-specific murine mAb 5C9 by DNA immunization, and modified 5C9 with ^{124}I, Cy5.5 and FD1080. The results of these studies support the targeted therapy of CLDN18.2-positive tumors by using immuno-PET imaging and near-infrared fluorescent II imaging to localize tumors and guide surgery for orthotopic CLDN18.2-positive tumors[21].

[00519] Due to the superior targeting specificity and high sensitivity of molecular imaging technology, we used the 18B10 antibody with GMP requirements to construct the immuno-PET molecular probe [^{89}Zr]Zr-DFO-18B10. The goal of this study was to assess the ability of [^{89}Zr]Zr-DFO-18B10 to characterize CLDN18.2 expression.

[00520] Heavy chain variable region of IMAB362 (SEQ ID NO: 72)

[00521] QVQLQQPGAELVRPGASVKLSCKASGYTFTSYWINWVKQRPGQGLEWIGNI YPSDSYTNYNQKFKDKATLTVDKSSSTAYMQLSSPTSEDSAVYYCTRSWRGNSFDYWGQGT TLTVSS

[00522] Light chain variable region of IMAB362 (SEQ ID NO: 73)

[00523] DIVMTQSPSSLTVTAGEKVTMSCKSSQSLLNSGNQKNYLTWYQQKPGQPPKL LIYWASTRESGVPDRFTGSGSGTDFTLTISSVQAEDLAVYYCQNDYSYPFTFGSGTKLEIK

[00524] *Example 6.3 Material and methods*

[00525] *1) Materials*

[00526] All reagents were obtained from Sigma–Aldrich. P-isothiocyanatobenzyl-desferrioxamine B (p-NCS-Bz-DFO) was purchased from Macrocyclics. The GMP grade CLDN18.2 antibody 18B10 (Hu18B10HaLa) was kindly provided by Transcenta Holding Ltd. (Suzhou, China). Radionuclide ^{89}Zr was produced and purified by the Cyclotron team of the Nuclear Medicine Department of Peking University Cancer Hospital.

[00527] *2) Radiolabeling of 18B10 with 89Zr*

[00528] For ^{89}Zr labeling, ^{89}Zr-oxalic acid was neutralized to pH 7.0 using 0.25 M 2-[4-(2-hydroxyethyl)-1-piperazinyl］ethanesulfonic acid (HEPES) and 1 M Na_2CO_3 buffer , and then mixed with previously described DFO-18B10 for 60 min at 37 °C. The reaction mixture was purified by PD-10 column (2.5 ml, 0.01 M Ph 7.4 PBS).

[00529] *3) Small-animal PET Imaging of [^{89}Zr]Zr-DFO-18B10*

[00530] Normal KM mice and BGC823$^{CLDN18.2}$/BGC823 model nude mice were injected with 7.4 MBq of [^{89}Zr]Zr-DFO-18B10 via the tail vein (n = 3). Then 10 min static PET scans were acquired at each time point (2, 24, 48, and 72 h p.i.). As a non-specific control group, BGC823$^{CLDN18.2}$ mice (n = 3) were fasted 6 h in advance, then injected with 7.4 MBq of ^{18}F-fluorodeoxyglucose (FDG) via the tail vein. The mice were anesthetized with 2% isoflurane before and during the ^{18}F-FDG PET imaging. With a small-animal PET/CT scanner (Super Nova PET/CT, Pingseng Healthcare, China), the PET images were reconstructed by Avatar 3, and the ROI-derived standard uptake value (SUV) was calculated by drawing ROIs over these organs.

[00531] *4) Ex Vivo Biodistribution.*

[00532] The KM mice were intravenously injected with 0.74 MBq of [^{89}Zr]Zr-DFO-18B10 via the tail vein and were then sacrificed at 2, 24, 48, 72 and 144 h p.i. (n = 4). The tissues including the blood, heart, liver, spleen, lung, kidneys, stomach, intestines, muscle, bone and brain were dissected. The radioactivity of the tissues was measured using a γ-counter. The radioactivity of each organ was calculated as % injected dose per gram (%ID/g). For the tumor model's ex vivo biodistribution, female nude mice bearing BGC823$^{CLDN18.2}$ and BGC823 tumor xenografts were injected by tail vein with 0.74 MBq of [^{89}Zr]Zr-DFO-18B10 to evaluate the distribution of [^{89}Zr]Zr-DFO-18B10 in major organs and tumors (n = 4 per group). The mice were sacrificed and dissected at 48 h p.i. (n = 4), and the tumor, kidney, blood, and other major organs were collected and weighed. The blocking study was also performed in BGC823$^{CLDN18.2}$ mice by a coinjection of 0.74 MBq of [^{89}Zr]Zr-DFO-18B10

with an excess dose of cold 18B10 (1 mg). At 48 h p.i., the blocked mice were sacrificed and dissected. Then, the organ biodistribution of [^{89}Zr]Zr-DFO-18B10 was determined.

[00533] *5) Dosimetry Estimation*

[00534] For human radiation dosimetry, animal biodistribution data were obtained by the standard method of organ dissection. The human organ radiation dosimetry data were extrapolated from the biodistribution data of [^{89}Zr]Zr-DFO-18B10 in KM mice by OLINDA/EXM 2.0 software (Vanderbilt University, America).

[00535] *6) Statistical Analysis*

[00536] Quantitative data are expressed as the mean ± standard deviation (SD), with all error bars denoting the SD. The means were compared using Student's t test, and P values of less than 0.05 were considered to indicate statistical significance.

[00537] *7) Conjugation and Identification DFO-18B10*

[00538] Both modification and radiolabeling methods for 18B10 have been reported in previous studies. Specifically, 18B10 (3.3 nmol) were dissolved in $NaHCO_3$ buffer (0.1 M, pH 9.5) after exchanging the solvent with 0.01M PBS. The pH value was adjusted to 9.0 with 0.1 M Na_2CO_3 solution. 60 nmol p-NCS-Bz-DFO dissolved in DMSO was then added to the above solution with a molar ratio of p-NCS-Bz-DFO to 18B10 as 20:1. After mixing and reacting at 37 °C for 1 h, the crude product was further purified by PD-10 column (2.5 ml, 0.01 M PBS) and stored at -80 °C in stabilizer.

[00539] The mass spectra of 18B10 and DFO-18B10 were measured by matrix-assisted laser desorption/ionization time-of-flight mass spectrometry (MALDI-TOF-MS) (Bruker Dalton, Germany). For nonreducing sodium dodecyl sulfate-polyacrylamide gel electrophoresis (SDS-PAGE), 10 μg antibody samples were diluted with 0.01 M PBS and ×5 nonreducing sample buffer without dithiothreitol, then separated on an 6% sodium dodecyl sulfate PAGE gel by electrophoresis. The gel was stained with 0.5% Coomassie blue.

[00540] *8) Assessment of CLDN18.2 binding affinity*

[00541] Enzyme-linked immunosorbent assays (ELISAs) were used to determine the binding potency between 18B10 and DFO-18B10 with human CLDN18.2 full length protein-VLP (CL2-H52P7). First, 100 μL solution of the CL2-H52P7 (2 μg/mL) was added to each well coated with a 96-well polystyrene StripwellTM microplate (Corning Costar, CLS2481-100EA), at 4 °C overnight. Then, the antigen solution was discarded, and the protein was washed five times with PBST (0.01 M pH 7.4 PBS and 0.2% Tween-20). After that, 5%

powdered milk (diluted with PBS) was added to the microplate for 2 h at 37 ℃ to block other nonspecific sites. Then, after discarding the 5% powdered milk, five times washed with PBST. After the plate was washed, the diluted sample (IgG, 18B10 and DFO-18B10) was added with seven concentration gradients, 0.001, 0.005, 0.01, 0.05, 0.1, 0.5, 1,10,50, 100, 500 and 1000 nM to the microplate (100 μL/well) and the membrane was covered for 2 h at 15-25 °C. The plate was washed again, and secondary antibody was added: goat anti-mouse IgG4 Fc (HRP) was diluted 1:3000 in the enzyme-labeled plate with a secondary antibody diluent (100 μL/well) and incubated at 15-25 °C for 1 h. For color development after washing, coloring solution (100 μL/well) was added, and the plate was covered with film and developed while protected from light at 15-25 °C for 20 min. For termination of the reaction, stop solution was added (50 μL/well. For detection, the optical density (OD) value of each well was read by a microplate reader at a detection wavelength of 450 nm. The EC_{50} value was also used to assess the affinity of anti-CLDN18.2 antibodies to CLDN18.2.

[00542] *9) Preparation of [^{89}Zr]Zr-DFO- IgG*

[00543] The preparation of DFO-IgG is the same as that of DFO-18B10. For ^{89}Zr labeling, ^{89}Zr-oxalic acid was neutralized to pH 7.0 using 0.25 M 2-[4-(2-hydroxyethy)-1-piperazinyl］ethanesulfonic acid (HEPES) and 1 M Na_2CO_3 buffer , then mixed with DFO-IgG for 60 min 37 °C. The reaction mixture was purified by PD-10 column (2.5 ml, 0.01 M Ph 7.4 PBS).

[00544] *10) Quality Control of [^{89}Zr]Zr-DFO-18B10*

[00545] Quality control of [^{89}Zr]Zr-DFO-18B10 tracer is carried out in accordance with the Guidelines for Quality Control of Positron Radiopharmaceuticals.

(1) pH: Take 1 drop of radiopharmaceuticals, drop it on a precision pH test strip, and compare it with the standard color swatch, that is, the pH value of the solution.

(2) Ethanol content: No ethanol is added during the preparation of the tracer preparation, and there is no need for inspection.

(3) Endotoxin: Take this product, according to the Chinese Pharmacopoeia (2020) General Rule 1143 for inspection, this product should contain less than 15 EU/mL of endotoxin.

(4) Sterility: Take this product, according to the Chinese Pharmacopoeia (2020) General Rule 1101 for inspection.

(5) Specific activity: Refers to the activity of an element of a radionuclide or the unit mass of its compound.

[00546] *11) Radiochemical Purity and Vitro Stability*

[00547] The radiochemical yield and radiochemical purity were measured by Radio-thin-layer chromatography (Radio-TLC) in a standard protocol. The pre-purification and post-purification products [^{89}Zr]Zr-DFO-18B10 (2uL) were dropped to the lower end of the TLC-SG test strip 1 cm, and then the TLC-SG test strip was placed in the eluent 0.5 M sodium citrate (PH=5.0) buffer. When the eluent is unfolded to 10 cm from the lower end, it is removed and dried, radio-TLC analysis is performed, and the Rf value is calculated. The Rf values of free Zr-89 and [^{89}Zr]Zr-DFO-18B10 are 0.9-1.0 and 0-0.1 respectively. The vitro stability study is conducted that [^{89}Zr]Zr-DFO-18B10 incubated with 0.01 M PBS or 5% HSA at room temperature (RT). Radio-TLC were performed at various incubation time (0, 2, 12, 24, 48, and 96 h).

[00548] *12) Cell Lines and Tumor-bearing Model*

[00549] The human stomach cancer cell line BGC823 was obtained at Peking University Cancer Hospital and Institute (Beijing, China). The BGC823$^{CLDN18.2}$ cell line was generated by transfection with the full-length CLDN18.2. The cells were cultured in RPMI-1640 medium which was supplemented with 10% FBS plus antibiotics from Invitrogen. All animal experiments were performed according to the National Institutes of Health guidelines for the care and use of laboratory animals and approved by the Animal Care and Ethics Committee of Peking University Cancer Hospital. For PET/CT imaging and vitro biodistribution experiments, BGC823 and BGC823$^{CLDN18.2}$ xenografts were established in 4 to 6-week-old female BALB/c nu/nu mice which were purchased from Beijing Vital River Laboratory Animal Technology Co., Ltd (Beijing, China). The right axillary of the mouse was subcutaneously injected with 1×10^6 BGC823/BGC823$^{CLDN18.2}$ cells suspended in 100 μL PBS. Tumors were grown for 3 weeks to reach an average volume of 100 mm^3.

[00550] *13) Assessment of CLDN18.2 Expression*

[00551] Western blotting was performed as previously described. After washing three times with cold PBS, 500 μL of RIPA lysis buffer was added to each cell dish for 10 min in an ice box. The cell lysate was centrifuged for 5 min at 15000 rpm at 4 °C, and the supernatant was collected and stored on ice. Equal amounts of supernatant (20 μg) were separated to extract protein by SDS−PAGE (250 mA, 90 min), and transferred over to a polyvinylidene fluoride (PVDF) membrane. Blots were incubated with the following primary antibodies: rabbit anti-human CLDN18.2 (ab213480, 1:500; Abcam). Blots were then incubated with an HRP-conjugated goat anti-rabbit secondary antibody (1:10000) Proteins were detected using to Clarity Western ECL Substrate. Immunoblots were imaged with the

Alliance Micro Q9 chemiluminescence imaging system (Alliance Micro Q9, UVITEC, Britain). Cells (2×10^5) were collected and washed with cold PBS twice, stained with 2 μg/mL CLDN18.2 antibody (1D5, Beijing cancer hospital) for 1 h at room temperature followed by Alexa Fluor 488-conjugated antibody for 30 min, and then subjected to flow cytometry with BD FACS Aria Flow cytometric analyses were performed on a Beckman Coulter Cytomics FC 500 MPL.

[00552] *14) Cellular Experiments.*

[00553] BGC823/BGC823$^{CLDN18.2}$ cells were cultured in RPMI-1640 culture medium (2.0×10^5 cells/mL) and added to a 24-well plate (1.0 mL per well) to culture overnight. [^{89}Zr]Zr-DFO-18B10 (20 μL, 37 kBq, 6.87×10^{-12} M) was added to wells (n = 4) containing adherent BGC823/BGC823$^{CLDN18.2}$ cells. The mixture was incubated in a 5% CO_2 incubator at 37 °C for 2, 10, 30, 60, and 120 min. After incubation, the culture medium was removed and the cells were washed 2 times with cold PBS (0.01 M). Inhibition for 60 and 120 min was performed in the presence of excess unlabeled 18B10 (50 μg). Then, the cells were collected after digestion by 1 M NaOH and counted in a gamma counter. The percentage of added dose per 2.0×10^5 cells (%AD/2.0×10^5 cells) was calculated according to the count.

[00554] *Example 6.4: Immunohistochemistry Studies*

[00555] Paraffin sections were deparaffinized with xylene. Following rehydration in distilled water, antigen was retrieved by heating in EDTA (pH 9.0) for 10 min. Endogenous peroxidase activity was blocked by incubating in 3% hydrogen peroxide at room temperature for 15 min. Nonspecific binding was blocked with goat blocking serum for 1 h at room temperature. Anti-CLDN18.2 rabbit monoclonal antibody (Abcam, ab222512) diluted at 1:500 was added, and the slides were incubated at 4 °C overnight. Following three washes, the slides were incubated with Envision (DAKO) for 45 min at room temperature. Diaminobenzidine was used as a chromogen. Sections were counterstained with hematoxylin, dehydrated, and mounted. Evaluation of immunohistochemical slides was performed using a Leica AT2 microscope.

[00556] *Example 6.5 Results and discussion*

[00557] *1) Molecular Characteristic of Conjugation*

[00558] The molecular weight of the CLDN18.2 antibody, 18B10, was approximately 148 kDa, which was further determined to be exactly 148,723 Da (Figure 14A). DFO-18B10 was chelated with an approximately double-DFO chelator with a molecular weight of 150320 Da (Figure 14B). SDS–PAGE showed that both 18B10 and DFO-18B10 had bands at

approximately 150 kDa with no other bands (Figure 14C), which indicated that the conjugation was of excellent quality as no antibody aggregates or antibody fragments were detected. The ELISA results showed that the EC_{50} value of DFO-18B10 binding to CLDN18.2 was not significantly different from that of 18B10 (0.413 nM ± 0.055 nM vs. 0.361 ± 0.058 nM, $P > 0.05$, Figure 14D). The binding assay demonstrated both 18B10 and DFO-18B10 can form a strong bond with CLDN18.2, and the conjugation of the chelator DFO had no impact on the affinity of 18B10 to CLDN18.2.

[00559] *2) Radiosynthesis, quality control, and in vitro stability*

[00560] The synthesis process of [^{89}Zr]Zr-DFO-18B10 is shown in Figure 15 panel A. [^{89}Zr]Zr-DFO-18B10 was manually prepared with a radiolabeling yield of 74.64% ± 4.4% (n = 3 nondecay corrected). The radiochemical purity (RCP) of [^{89}Zr]Zr-DFO-18B10 was more than 99% in 0.01 M PBS (pH 7.4) (Figure 15 panel B). The *in vitro* stability of [^{89}Zr]Zr-DFO-18B10 in 0.01 M PBS or 5% HSA was demonstrated by an RCP of more than 85% after 96 h at RT. (Figure 15 panel C). The excellent *in vitro* stability also showed that the 18B10 structural modification and labeling method was feasible. Quality control results are shown in Table 4.

[00561] Table 4. Quality control of [^{89}Zr]Zr-DFO-18B10

Parameter	QC specification	QC result
Appearance	Clear, colorless	Pass
Volume	1-2 mL	1 mL
pH	4.0-8.0	7.4
Radiochemical purity	>95%	>99%
Ethanol	<5%	0
Endotoxins	<15 EU/mL	Pass
Sterility	Sterile	Pass
Specific activity	18.5-296 GBq/μmol	24.15 ± 1.34 GBq/μmol

[00562] *3) In Vitro CLDN18.2 Expression of Cell Lines.*

[00563] Western blotting results confirmed that the expression of CLDN18.2 in BGC823$^{CLDN18.2}$ cells was significantly different from that in BGC823 cells (Figure 16 panel A). The relative expression of CLDN18.2 in the BGC823$^{CLDN18.2}$ and BGC823 cell lines was 1.37 ± 0.24 and 0.23 ± 0.01, respectively ($P = 0.0013$, Figure 16 panel B). Flow cytometry experiments revealed that 86.2% of cells were positively stained with anti-CLDN18.2

antibody (1D5) in the BGC823$^{CLDN18.2}$ group (Figure 16 panel C). The differences in CLDN18.2 expression measured by western blotting and flow cytometry were then validated between the human gastric cancer cell lines BGC823 and BGC823$^{CLDN18.2}$. The result of the cellular uptake experiment showed that the uptake of [^{89}Zr]Zr-DFO-18B10 in BGC823$^{CLDN18.2}$ cells increased in a time-dependent manner (7.33 ± 0.84% at 10 min, 7.97% ± 0.56% at 30 min, 11.47% ± 0.32% at 60 min, 13.37% ± 2.04% at 120 min), while no significant changes were observed in the BGC823 group (4.21% ± 0.21% at 10 min, 3.77% ± 0.53% at 30 min, 4.57% ± 0.36% at 60 min, 5.54% ± 0.21% at 120 min). The uptake by BGC823$^{CLDN18.2}$ cells (CLDN18.2 positive) was significantly higher than that by BGC823 cells (CLDN18.2 negative) at each selected time point ($p < 0.0004$). Meanwhile, an excess of unlabeled 18B10 significantly blocked the uptake of [^{89}Zr]Zr-DFO-18B10 (11.47% ± 0.32% vs. 3.24% ± 0.36% at 60 min, 13.37% ± 2.04% vs. 5.64% ± 0.21% at 120 min) (Figure 16 panel D). In the cellular uptake experiment, the uptake of [^{89}Zr]Zr-DFO-18B10 by BGC823$^{CLDN18.2}$ cells at 60 min was 2.51-fold higher than that of BGC823 cells and 3.54-fold higher than that of the blocking group. The specificity of [^{89}Zr]Zr-DFO-18B10 for CLDN18.2 was thus demonstrated at the cellular level.

[00564] *4) Dosimetry Estimation*

[00565] The biodistribution study of [^{89}Zr]Zr-DFO-18B10 demonstrated favourable pharmacokinetics with a relatively long half-life *in vivo* (Supporting Information Figure 20A). Human organ radiation dosimetry is shown in Table 5. The liver received the highest dose (0.360 mSv/MBq), followed by the gallbladder wall (0.155 mSv/MBq). The effective dose was 0.0705 mSv/MBq. When a patient was injected with 74 MBq of [^{89}Zr]Zr-DFO-18B10 for imaging, its effective radiation dose was less than 5.217 mSv, which is acceptable in routine nuclear medicine research. The estimated human radiation burden due to a single i.v. [^{89}Zr]Zr-DFO-18B10 injection is comparable to that of other ^{89}Zr-labelled monoclonal antibodies [22–24], and is suitable for clinical research.

[00566] Table 5. Estimates of the Mean Absorbed Radiation Dose

Organ	mSv/MBq
Adrenals	1.31E-01
Brain	3.08E-02
Esophagus	7.94E-02
Eyes	1.55E-02
Gallbladder Wall	1.55E-01
Left colon	3.65E-02
Small Intestine	5.86E-02

Stomach Wall	6.15E-02
Right colon	4.82E-02
Rectum	2.96E-02
Heart Wall	9.19E-02
Kidneys	1.33E-01
Liver	3.60E-01
Lungs	2.00E-01
Pancreas	6.66E-02
Prostate	1.18E-02
Salivary Glands	1.41E-02
Red Marrow	4.61E-02
Osteogenic Cells	1.09E-01
Spleen	1.38E-01
Testes	4.82E-03
Thymus	5.37E-02
Thyroid	3.68E-02
Urinary Bladder Wall	8.09E-03
Total Body	2.72E-02
Effective Dose	**7.05E-02**

[00567] *5) Small-animal PET/CT Imaging and IHC Analysis*

[00568] Small-animal PET/CT imaging at different time points (2, 24, 48, 72 and 120 h) after injection of [^{89}Zr]Zr-DFO-18B10 into KM mice, showed high uptake in the heart, liver and spleen (Supporting Information Figure 20B). The standard uptake value AVERAGE (SUVmean) of some organs measured by regions of interest (ROIs) is shown in Supporting Information Figure 20C. After 2 h, the SUVmean in the heart was 2.57 ± 0.02, in the liver was 2.27 ± 0.01 and in the spleen was 1.86 ± 0.01. The ratio of heart to muscle (H/M) was 20.30 ± 0.91. After 120 h, the SUVmean in the heart, liver and spleen were 0.49 ± 0.01, 1.36 ± 0.02 and 1.21 ± 0.01, respectively, and almost no special intake was observed in the stomach. The images are consistent with the biodistribution results.

[00569] The *in vivo* distribution and metabolic characteristics of [^{89}Zr]Zr-DFO-18B10 were evaluated in real time and noninvasively via small-animal PET/CT imaging at 2, 24, 48, 72 h and 96 h p.i. of the radiotracer. Meanwhile, we set up the following three control groups, which were blocked by excess 18B10, negative CLDN18.2 expression in BGC823 cells and nonspecific targeting of [^{89}Zr]Zr-DFO-IgG (7.4 MBq), respectively. SUVmean data were collected for organs of BGC823$^{CLDN18.2}$ or BGC823 mice by outlining the ROI from the immune-PET images (Figure 17A, 17B, 17C, 17D and 17E). The tumor sites in the [^{89}Zr]Zr-DFO-18B10 group still had obvious uptake at 96 h p.i. In the BGC823$^{CLDN18.2}$ model with

[^{89}Zr]Zr-DFO-18B10, the SUVmean continued to increase within 48 h p.i. and reached a maximum uptake value of 1.09 ± 0.03 at 48 h. In addition, until 96 h p.i., the SUVmean of the BGC823$^{CLDN18.2}$ model was significantly different from that of the BGC823 model and blocking group (1.03 ± 0.03, 0.41 ± 0.05, 0.51 ± 0.07, respectively, $P < 0.0002$). Using [^{89}Zr]Zr-DFO-IgG as a negative control probe, the results showed that in the BGC823$^{CLDN18.2}$ model mice except for the tumor uptake value slightly higher than [^{89}Zr]Zr-DFO-18B10 at 2 h after injection (0.51 ± 0.01 vs. 0.37 ± 0.02), the ^{89}Zr-DFO-IgG tumor uptake value at all other time points (24 h, 48 h, 72 h and 96 h) was significantly lower than that of [^{89}Zr]Zr-DFO-18B10 (0.55 ± 0.04 vs. 0.96 ± 0.12, 0.53 ± 0.02 vs. 1.10 ± 0.12, 0.54 ± 0.04 vs. 1.06 ± 0.06 and 0.47 ± 0.01 vs. 1.03 ± 0.01) (Figure 21). Over time, compared with other imaging groups, the uptake of [^{89}Zr]Zr-DFO-18B10 was mostly concentrated in the tumor in the BGC823$^{CLDN18.2}$ model, and the uptake values of the heart, liver, and other organs were greatly reduced.

[00570] For comparison with the gold-standard probe ^{18}F-fluorodeoxyglucose (FDG), BGC823$^{CLDN18.2}$ tumor-bearing mice were given ^{18}F-FDG and images were collected 1 h p.i. (Figure 18A). The results showed that the uptake of ^{18}F-FDG in CLDN18.2-positive mice was similar to the background uptake. The tumor accumulation of [^{89}Zr]Zr-DFO-18B10 in BGC823$^{CLDN18.2}$ mice 48 h p.i. was approximately 4.15-fold that of the blocking group, 2.27-fold that of the BGC823 group, and 2.05-fold that of the [^{89}Zr]Zr-DFO-IgG group (SUVmean values were 1.11 ± 0.02, 0.27 ± 0.01, 0.49 ± 0.03, 0.54 ± 0.06, respectively) (Figure 18B). The tumor/heart (T/H) ratios and tumor/muscle (T/M) ratios at each time point after injection of [^{89}Zr]Zr-DFO-18B10 were significantly higher than those of the other control groups (Figure 18C-18D), and at 96 h p.i., the T/H and T/M ratios reached their maximum of 2.37 ± 0.04, 14.95 ± 1.63, respectively.

[00571] The T/NT value of [^{89}Zr]Zr-DFO-18B10 was significantly different 48 h p.i. when comparing the BGC823$^{CLDN18.2}$ model to other groups. Compared with our previous research, 18B10 is a humanized antibody with better immune responsiveness to the CLDN18.2 receptor. Second, the patient needs to receive iodine to block the thyroid gland before and during ^{124}I imaging, which greatly reduces patient compliance[21]. Labelling with ^{89}Zr would appear to be more robust and better available. Nevertheless, a remarkably high background in the liver and spleen was also noted with [^{89}Zr]Zr-DFO-18B10, which might be a result of nonspecific binding and hepatobiliary clearance. This is very similar to previous studies on the ^{89}Zr-labelled antibody[25,26]. From an imaging perspective, this not only results in problems for tumor localization in the liver and spleen region, but it also might lead to false-

positive results when "tumor CLDN18.2 expression" and further cause erroneous selection of candidate patients for this therapy. Although the interactions between FcγR expressed on immune effector cells and the Fc region of antibodies can trigger antibody-mediated therapeutic responses, they may not be favorable in the context of molecular imaging. According to our research, there are three initial resolutions to reduce nonspecific uptake by the liver and spleen[27,28]. Firstly, the preparation of probes using antibody fragments such as Fab, $F(ab)_2$ to replace intact antibodies not only avoids the interaction of the Fc region with the immune system, but also allows the probes to have a faster pharmacokinetic profile. Secondly, another strategy is predicated on genetically engineering the Fc region of an IgG to abrogate its binding with FcγRs on immune cells while maintaining its ability to bind FcRn. Thirdly, a more facile and modular approach may lie in manipulating the glycans of the Fc region. In addition, from the nature of the nuclide, ^{89}Zr is a radioactive metal ion that first ligates the antibody by a suitable chelating agent (typically using a lysine group) and then indirectly labels the antibody by non-covalently chelating the radioactive metal ion. Once antibodies have been internalized into the tumor cells, they are subject to catabolism through lysosomal degradation. The catabolites of radiometal ion chelates remain trapped (residualized) inside the cells, leading to an accumulation of radiometal (and PET signal) in the target tumor tissue and metabolic organ over time. However, iodine is usually labeled directly onto antibodies through a simple and widely used procedure, and most iodine-containing catabolites are nonpolar molecules that are rapidly lost from the liver and spleen[29]. Based on this property of radionuclide iodine, we are also conducting a study related to ^{124}I labeled 18B10, which may be more suitable for clinical translation in the future.

[00572] We also performed ^{18}F-FDG PET/CT imaging as a reference. The tumor SUVmean of [^{89}Zr]Zr-DFO-18B10 was higher than that of ^{18}F-FDG (1.10 ± 0.12 vs. 0.40 ± 0.02) at the tumor sites in the $BGC823^{CLDN18.2}$ model, and the T/M value of [^{89}Zr]Zr-DFO-18B10 was also much higher than that of ^{18}F-FDG (10.23 ± 1.30 vs. 1.80 ± 0.22).

[00573] The results of IHC revealed high and homogenous CLDN18.2 expression in $BGC823^{CLDN18.2}$ tumors, and the BGC823 xenograft tumors were negative for CLDN18.2 (Figure 18E). The stomachs of $BGC823^{CLDN18.2}$ and BGC823 tumor-bearing mice showed substantially positive expression of CLDN18.2. Neither the liver nor spleen tissue of the two types of tumor-bearing mice expressed CLDN18.2. The IHC results showed that the $BGC823^{CLDN18.2}$ tumors were strongly positive for CLDN18.2 (+++), while the BGC823 tumors were negative (-), which was consistent with the imaging and western blotting results. These results prove that the [^{89}Zr]Zr-DFO-18B10 probe we constructed has the ability to

specifically target CLDN18.2. In addition, a strong positive expression of CLDN18.2 (+++) was also observed in the gastric mucosa of all mice, but neither PET/CT imaging nor biodistribution showed any obvious uptake and retention of the probe in the stomach, likely because the expression of CLDN18.2 *in vivo* was limited to the gastric mucosa, and monoclonal antibodies had difficulty accessing the hidden CLDN18.2 binding epitope in the gastric mucosa[29] (Figure 22).

[00574] *6) Ex vivo biodistribution*

[00575] The biodistribution of [^{89}Zr]Zr-DFO-18B10 in BGC823$^{CLDN18.2}$ and BGC823 tumor–bearing mice is presented in Figure 19. At 48 h p.i., the livers in all three groups showed relatively high uptake (8.39 ± 0.59 %ID/g in BGC823$^{CLDN18.2}$ group, 9.28 ± 0.19 %ID/g in BGC823 group and 20.96 ± 0.88 %ID/g in blocking the group, respectively). The uptake value of the spleen was second to that of the liver (3.54 ± 0.26 %ID/g in BGC823$^{CLDN18.2}$ group, 2.08 ± 0.29 %ID/g in BGC823 group and 1.93 ± 0.24 %ID/g in the blocking group, respectively). Tumor uptake in BGC823$^{CLDN18.2}$ tumor bearing mice was higher (2.05 ± 0.16 %ID/g) than that in the BGC823 mice (0.69 ± 0.02 %ID/g) and blocking group (0.72 ± 0.02 %ID/g). (Figure 19A). The tumor/liver (T/L) and tumor/brain (T/B) ratios of BGC823$^{CLDN18.2}$ tumors were significantly higher than those of the other two control groups. (T/L: 0.075 ± 0.001 in the BGC823 group vs. 0.25 ± 0.003 in the BGC823$^{CLDN18.2}$ group vs. 0.035 ± 0.002 in the blocking group, T/B: 16.03 ± 1.66 in the BGC823 group vs. 40.35 ± 3.68 in the BGC823$^{CLDN18.2}$ group vs. 3.01 ± 0.53 in the blocking group, Figure 19B, D). The tumor/stomach (T/S) ratios were not significantly different among the three groups (2.00 ± 0.13 in BGC823 vs. 2.04 ± 0.43 in BGC823$^{CLDN18.2}$ vs. 1.47 ± 0.50 in blocking group, Figure 19C). Consistent with the PET/CT results, in vitro biodistribution data at 48 h p.i. showed that [^{89}Zr]Zr-DFO-18B10 aggregated in the liver and spleen, and the liver uptake in the blocking group was significantly higher than that in the other two groups, possibly because tumor uptake was blocked, resulting in the probes entering the liver directly through the bloodstream for metabolism. The difference in tumor uptake values in the three groups also reflects the excellent specificity of [^{89}Zr]Zr-DFO-18B10 for CLDN18.2-positive tumors.

[00576] *Example 6.6 Conclusion*

[00577] We successfully prepared ^{89}Zr labelling of a GMP grade anti-CLDN18.2 recombinant humanized antibody 18B10. [^{89}Zr]Zr-DFO-18B10 exhibited good specificity at the cellular level and rapid tumor accumulation which remained positive from 24 to 96 h. It provides a promising molecular probe for detecting the treatment effects of therapeutic

antibodies in humans in real time. It also provides a possibility for the screening and efficacy evaluation of patients targeted for CLDN18.2 therapy in the future.

[00578] References for Example 6 can be seen in Table 8.

[00579] **Example 7**

[00580] *Example 7.1 Radiolabeling and Quality Control of ^{177}Lu-18B10*

[00581] TZ-DOTA was synthesized with TZ-NHS and TZ-NHS at PH8.4, and TZ-DOTA reacted with ^{177}Lu solution at 60℃ for about 10 minutes at PH5.5-6 to get TZ-^{177}Lu. TCO-NHS was mixed with antibody precursor 18B10 to obtain 18B10-TCO. TZ-^{177}Lu and 18B10-TCO reacted at 37℃ for 5 min (300μg antibody per 1mCi ^{177}Lu) and purified by PD-10 column. The product ^{177}Lu-DOTA-18B10 was finally obtained. The steps and conditions for ^{177}Lu labeling are shown in Figure 23A. The labeling rate, radiochemical purity and yield of ^{177}Lu labeled 18B10 were 85.61%, 98.87% and 50% respectively. The product had good stability, and the radiochemical purity was still more than 95% at 168h after labeling (Figure 23B).

[00582] *Example 7.2 Small-Animal PET Imaging*

[00583] BGC823/AGS CLDN18.2-positive and BGC823/AGS CLDN18.2-negative tumor-bared mouse models (balb/c nude mice, female, 5weeks) were constructed and then ^{177}Lu-DOTA-18B10 imaging was performed by Micro-PET (Super Nova PET/CT, PINGSENG, China). A block control group (n=4) was set in BGC823$^{CLDN18.2}$ mice. The imaging time points were 4h, 24h, 48h, 72h, and 144h post-injection. Each mouse was injected with 300μCi ^{177}Lu-DOTA-18B10. In the positive group, the imaging was good and the tumor uptake was obvious, which reached the peak at about 72 hours and could be blocked (Figures 24A-24B). There was no significant tumor uptake in the negative group (Figures 25-26). CLDN18.2 immunohistochemical staining was performed on mouse tumor tissues dissected at the end of imaging. The expression of CLDN18.2 was positive in the positive imaging group and negative in the negative imaging group. The histochemistry was consistent with the imaging results (Figure 27).

[00584] *Example 7.3 Cell uptake*

[00585] BGC823/AGS$^{CLDN18.2}$ cells and BGC823/AGS cells after digestion were re-suspended with RPMI-1640 medium at appropriate concentrations, then added to 24-well plate 1ml per well and incubated overnight. On the second day, ^{177}Lu-DOTA-18B10 was added to the well at 0.037MBq per well (500ug unlabeled precursor was added to the block group at the same time, n=4). Cells were incubated in 5% CO_2 incubators at 37°C for 10 min,

30 min, 60 min, and 120 min (block group for 60 min, 120 min), washed and lysed, and then collected and tested with γ-counter instrument. Cellular uptake results were expressed as percentage injected activity (%IA) per 10^5 cells. The results showed that BGC823/AGS$^{CLDN18.2}$ positive cells had significant uptake of ^{177}Lu-DOTA-18B10, which was significantly different from the negative and block groups (Figure 28).

[00586] *Example 7.4 Saturated binding experiment*

[00587] AGS$^{CLDN18.2}$ cells after digestion and centrifugation were re-suspended with RPMI-1640 medium to an appropriate concentration, then added to 24-well plate with 1ml per well and incubated overnight. On the second day, ^{177}Lu-DOTA-18B10 was added to the well (n=4) at different concentration gradients (8 concentrations of 1.25~160 nmol/L), incubated in 5% CO_2 incubator at 37°C for 120 minutes, and cells were collected after washing and lysis and tested with γ-counter instrument. The values were fitted with GraphPad Prism. The results showed that Kd constant in the saturated binding test was 12.87, indicating that the probe is able to target CLDN18.2 molecules specifically (Figure 29A).

[00588] *Example 7.5 Pharmacokinetic experiment*

[00589] Pharmacokinetics experiments were performed on normal KM mice (female, n=6) by injecting 0.56MBq ^{177}Lu-DOTA-18B10 into the tail vein. At 1 minute, 3 minutes, 5 minutes, 10 minutes, 15 minutes, 30 minutes and 1 hour, 2 hours, 4 hours, 8 hours, 12 hours, 24 hours, 48 hours, 72 hours, 96 hours, 120 hours, 192 hours after injection, periorbital venous blood was collected by capillary tube and radioactive detection was performed with γ-counter. The collected data were analyzed by GraphPad Prism to calculate pharmacokinetics. The results showed ^{177}Lu-DOTA-18B10 has a good pharmacokinetics, the half-life (slow) is 22.29 h and the half-life (fast) is 0.4512 h (Figure 29B).

[00590] *Example 7.6 Biodistribution*

[00591] ^{177}Lu-DOTA-18B10 was injected into mice through the caudal vein, and the mice were anesthetized and killed at a predetermined time point. Major organs and tissues of the mice, such as blood, stomach, intestine, bone, muscle, heart, lung, spleen, liver, kidney and tumor, were collected, and the radiation was detected by γ-counter instrument. Biodistribution results are expressed as the percent of injected dose per gram (%ID/g). Each mouse was injected with ^{177}Lu-DOTA-18B10 of 0.44-0.56 MBq, and tissue samples were taken at 8 h, 24 h, 48 h, 72 h, and 144 h after injection (n=4). In the block group, an equivalent dose of ^{177}Lu-DOTA-18B10 was injected with 50μg/g body weight of unlabeled 18B10 and sampled at 48h time point (n=4). The results showed that the biodistribution was

consistent with the PET imaging. The tumor distribution was high and could be blocked by unlabeled precursor (Figures 30 and 31).

[00592] *Example 7.7 Therapeutic experiments*

[00593] Three groups of BGC823/ AGS CLDN18.2 positive tumor-bearing mice (n=6) with tumor volume of about 100mm^3 were prepared, and 300μCi/150μCi ^{177}Lu-DOTA-18B10 were injected into caudal vein as treatment group and equal volume of PBS was injected as blank control group, respectively. Tumor volume and mouse body weight were measured and recorded every other day until day 16 to 17 after injection. The results showed that no matter BGC823$^{CLDN18.2}$ or AGS$^{CLDN18.2}$ model mice, ^{177}Lu-DOTA-18B10 had significant therapeutic effect (Figure 32). The efficacy of 300μCi group was better than that of 150μCi group, and both were better than blank control group (Figure 32). HE staining of the tumor tissue sampled on the last day also clearly showed obvious tumor tissue damage in the treatment group (Figure 34). In addition, HE staining of all important organs (heart, liver, spleen, lung, kidney, stomach, intestine, and muscle) from the last day and weight records of all three groups showed that ^{177}Lu-DOTA-18B10 treatment had no significant effect on body weight and normal organs of mice (Figure 35).

[00594] **Example 8**

[00595] *Example 8.1 Abstract*

[00596] Claudin 18.2 (CLDN18.2), due to its highly selective expression in tumor cells, has made breakthrough progress in clinical research and is expected to be integrated in routine tumor diagnosis and treatment. **Methods:** In this research, we developed a molecular probe for PET imaging and treatment by labeling a scFv-Fc antibody that specifically targets CLDN18.2 with radionuclides (^{124}I and ^{177}Lu) and evaluated the diagnostic and therapeutic potentials in tumor bearing model models. **Results:** The molecular probes ^{124}I-SF106 and ^{177}Lu-DOTA-SF106 possess high radiochemical purity (RCP, 95.63 ± 2.90% and 97.05 ± 1.1%) and exhibit good stability in phosphate buffer saline and 5% human serum albumin (RCP, 92.44 ± 4.68% and 91.03 ± 2.42% at 120 h). ^{124}I-SF106 uptake in cells expressing CLDN18.2 was well targeted and specific, and the dissociation constant was 17.74 nM. ^{124}I-SF106 micro-PET imaging showed maximum standardized uptake value (SUVmax) achieved peak uptake in CLDN18.2 positive tumors at 48 h after injection and was significantly higher

than CLDN18.2-negative tumors (1.83 ± 0.02vs 1.23 ± 0.04, $p < 0.001$). The SUVmax ratio of the tumor to muscle and liver in the $BGC823^{CLDN18.2}$ mouse model with CLDN18.2 positive was significantly higher than that in the BGC823 mouse model with CLDN18.2 negative. ^{124}I-SF106 dosimetric study showed that the effective dose was 0.0705 mSv/MBq in human, which was medical safety standards for further clinical applications. The results of preliminary treatment experiments showed that 3 MBq of ^{177}Lu-DOTA-SF106 in the CLDN18.2-expressing tumor-bearing mice could significantly inhibit tumor growth. **Conclusion:** These results indicate that radionuclide-labeled scFv-Fc molecular probes (^{124}I-SF106 and ^{177}Lu-DOTA-SF106) provide a new possibility for the diagnosis and treatment of CLDN18.2 positive cancer patients in clinical practice. Graphic Abstract is shown as in Figure 36.

[00597] *Example 8.2 introduction*

[00598] Gastric carcinoma (GC) is among the most prevalent malignancies worldwide. In developing countries, about 80% of gastric cancer patients are diagnosed at advanced stage (*1–3*). For these patients, radiotherapy and chemotherapy were the main treatments, which aim to improve symptoms and extend survival time. However, the prognosis is dismal, and the median survival time is only 4-13 months (*4,5*). Targeted therapy is an emerging therapeutic approach that holds great promise for improving patient survival and has valuable clinical applications (*6*).

[00599] CLDN18.2 has been confirmed as a target for therapeutic antibodies. In a study by Jin Haek et al., 74.4% of study patients showed expression of CLDN18.2 (*7*). CLDN18.2 is a subtype of the tight junction protein family, present in the TJ supramolecular complex of normal gastric mucosal cells (*8–10*). However, malignant tumor cells lose their polarity, exposing the epitope of CLDN18.2 and allowing in vivo antibody binding (*11,12*). Zolbetuximab (IMAB362) is a novel chimeric IgG1 antibody, that has shown significant improvement in progression-free survival and overall survival of patients with CLDN18.2-

positive gastric or gastroesophageal junction cancer when used in combination with chemotherapy (*13*,*14*).

[00600] CLDN18.2 expression is mainly evaluated by immunohistochemistry in clinical research and diagnosis, and as is inherently limited, such as the scope of tissue biopsy, the quality of tumor sections, and tumor heterogeneity, which may not fully reflect the true level of CLDN18.2 expression in patients.

[00601] Current clinical studies utilize immunohistochemistry (IHC) methods to evaluate CLDN18.2 expression, and as such is inherently limited by several aspects including quality and quantity of tumor slides required, heterogeneity of the tumor as well as challenges of performing on treatment biopsies. However, as such is inherently limited by several aspects including size and location of tissue biopsy samples, quality and quantity of tumor slides required, heterogeneity of the tumor. Thus, real-time controllable detection technology to accurately detect CLDN18.2 expression and distribution throughout the body at baseline and on treatment would be valuable. Positron emission tomography (PET) is a widely used clinical diagnostic method that detects target molecule distribution in patients through radionuclide probe. Our previous report on HER2-positive lesion detection in gastric cancer patients using a ^{124}I-trastuzumab PET radioligand confirmed its feasibility (*15*).

[00602] Previously, we reported a molecular probe based on CLDN18.2-specific antibody 5C9, modified with ^{124}I, Cy5.5, and FD1080. This probe was capable of detecting CLDN18.2 expression in solid tumors and guiding surgical treatment of CLDN18.2-overexpression tumors (*16*). Compared to full-length antibodies, single-chain variable fragment-crystallizable protein (scFv-Fc) structures offers greater editability, and may enhance tissue permeability, accelerate blood clearance, and decrease the background noise of tumor imaging (*17–19*). The fusion of intact Fc regions enables scFv-Fc antibodies with comparable pharmacokinetics to intact antibodies (*20*). In this study, we successfully

developed a novel single-chain fragment variable fragment crystallin antibody (Hu18B10HaLa scFv-Fc, also referred to as SF106 in this study) and labeled the radionuclide iodine-124 to explore its potential for PET imaging. Additionally, we obtained the therapeutic molecular probe ^{177}Lu-DOTA-SF106 by labelling with lutetium-177 radionuclide and performed preliminary testing of its inhibition on tumour growth in a CLDN18.2 expression mouse tumor model.

[00603] *Example 8.3 MATERIAS AND METHODS*

[00604] *1) Antibody, Cell Culture and Tumor Bearing Model Models Construction*

[00605] The scFv-Fc antibody targeting CLDN18.2 was produced using hybridoma technology. The study mainly used gastric cancer cell lines, BGC823 and AGS, as well as BGC823$^{CLDN18.2}$ and AGS $^{CLDN18.2}$ cells with high levels of CLDN18.2 expression. In vitro cell uptake experiments were conducted using unlabeled SF106 antibody to block uptake of radiolabeled SF106 antibody. Further information is provided in supplementary materials.

[00606] *2) Radionuclide labeling and In Vitro Study*

[00607] In this study, ^{124}I-SF106 and ^{177}Lu-DOTA-SF106 probes were constructed through SF106 antibody radiolabeling with the radionuclides ^{124}I and ^{177}Lu, respectively. The radiochemical purity and in vitro stability of the labeled products were studied. The detailed operation is provided in supplementary materials.

[00608] *3) Radioimmunoimaging and Radionuclide Therapy Studies*

[00609] All animal experiments were carried out in compliance with the guidelines of the Peking University Institutional Animal Care and Use Committee (EAEC 202201). GBC823 and BGC823$^{CLDN18.2}$ models were injected with ^{124}I-SF106, and PET static imaging was performed at different times after injection. The AGS$^{CLDN18.2}$ model was randomly divided into experimental group and control group. The experimental group was injected with ^{177}Lu-DOTA-SF106, and the control group was injected with the same volume of PBS for tumor inhibition experiments.

[00610] *4) Statistical Analysis*

[00611] All data are expressed as the mean ± standard deviation (SD). Mann–Whitney t tests were performed for the in vitro studies. Data from different groups were analyzed using two-way ANOVA multiple comparisons, and *P* values of less than 0.05 were considered as statistical significance. The significance is represented with asterisks (*) according to the following values: $P < 0.05$ (*), $P < 0.01$ (**), and $P < 0.001$ (***).

[00612] *Example 8.4 RESULTS*

[00613] *1) Construction and Molecular Detection of SF106 Antibody*

[00614] scFv-Fc (SF106) antibody was constructed by fusing scFv to human Fc of IgG1(SEQ ID NO: 49), the scFv was designed from the VH-linker-VL orientation. The VH and VL sequences are from Hu18B10HaLa, and the linker is (GGGGS)4. (Figure 37A). The molecular weight of SF106 antibody was further verified to be 108,303 Da by MALDI-TOF-MS (Figure 37B). The SDS-page test showed that the SF106 had only one band at 108 kDa. Meanwhile, a molecular fragment close to 55 kDa was detected after denaturing at 90℃ for 10 minutes (Figure 42B). FACS analysis of SF106 binding to HEK293-human CLDN18.2-hi cells showed that the half maximal effective concentration (EC50) values were 11.31 nM (Figure 37C).

[00615] *2) Radiolabeling of ^{124}I-SF106 and In Vitro Stability*

[00616] The ^{124}I labeling process of SF106 antibody is shown in Figure 38 panel A. The trial labeling by nonradioactive natural iodine (^{nat}I), the products were tested by MALDI-TOF with an average molecular weight of 108963 Da, about 360 Da increase relative to the SF106 antibody, at the same time, we verified the labeled antibody molecules by SDS-PAGE (Figure 42A and 42B). The labeling rate of ^{124}I-SF106 was 95.63 ± 2.90% (n = 3) and the radiochemical purity (RCP) of ^{124}I-SF106 after purification was 98.18 ± 0.93% (n = 3) (Figure 42C and 42D). The stability experiment showed that the radiochemical purity of ^{124}I-

SF106 was 92.44 ± 4.68% (n = 3) and 91.03 ± 2.42% (n = 3) which were incubated in 0.01M PBS and 5% HSA solutions for 120 h, respectively (Figure 37B).

[00617] *3) In Vitro Cellular Uptake and Biological Evaluations of ^{124}I-SF106*

[00618] Flow cytometry results showed that 71.0% of BGC823$^{CLDN18.2}$ cells had a positive signal with CLDN18.2 antibody (1D5) (Figure 37C). The uptake of ^{124}I-SF106 in BGC823$^{CLDN18.2}$ cells was significantly higher than that in BGC823 cells at all selected time points of this experiment (0.47 ± 0.02% vs 0.2 ± 0.01% at 10 min, 0.67 ± 0.03% vs 0.20 ± 0.05% at 30 min, 0.93 ± 0.02% vs 0.17 ± 0.02% at 60 min, 0.96 ± 0.04% vs 0.22 ± 0.09% at 120 min, $P < 0.001$).

[00619] The uptake of ^{124}I-SF106 in BGC823$^{CLDN18.2}$ cells increased with incubation time, and no significant changes in BGC823 cells. ^{124}I-SF106 uptake in BGC823$^{CLDN18.2}$ cells were significantly reduced by SF106 blocking after 120 min incubation in advance (unblocked group vs blocked group: 0.96 ± 0.04% vs 0.21 ± 0.02%, $P < 0.001$) (Figure 37D).

[00620] The binding constant (K_d = 17.74 nmol/L) of ^{124}I-SF106 to CLDN18.2 receptors was determined by a cell saturation binding assay using BGC823$^{CLDN18.2}$ cells (Figure 42E).

[00621] *4) Dosimetry Estimation of ^{124}I-SF106*

[00622] The study showed that the half-life of ^{124}I-SF106 in the elimination phase was 27.68 h, and the half-life in the distribution phase was 0.6354 h in vivo (Figure 42F). Human organ radiation dosimetry was estimated from the biodistribution data of ^{124}I-SF106 using OLINDA/EXM 2.0 software package. Osteogenic cells received the highest dose (0.513 mSv/MBq) followed by lungs (0.234 mSv/MBq) from TABLE 6. The radiation dose for the kidneys and liver was 0.137 mSv/MBq and 0.187 mSv/MBq, and the effective dose was 0.0873 mSv/MBq, this is acceptable in nuclear medicine research.

[00623] *5) Micro-PET/CT Imaging of ^{124}I-SF106 in Tumor-Bearing Mice*

[00624] The distribution and metabolic characteristics of ^{124}I-SF106 were assessed by Micro-PET/CT imaging at different time points (4, 24, 48,72, 96 and 120 h) after injection of

the tumor-bearing mouse model. Maximum intensity projection (MIP) images of Micro-PET/CT were shown in Figure 39. A significant accumulation of ^{124}I-SF106 was observed in the CLDN18.2-expressing BGC823$^{CLDN18.2}$ tumor, showing favorable imaging results from 24 to 120 h after injection. The signal of ^{124}I-SF106 in the BGC823$^{CLDN18.2}$ tumor-bearing mouse model had a peak uptake at 48 h, and the highest SUVmax was 1.83 ± 0.02. In contrast, BGC823 tumor-bearing mice without CLDN18.2 expression exhibited a lower concentration of ^{124}I-SF106, with the highest SUVmax at 1.23 ± 0.04 at 48 h. Furthermore, co-injection of unlabeled SF106 antibody in the blocking group effectively reduced the concentration of ^{124}I-SF106 in tumor of CLDN18.2-expressing BGC823$^{CLDN18.2}$ tumor-bearing mice (Figure 40 panel A; Figure 43 panel A, panel B and panel C). In normal tissues, ^{124}I-SF106 was mostly detected in the liver and blood. Meanwhile, we verified the biodistribution of ^{124}I-SF106 in KM mice and ^{125}I-SF106 in BGC823$^{CLDN18.2}$ tumor-bearing mouse model. The results showed that the molecular probes were mainly distributed in the blood and gradually decreased with time, and the metabolic trend of ^{125}I-SF106 in tumors was consistent with the imaging results (Figures 43 panel D and panel E).

[00625] For imaging, we performed co-injection of the anti-CLDN18.2 monoclonal antibody Hu18B10HaLa specifically targeting CLDN18.2 for target blocking, while using ^{124}I-IgG as a control group (Figure 44 panel A). The co-injection of Hu18B10HaLa reduced the uptake of ^{124}I-SF106 by tumors significantly. The SUVmax value was significantly lower in the tumor than that of the ^{124}I-SF106 group at each time point, while the SUVmax value in the tumor gradually decreased with imaging time in the ^{124}I-IgG group (Figure 44 panel B).

[00626] In addition, the SUVmax ratio of tumor to muscle of ^{124}I-SF106 in BGC823C$^{LDN18.2}$ tumor-bearing mouse was significantly higher than that in BGC823 tumor-bearing mice at each imaging time ($P < 0.05$), and co-injection of SF106 can significantly reduce the ratio of tumor to muscle in BGC823C$^{LDN18.2}$ tumor-bearing mouse (Figure 40

panel B). The tumor to liver (T/L) ratios at each time point after injection of ^{124}I-SF106 were significantly higher than those of the other control groups, and tumor/heart (T/H) ratios were higher than those of the other control groups at 72 h after injection (Figures 40 panel C and panel D). These results indicate that ^{124}I-SF106 has specific targeting effect on CLDN18.2 in vivo.

[00627] *6) Immunohistochemistry*

[00628] Immunohistochemistry results showed high expression of CLDN18.2 in tumors in BGC823$^{CLDN18.2}$ tumor-bearing mouse model, while there was no expression of CLDN18.2 in BGC823 tumor tissue (Figures 40 panel E and panel F), which was consistent with Micro-PET/CT imaging results.

[00629] *7) Radioligand Therapy Studies*

[00630] SF106 antibody was labeled with ^{177}Lu using a two-step method, as illustrated in Figure 41 panel A. Mass spectrometry was employed to detect the intermediate product coupled with DOTA. The molecular weight of DOTA-SF106 was found to be 110339.972, which is 2036.848 higher than that of SF106, equivalent to 2.67 times the DOTA molecular weight (Figure 45 panel A). The quality test results of the labeled product revealed that the labeling rate of ^{177}Lu-DOTA-SF106 exceeded 79.36% following a 30-minute labeling reaction. Furthermore, the radiochemical purity after purification via a PD10 column demonstrated a purity level greater than 95.95% (Figures 45 panel C and panel D). An in vitro stability test was performed on the ^{177}Lu-DOTA-SF106 product, revealing a radiochemical purity above 89.37% after 120 h in 0.01 M PBS solution and a purity greater than 95.91% after 120 h in 5% HSA solution (Figure 45 panel B).

[00631] We injected ^{177}Lu-DOTA-SF106 into BGC823$^{CLDN18.2}$ and BGC823 tumor-bearing mouse for small-animal SPECT/CT imaging at different time. The results showed that there was a significant accumulation of ^{177}Lu-DOTA-SF106 in tumors with high

expression of CLDN18.2 at 24h after injection , and ^{177}Lu-DOTA-SF106 were mainly accumulates in liver and spleen tissues in vivo (Figures 41 panel B and panel C).

[00632] In order to preliminarily study the inhibitory effect of ^{177}Lu-DOTA-SF106 on the growth of tumors expressing CLDN18.2, an experimental group and a control group (n = 6) were set up for this experiments. Each mouse in the experimental group was injected with about 3 MBq of ^{177}Lu-DOTA-SF106, and the control group was injected with the same volume of PBS solution. After injection, the tumor size and weight changes of each group were monitored as shown in Figure 41 panel D and panel E. At the end of the treatment on the 18 th day, The tumor volume of ^{177}Lu-DOTA-SF106 group was 380.73 ± 174.77, which was significantly different from that of PBS group (1040.04 ± 422.40) ($P < 0.001$), that means the tumor growth of mice was significantly slowed down after injection of ^{177}Lu-DOTA-SF106. At the end of the treatment, the weight of the mice in the experimental group was 13.13 ± 0.90, and the weight of the mice in the PBS group was 13.13 ± 1.79. Compared with the initial weight, the weight of the two groups of mice decreased, but there was no significant difference in the weight of the two groups of mice, and no mice died during the experiment.

[00633] *Example 8.5 DISCUSSION*

[00634] CLDN18.2, as a novel target for the diagnosis and treatment of gastric cancer, has been extensively studied with monoclonal antibodies (mAbs), nanobodies, bispecific antibodies (BsAbs), chimeric antigen receptor T (CAR-T) cells, and antibody-drug conjugates (ADCs) (*21*,*22*). Among them, zobetuximab mAb has significantly prolonged patient survival in clinical studies and may become the standard therapeutic drug for clinical patients (*23–25*).

[00635] In clinical diagnosis and treatment, CLDN18.2 expression is mainly measured through endoscopic biopsy to obtain tissue samples for immunohistochemical detection

(*26*,*27*). However, due to sampling time, sampling range and size, and other factors, sample test results have certain limitations and cannot fully reflect the true level of CLDN18.2 expression in patients (*28*). Compared with mmunohistochemical detection, positron emission tomography (PET) can provide non-invasively, real-time, quantitative and comprehensive measurement of expression and distribution status of targets in vivo through radioactive molecular probes, which can provide more comprehensive and accurate results for clinical management (*29*). Consequently, the generation of novel PET molecular tracers for CLDN18.2 is crucial for the advancement and implementation of CLDN18.2 targeted therapy.

[00636] We developed a radioactive molecular probe that targets CLDN18.2 using an scFv-Fc antibody, with a molecular weight of 108 kDa and a strong affinity for CLDN18.2. By antibody engineering, the molecular weight of the scFv-Fc antibody was reduced compared to the intact antibody. This approach accelerated the metabolic rate of the antibody in vivo, minimizing radiation and toxicity to normal organs (*30*). The minimum structure of antigen binding was retained, enhancing the permeability of the antibody to solid tumors while maintaining high affinity. These optimizations make the antibody well-suited for immunoimaging applications (*18*,*31*).

[00637] Radionuclide ^{124}I has a half-life of about 4.2 days, which is extensively used in both experimental and clinical PET imaging studies. An important characteristic of ^{124}I is that it allows antibody labeling without compromising the antibody's immune activity (*32*,*33*). In our prior research, we efficaciously tagged PD-1 antibody and HER2 antibody with ^{124}I, and demonstrated favorable biodistribution and imaging traits via PET/CT at a secure radiation dosage (*15*,*34*). Furthermore, the procedure for utilizing the antibody labeled with ^{124}I is uncomplicated, and the endpoint product can be refined after undergoing a one-minute reaction at ambient temperature, This facilitates the preparation and commercialization of the

molecular probe. The ^{124}I-SF106 labeling efficiency in this study was highly satisfactory with a rate of 95.63 ± 2.90 % and radiochemical purity of 98.18 ± 0.93 % and displayed excellent in vitro stability.

[00638] We chose the BGC823 cell line of human gastric cancer as a negative model, while BGC823 cells expressing CLDN18.2 were chosen to serve as a positive model. It has been confirmed that ^{124}I-SF106 exhibits specific uptake maintains good affinity towards cells expressing CLDN18.2, with a K_d value of 17.74 nmol/L.

[00639] Immune PET imaging revealed that the distribution of ^{124}I-SF106 in animal models was analogous to that of intact antibodies with SUVmax peaking at 48 h. In comparison to full antibodies, the time to attain maximum tumor uptake is reduced, while offering a greater amount of uninterrupted imaging data than nanobodies (*16,35*). The uptake of probes in tumor tissues exhibited a significantly higher level compared to those in muscle, liver, and heart tissues, resulting in a favorable ratio between tumor tissue and other organs. The expression of CLDN18.2 in patients can be comprehensively detected by PET noninvasive imaging, which can provide reference for clinical research and continuous observation of targeted therapy.

[00640] The scFv-Fc antibodies exhibit similar in vivo metabolism and distribution as full antibodies, and PET imaging revealed prolonged retention times in tumor. We developed a therapeutic radiolabeled molecular probe, ^{177}LU-DOTA-SF106, which demonstrated excellent radiochemical purity and in vitro stability. Tumor-bearing mice expressing CLDN18.2 were treated with ^{177}LU-DOTA-SF106 for targeted therapy. The experimental group received an injection of approximately 3 MBq of ^{177}LU-DOTA-SF106, which significantly inhibited tumor growth. At the end of the study, a significant difference in tumor volume was observed between the experimental and control groups. It should be noted that the weight of both mouse groups decreased, which may be caused by external factors. Further

investigation is required to determine the cause of this phenomenon. There was no significant difference in body weight between the experimental group and the control group under the same factors, indicating that injection of 3 MBq ^{177}LU-DOTA-SF106 did not cause abnormal changes in body weight.

[00641] In this research, we developed a molecular probe ^{124}I-SF106 and confirmed its effective targeting and high specificity toward CLDN18.2 both in cells and tumor-bearing mouse models. PET/CT imaging demonstrated an improved ratio between tumor tissue and other organs at 48 h and post-injection. Further optimization could be done by refining the antibody's structure to enable effective infiltration into cancerous tissues and swift elimination from non-specific organs, thereby achieving an optimal imaging result. Moreover, the treatment study is only a preliminary proof of concept and requires further confirmation. Furthermore, It is understood animal models cannot always be replicated 100% in human, and more optimization and validation are necessary for ^{124}I-SF106 in clinical translation.

[00642] *Example 8.6 CONCLUSION*

[00643] Here, we have successfully radiolabeled SF106 antibody using radionuclides ^{124}I and ^{177}Lu, and the molecular probe has excellent radiochemical purity and stability. The radiopharmaceutical ^{124}I-SF106 exhibited excellent targeting of CLDN18.2 in vivo and produced a favorable PET imaging on tumors. The therapeutic radiolabeled molecular probe ^{177}Lu-DOTA-SF106 exhibits significant antitumor activity against transplanted CLDN18.2 expressing tumors in mice. Thus, the radiolabeled molecular probe we developed is anticipated to offer a novel option for detecting and treating patients with CLDN18.2 overexpression.

[00644] *Example 8.7 KEY POINTS*

[00645] QUESTION:

[00646] What is the potential application of a scFv-Fc radionuclide probe targeting cldn18.2 in the diagnosis and treatment of tumors?

[00647] PERTINENT FINDINGS:

[00648] The cldn18.2-targeting antibody has achieved significant progress in anti-tumor research. The metabolic properties of the scFv-Fc antibody and monoclonal antibody are similar, rendering it highly promising for radionuclide probe studies.

[00649] IMPLICATIONS FOR PATIENT CARE:

[00650] This study observed promising PET imaging outcomes in animal models after injection with ^{124}I-labeled radioactive scFv-Fc (SF106) probes. Additionally, we have a favorable results of radioimmunotherapy studies with ^{177}Lu-DOTA-SF106 in animal models. These findings offer new insights into the diagnosis and treatment of cancers that exhibit high levels of CLDN18.2 expression.

[00651] *Example 8.8 Supplementary Materials*

[00652] *Experimental methods*

[00653] *1) Antibody*

[00654] The antibody scFv-Fc (SF106) targeting CLDN18.2 was constructed by fusing the scFv of Hu18B10HaLa with human Fc of IgG1, kindly provided by Suzhou Transcenta Therapeutics Co., Limited. (Suzhou, China). Specifically, the cDNA of scFv antibody targeting CLDN18.2 was screened by hybridoma technology, and scFv-Fc was inserted into pcDNA3.1(+) vector and plasmid was extracted and confirmed by sequencing. ExpiCHO cells were transfected using the ExpiCHO transfection kit with the plasmid prepared above. Transfected cells were cultured in shake flasks at 125 rpm at 8% CO_2 and 37°C incubator. Cell culture was harvested on day 10, and the harvested antibodies were purified by affinity chromatography with MabselectSure resin. The resulting antibody was analyzed to determine purity using SDS-PAGE and size exclusion chromatography (TSKgel G3000SWXL, TOSOH). The production flow is shown in the figure 37A. SF106 was detected by SDS-Page and matrix assisted laser desorption ionization time-of-flight mass spectrometry (MALDI-TOF-MS) (Bruker Dalton, Germany) (Figure 37B)

[00655] *2)Cell culture*

[00656] Human gastric cancer cell line BGC823, AGS and expressing CLDN18.2 cell line $BGC823^{CLDN18.2}$, $AGS^{CLDN18.2}$ was maintained at Peking University Cancer Hospital and Institute (Beijing, China). HEK293-human CLDN18.2-hi cells was maintained at Suzhou Transcenta Therapeutics Co., Limited. (Suzhou, China). Cells were cultured in RPMI 1640 (HEK293 cells with DMEM) supplemented with 10% fetal bovine serum and 1% pen-Strep solution (penicillin: 10000 units/mL; streptomycin: 10 mg/mL) at 37 ℃ and 5% CO_2.

[00657] *3)Animal Model*

[00658] KM and BABL/c nude mice, purchased from Charles River (Beijing, China), were used in this experiment. Tumor-bearing mice were administered with BGC823, AGS, $BGC823^{CLDN18.2}$ or $AGS^{CLDN18.2}$ (1×10^6) cells in the right axilla of BABL/c nude mice until tumors grew to diameter of 6-10 mm. All animal experiments were carried out in compliance with the guidelines of the Peking University Institutional Animal Care and Use Committee (EAEC 202201). For the study of radionuclide ^{124}I, all animals were given KI (0.5%) aqueous solution as a pre-blocking agent three days prior to the commencement of the experiment.

[00659] *4)Preparation of $^{nat/124/125}I$-SF106 and ^{177}Lu-DOTA-SF106*

[00660] Non-radioactive $K^{nat}I$ solution 50 μL (4mg/mL) radionuclides were mixed with 500 μL phosphate buffer (0.1 M) in a reaction tube. Then, add 100 μL of SF106 (4.2 mg/mL) and 15 μL of NBS (1 mg/mL). The mixture was allowed to react for 1 min at room temperature and suspended for 100 μL of human serum albumin (HSA, 10%). Then, the final radiopharmaceuticals was purified by the PD-10 column with 2.5 mL of 0.01M PBS.

[00661] Radionuclide ^{124}I was produced in our department using a medical cyclotron with a solid target system. ^{124}I radionuclides were mixed with 500 μL of phosphate buffer (0.1 M) in a reaction tube. Then, add 100 μL of SF106 (4.2 mg/mL) and 15 μL of NBS (1 mg/mL). The mixture was allowed to react for 1 min at room temperature and suspended in

100 μL of human serum albumin (HSA, 10%). Then, the final product was purified by the PD-10 column with 2.5 mL of 0.01M PBS. Before and after purification, the radiochemical purity of the compounds was measured using a thin layer radioactive chromatography scanner (Radio-TLC).

[00662] ^{125}I radionuclides were mixed with 500 μL of phosphate buffer (0.1 M) in a reaction tube. Then, add 100 μL of SF106 (4.2 mg/mL) and 15 μL of NBS (1 mg/mL). The mixture was allowed to react for 1 min at room temperature and suspended for 100 μL of human serum albumin (HSA, 10%). Then, the final product was purified by the PD-10 column with 2.5 mL of 0.01M PBS. Before and after purification, the radiochemical purity of the compounds was measured using a thin layer radioactive chromatography scanner (Radio-TLC). ^{124}I radiolabel with IgG and Hu18B10HaLa with the same protocol as SF106.

[00663] ^{177}Lu labeled antibody was prepared by adding DOTA (10mg/ml) with 20 times the molar amount of antibody to the reaction tube containing 100 μL SF106 (4.6mg/ml), the reaction pH (8-8.5) was adjusted by metal-free sodium carbonate buffer, then at 37°C coupled for 1 h, purified by PD-10 column, and the obtained DOTA-SF106 antibody was detected by MALDI-TOF-MS. 120 μL of 0.05M hydrochloric acid / 1M sodium acetate buffer containing 65.68 MBq ^{177}Lu was added to 250 μL conjugated DOTA-SF106 antibody (0.44mg/ml), conjugated at 37°C for 30min, and purified by PD-10 column. Before and after purification, the radiochemical purity of the compounds was measured using a thin layer radioactive chromatography scanner (Radio-TLC).

[00664] *5)Molecular property detection*

[00665] Cells BGC823 and BGC823$^{CLDN18.2}$ (2-5 × 10^5) were collected and washed with cold PBS Five times and stained with 200 μL (1 μg/mL) CLDN18.2 antibody (1D5) for 30 min at 37℃ followed by cold PBS five times and then subjected to flow cytometry with BD FACSAria. All experiments were conducted to avoid light measures.

[00666] The antibody affinity was detected by FACS, and HEK293-human CLDN18.2-hi cells were incubated with different concentrations of FITC conjugated SF106 antibody (87.405, 29.135, 9.7115, 3.237, 1.079, 0.3595, 0.12, 0.04, 0.0135, 0.0045, 0.001 nM) and set up isotype controls (n=3). Fluorescence signals were detected of 1×10^4 cells. The results shown in Figure 42B, EC50 was 11.31nM

[00667] Mass spectrometric detection of ^{nat}I-SF106 and DOTA-SF106. The 2 μL labeled sample was added to the target spot area, and the average molecular weight was detected by matrix assisted laser desorption ionization time-of-flight mass spectrometry (MALDI-TOF-MS). At the same time, 15 μl of SF106, ^{124}I-SF106 and ^{nat}I-SF106 were loaded for SDS-PAGE electrophoresis, stained with Coomassie brilliant blue, and analyzed by Micro-PET imaging.

[00668] *6)Stability*

[00669] The radiochemical purity of ^{124}I-SF106 and ^{177}Lu-DOTA-SF106 was measured by Radio-TLC. 2 - 5μL of ^{124}I-SF106 or ^{177}Lu-DOTA-SF106 stored in 0.01 M PBS or 5 % HSA solution was spotted on SG-ITLC paper, respectively. Saline was utilized as the developer in the detection of ^{124}I-SF106, while saturated EDTA solution was employed in the detection of ^{177}Lu-DOTA-SF106.

[00670] *7)Cellular Experiments*

[00671] BGC823 and BGC823$^{CLDN18.2}$ cells were suspended in RPMI-1640 cultured medium plus 10% FBS and antibiotics (1×10^5 cells/mL), after 24 hours to allow the cells to adhere to the well on a 24-well plate for uptake and saturation binding experiments.

[00672] Cell uptake experiments. 500 μL (74 kBq) ^{124}I-SF106 mixture with serum-free medium was added to each well (n = 4), and 100 μg SF106 was added as blocking at the last time point. The 24-well plate was cultured at 37℃ and the reaction was terminated at 10, 30, 60, and 120 min. Thereafter, the 24-well plate was washed three times with 0.01M PBS and

collected in counting tubes after dissolution with cell lysis solution for measurement on γ-counter.

[00673] The saturation binding experiment. The ^{124}I-SF106 product concentration was divided into six concentration gradients (0.185 kBq, 0.37 kBq, 1.85 kBq, 3.7 kBq, 18.5 kBq, and 37 kBq, and n=4) and added to a 24-well plate, respectively. Each gradient was repeated four times, and 100 μL of product solution was added to each well. The 24-well plate was cultured at 37℃ for 120 minutes. Thereafter, the 24-well plate was washed three times with 0.01M PBS and collected in counting tubes after dissolution with cell lysis solution for measurement on γ-counter. The value of the binding constant K_d was calculated according to the fitting curve of the summarized data.

[00674] *8)Pharmacokinetics Experiments*

[00675] KM female mice were intravenously injected with 0.37 MBq ^{124}I-SF106 via the tail vein. Blood samples were collected at 1 min, 5 min, 10 min, 15 min, 30 min, 1 h, 2 h, 4 h, 8 h, 24 h, 48 h, 96 h and 120 h by capillary tubes from the periorbital vein (n = 6), and radioactivity measured using a γ-counter after weighing. Results are expressed as the percent of injected dose per gram (%ID/g).

[00676] *9)Biodistribution studies.*

[00677] BGC823$^{CLDN18.2}$ tumor-bearing mice female mice were intravenously injected with 0.37 MBq ^{125}I-SF106 via the tail vein. Mice were sacrificed in groups by cervical dislocation after intravenous injection at 4 h, 24 h, 48 h, 96 h, and 120 h (n=3). The main organs, including the blood, heart, liver, spleen, lung, kidneys, stomach, intestines, muscle, bone, brain and tumor were collected, weighed, and measured for radioactivity using the γ-counter. The reference standard was repeated 10 times with a 1% injection dose. The results are expressed as the percent of injected dose per gram (%ID/g).

[00678] KM female mice were intravenously injected with 0.37 MBq ^{124}I-SF106 via the tail vein. Mice were sacrificed in groups by cervical dislocation after intravenous injection at 4 h, 24 h, 96 h, and 120 h (n=3). The main organs, including the blood, heart, liver, spleen, lung, kidneys, stomach, intestines, muscle, bone, and brain, were collected, weighed, and measured for radioactivity using the γ-counter. The reference standard was repeated 10 times with a 1% injection dose. The results are expressed as the percent of injected dose per gram (%ID/g).

[00679] *10)Micro-PET/CT and Small-Animal SPECT/CT Imaging*

[00680] Micro-PET/CT was used to explore the metabolism and distribution of ^{124}I-SF106 in CLDN18.2-expressing tumor-bearing mice. 3.7 MBq of ^{124}I-SF106 was injected to the BGC823$^{CLDN18.2}$ tumor-bearing mouse, while unlabeled SF106 antibody was injected as a blocking agent with ^{124}I-SF106 for the control group. Tumor-bearing mice without CLDN18.2 were used as the negative control and were injected with the same dose of ^{124}I-SF106. The mice were anesthetized and imaged via Micro-PET/CT at 4h, 24h, 48h, 72h, 96h, and 120h after injection, and PET images were reconstructed using Avatar 3. The standard uptake value (SUV) was calculated by drawing regions of interest (ROI) on the selected tissue.

[00681] SPECT/CT was performed using a small-animal SPECT/CT system (Mediso Inc.). The BGC823$^{CLDN18.2}$ or BGC823 tumor-bearing mouse were injected with ~37 MBq of ^{177}Lu-DOTA-SF106, and imaged at 24, 48, 96, and 120 h postinjection. The raw SPECT data were reconstructed in a whole-body region. The SPECT and CT images were then fused by the Nucline v 2.01 (Mediso Inc.). The maximum intensity projection (MIP) was given for whole-body imaging by the posterior view.

[00682] *11)Immunohistochemistry*

[00683] After immune imaging, the tumor tissues of the ^{124}I-SF106 in BGC823$^{CLDN18.2}$ and BGC823 tumor-bearing mice were obtained for paraffin embedding. Tissue sections were incubated at 4℃ overnight with Anti-CLDN18.2 antibody (ab222512, 1:500; Abcam) and then incubated for 30 min with goat anti-rabbit IgG H&L (HRP) (ab205718, 1:10000; Abcam) at room temperature. Tissue sections developed color with 3,3-N-Diaminobenzidine (DAB) solution and then mounted with cover slips after counterstained with hematoxylin.

[00684] *12)Targeted Radionuclide Therapy*

[00685] The therapeutic efficacy and safety of ^{177}Lu-DOTA-SF106 were evaluated in BALB/c nude mice with AGS$^{CLDN18.2}$ tumor models. The animals were randomly divided into two groups (n = 6), with one group being injected with PBS and the other with about 3 MBq ^{177}Lu-DOTA-SF106 having a specific activity of 10 MBq/nmol. The tumor volume and body weight were measured on day 0 after injection, and subsequently every 2 days from day 1 until day 18 after injection. The tumor volume (mm^3) was calculated using the ellipsoid formula: [length (mm)] × [width (mm)]^2 / 2. The graph were constructed based on measurements of tumor volume and weight at each time point.

[00686] **Table 6: Estimates of the Mean Absorbed Radiation Dose**

Target Organ	Total
Adrenals	1.12×10^{-1}
Brain	1.48×10^{-1}
Breasts	2.94×10^{-2}
Esophagus	8.09×10^{-2}
Eyes	6.12×10^{-2}
Gallbladder Wall	5.45×10^{-2}
Left colon	4.93×10^{-2}
Small Intestine	1.25×10^{-1}
Stomach Wall	5.36×10^{-2}
Right colon	3.86×10^{-2}
Rectum	1.16×10^{-1}
Heart Wall	2.07×10^{-1}
Kidneys	1.37×10^{-1}
Liver	1.87×10^{-1}
Lungs	2.34×10^{-1}
Ovaries	3.43×10^{-2}
Pancreas	6.42×10^{-2}

Salivary Glands	4.41×10^{-2}
Red Marrow	9.65×10^{-2}
Osteogenic Cells	5.13×10^{-1}
Spleen	1.46×10^{-1}
Thymus	7.19×10^{-2}
Thyroid	5.18×10^{-2}
Urinary Bladder Wall	2.38×10^{-2}
Uterus	3.54×10^{-2}
Total Body	7.91×10^{-2}
Effective Dose	8.73×10^{-2}

[00687] Example 9

[00688] *Example 9.1 Abstract*

[00689] **Background:** Gastric cancer (GC), being one of the most prevalent and deadliest tumors worldwide, is often diagnosed at an advanced stage with limited treatment options and poor prognosis. The development of a CLDN18.2-targeted radioimmunotherapy probe is a potential treatment option for GC.

[00690] **Methods:** CLDN18.2 antibody Humanized 18B10 (Hu18B10HaLa) was chelated by DOTA and radiolabeled with therapeutic radioactive nuclide ^{177}Lu, and its specificity and targeting ability were evaluated by cell uptake, imaging and biodistribution experiments. In BGC823$^{CLDN18.2}$/AGS$^{CLDN18.2}$ mouse models, the efficacy of ^{177}Lu-DOTA-18B10 radioimmunotherapy against CLDN18.2-expressing tumor tissue was demonstrated, and the toxicity was tested by H&E saining and blood sample assay.

[00691] **Results:** ^{177}Lu-DOTA-18B10 were constructed in 85.61% labeling rate, with 18.50 MBq/n mol specific activity and stability≥94% after 7 days. It exhibited specific high tumor uptake in CLDN18.2-positive xenografts of GC mouse models. Imaging, biodistribution and dosimetry analysis indicated that the heart wall and spleen might be the primary organs affected. Survival studies in BGC823$^{CLDN18.2}$ and AGS$^{CLDN18.2}$ tumor-bearing mouse models indicated that low doses of 5.55 MBq (150 μCi) and high dose of 11.10 MBq (300 μCi) of ^{177}Lu-DOTA-18B10 significantly inhibited tumor growth compared to the saline control group, with the 300 μCi group showing superior therapeutic efficacy. Histological staining with hematoxylin and eosin (H&E) and Ki67 immunohistochemistry of residual tissues confirmed tumor tissue destruction and reduced tumor cell proliferation following treatment. H&E showed there was no significant toxicity observed in the heart, spleen and

other important organs when treated with high-dose of ^{177}Lu-DOTA-18B10, and no apparent hematotoxicity or liver toxicity was observed in toxicity experiments.

[00692] **Conclusion:** In preclinical studies, ^{177}Lu-DOTA-18B10 demonstrated significant antitumor efficacy with acceptable toxicity to normal tissues. It exhibits strong potential for clinical translation, providing a new promising treatment option for CLDN18.2-overexpressing tumors, including GC.

[00693] *Example 9.2 Introduction*

[00694] Gastric cancer (GC) is the third leading cause of cancer-related deaths worldwide. The high mortality rate of GC may be attributed to the fact that most cases are diagnosed at an advanced stage, where treatment options mostly involve conventional chemotherapy[1]. Patients at this stage often have a poor prognosis, with an overall 5-year survival rate of less than 20% [2,3]. Despite numerous studies conducted on this topic[4-6], the demand for GC treatment remains unmet due to the large population of patients and the limited number of approved first-line therapies for advanced-stage GC[7-9]. This is especially true for human epidermal growth factor receptor-2 (HER2)-negative patients who lack effective targeted treatment options, resulting in a less optimistic survival.

[00695] Research on novel targets and drugs for GC is ongoing. In recent years, the development of neoadjuvant therapy, targeted drugs, and immunotherapy has opened up new avenues for cancer treatment. However, data from the past five years indicate that the 5-year survival rate for advanced-stage GC remains low under current treatment modalities[10,11]. Finding a more effective treatment method that can be applied to a broader range of patients is a key focus of many clinical researchers, aiming to further improve the survival rates of GC patients.

[00696] GC is a tumor that exhibits moderate sensitivity to radiation[12]. Radiation therapy is widely used in cancer treatment to induce DNA damage in actively proliferating malignant cells, effectively killing tumor cells. Additionally, radiation exposure can increase antigen exposure, enhance antigen presentation, and assist in reshaping the immune microenvironment and improving the efficacy of immunotherapy[13,14]. However, the poor tolerance of surrounding organs to external radiation therapy complicates the delivery of radiation[15]. Moreover, compared to localized GC, advanced metastatic GC often cannot be cured by chemotherapy or external radiation alone. In such cases, targeted radioimmunotherapy (RIT) may be a promising approach. Targeted radiotherapy provides an opportunity to deliver radiation selectively to disease sites in patients with metastases, regardless of disease stage, offering a potential clinical treatment strategy for advanced tumor

patients. ^{177}Lu is a therapeutic radioactive isotope that emits β-rays, possessing strong tissue penetration and cytotoxicity[16]. When labeling substances such as monoclonal antibodies that specifically target tumor-expressed molecules, ^{177}Lu can be used to deliver targeted radiation therapy to systemic lesions in patients with tumors such as GC, serving as a powerful tool for preventing and treating systemic micro-metastases. Additionally, this targeted radiation can minimize radiation exposure to healthy tissues, which is an ability not possessed by traditional external radiation therapy[16,17].

[00697] Claudin-18.2 (CLDN18.2) is a member of the human Claudin family, a four-transmembrane protein that plays a crucial role in tight junction structure[18], participating in the formation of cell-cell adhesion and maintenance of cell polarity[19,20]. Under normal conditions, CLDN18.2 expression is strictly limited to differentiated epithelial cells of the gastric mucosa, with concealed expression and limited expression level, contributing to barrier function maintenance[21]. However, in various human tumors, including GC and its metastases, abnormal activation of CLDN18.2 occurs[21,22], with highly selective and stable expression in specific tumor tissues, contributing to tumor cell proliferation, differentiation, and migration[23,24]. It has been reported that over 50% of GC patients express CLDN18.2, with expression rates reaching up to 80% in some populations, and the expression can be observed in both primary and metastatic lesions[21,25]. This highly specific expression in tumors and the expression rate exceeding 50% in GC patients make CLDN18.2 a potential target for effective anti-tumor drug therapy. The mutually exclusive expression of CLDN18.2 and HER2 in some populations[25,26] brings hope to a large number of HER2-negative and treatment-resistant GC patients.

[00698] In clinical trials, anti-CLDN18.2 antibodies have demonstrated certain anti-tumor effects in patients with advanced gastric adenocarcinoma[26-28]. Leftideciximab (IMAB362) is the first antibody targeting CLDN18.2, and when used in combination with first-line chemotherapy, it has shown longer progression-free survival (PFS) and overall survival (OS)[28,29].

[00699] Osemitamab, a subsequently developed novel anti-CLDN18.2 monoclonal antibody (humanized from 18B10). Compared to IMAB362, Osemitamab has higher affinity, stronger FcgRIIIa binding capacity, increased ADCC/CDC/ADCP activity, and greater anti-tumor activity due to reduced fucosylation[30]. In a Phase I clinical study (NCT04396821), Osemitamab in combination with chemotherapy achieved partial relief in 73.3% of patients with advanced gastric and gastroesophageal junction cancer (GC/GEJ)[31]. Currently, Osemitamab has entered in Phase III clinical trial (TranStar 301). TranStar 301 is a

randomized, double-blind, placebo-controlled phase III clinical trial conducted worldwide to evaluate the first-line treatment efficacy of Osemitamab combined with Nivolumab and chemotherapy in patients with HER2 negative, CLDN18.2 expression locally advanced or metastatic GC/GEJ. The U.S. Food and Drug Administration (FDA) has granted orphan drug designation to 18B10 for the treatment of GC/GEJ and pancreatic cancer.

[00700] Recently, the results of a Phase I clinical trial targeting CLDN18.2 with chimeric antigen receptor T-cell (CAR-T) therapy (NCT03874897) showed favorable efficacy in patients with CLDN18.2-high expressing digestive system tumors[32]. However, these therapeutic agents also present some challenges. The efficacy of IMAB362 has shown significant variability in different clinical trials, and the incidence of adverse reactions such as nausea and vomiting are relatively high[33]. The efficacy of 18B10 as a monotherapy is yet to be confirmed. CAR-T therapy for solid tumors carries a significant risk of severe side effects and off-target toxicity[34]. Therefore, researchers are striving to develop more effective and less toxic treatment approaches that can better utilize CLDN18.2 as a target. Targeted RIT based on therapeutic radionuclides offers a potential solution for the realization of this clinical strategy. Recently, clinical trials have demonstrated that targeted RIT can inhibit tumor growth[35,36], and in some cases, even eradicate certain types of cancer[37-39].

[00701] Furthermore, radiation from radionuclides can increase antigen exposure, enhance antigen presentation, and transform the tumor immune microenvironment from 'cold' to 'hot', providing a favorable environment for immunotherapies[14,40]. In terms of safety, RIT agents, including those labeled with ^{177}Lu, have shown good toxicity control in human patients[41,42]. From a technical perspective, 18B10 antibody exhibits high tumor uptake, prolonged retention time, fulfilling the required characteristics of a radionuclide therapy probe, and matching well with the half-life of ^{177}Lu, making it a suitable precursor for RIT probe construction.

[00702] In previous studies conducted in our laboratory, we have developed various in vivo imaging techniques targeting the CLDN18.2 protein. We have constructed high-resolution positron emission computed tomography (PET) probes that allow comprehensive, real-time, and non-invasive monitoring of CLDN18.2 in vivo. Among them, the studies of ^{89}Zr-DFO-18B10[31] and ^{124}I-5C9[43] in mouse models and the first clinical study of ^{124}I-18B10 in humans (NCT04883970)[44] have shown that radiotracer probes exhibit good tracing capability for CLDN18.2-positive tumors. Therefore, CLDN18.2-targeted probes serve as an important complement to routine clinical practice, enabling accurate and comprehensive protein targeting to guide the treatment of CLDN18.2-positive tumors[43]. Utilizing these

diagnostic PET probes allows for comprehensive assessment of CLDN18.2 expression in patients who may benefit from RIT, facilitating the selection of potential beneficiaries and the customization of precise treatment plans. The development of therapeutic nuclides labeled RIT probes can be synergistic with these diagnostic probes, achieving an integrated approach to the diagnosis and treatment of CLDN18.2 overexpressing tumors, thus providing a more precise and efficient method for combating cancer.

[00703] Therefore, the development of CLDN18.2 targeted RIT has a solid foundation and broad prospects. The aim of this study is to construct a CLDN18.2-targeted ^{177}Lu-labeled RIT probe: ^{177}Lu-DOTA-18B10, and evaluate its preclinical anti-tumor efficacy and safety. In this manuscript, we report significant therapeutic effects and acceptable toxicity of ^{177}Lu-DOTA-18B10 in a GC xenograft mouse model, providing a new and powerful treatment approach for CLDN18.2 overexpressing tumors, including GC.

[00704] *Example 9.3 Methods*

[00705] For detailed information on the supplementary method of cell culture, flow cytometry, and xenograft mouse models, cell uptake experiment and saturation binding experiment, SPECT imaging and ROI analysis, biodistribution, dosimetry estimation, and pharmacokinetics, please refer to the Supplementary Materials.

[00706] *1) Radiolabeling of ^{177}Lu-DOTA-18B10 and quality control*

[00707] A metal-free buffer solution of $NaHCO_3$+Na_2CO_3 was prepared in advance. DOTA was dissolved in DMSO at a concentration of 10 mg/ml. The GMP grade CLDN18.2 antibody 18B10(Hu18B10HaLa) was provided by Transcenta Therapeutics Co., Ltd. (China). Please refer to the Supplementary Materials for more details.

[00708] *2) Therapeutic experiments in xenograft mouse models*

[00709] The constructed BGC823$^{CLDN18.2}$ or AGS$^{CLDN18.2}$ subcutaneous xenograft mouse were randomly divided into three groups (n = 6-8 per group). After grouping, each group of mice received a tail vein injection of 50 μL containing 150 μCi of ^{177}Lu-DOTA-18B10, 300 μCi of ^{177}Lu-DOTA-18B10, or 0.9% saline solution. The body weight and tumor size of the mice were monitored once a day after the injection. After 15-16 days, the mice were euthanized, and the residual tumor tissue from the treatment group and some normal organs were collected for further studies.

[00710] *3) Histological staining of residual tissues*

[00711] The collected mouse tumor residual tissues and organ tissues were fixed in 10% neutral formalin. After a minimum of 10 half-lives, the tissues were embedded in paraffin and sectioned for subsequent hematoxylin-eosin (H&E) staining, Ki67 immunohistochemistry

(IHC), and CLDN18.2 IHC. The stained sections were analyzed by dedicated pathologists. Please refer to the Supplementary Materials for more details.

[00712] *4) Toxicity experiment*

[00713] Daily monitoring of mice for toxic reactions such as lethargy, reduced appetite, and skin ecchymosis. In the therapeutic experiments, tumor-bearing mice were weighed every other day to observe whether there was a significant weight loss. In subsequent toxicity experiments, male and female normal balb/c nude mice (8-10 per gender) were divided into two groups: one receiving the maximum therapeutic dose (300 μCi) and the other receiving saline injection. Blood samples were collected for hematological analysis and liver function testing. Please refer to the Supplementary Materials for more details.

[00714] *5) Statistical analysis*

[00715] All data were compared between two groups using a two-tailed t-test, and a p-value less than 0.05 was considered statistically significant. GraphPad Prism 8 was used for data analysis and some of the figures. The results of repeated experiments are presented as the mean ± standard deviation unless otherwise stated.

[00716] *Example 9.4 Results*

[00717] *1) Construction and validation of ^{177}Lu-DOTA-18B10*

[00718] To develop and evaluate a radiolabeled immunotherapeutic probe targeting the CLDN18.2 protein, we used the unlabeled CLDN18.2 targeted monoclonal antibody 18B10 as a precursor, DOTA as a bioconjugate and chelating agent, labeled 18B10 with ^{177}Lu (Figure 46A). Through multiple labeling experiments, the specific activity of the labeled product was approximately 18.50 MBq/nmol, with a labeling rate of about 85.61%, and a radiochemical yield of about 51.50%, indicating high specific activity and radiochemical yield of the labeled product. Subsequently, the radiolabeled conjugate was purified, resulting in a higher radiochemical purity (≥99%). The probe product exhibited ≥94% stability after incubation at room temperature in PBS and 5% HSA for 7 days (Figure 51).

[00719] *2) Specific binding of ^{177}Lu-DOTA-18B10 to CLDN18.2*

[00720] CLDN18.2-transfected BGC823 and AGS GC cell lines were used as positive cell lines (BGC823$^{CLDN18.2}$, AGS$^{CLDN18.2}$), and non-transfected BGC823 and AGS GC cell lines were used as negative control groups, to perform cell uptake experiments (cell binding assays) to validate the immunoreactivity of the radiolabeled conjugate to CLDN18.2 protein in vitro. The transfected cell lines were confirmed to have higher CLDN18.2 expression compared to the non-transfected cell lines through flow cytometric analysis (Figure 52). IHC staining of

CLDN18.2 in xenograft tumors formed by subcutaneous injection of cells in balb/c nude mice further confirmed this point (Figure 47E).

[00721] The cell uptake experiment results demonstrated that CLDN18.2-positive cell lines exhibited significantly higher uptake of the radiolabeled probe ^{177}Lu-DOTA-18B10 compared to the negative cell lines, and this uptake could be blocked by excess unlabeled 18B10 precursor (at 60 min) (Figure 46B). The difference between BGC823$^{CLDN18.2}$ and BGC823 cells was approximately 4.26-fold, and between AGS$^{CLDN18.2}$ and AGS cells, it reached 4.94-fold, indicating the specific binding of the probe to the target protein.

[00722] Furthermore, using a gradient density plate of BGC823$^{CLDN18.2}$ cells, we obtained the binding constant (Kd = 12.87) of the cell binding experiment (Figure 46C), reflecting a strong binding capability between the probe product and the cellular CLDN18.2 protein.

[00723] *3) ^{177}Lu-DOTA-18B10 exhibits favorable imaging efficacy and biodistribution in GC mouse models*

[00724] We constructed in vivo models in balb/c nude mice using the same cell lines as in the cell experiments. Histological staining of tumor tissues derived from BGC823$^{CLDN18.2}$ and AGS$^{CLDN18.2}$ cell lines showed extensive and homogeneous expression of CLDN18.2, while tumors formed by non-transfected BGC823 cells exhibited low CLDN18.2 expression (Figure 47E). In BGC823$^{CLDN18.2}$, BGC823, AGS$^{CLDN18.2}$, and AGS subcutaneous xenograft models, small animal SPECT live imaging experiments were performed using the ^{177}Lu-DOTA-18B10 probe (n=3). Ex vivo biodistribution experiments were conducted in BGC823$^{CLDN18.2}$ and BGC823 models to assess the in vivo CLDN18.2 levels (n=4).

[00725] After intravenous injection of approximately 7.4 MBq (200 μCi, 60 μg) of ^{177}Lu-DOTA-18B10, we performed SPECT imaging of the mice. The imaging indicated high tumor uptake in the positive models and low tumor uptake in the negative models (Figure 47A, C), while other non-target organs showed relatively low uptake, except for slightly higher uptake in the spleen. IHC confirmed that CLDN18.2 was not expressed in spleen (Figure 53). In the BGC823$^{CLDN18.2}$ model, tumor uptake reached its highest point at 72 hours (15.98 %ID/cc), and in the AGS$^{CLDN18.2}$ model, it also peaked at 72 hours (14.29 %ID/cc, Figure 47B). In the block group co-injected with excess unlabeled 18B10 precursor, the uptake of the two CLDN18.2-positive tumors could be blocked, confirming the specificity of tumor uptake of the probe (Figure 47C, D).

[00726] The ex vivo biodistribution experiments validated the results of the imaging experiments. In BGC823$^{CLDN18.2}$ tumor-bearing mice with CLDN18.2 positivity, the ^{177}Lu-DOTA-18B10 probe exhibited high tumor uptake, which increased over time, reaching its

peak (16.57 %ID/g) at 48 h post-injection (Figure 48 panel A). The uptake in other organs decreased with time, and the radioactivity concentration was highest in the blood and spleen, reaching a maximum of 25.55 and 26.03 %ID/g, respectively (Figure 48 panel A). The tumor/non-tumor (T/NT) ratio was also calculated (Figure 54), which represents the ratio of radioactive probe accumulation in the tumor versus non-tumor organs. As shown in the Figure 54, the T/NT values of all organs increased slightly or significantly with time (T/muscle and T/bone rise first and then fall), indicating that the difference in the distribution of the ^{177}Lu-DOTA-18B10 probe between tumors and other non-specific organs became increasingly obvious with time. The tumor uptake in BGC823 tumor-bearing mice without CLDN18.2 expression and in the block positive model (co-injected with excess unlabeled 18B10) decreased to 6.12 and 5.48 %ID/g at 48 h, respectively, which was significantly lower than that in the non-blocked CLDN18.2-positive tumors (Figure 48 panel B), indicating the probe's high tumor uptake was specific. The biodistribution pattern of the probe in organs in the negative and block groups of mice was similar to that in the positive mice, except for reduced spleen uptake in the block group mice (Figure 48 panel B).

[00727] Based on the biodistribution results in mice, we performed dosimetry calculations for human organ radiation, as shown in Table 7. The highest dose was in the heart wall (2.680 mSv/MBq), followed by the spleen (0.583 mSv/MBq). Assuming 35 MBq of ^{177}Lu-DOTA-18B10 was injected into a human body, the effective radiation dose was less than 4.9 mSv, which is acceptable in routine clinical nuclear medicine practice.

[00728] Table 7

Target Organ	Absorbed dose (mSv/MBq)
Adrenals	8.21E-02
Brain	6.88E-02
Breasts	7.36E-02
Gallbladder Wall	8.26E-02
LLI Wall	7.18E-02
Small Intestine	3.18E-01
Stomach Wall	1.48E-01
ULI Wall	7.60E-02
Heart Wall	2.68E+00
Kidneys	2.77E-01
Liver	5.34E-01

Lungs	2.86E-01
Muscle	3.54E-02
Ovaries	7.32E-02
Pancreas	8.34E-02
Red Marrow	5.82E-02
Osteogenic Cells	2.20E-01
Skin	6.63E-02
Spleen	5.83E-01
Testes	6.74E-02
Thymus	9.24E-02
Thyroid	6.98E-02
Urinary Bladder Wall	7.04E-02
Uterus	7.32E-02
Total Body	1.15E-01
Effective Dose (mSv/MBq)	1.40E-01

[00729] Results from pharmacokinetic experiments in normal KM mice showed that ^{177}Lu-DOTA-18B10 exhibited favorable pharmacokinetics with a relatively long half-life. The value of the slow half-life was 22.39 h, and the value of the fast half-life was 0.4512 h (Figure 55).

[00730] *4) ^{177}Lu-DOTA-18B10 demonstrates compelling therapeutic efficacy in GC mouse models*

[00731] Based on the biodistribution and radiation dosimetry estimation results, we selected doses of 5.55 MBq (150 μCi) and 11.10 MBq (300 μCi) for the administration of the RIT probe ^{177}Lu-DOTA-18B10 in the animal therapeutic experiments. To evaluate the therapeutic potential of this probe, we divided the BGC823$^{CLDN18.2}$ mouse models carrying CLDN18.2-positive xenografts into three groups (n = 6), which were respectively treated with 150 μCi, 300 μCi of ^{177}Lu-DOTA-18B10, and an equal volume of saline solution as a control (100 μL via tail vein injection). Consistent with expectations, the subcutaneous tumors in the saline control group of the BGC823$^{CLDN18.2}$ balb/c nude mice model rapidly progressed (Figure 49A), setting a high standard for in vivo efficacy in these tumors. In the 150 μCi/300 μCi treatment groups and the control group, we monitored tumor volume and

mouse body weight for 16-17 days continuously. We plotted the tumor volume curves and observed significant tumor growth inhibition in the treatment groups compared to the control group (Figure 49A, ***: $p < 0.001$). As for the two treatment doses, the 300 μCi group appeared to have a sustained superior efficacy compared to the 150 μCi group, suggesting a dose-dependent treatment effect. At the end of the 16-17-day observing period, mice in each group were euthanized, and the BGC823$^{CLDN18.2}$ tumors were resected and measured for volume. The tumor volume in the 150 μCi group was significantly smaller than the control group, and the tumor volume in the 300 μCi group was significantly smaller than both the 150 μCi group and the control group (Figure 49B). Combine together, ^{177}Lu-DOTA-18B10 exhibited impressive therapeutic efficacy in GC mouse models.

[00732] Given the impressive therapeutic efficacy achieved by ^{177}Lu-DOTA-18B10 in the BGC823$^{CLDN18.2}$ model, to validate the broad applicability of this RIT probe, we further conducted the treatment experiment in another GC cell line model, AGS$^{CLDN18.2}$ subcutaneous xenograft model. Since the imaging experiments yielded similar results in both models, the treatment experiment in AGS$^{CLDN18.2}$ model followed the same grouping scheme as BGC823$^{CLDN18.2}$ model. The results showed that the tumor in the saline control group of the AGS$^{CLDN18.2}$ model also progressed rapidly (Figure 49A). The treatment groups exhibited similar outcomes to the BGC823$^{CLDN18.2}$ model: the 300 μCi group appeared to have sustained superior efficacy compared to the 150 μCi group, and the tumor volume measurements on the last day of treatment indicated that the average tumor volume in the 150 μCi group was significantly smaller than the control group, while the average tumor volume in the 300 μCi group was significantly smaller than both the 150 μCi group and the control group (Figure 49B). Furthermore, the efficacy in the AGS$^{CLDN18.2}$ model seemed to be superior to the BGC823$^{CLDN18.2}$ model, as the AGS$^{CLDN18.2}$ treatment group not only exhibited an obviously controlled tumor growth curve but also some individual mice showed tumor volumes in the late treatment period that were even lower than the initial volume before treatment, approaching a near complete response (CR) level (Figure 49A, B).

[00733] In conclusion, ^{177}Lu-DOTA-18B10 RIT demonstrates profound and persistent anti-tumor responses in CLDN18.2-positive GC mouse models, achieving impressive anti-tumor effects even in the low-dose groups.

[00734] *5) Tumor histopathology confirms histological changes induced by the treatment*

[00735] On the final day of the therapeutic experiment, after euthanizing the mice, we resected and processed the residual tumor tissue at the implantation site. The tissue samples were paraffin-embedded, sliced, and subjected to H&E staining, as well as IHC staining for

CLDN18.2 and Ki67. H&E staining results revealed that both the $BGC823^{CLDN18.2}$ and $AGS^{CLDN18.2}$ models in the saline control group exhibited normal tumor tissue structure, while the tumors in the 150 μCi and 300 μCi treatment groups showed increasingly severe tissue destruction (Figure 49C). Additionally, the expression of Ki67 in the saline control, 150 μCi, and 300 μCi groups displayed a progressively decreasing pattern, directly proportional to the degree of tissue damage, indicating a reduction in tumor proliferation activity (Figure 49C).

[00736] *6) ^{177}Lu-DOTA-18B10 treatment shows no significant toxicity*

[00737] To assess the toxicity of the probe, we administered 300 μCi ^{177}Lu-DOTA-18B10 or saline solution via tail vein injection to female or male balb/c nude mice (n = 4 per group per gender). After injection, the mice did not exhibit significant toxic reactions such as drowsiness, loss of appetite, and skin ecchymosis in both groups. Complete blood count analyses within 13 days after injection and liver function on the 13th day were examined and compared between the two groups. The results showed mild hepatotoxicity but no significant heme toxicity associated with ^{177}Lu-DOTA-18B10 (Figure 50). Complete blood count analyses conducted every other day indicated no significant differences in white blood cells (WBCs), red blood cells (RBCs), and platelets (PLT) between the 300 μCi ^{177}Lu-DOTA-18B10 injection group and the saline control group at different time points, and the values remained within the normal range for both female and male mice (Figure 50). Liver function tests conducted on the 13th day after probe injection revealed no significant changes in ALT and TBIL compared to the saline control group, with only a mild increase in AST (more pronounced in female mice, Figure 50). Furthermore, mice in each group were weighed every other day until the last day, and none of the groups showed significant weight loss (Figure 56).

[00738] After euthanizing the mice on the final day of treatment, we resected important organs from both the 300 μCi ^{177}Lu-DOTA-18B10 group and the saline control group for paraffin embedding and sectioning. H&E staining was performed on the sections to observe tissue toxicity. H&E staining results showed no apparent histological damage or other changes in vital organs (including the stomach, liver, spleen, heart, lungs, kidneys, intestines, muscles, etc.) in the probe injection group compared to the saline group (Figure 57). These findings further suggest that the in vivo toxicity of ^{177}Lu-DOTA-18B10 is acceptable.

[00739] All the experimental results mentioned above indicate that the therapeutic probe ^{177}Lu-DOTA-18B10 does not exhibit significant toxicity to vital organs, suggesting that its future application in humans may not have severe adverse effects.

[00740] *Example 9.5 Discussion*

[00741] In recent years, GC, as one of the tumors with high global incidence and mortality rates, has seen an increasing number of treatment modalities. However, there is a lack of breakthroughs in clinical efficacy progress[2,3]. GC is often diagnosed at advanced stages, and surgical resection is only suitable for early-stage GC, with potential surgical complications. The overall survival rate of radiotherapy and chemotherapy is not satisfactory, with a 5-year survival rate of only 30%, and a disease remission rate of 25-55%, which may also result in severe hematological side effects[45]. Currently, PD-1/PD-L1 immune checkpoint inhibitors have been approved for the treatment of advanced gastrointestinal cancers. However, compared to colorectal and lung cancers, the development of immunotherapeutic drugs for GC still lags behind, and the target population is not well-defined[46]. Trastuzumab, a targeted therapy drug, has extended the overall survival of patients with advanced HER2-positive gastric diseases as a first-line treatment. However, HER2-positive patients account for only 7-22% of all GC patients, and HER2 expression is dynamic[47].

[00742] The development of new and long-lasting effective treatments for GC is an urgent clinical need. The emerging target CLDN18.2 has become the most promising therapeutic target in the field of GC. Considering the high specific expression of CLDN18.2 on the membrane surface of GC cells, targeted therapies[28] and CAR-T cell therapies (NCT03874897)[32] based on CLDN18.2 have achieved certain successes in improving efficacy. GMP grade CLDN18.2 antibody 18B10 is also a promising treatment choice. Currently, 18B10 has already entered in Phase III clinical trial (TranStar 301), having a broad application prospect.

[00743] However, the efficacy of CLDN18.2-targeted drugs is unstable, and adverse reactions such as nausea and vomiting are significant[28,33]. Furthermore, CAR-T cell therapy for solid tumors is still in the early stages of exploration, with small sample sizes and potential risks of cytokine storms. The occurrence of off-target adverse reactions is also relatively high[48]. Most importantly, these current treatment modalities have not yet provided satisfactory improvements in survival.

[00744] Finding ways to overcome the current issues in CLDN18.2 treatment while effectively utilizing CLDN18.2 as an excellent target to provide new and reliable treatment options for patients with advanced GC has become the focus of researchers' efforts. The emergence of targeted RIT offers the possibility to achieve this goal by combining the specific targeting of CLDN18.2 with the good cytotoxic effects of radiation damage.

[00745] Radioimmunotherapy, also known as radionuclide therapy, utilizes radioactive isotopes coupled with targeted carriers to induce DNA damage specifically in the diseased

target cells while avoiding damage to normal tissues. The advantages of radionuclide therapy include high specificity, which reduces adverse effects on normal tissues compared to external beam radiation therapy and chemotherapy. It also allows for close monitoring and targeted eradication of both overt and occult (subclinical) metastatic lesions. Furthermore, once the target lesions are accurately identified, the high-energy ionizing radiation caused by therapeutic radioactive isotopes demonstrates significant killing capacity against highly proliferative malignant cells.

[00746] In this study, we developed a probe named ^{177}Lu-DOTA-18B10, which targets CLDN18.2 using 18B10 monoclonal antibody as a precursor and is labeled with ^{177}Lu, a therapeutic radionuclide. We validated the good molecular imaging, favorable biodistribution, and pharmacokinetics of ^{177}Lu-DOTA-18B10 in a GC mouse model. Imaging and biodistribution data indicated potential toxic risks to the heart wall and spleen, but histology confirmed no obvious tissue damage in the hearts and spleens of the mouse model, and no significant abnormalities were observed in mouse blood cell counts, suggesting acceptable heart and spleen toxicity. Negative CLDN18.2 IHC confirmed the non-specific uptake in the spleen, suggesting that the high uptake in the spleen may be due to the enhanced antibody-dependent cell-mediated cytotoxicity (ADCC) and antibody-dependent cellular phagocytosis (ADCP) effects of 18B10[30], leading to its retention in the spleen.

[00747] Moreover, this study explored the therapeutic efficacy of ^{177}Lu-DOTA-18B10 RIT against CLDN18.2-positive tumors and determined the optimal therapeutic dose in a GC animal model. Safety under the treatment dose of the probe was also verified. We achieved significant therapeutic effects with acceptable toxicity evaluation in the model mice. Treatment with radioactive therapy drug ^{177}Lu-DOTA-18B10 at doses of 150 μCi and 300 μCi both resulted in significant and persistent antitumor efficacy in the model mice, accompanied by only acceptable hepatotoxicity and no other toxic manifestations. Tumors in both BGC823$^{CLDN18.2}$ and AGS$^{CLDN18.2}$ GC models were effectively controlled in both treatment groups, with better tumor volume control, greater tumor tissue destruction and cell proliferation reduction in the 300 μCi group. Among the two models, AGS$^{CLDN18.2}$ model showed better therapeutic efficacy than the BGC823$^{CLDN18.2}$ model. Comparing the IHC staining results of CLDN18.2 protein expression in both tumor tissues, AGS$^{CLDN18.2}$ tumor tissue exhibited a higher expression rate of CLDN18.2, reaching over 95%, while the expression rate of CLDN18.2 in BGC823$^{CLDN18.2}$ tumor tissue was approximately 70-80%, which is slightly lower. Therefore, the increased targets might be the reason for the better anti-tumor efficacy of the probe in the AGS$^{CLDN18.2}$ model. Additionally, the differential

sensitivity of different tumor cells to DNA damage may also contribute to differences in treatment responsiveness.

[00748] According to previous studies, several antibody conjugates labeled with ^{177}Lu have been tested in clinical trials, and their toxicity in human patients has been well established and controlled[41,42]. Meanwhile, increasing evidence suggests that RIT and targeted RIT may impede tumor growth[35,36], and even eradicate certain types of cancer[37-39]. The 18B10 monoclonal antibody targeting CLDN18.2 has also entered clinical trials, demonstrating both safety and efficacy[30,31]. This study confirmed the compelling therapeutic efficacy, acceptable toxicity in animal models, and acceptable estimations of human radiation dose for ^{177}Lu-DOTA-18B10, suggesting the feasibility of clinical translation of this RIT probe for human applications. Previous studies in our laboratory have demonstrated good in vivo tracking ability of CLDN18.2 in mice and humans using diagnostic PET probes labeled with ^{89}Zr-18B10 or ^{124}I-18B10 (18B10 was humanized from 18B10, a mouse-derived hybridoma antibody)[31,44]. Particularly, ^{124}I-18B10 successfully depicted the distribution of CLDN18.2 protein throughout the body in patients with gastrointestinal tumors[44]. Therefore, these PET probes can serve as diagnostic and whole-body monitoring tools prior to or during the treatment with ^{177}Lu-labeled therapeutic probes, effectively selecting potential beneficiaries of targeted RIT and enabling integrated tumor diagnosis and treatment. Furthermore, non-invasive intravital imaging can also be performed using SPECT instrumentation following injection of ^{177}Lu-DOTA-18B10.

[00749] When it comes to the choice between high and low radiation doses, there are slight differences between mice and humans. However, insights can be gained from mouse experiments. In situations where toxicity is acceptable, we believe it is preferable to prioritize treatment probes with higher radiation doses to achieve better anti-tumor effects. However, if significant adverse reactions occur, the dose can be reduced as necessary, while still maintaining a certain level of tumor control. In future research, we can explore the possibility of administering small doses multiple times in a periodic manner, aiming to maintain the anti-tumor effects of RIT while minimizing systemic toxicity. This approach is supported by previous studies[41,42] and the observed expression of CLDN18.2 in residual tumor tissue after probe injection.

[00750] The toxicity experimental results of this study suggest that the liver may be the main affected organ. However, among the three common liver function indicators, only AST showed an increase. The increase was less pronounced in males. Furthermore, when considering the absence of significant abnormalities in the H&E staining of liver tissues from

the treatment group, as well as the results of biodistribution, we conclude that the liver did not exhibit severe toxic reactions.

[00751] These preclinical results from our study indicate that further clinical evaluation of the therapeutic effects of the ^{177}Lu-DOTA-18B10 probe in patients with tumors expressing high levels of CLDN18.2 is warranted. Additionally, although this study primarily focused on validating the efficacy of targeted RIT against CLDN18.2 in GC, considering the upregulation of CLDN18.2 expression in numerous common tumors such as pancreatic cancer (>50%), esophageal cancer, and lung cancer[21], this therapeutic probe holds significant potential for broader application in malignancies with high CLDN18.2 expression.

[00752] *Example 9.6 Conclusion*

[00753] In conclusion, this study represents the first use of the therapeutic radionuclide ^{177}Lu-labeled CLDN18.2-targeting GMP grade monoclonal antibody 18B10, establishing a targeted RIT probe for CLDN18.2. A series of preclinical experiments were conducted to confirm the significant efficacy and low toxicity of the ^{177}Lu-DOTA-18B10 probe in preclinical models of GC. This probe demonstrates great potential as a RIT drug for clinical translation, which can offer a promising new treatment option for many CLDN18.2-overexpressing tumors including GC, lead to improved survival outcomes for an increasing number of patients.

[00754] Ethics approval and informed consent: All animal experiments were approved by the Peking University Cancer Hospital Animal Care and Use Committee (reference number: EAEC 2022-01).

[00755] *Example 9.7 Supplemental materials*

[00756] Supplementary Methods

[00757] *1) Radiolabeling of ^{177}Lu-DOTA-18B10 and quality control.*

[00758] The molar ratio of 18B10 monoclonal antibody(Hu18B10HaLa) to the chelator DOTA was 1:10. The pH of the mixture was adjusted to around 9.0 using the buffer solution, and the reaction was carried out at room temperature with gentle rotation for 2 hours (h). The resulting DOTA-18B10 conjugate was purified using PD-10 size exclusion columns (GE Healthcare, England) and exchanged with PBS solution. Next, a labeling buffer of HCl+$NaHCO_3$ was prepared, and the DOTA-18B10 was mixed with the labeling buffer. ^{177}Lu (supplied by Isotope Technologies Munich SE, Germany) was added to the reaction system, and the final pH was adjusted to around 5.0. The reaction was conducted at 37°C for 30 minutes. After obtaining the product, it was further purified using a pre-treated PD-10 column with PBS. Before and after purification, instant thin-layer chromatography (iTLC)

analysis was performed using SG-iTLC paper with saturated EDTA solution as the developing agent to determine the labeling efficiency and radiochemical purity of the labeled product. Stability assessment was carried out by storing the final product in 0.01 M PBS and 5% human serum albumin (HSA) at room temperature. iTLC analysis was performed every day for 7 days to measure the radiochemical purity changes of the product.

[00759] *2) Histological staining of residual tissues.*

[00760] The Ki67 IHC utilized an antibody (SP6) from Abcam (ab16667) at a 1:200 dilution with citrate retrieval, while the CLDN18.2 IHC used an antibody (EPR19202) from Abcam (ab222512) at a 1:500 dilution with EDTA9.0 retrieval. The IHC experimental steps included dewaxing the paraffin sections in xylene, graded ethanol soaking, antigen retrieval by microwave, blocking endogenous peroxidase with 3% H_2O_2, goat serum blocking for 1 hour, incubation with primary antibodies overnight at 4°C, followed by 40 minutes of secondary antibody incubation. Diaminobenzidine was then used for visualization, followed by hematoxylin counterstaining, 1% hydrochloric acid alcohol and ammonia. The sections were then dehydrated and mounted with resin. The sections were observed and captured using Leica AT2 microscope (Germany) and 3DHISTECH Pannoramic MIDI (Hungary).

[00761] *3) Toxicity experiment.*

[00762] Blood samples were collected from orbital blood every other day for hematological analysis. The complete blood count analyses were determined using the TEK-II fully automated animal blood analyzer (Tekang Technology, China). Nineteen parameters were recorded, and three are represented (white blood cell count, red blood cell count, and platelet count). These values were compared with the baseline measurements taken before RIT and the normal range values for female or male balb/c nude mice (doi: 10.1158/1078-0432.CCR-21-1533). On the final day of the toxicity experiment (day 13 post-injection), the mice were euthanized, and blood serum specimens were collected for liver function testing. Additionally, important organ tissues were collected for H&E staining to observe the toxicity in the liver and other vital organs. The collected serum samples were stored frozen for at least 10 half-lives before further testing. The levels of alanine aminotransferase (ALT), aspartate aminotransferase (AST), and total bilirubin (TBIL) were measured using TBIL content assay kit, glutamic oxaloacetic transaminase (GOT)/AST assay kit, and glutamic pyruvictransaminase (GPT)/ALT assay kit (RXSH0658, RXWB0098, RXWB0374; Ruixin Biotechnology, China), and analyzed by Epoch Microplate spectrophotometer (BioTek Instruments, USA).

[00763] *4) Cell culture, flow cytometry, and xenograft mouse models*

[00764] The BGC823, BGC823$^{CLDN18.2}$, AGS, and AGS$^{CLDN18.2}$ cell lines were obtained from the central laboratory of Peking University Cancer Hospital (China). The cells were cultured in RPMI-1640 medium (Corning) containing 10% fetal bovine serum and 1% antibiotics. The culture plates were placed in a 37℃-incubator containing 5% CO_2. Flow cytometry was used to determine the expression levels of CLDN18.2 on the above cells. After washing the cells with PBS twice, cells were stained with 2 μl (2 μg/mL) of CLDN18.2 antibody (1D5, Beijing Cancer Hospital, China) at 4°C for 30 minutes, followed by incubation with FITC-conjugated secondary antibody (Beijing Cancer Hospital Central Laboratory, China) for 30 minutes. Flow cytometric analyses were performed using the BD FACS Aria instrument.

[00765] Xenograft mouse models were established using female 4-5-week-old balb/c nude mice (Vital River, China). The aforementioned cells were implanted subcutaneously into the posterior upper axilla of nude mice to create the xenograft tumor models. Imaging, biodistribution, and treatment experiments were conducted when the tumor volume reached approximately 100-300 mm^3. The mice were kept in a pathogen-free environment that met the conditions for mouse breeding. All animal experiments and procedures followed the Institutional Animal Care and Use Committee guidelines. Tumor size was measured using a caliper along the longest axis (length) and the axis perpendicular to the longest axis (width). Tumor volume was calculated using the equation: Volume = (length × width^2) / 2.

[00766] *5) Cell uptake experiment and saturation binding experiment*

[00767] The digested and centrifuged BGC823, BGC823$^{CLDN18.2}$, AGS, and AGS$^{CLDN18.2}$ cells were resuspended in culture medium at a concentration of approximately 0.5*10^5 cells/mL. Subsequently, they were added to 24-well plates with 500 μL per well. After cell adhesion, each well was added with 0.037 MBq of labeled probe (the block group was co-injected with excess unlabeled 18B10 precursor, n=4). The plates were then incubated in an incubator for 10 minutes, 30 minutes, 1 hour, and 2 hours (the block group was incubated for 1 hour). After removing the supernatant and washing with PBS, the cells were lysed with 0.1 M NaOH, and the lysate was collected in different counting tubes for detection using a γ-counter instrument. The cell uptake results were expressed as the percentage of added dose (%AD) per 10^5 cells.

[00768] For the saturation binding experiment, AGS$^{CLDN18.2}$ cells were treated with eight concentrations of the probe (1.25, 2.5, 5, 10, 20, 40, 80, 160 nmol/L, n=4). The cells were processed as described above, and the wells for measurement were transferred to counting

tubes. The radioactive counts were measured using a γ-counter instrument, and the data were further analyzed using GraphPad Prism software to fit the curves and calculate the dissociation constant (Kd) between ^{177}Lu-DOTA-18B10 and cell CLDN18.2, thereby determining their affinity.

[00769] *6) SPECT imaging and ROI analysis*

[00770] Single photon emission computed tomography (SPECT) imaging of the tumor-bearing mouse models was performed using SPECT/CT scan (Mediso Inc., Hungary). BGC823, BGC823$^{CLDN18.2}$, AGS, and AGS$^{CLDN18.2}$ tumor-bearing mice (n=3) received a tail vein injection of 7.40 MBq of ^{177}Lu-DOTA-18B10 (100 μL). The mice were anesthetized and subjected to SPECT imaging at 4, 24, 48, 72, and 144 h after injection. The Block group received a co-injection of excess unlabeled 18B10 to observe the specific blocking effect. During the SPECT/CT scan, mice were anesthetized by inhalation of 2% isoflurane in O_2. The pinhole SPECT images (20% width; frame time: 20 s) were acquired for 18.5 mins and subsequently CT images were acquired (50 kVp, 0.67 mA, rotation 210°, exposure time: 300 ms). After acquiring and reconstructing the images, regions of interest (ROIs) were delineated for the tumors, blood pool and major organs (liver, spleen, muscle), and the percent injected dose/cubic centimeter (%ID/cc) data were obtained for subsequent analysis.

[00771] *7) Biodistribution, dosimetry estimation, and pharmacokinetics*

[00772] The ex vivo biodistribution experiment involved the intravenous injection of radiolabeled drug ^{177}Lu-DOTA-18B10 into BGC823$^{CLDN18.2}$ (positive model) and BGC823 (negative model) xenograft-bearing mice (n=4, each with a dose of 0.37-0.56 MBq). The positive model block group received a co-injection of excess unlabeled 18B10 precursor at the same time. The mice were anesthetized and euthanized at 8, 24, 48, 72, and 144 h post-injection (negative model group and block group only have 48-hour time point). Blood and major organs (heart, liver, spleen, lung, kidney, stomach, intestine, bone, muscle) were collected, rinsed, dried, weighed using an electronic balance, and placed in counting tubes for detection using a γ-counter instrument. The calculated biodistribution results were reported as the percentage of injected dose per gram (%ID/g). All counts were background and decay corrected.

[00773] Dosimetry estimation involved using the biodistribution data of ^{177}Lu-DOTA-18B10 in the aforementioned animal models to estimate the radiation doses to human organs using the OLINDA/EXM software (2.0, Vanderbilt University, America).

[00774] Pharmacokinetics experiments were conducted in normal KM mice (female, n=6) after intravenous injection of 0.37-0.56 MBq of ^{177}Lu-DOTA-18B10. Blood samples were

collected from the periorbital veins at 1, 3, 5, 10, 15, 30 minutes and 1, 2, 4, 8, 11, 24, 48, 71, 94, and 148 h. The samples were analyzed for radioactivity using a γ-counter, and the data were processed and analyzed using GraphPad Prism software.

[00775] Table 8: REFERENCES FOR EXAMPLES 1-5

1. Tsukita S, Furuse M, Itoh M. Multifunctional strands in tight junctions. Nat Rev Mol Cell Biol. 2001;2(4):285-93.
2. Gunzel D, Yu AS. Claudins and the modulation of tight junction permeability. Physiol Rev. 2013;93(2):525-69.
3. Zihni C, Mills C, Matter K, Balda MS. Tight junctions: from simple barriers to multifunctional molecular gates. Nat Rev Mol Cell Biol. 2016;17(9):564-80.
4. Niimi T, Nagashima K, Ward JM, Minoo P, Zimonjic DB, Popescu NC, et al. claudin-18, a novel downstream target gene for the T/EBP/NKX2.1 homeodomain transcription factor, encodes lung- and stomach-specific isoforms through alternative splicing. Mol Cell Biol. 2001;21(21):7380-90.
5. Sahin U, Koslowski M, Dhaene K, Usener D, Brandenburg G, Seitz G, et al. Claudin-18 splice variant 2 is a pan-cancer target suitable for therapeutic antibody development. Clinical cancer research : an official journal of the American Association for Cancer Research. 2008;14(23):7624-34.
6. Iwaya M, Hayashi H, Nakajima T, Matsuda K, Kinugawa Y, Tobe Y, et al. Colitis-associated colorectal adenocarcinomas frequently express claudin 18 isoform 2: implications for claudin 18.2 monoclonal antibody therapy. Histopathology. 2021;79(2):227-37.
7. Kyuno D, Takasawa A, Takasawa K, Ono Y, Aoyama T, Magara K, et al. Claudin-18.2 as a therapeutic target in cancers: cumulative findings from basic research and clinical trials. Tissue Barriers. 2021:1967080.
8. Klempner SJ, Ajani JA, Al-Batran S-E, Bang Y-J, Catenacci DVT, Enzinger PC, et al. Phase II study of zolbetuximab plus pembrolizumab in claudin 18.2: Positive locally advanced or metastatic gastric or gastroesophageal junction adenocarcinoma (G/GEJ)—ILUSTRO Cohort 3. 2021;39(3_suppl):TPS260-TPS.
9. Yamaguchi K, Shitara K, Al-Batran SE, Bang YJ, Catenacci D, Enzinger P, et al. 198TiP - SPOTLIGHT: Comparison of zolbetuximab or placebo + mFOLFOX6 as first-line treatment in patients with claudin18.2+/HER2– locally advanced unresectable or metastatic gastric or gastroesophageal junction adenocarcinoma (GEJ): A randomized phase III study. Annals of Oncology. 2019;30:ix66-ix7.
10. Xu RH, Ajani JA, Al-Batran SE, Bang YJ, Catenacci D, Enzinger PC, et al. 195TiP GLOW: Phase III study of first-line zolbetuximab + CAPOX versus placebo + CAPOX in Claudin18.2^{+}/HER2^{-} advanced/metastatic gastric or gastroesophageal junction adenocarcinoma (G/GEJ). Annals of Oncology. 2020;31:S1315-S6.
11. Sahin U, Türeci Ö, Manikhas G, Lordick F, Rusyn A, Vynnychenko I, et al. FAST: A randomised phase II study of zolbetuximab (IMAB362) plus EOX vs EOX alone for first-line treatment of advanced CLDN18.2 positive gastric and gastro-oesophageal adenocarcinoma. Annals of oncology : official journal of the European Society for Medical Oncology. 2021.
12. Qi C, Gong J, Li J, Liu D, Qin Y, Ge S, et al. Claudin18.2-specific CAR T cells in gastrointestinal cancers: phase 1 trial interim results. Nature medicine. 2022.
13. Kage H, Flodby P, Zhou B, Borok Z. Dichotomous roles of claudins as tumor

promoters or suppressors: lessons from knockout mice. Cell Mol Life Sci. 2019;76(23):4663-72.
14. Zhao C, Rong Z, Ding J, Wang L, Wang B, Ding L, et al. Targeting Claudin 18.2 Using a Highly Specific Antibody Enables Cancer Diagnosis and Guided Surgery. Molecular pharmaceutics. 2022.
15. H. Zhu JD, X. Chong, C. Ji, C. Zhang, F. Teng, Y. Gu, X. Qian, Z. Yang, L. Shen, J. Gao. Molecular imaging evaluation of a novel Claudin18.2. specific monoclonal antibody labeled with radionuclide. Annals of Oncology. 2021(32).
16. Wang S, Zhu H, Ding J, Wang F, Meng X, Ding L, et al. Positron Emission Tomography Imaging of Programmed Death 1 Expression in Cancer Patients Using 124I-Labeled Toripalimab: A Pilot Clinical Translation Study. Clin Nucl Med. 2021;46(5):382-8.
17. Jiang H, Shi Z, Wang P, Wang C, Yang L, Du G, et al. Claudin18.2-Specific Chimeric Antigen Receptor Engineered T Cells for the Treatment of Gastric Cancer. J Natl Cancer Inst. 2019;111(4):409-18.
18. Zhang J, Dong R, Shen L. Evaluation and reflection on claudin 18.2 targeting therapy in advanced gastric cancer. Chinese journal of cancer research = Chung-kuo yen cheng yen chiu. 2020;32(2):263-70.
19. Gerwing M, Herrmann K, Helfen A, Schliemann C, Berdel WE, Eisenblatter M, et al. The beginning of the end for conventional RECIST - novel therapies require novel imaging approaches. Nature reviews Clinical oncology. 2019.
20. Bensch F, van der Veen EL, Lub-de Hooge MN, Jorritsma-Smit A, Boellaard R, Kok IC, et al. (89)Zr-atezolizumab imaging as a non-invasive approach to assess clinical response to PD-L1 blockade in cancer. Nature medicine. 2018;24(12):1852-8.
21. Niemeijer AN, Leung D, Huisman MC, Bahce I, Hoekstra OS, van Dongen G, et al. Whole body PD-1 and PD-L1 positron emission tomography in patients with non-small-cell lung cancer. Nature communications. 2018;9(1):4664.
22. Kok IC, Hooiveld JS, van de Donk PP, Giesen D, van der Veen EL, Lub-de Hooge MN, et al. (89)Zr-pembrolizumab imaging as a non-invasive approach to assess clinical response to PD-1 blockade in cancer. Annals of oncology : official journal of the European Society for Medical Oncology. 2022;33(1):80-8.
23. Türeci O, Sahin U, Schulze-Bergkamen H, Zvirbule Z, Lordick F, Koeberle D, et al. A multicentre, phase IIa study of zolbetuximab as a single agent in patients with recurrent or refractory advanced adenocarcinoma of the stomach or lower oesophagus: the MONO study. Annals of Oncology. 2019;30(9):1487-95.
24. Sahin U, Schuler M, Richly H, Bauer S, Krilova A, Dechow T, et al. A phase I dose-escalation study of IMAB362 (Zolbetuximab) in patients with advanced gastric and gastro-oesophageal junction cancer. European Journal of Cancer. 2018;100:17-26.

[00776] Table 9: REFERENCES FOR EXAMPLE 6

[1] H. Sung, J. Ferlay, R.L. Siegel, M. Laversanne, I. Soerjomataram, A. Jemal, F. Bray, Global Cancer Statistics 2020: GLOBOCAN Estimates of Incidence and Mortality Worldwide for 36 Cancers in 185 Countries, CA Cancer J Clin. 71 (2021) 209–249. https://doi.org/10.3322/caac.21660.

[2] W. Cao, H.-D. Chen, Y.-W. Yu, N. Li, W.-Q. Chen, Changing profiles of cancer burden worldwide and in China: a secondary analysis of the global cancer statistics 2020, Chin Med J (Engl). 134 (2021) 783–791. https://doi.org/10.1097/CM9.0000000000001474.

[3] H. Qiu, S. Cao, R. Xu, Cancer incidence, mortality, and burden in China: a time-trend

analysis and comparison with the United States and United Kingdom based on the global epidemiological data released in 2020, Cancer Commun (Lond). 41 (2021) 1037–1048. https://doi.org/10.1002/cac2.12197.

[4] Y.Y. Janjigian, K. Shitara, M. Moehler, M. Garrido, P. Salman, L. Shen, L. Wyrwicz, K. Yamaguchi, T. Skoczylas, A. Campos Bragagnoli, T. Liu, M. Schenker, P. Yanez, M. Tehfe, R. Kowalyszyn, M.V. Karamouzis, R. Bruges, T. Zander, R. Pazo-Cid, E. Hitre, K. Feeney, J.M. Cleary, V. Poulart, D. Cullen, M. Lei, H. Xiao, K. Kondo, M. Li, J.A. Ajani, First-line nivolumab plus chemotherapy versus chemotherapy alone for advanced gastric, gastro-oesophageal junction, and oesophageal adenocarcinoma (CheckMate 649): a randomised, open-label, phase 3 trial, Lancet. 398 (2021) 27–40. https://doi.org/10.1016/S0140-6736(21)00797-2.

[5] E. Van Cutsem, V.M. Moiseyenko, S. Tjulandin, A. Majlis, M. Constenla, C. Boni, A. Rodrigues, M. Fodor, Y. Chao, E. Voznyi, M.-L. Risse, J.A. Ajani, V325 Study Group, Phase III study of docetaxel and cisplatin plus fluorouracil compared with cisplatin and fluorouracil as first-line therapy for advanced gastric cancer: a report of the V325 Study Group, J Clin Oncol. 24 (2006) 4991–4997. https://doi.org/10.1200/JCO.2006.06.8429.

[6] K. Shitara, Chemotherapy for advanced gastric cancer: future perspective in Japan, Gastric Cancer. 20 (2017) 102–110. https://doi.org/10.1007/s10120-016-0648-7.

[7] M. Pavel, K. Öberg, M. Falconi, E.P. Krenning, A. Sundin, A. Perren, A. Berruti, ESMO Guidelines Committee. Electronic address: clinicalguidelines@esmo.org, Gastroenteropancreatic neuroendocrine neoplasms: ESMO Clinical Practice Guidelines for diagnosis, treatment and follow-up, Ann Oncol. 31 (2020) 844–860. https://doi.org/10.1016/j.annonc.2020.03.304.

[8] L. Shen, Anticancer drug R&D of gastrointestinal cancer in China: Current landscape and challenges, Innovation (Camb). 3 (2022) 100249. https://doi.org/10.1016/j.xinn.2022.100249.

[9] S. Tsukita, M. Furuse, M. Itoh, Multifunctional strands in tight junctions, Nat Rev Mol Cell Biol. 2 (2001) 285–293. https://doi.org/10.1038/35067088.

[10] D. Günzel, A.S.L. Yu, Claudins and the modulation of tight junction permeability, Physiol Rev. 93 (2013) 525–569. https://doi.org/10.1152/physrev.00019.2012.

[11] T. Otani, M. Furuse, Tight Junction Structure and Function Revisited, Trends Cell Biol. 30 (2020) 805–817. https://doi.org/10.1016/j.tcb.2020.08.004.

[12] S. Tabariès, P.M. Siegel, The role of claudins in cancer metastasis, Oncogene. 36 (2017) 1176–1190. https://doi.org/10.1038/onc.2016.289.

[13] I. Hashimoto, T. Oshima, Claudins and Gastric Cancer: An Overview, Cancers (Basel). 14 (2022) 290. https://doi.org/10.3390/cancers14020290.

[14] U. Sahin, Ö. Türeci, G. Manikhas, F. Lordick, A. Rusyn, I. Vynnychenko, A. Dudov, I. Bazin, I. Bondarenko, B. Melichar, K. Dhaene, K. Wiechen, C. Huber, D. Maurus, A. Arozullah, J.W. Park, M. Schuler, S.-E. Al-Batran, FAST: a randomised phase II study of zolbetuximab (IMAB362) plus EOX versus EOX alone for first-line treatment of advanced CLDN18.2-positive gastric and gastro-oesophageal adenocarcinoma, Ann Oncol. 32 (2021) 609–619. https://doi.org/10.1016/j.annonc.2021.02.005.

[15] A phase I study of TST001, a high affinity humanized anti-CLDN18.2 monoclonal antibody, in combination with capecitabine and oxaliplatin (CAPOX) as a first-line treatment of advanced G/GEJ cancer. | Journal of Clinical Oncology, (n.d.). https://ascopubs.org/doi/10.1200/JCO.2022.40.16_suppl.4062 (accessed November 2, 2022).

[16] C. Qi, J. Gong, J. Li, D. Liu, Y. Qin, S. Ge, M. Zhang, Z. Peng, J. Zhou, Y. Cao, X.

Zhang, Z. Lu, M. Lu, J. Yuan, Z. Wang, Y. Wang, X. Peng, H. Gao, Z. Liu, H. Wang, D. Yuan, J. Xiao, H. Ma, W. Wang, Z. Li, L. Shen, Claudin18.2-specific CAR T cells in gastrointestinal cancers: phase 1 trial interim results, Nat Med. 28 (2022) 1189–1198. https://doi.org/10.1038/s41591-022-01800-8.

[17] L. Fan, X. Chong, M. Zhao, F. Jia, Z. Wang, Y. Zhou, X. Lu, Q. Huang, P. Li, Y. Yang, Z. Hu, Q. Li, X. Zhang, L. Shen, Ultrasensitive Gastric Cancer Circulating Tumor Cellular CLDN18.2 RNA Detection Based on a Molecular Beacon, Anal Chem. 93 (2021) 665–670. https://doi.org/10.1021/acs.analchem.0c04055.

[18] T. Gu, H. Shi, Relationship of 18F-FDG PET/CT Parameters and CLDN18.2 Expression Status in Gastric Cancer, Journal of Nuclear Medicine. 63 (2022) 3028–3028.

[19] G. Hu, W. Zhu, Y. Liu, Y. Wang, Z. Zhang, S. Zhu, W. Duan, P. Zhou, C. Fu, F. Li, L. Huo, Development and comparison of three 89Zr-labeled anti-CLDN18.2 antibodies to noninvasively evaluate CLDN18.2 expression in gastric cancer: a preclinical study, Eur J Nucl Med Mol Imaging. 49 (2022) 2634–2644. https://doi.org/10.1007/s00259-022-05739-3.

[20] G. Hu, W. Zhu, Y. Liu, W. Duan, P. Zhou, F. Li, L. Huo, Study of 89Zr-labeled recombinant antibody VHH-Fc for noninvasive evaluation of CLDN18.2 expression in gastric cancer, Journal of Nuclear Medicine. 63 (2022) 2525–2525.

[21] C. Zhao, Z. Rong, J. Ding, L. Wang, B. Wang, L. Ding, L. Meng, X. Meng, F. Wang, Z. Yang, C. Shou, H. Zhu, Targeting Claudin 18.2 Using a Highly Specific Antibody Enables Cancer Diagnosis and Guided Surgery, Mol Pharm. 19 (2022) 3530–3541. https://doi.org/10.1021/acs.molpharmaceut.1c00947.

[22] P.K.E. Börjesson, Y.W.S. Jauw, R. de Bree, J.C. Roos, J.A. Castelijns, C.R. Leemans, G.A.M.S. van Dongen, R. Boellaard, Radiation dosimetry of 89Zr-labeled chimeric monoclonal antibody U36 as used for immuno-PET in head and neck cancer patients, J Nucl Med. 50 (2009) 1828–1836. https://doi.org/10.2967/jnumed.109.065862.

[23] R. Laforest, S.E. Lapi, R. Oyama, R. Bose, A. Tabchy, B.V. Marquez-Nostra, J. Burkemper, B.D. Wright, J. Frye, S. Frye, B.A. Siegel, F. Dehdashti, [89Zr]Trastuzumab: Evaluation of Radiation Dosimetry, Safety, and Optimal Imaging Parameters in Women with HER2-Positive Breast Cancer, Mol Imaging Biol. 18 (2016) 952–959. https://doi.org/10.1007/s11307-016-0951-z.

[24] Pharmacokinetics, Biodistribution, and Radiation Dosimetry for 89Zr-Trastuzumab in Patients with Esophagogastric Cancer | Journal of Nuclear Medicine, (n.d.). https://jnm.snmjournals.org/content/59/1/161.long (accessed November 1, 2022).

[25] C.G. England, E.B. Ehlerding, R. Hernandez, B.T. Rekoske, S.A. Graves, H. Sun, G. Liu, D.G. McNeel, T.E. Barnhart, W. Cai, Preclinical Pharmacokinetics and Biodistribution Studies of 89Zr-Labeled Pembrolizumab, J Nucl Med. 58 (2017) 162–168. https://doi.org/10.2967/jnumed.116.177857.

[26] N.B. Sobol, J.A. Korsen, A. Younes, K.J. Edwards, J.S. Lewis, ImmunoPET Imaging of Pancreatic Tumors with 89Zr-Labeled Gold Nanoparticle-Antibody Conjugates, Mol Imaging Biol. 23 (2021) 84–94. https://doi.org/10.1007/s11307-020-01535-3.

[27] D. Vivier, S.K. Sharma, P. Adumeau, C. Rodriguez, K. Fung, B.M. Zeglis, The Impact of FcγRI Binding on Immuno-PET, J Nucl Med. 60 (2019) 1174–1182. https://doi.org/10.2967/jnumed.118.223636.

[28] P. Adumeau, R. Raavé, M. Boswinkel, S. Heskamp, H.J.C.T. Wessels, A.J. van Gool, M. Moreau, C. Bernhard, L. Da Costa, V. Goncalves, F. Denat, Site-Specific, Platform-Based Conjugation Strategy for the Synthesis of Dual-Labeled Immunoconjugates for Bimodal PET/NIRF Imaging of HER2-Positive Tumors, Bioconjug Chem. 33 (2022) 530–

540. https://doi.org/10.1021/acs.bioconjchem.2c00049.

[29] L.E. Lamberts, S.P. Williams, A.G.T. Terwisscha van Scheltinga, M.N. Lub-de Hooge, C.P. Schröder, J.A. Gietema, A.H. Brouwers, E.G.E. de Vries, Antibody positron emission tomography imaging in anticancer drug development, J Clin Oncol. 33 (2015) 1491–1504. https://doi.org/10.1200/JCO.2014.57.8278.

[30] J. Zhang, R. Dong, L. Shen, Evaluation and reflection on claudin 18.2 targeting therapy in advanced gastric cancer, Chin J Cancer Res. 32 (2020) 263–270. https://doi.org/10.21147/j.issn.1000-9604.2020.02.13.

[00777] Table 10: REFERENCES FOR EXAMPLE 8

[1] Correa P. Gastric Cancer: Overview. *Gastroenterol Clin North Am.* 2013;42:211-217.
[2] Bass AJ, Thorsson V, Shmulevich I, et al. Comprehensive molecular characterization of gastric adenocarcinoma. *Nature*. 2014;513:202-209.
[3] Cristescu R, Lee J, Nebozhyn M, et al. Molecular analysis of gastric cancer identifies subtypes associated with distinct clinical outcomes. *Nat Med*. 2015;21:449-456.
[4] Thomassen I, van Gestel YR, van Ramshorst B, et al. Peritoneal carcinomatosis of gastric origin: A population-based study on incidence, survival and risk factors. *International Journal of Cancer*. 2014;134:622-628.
[5] Xu C-D. Clinical Study of Nimotuzumab Combined with Chemotherapy in the Treatment of Late Stage Gastric Cancer. *Asian Pac J Cancer Prev*. 2014;15:10273-10276.
[6] Rosenbaum MW, Gonzalez RS. Targeted therapy for upper gastrointestinal tract cancer: current and future prospects. *Histopathology*. 2021;78:148-161.
[7] Sahin U, Türeci Ö, Manikhas G, et al. FAST: a randomised phase II study of zolbetuximab (IMAB362) plus EOX versus EOX alone for first-line treatment of advanced CLDN18.2-positive gastric and gastro-oesophageal adenocarcinoma. *Ann Oncol*. 2021;32:609-619.
[8] Sahin U, Koslowski M, Dhaene K, et al. Claudin-18 Splice Variant 2 Is a Pan-Cancer Target Suitable for Therapeutic Antibody Development. *Clinical Cancer Research*. 2008;14:7624-7634.
[9] Niimi T, Nagashima K, Ward JM, et al. claudin-18, a Novel Downstream Target Gene for the T/EBP/NKX2.1 Homeodomain Transcription Factor, Encodes Lung- and Stomach-Specific Isoforms through Alternative Splicing. *Mol Cell Biol*. 2001;21:7380-7390.
[10] Türeci Ö, Koslowski M, Helftenbein G, et al. Claudin-18 gene structure, regulation, and expression is evolutionary conserved in mammals. *Gene*. 2011;481:83-92.
[11] Jun K-H, Kim J-H, Jung J-H, Choi H-J, Chin H-M. Expression of claudin-7 and loss of claudin-18 correlate with poor prognosis in gastric cancer. *International Journal of Surgery*. 2014;12:156-162.
[12] Sentani K, Oue N, Tashiro T, et al. Immunohistochemical Staining of Reg IV and Claudin-18 is Useful in the Diagnosis of Gastrointestinal Signet Ring Cell Carcinoma. *The American Journal of Surgical Pathology*. 2008;32:1182.
[13] Schuler MH, Al-Batran S-E, Zvirbule Z, et al. Expression of Claudin 18.2 and HER2 in gastric, gastroesophageal junction, and esophageal cancers: Results from the FAST study. *JCO*. 2017;35:4038-4038.
[14] Zhao S, Su L, Chen Y, et al. Phase 2 randomized controlled trial of intravenous or intraperitoneal paclitaxel plus mFOLFOX6 vs. mFOLFOX6 as first-line treatment of advanced gastric cancer. *Frontiers in Oncology*. 2022;12.
[15] Guo X, Zhou N, Chen Z, et al. Construction of 124I-trastuzumab for noninvasive PET imaging of HER2 expression: from patient-derived xenograft models to gastric cancer

patients. *Gastric Cancer*. 2020;23:614-626.
[16] Zhao C, Rong Z, Ding J, et al. Targeting Claudin 18.2 Using a Highly Specific Antibody Enables Cancer Diagnosis and Guided Surgery. *Molecular Pharmaceutics*. 2022;19:3530-3541.
[17] Thurber GM, Schmidt MM, Wittrup KD. Antibody tumor penetration. *Adv Drug Deliv Rev*. 2008;60:1421.
[18] Sundaresan G, Yazaki PJ, Shively JE, et al. 124I-Labeled Engineered Anti-CEA Minibodies and Diabodies Allow High-Contrast, Antigen-Specific Small-Animal PET Imaging of Xenografts in Athymic Mice. *Journal of Nuclear Medicine*. 2003;44:1962-1969.
[19] Kenanova V, Olafsen T, Crow DM, et al. Tailoring the Pharmacokinetics and Positron Emission Tomography Imaging Properties of Anti–Carcinoembryonic Antigen Single-Chain Fv-Fc Antibody Fragments. *Cancer Res*. 2005;65:622-631.
[20] Martin WL, West AP, Gan L, Bjorkman PJ. Crystal Structure at 2.8 Å of an FcRn/Heterodimeric Fc Complex: Mechanism of pH-Dependent Binding. *Molecular Cell*. 2001;7:867-877.
[21] Cao W, Xing H, Li Y, et al. Claudin18.2 is a novel molecular biomarker for tumor-targeted immunotherapy. *Biomarker Research*. 2022;10:38-58.
[22] Jiang H, Shi Z, Wang P, et al. Claudin18.2-Specific Chimeric Antigen Receptor Engineered T Cells for the Treatment of Gastric Cancer. *J Natl Cancer Inst*. 2019;111:409-418.
[23] Carrasco-Garcia E, García-Puga M, Arevalo S, Matheu A. Towards precision medicine: linking genetic and cellular heterogeneity in gastric cancer. *Ther Adv Med Oncol*. 2018;10:1758835918794628.
[24] Collaborators G 2016 C of D. Global, regional, and national age-sex specific mortality for 264 causes of death, 1980–2016: a systematic analysis for the Global Burden of Disease Study 2016. *Lancet (London, England)*. 2017;390:1151-1210.
[25] Qiu H, Cao S, Xu R. Cancer incidence, mortality, and burden in China: a time‐trend analysis and comparison with the United States and United Kingdom based on the global epidemiological data released in 2020. *Cancer Communications*. 2021;41:1037-1048.
[26] Dottermusch M, Krüger S, Behrens H-M, Halske C, Röcken C. Expression of the potential therapeutic target claudin-18.2 is frequently decreased in gastric cancer: results from a large Caucasian cohort study. *Virchows Arch*. 2019;475:563-571.
[27] Tureci Ö, Itoh K, Yamaguchi R, Mukhina S, Sahin U, Rohde C. High Prevalence of Claudin 18.2 Expression in Japanese Patients with Gastric Cancer. *JCO*. 2017;35:e15584-e15584.
[28] Yamashita K, Iwatsuki M, Harada K, et al. Can PD-L1 expression evaluated by biopsy sample accurately reflect its expression in the whole tumour in gastric cancer? *Br J Cancer*. 2019;121:278-280.
[29] Zhang M, Li S, Zhang H, Xu H. Research progress of 18F labeled small molecule positron emission tomography (PET) imaging agents. *European Journal of Medicinal Chemistry*. 2020;205:112629.
[30] Sivolapenko GB, Douli V, Sirmalis G, et al. Breast cancer imaging with radiolabelled peptide from complementarity-determining region of antitumour antibody. *The Lancet*. 1995;346:1662-1666.
[31] Kenanova V, Olafsen T, Crow DM, et al. Tailoring the Pharmacokinetics and Positron Emission Tomography Imaging Properties of Anti–Carcinoembryonic Antigen Single-Chain Fv-Fc Antibody Fragments. *Cancer Res*. 2005;65:622-631.
[32] Chacko A-M, Divgi CR. Radiopharmaceutical chemistry with iodine-124: A non-standard radiohalogen for positron emission tomography. *Medicinal Chemistry*.

2011;7:395-412.
[33] Divgi CR, Pandit-Taskar N, Jungbluth AA, et al. Preoperative characterisation of clear-cell renal carcinoma using iodine-124-labelled antibody chimeric G250 (124I-cG250) and PET in patients with renal masses: a phase I trial. *The Lancet Oncology*. 2007;8:304-310.
[34] Wang S, Zhu H, Ding J, et al. Positron Emission Tomography Imaging of Programmed Death 1 Expression in Cancer Patients Using 124I-Labeled Toripalimab: A Pilot Clinical Translation Study. *Clinical Nuclear Medicine*. 2021;46:382.
[35] Liu Q, Jiang L, Li K, et al. Immuno-PET imaging of 68Ga-labeled nanobody Nb109 for dynamic monitoring the PD-L1 expression in cancers. *Cancer Immunol Immunother*. 2021;70:1721-1733.

[00778] Table 11: REFERENCES FOR EXAMPLE 9

1. Smyth EC, Nilsson M, Grabsch HI, van Grieken NC, Lordick F. Gastric cancer. Lancet (London, England). 2020; 396: 635-648.
2. Siegel RL, Miller KD, Wagle NS, Jemal A. Cancer statistics, 2023. CA Cancer J Clin. 2023; 73: 17-48.
3. Cao W, Chen HD, Yu YW, Li N, Chen WQ. Changing profiles of cancer burden worldwide and in china: A secondary analysis of the global cancer statistics 2020. Chinese medical journal. 2021; 134: 783-791.
4. Rosenbaum MW, Gonzalez RS. Targeted therapy for upper gastrointestinal tract cancer: Current and future prospects. Histopathology. 2021; 78: 148-161.
5. Fuchs CS, Doi T, Jang RW, Muro K, Satoh T, Machado M, et al. Safety and efficacy of pembrolizumab monotherapy in patients with previously treated advanced gastric and gastroesophageal junction cancer: Phase 2 clinical keynote-059 trial. JAMA oncology. 2018; 4: e180013.
6. Bang YJ, Ruiz EY, Van Cutsem E, Lee KW, Wyrwicz L, Schenker M, et al. Phase iii, randomised trial of avelumab versus physician's choice of chemotherapy as third-line treatment of patients with advanced gastric or gastro-oesophageal junction cancer: Primary analysis of javelin gastric 300. Ann Oncol. 2018; 29: 2052-2060.
7. Shitara K. Chemotherapy for advanced gastric cancer: Future perspective in japan. Gastric cancer : official journal of the International Gastric Cancer Association and the Japanese Gastric Cancer Association. 2017; 20: 102-110.
8. Pavel M, Öberg K, Falconi M, Krenning EP, Sundin A, Perren A, et al. Gastroenteropancreatic neuroendocrine neoplasms: Esmo clinical practice guidelines for diagnosis, treatment and follow-up. Ann Oncol. 2020; 31: 844-860.
9. Janjigian YY, Shitara K, Moehler M, Garrido M, Salman P, Shen L, et al. First-line nivolumab plus chemotherapy versus chemotherapy alone for advanced gastric, gastro-oesophageal junction, and oesophageal adenocarcinoma (checkmate 649): A randomised, open-label, phase 3 trial. Lancet (London, England). 2021; 398: 27-40.
10. Shen L. Anticancer drug r&d of gastrointestinal cancer in china: Current landscape and challenges. Innovation (Cambridge (Mass.)). 2022; 3: 100249.
11. Shen L, Shan YS, Hu HM, Price TJ, Sirohi B, Yeh KH, et al. Management of

gastric cancer in asia: Resource-stratified guidelines. The Lancet. Oncology. 2013; 14: e535-47.
12. Wang P, Zhou H, Han G, Ni Q, Dai S, Huang J, et al. Assessment of the value of adjuvant radiotherapy for treatment of gastric adenocarcinoma based on pattern of post-surgical progression. World journal of surgical oncology. 2021; 19: 205.
13. Kammerer-Jacquet SF, Deleuze A, Saout J, Mathieu R, Laguerre B, Verhoest G, et al. Targeting the pd-1/pd-l1 pathway in renal cell carcinoma. International journal of molecular sciences. 2019; 20:
14. Luo L, Lv M, Zhuang X, Zhang Q, Qiao T. Irradiation increases the immunogenicity of lung cancer cells and irradiation-based tumor cell vaccine elicits tumor-specific t cell responses in vivo. OncoTargets and therapy. 2019; 12: 3805-3815.
15. Cheng Y, Dong Y, Hou Q, Wu J, Zhang W, Tian H, et al. The protective effects of xh-105 against radiation-induced intestinal injury. Journal of cellular and molecular medicine. 2019; 23: 2238-2247.
16. O'Donoghue JA, Bardiès M, Wheldon TE. Relationships between tumor size and curability for uniformly targeted therapy with beta-emitting radionuclides. Journal of nuclear medicine : official publication, Society of Nuclear Medicine. 1995; 36: 1902-9.
17. Hindié E, Zanotti-Fregonara P, Quinto MA, Morgat C, Champion C. Dose deposits from 90y, 177lu, 111in, and 161tb in micrometastases of various sizes: Implications for radiopharmaceutical therapy. Journal of nuclear medicine : official publication, Society of Nuclear Medicine. 2016; 57: 759-64.
18. Türeci O, Koslowski M, Helftenbein G, Castle J, Rohde C, Dhaene K, et al. Claudin-18 gene structure, regulation, and expression is evolutionary conserved in mammals. Gene. 2011; 481: 83-92.
19. Günzel D, Yu AS. Claudins and the modulation of tight junction permeability. Physiological reviews. 2013; 93: 525-69.
20. Otani T, Furuse M. Tight junction structure and function revisited. Trends in cell biology. 2020; 30: 805-817.
21. Sahin U, Koslowski M, Dhaene K, Usener D, Brandenburg G, Seitz G, et al. Claudin-18 splice variant 2 is a pan-cancer target suitable for therapeutic antibody development. Clin Cancer Res. 2008; 14: 7624-34.
22. Iwaya M, Hayashi H, Nakajima T, Matsuda K, Kinugawa Y, Tobe Y, et al. Colitis-associated colorectal adenocarcinomas frequently express claudin 18 isoform 2: Implications for claudin 18.2 monoclonal antibody therapy. Histopathology. 2021; 79: 227-237.
23. Tabariès S, Siegel PM. The role of claudins in cancer metastasis. Oncogene. 2017; 36: 1176-1190.
24. Hashimoto I, Oshima T. Claudins and gastric cancer: An overview. Cancers. 2022; 14:
25. Baek JH, Park DJ, Kim GY, Cheon J, Kang BW, Cha HJ, et al. Clinical implications of claudin18.2 expression in patients with gastric cancer. Anticancer Res. 2019; 39: 6973-6979.
26. Shitara K, Lordick F, Bang YJ, Enzinger P, Ilson D, Shah MA, et al. Zolbetuximab plus mfolfox6 in patients with cldn18.2-positive, her2-negative, untreated, locally advanced unresectable or metastatic gastric or gastro-oesophageal junction adenocarcinoma (spotlight): A multicentre, randomised, double-blind, phase 3 trial. Lancet (London, England). 2023; 401: 1655-1668.
27. Kyuno D, Takasawa A, Takasawa K, Ono Y, Aoyama T, Magara K, et al. Claudin-

18.2 as a therapeutic target in cancers: Cumulative findings from basic research and clinical trials. Tissue barriers. 2022; 10: 1967080.
28. Sahin U, Türeci Ö, Manikhas G, Lordick F, Rusyn A, Vynnychenko I, et al. Fast: A randomised phase ii study of zolbetuximab (imab362) plus eox versus eox alone for first-line treatment of advanced cldn18.2-positive gastric and gastro-oesophageal adenocarcinoma. Ann Oncol. 2021; 32: 609-619.
29. Lordick F, Al-Batran SE, Ganguli A, Morlock R, Sahin U, Türeci Ö. Patient-reported outcomes from the phase ii fast trial of zolbetuximab plus eox compared to eox alone as first-line treatment of patients with metastatic cldn18.2+ gastroesophageal adenocarcinoma. Gastric cancer : official journal of the International Gastric Cancer Association and the Japanese Gastric Cancer Association. 2021; 24: 721-730.
30. Hristodorov D, Fischer R, Linden L. With or without sugar? (a)glycosylation of therapeutic antibodies. Molecular biotechnology. 2013; 54: 1056-68.
31. Chen Y, Hou X, Li D, Ding J, Liu J, Wang Z, et al. Development of a cldn18.2-targeting immuno-pet probe for non-invasive imaging in gastrointestinal tumors. Journal of pharmaceutical analysis. 2023; 13: 367-375.
32. Qi C, Gong J, Li J, Liu D, Qin Y, Ge S, et al. Claudin18.2-specific car t cells in gastrointestinal cancers: Phase 1 trial interim results. Nat Med. 2022; 28: 1189-1198.
33. Türeci O, Sahin U, Schulze-Bergkamen H, Zvirbule Z, Lordick F, Koeberle D, et al. A multicentre, phase iia study of zolbetuximab as a single agent in patients with recurrent or refractory advanced adenocarcinoma of the stomach or lower oesophagus: The mono study. Ann Oncol. 2019; 30: 1487-1495.
34. Han X, Wang Y, Wei J, Han W. Multi-antigen-targeted chimeric antigen receptor t cells for cancer therapy. Journal of hematology & oncology. 2019; 12: 128.
35. Wei W, Liu Q, Jiang D, Zhao H, Kutyreff CJ, Engle JW, et al. Tissue factor-targeted immunopet imaging and radioimmunotherapy of anaplastic thyroid cancer. Advanced science (Weinheim, Baden-Wurttemberg, Germany). 2020; 7: 1903595.
36. Larson SM, Carrasquillo JA, Cheung NK, Press OW. Radioimmunotherapy of human tumours. Nat Rev Cancer. 2015; 15: 347-60.
37. Green DJ, O'Steen S, Lin Y, Comstock ML, Kenoyer AL, Hamlin DK, et al. Cd38-bispecific antibody pretargeted radioimmunotherapy for multiple myeloma and other b-cell malignancies. Blood. 2018; 131: 611-620.
38. Cheal SM, Xu H, Guo HF, Patel M, Punzalan B, Fung EK, et al. Theranostic pretargeted radioimmunotherapy of internalizing solid tumor antigens in human tumor xenografts in mice: Curative treatment of her2-positive breast carcinoma. Theranostics. 2018; 8: 5106-5125.
39. Cheal SM, McDevitt MR, Santich BH, Patel M, Yang G, Fung EK, et al. Alpha radioimmunotherapy using (225)ac-proteus-dota for solid tumors - safety at curative doses. Theranostics. 2020; 10: 11359-11375.
40. Xie G, Gu D, Zhang L, Chen S, Wu D. A rapid and systemic complete response to stereotactic body radiation therapy and pembrolizumab in a patient with metastatic renal cell carcinoma. Cancer biology & therapy. 2017; 18: 547-551.
41. Hennrich U, Eder M. [(177)lu]lu-psma-617 (pluvicto(tm)): The first fda-approved radiotherapeutical for treatment of prostate cancer. Pharmaceuticals (Basel, Switzerland). 2022; 15:
42. Schuchardt C, Zhang J, Kulkarni HR, Chen X, Müller D, Baum RP. Prostate-specific membrane antigen radioligand therapy using (177)lu-psma i&t and (177)lu-psma-617 in patients with metastatic castration-resistant prostate cancer:

Comparison of safety, biodistribution, and dosimetry. Journal of nuclear medicine : official publication, Society of Nuclear Medicine. 2022; 63: 1199-1207.

43. Zhao C, Rong Z, Ding J, Wang L, Wang B, Ding L, et al. Targeting claudin 18.2 using a highly specific antibody enables cancer diagnosis and guided surgery. Molecular pharmaceutics. 2022; 19: 3530-3541.

44. Wang S, Qi C, Ding J, Li D, Zhang M, Ji C, et al. First-in-human cldn18.2 functional diagnostic pet imaging of digestive system neoplasms enables whole-body target mapping and lesion detection. European journal of nuclear medicine and molecular imaging. 2023;

45. Van Cutsem E, Moiseyenko VM, Tjulandin S, Majlis A, Constenla M, Boni C, et al. Phase iii study of docetaxel and cisplatin plus fluorouracil compared with cisplatin and fluorouracil as first-line therapy for advanced gastric cancer: A report of the v325 study group. Journal of clinical oncology : official journal of the American Society of Clinical Oncology. 2006; 24: 4991-7.

46. Hu C, Xu Z, Chen S, Lv H, Wang Y, Wang X, et al. Overexpression of b7h5/cd28h is associated with worse survival in human gastric cancer. Journal of cellular and molecular medicine. 2020; 24: 1360-1369.

47. Van Cutsem E, Bang YJ, Feng-Yi F, Xu JM, Lee KW, Jiao SC, et al. Her2 screening data from toga: Targeting her2 in gastric and gastroesophageal junction cancer. Gastric cancer : official journal of the International Gastric Cancer Association and the Japanese Gastric Cancer Association. 2015; 18: 476-84.

48. Feng J, Xu H, Cinquina A, Wu Z, Chen Q, Zhang P, et al. Treatment of aggressive t cell lymphoblastic lymphoma/leukemia using anti-cd5 car t cells. Stem cell reviews and reports. 2021; 17: 652-661.

CLAIMS

1. A method of detecting or visualizing CLDN18.2 protein at a site of interest in a subject, comprising:

   a) administering to the subject a detectably effective amount of an anti-CLDN18.2 antibody-radionuclide conjugate; and

   b) conducting radionuclide imaging to the subject at a subsequent time point after the administration of the anti-CLDN18.2 antibody-radionuclide conjugate to obtain an image; and

   c) determining or visualizing presence of the CLDN18.2 protein in the site of interest of the subject from the image,

   wherein the presence and/or location of the radionuclide uptake above background is indicative of the presence and/or location of the CLDN18.2 protein, and

   wherein the anti-CLDN18.2 antibody-radionuclide conjugate comprises an anti-CLDN18.2 antibody-diagnostic radionuclide conjugate.

2. The method of claim 1, wherein the subject has not been treated with, or is not receiving CLDN18.2 targeted therapy.

3. A method of diagnosing a subject as having a CLDN18.2 associated disease, the method comprising:

   a) administering to the subject a detectably effective amount of an anti-CLDN18.2 antibody-radionuclide conjugate; and

   b) conducting radionuclide imaging to the subject at a subsequent time point after the administration of the anti-CLDN18.2 antibody-radionuclide conjugate to obtain an image;

   c) diagnosing the CLDN18.2 associated disease in the subject based on presence and/or location of the CLDN18.2 protein in the site of interest of the subject as determined from the image;

   wherein the presence and/or location of the radionuclide uptake above background is indicative of the presence and/or location of the CLDN18.2 protein, and

   wherein the anti-CLDN18.2 antibody-radionuclide conjugate comprises an anti-CLDN18.2 antibody-diagnostic radionuclide conjugate.

4. The method of claim 3, wherein the subject has not been treated with, or is not receiving CLDN18.2 targeted therapy.

5. A method of identifying a subject in need as likely to be responsive to a CLDN18.2 targeted therapy, the method comprising:

a) administering to the subject a detectably effective amount of an anti-CLDN18.2 antibody-radionuclide conjugate; and

b) conducting radionuclide imaging to the subject at a subsequent time point after the administration of the anti-CLDN18.2 antibody-radionuclide conjugate to obtain an image;

c) identifying the subject as likely to respond to the CLDN18.2 targeted therapy based on presence and/or location of the CLDN18.2 protein in the site of interest of the subject as determined from the image,

wherein the presence and/or location of the radionuclide uptake above background is indicative of the presence and/or location of the CLDN18.2 protein, and

wherein the anti-CLDN18.2 antibody-radionuclide conjugate comprises an anti-CLDN18.2 antibody-diagnostic radionuclide conjugate.

6. The method of claim 5, wherein the subject has not been treated with, or is not receiving CLDN18.2 targeted therapy.

7. The method of any one of the preceding claims, wherein the diagnostic radionuclide is selected from the group consisting of: ^{18}F, ^{32}P, ^{33}P, ^{45}Ti, ^{47}Sc, ^{52}Fe, ^{59}Fe, ^{62}Cu, ^{64}Cu, ^{67}Cu, ^{67}Ga, ^{68}Ga, ^{75}Sc, ^{77}As, ^{86}Y, ^{90}Y, ^{89}Sr, ^{89}Zr, ^{94}Tc, ^{94}Tc, ^{99m}Tc, ^{99}Mo, ^{105}Pd, ^{105}Rh, ^{111}Ag, ^{111} In, ^{123}I, ^{124}I, ^{125}I, ^{131}I, ^{142}Pr, ^{143}Pr, ^{149}Pm, ^{153}Sm, $^{154"1581}Gd$, ^{161}Tb, ^{166}Dy, ^{166}Ho, ^{169}Er, ^{175}Lu, ^{177}Lu, ^{186}Re, ^{188}Re, ^{189}Re, ^{194}Ir, ^{198}Au, ^{199}Au, ^{211}At, ^{211}Pb, ^{212}Bi, ^{212}Pb, ^{213}Bi, ^{223}Ra and ^{225}Ac.

8. The method of any of the preceding claims, wherein the method further comprises:
d) administering a therapeutically effective amount of a CLDN18.2 targeted therapy to the subject identified as having presence of the CLDN18.2 protein in the site of interest, diagnosed as having a CLDN18.2 associated disease, and/or identified as likely to be responsive to a CLDN18.2 targeted therapy.

9. The method of claim 8, wherein the CLDN18.2 targeted therapy comprises a therapy selected from the group consisting of an anti-CLDN18.2 antibody therapy, a CLDN18.2

targeted compound, a CLDN18.2 targeted nucleic acid therapy, a CLDN18.2 targeted peptide, a CLDN18.2 targeted cell therapy, and a CLDN18.2 targeted gene therapy.

10. The method of claim 9, wherein the anti-CLDN18.2 antibody therapy comprises an anti-CLDN18.2 antibody-therapeutic radionuclide conjugate, wherein the therapeutic radionuclide is from the group consisting of: ^{111}In, ^{111m}In, ^{177}Lu, ^{212}Bi, ^{213}Bi, ^{211}At, ^{62}Cu, ^{64}Cu, ^{67}Cu, ^{90}Y, ^{124}I, ^{125}I, ^{131}I, ^{32}P, ^{33}P, ^{47}Sc, ^{111}Ag, ^{67}Ga, ^{142}Pr, ^{153}Sm, ^{161}Tb, ^{166}Dy, ^{166}Ho, ^{186}Re, ^{188}Re, ^{189}Re, ^{212}Pb, ^{223}Ra, ^{225}Ac, ^{59}Fe, ^{75}Se, ^{77}As, ^{89}Sr, ^{99}Mo, ^{105}Rh, ^{109}Pd, ^{143}Pr, ^{149}Pm, ^{169}Er, ^{194}Ir, ^{198}Au, ^{199}Au, ^{199}Au, and ^{211}Pb.

11. The method of claim 10, wherein the therapeutic radionuclide is ^{177}Lu or ^{124}I.

12. The method of claim 10 or 11, wherein the therapeutic radionuclide is the same as the diagnostic radionuclide.

13. The method of claim 12, wherein both the therapeutic radionuclide and the diagnostic radionuclide are ^{177}Lu or ^{124}I.

14. The method of claim 10, wherein the anti-CLDN18.2 antibody-diagnostic radionuclide conjugate is identical to the anti-CLDN18.2 antibody-therapeutic radionuclide.

15. The method of any of the claims 8-14, wherein the therapeutically effective amount is at least 100%, 150%, 200%, 300%, 400%, 500%, 600%, 700%, 800%, 900%, or 1000% of the detectably effective amount.

16. A method of monitoring progression of a CLDN18.2 associated disease in a subject during a monitoring time period, the method comprising:

d) administering to the subject a detectably effective amount of an anti-CLDN18.2 antibody-radionuclide conjugate after the monitoring time period;

e) conducting radionuclide imaging to the subject at a subsequent time point after the administration of the anti-CLDN18.2 antibody-radionuclide conjugate to obtain a post-monitor image; and

f) comparing the post-monitor image with a pre-monitor image, to determine change in the level of the CLDN18.2 protein during the monitoring time period from the image, wherein the level of the radionuclide conjugate above background is indicative of the level of the CLDN18.2 protein,

wherein the change is indicative of presence or absence of disease progression, wherein the anti-CLDN18.2 antibody-radionuclide conjugate comprises an anti-CLDN18.2 antibody-diagnostic radionuclide conjugate.

17. The method of claim 16, wherein the pre-monitor image is obtained from the subject before the monitoring time period by:

administering with the effective amount of the anti-CLDN18.2 antibody-radionuclide conjugate, followed by conducting radionuclide imaging to the subject at a subsequent time point after the administration of the anti-CLDN18.2 antibody-radionuclide conjugate to obtain the pre-monitor image.

18. The method of claim 16, wherein increase in the CLDN18.2 level during the monitoring time period is indicative of disease progression, and absence of the increase in the CLDN18.2 level during the monitoring time period is indicative of absence of disease progression.

19. The method of claim 16, wherein the subject has not been treated with, or is not receiving CLDN18.2 targeted therapy.

20. The method of claim 3 or 16, wherein the disease is tumor.

21. The method of claim 16, wherein the progression is metastasis of the tumor.

22. The method of claim 16, the level of the CLDN18.2 protein comprises amount, distribution and/or location of the CLDN18.2 protein.

23. The method of claim 16, wherein the subject is at risk of metastasis.

24. A method of monitoring therapeutic efficacy in a subject having a CLDN18.2 associated disease and having been treated with a therapy for a therapeutic period, the method comprising:

d) administering to the subject a detectably effective amount of an anti-CLDN18.2 antibody-radionuclide conjugate after the therapeutic period;

e) conducting radionuclide imaging to the subject at a subsequent time point after the administration of the anti-CLDN18.2 antibody-radionuclide conjugate to obtain a post-treatment image; and

f) comparing the post-treatment image with a pre-treatment image, to determine change in the level of the CLDN18.2 protein during the therapeutic period from the image,

wherein the level of the radionuclide conjugate above background is indicative of the level of the CLDN18.2 protein,

wherein the change is indicative of presence or absence of therapeutic efficacy, wherein the anti-CLDN18.2 antibody-radionuclide conjugate comprises an anti-CLDN18.2 antibody-diagnostic radionuclide conjugate.

25. The method of claim 24, wherein the pre-treatment image is obtained from the subject before the therapeutic period by:

administering with the effective amount of the anti-CLDN18.2 antibody-radionuclide conjugate, followed by conducting radionuclide imaging to the subject at a subsequent time point after the administration of the anti-CLDN18.2 antibody-radionuclide conjugate to obtain the pre-treatment image.

26. The method of claim 24 or 25, wherein increase in the CLDN18.2 level during the therapeutic period is indicative of absence of therapeutic efficacy or poor therapeutic efficacy, and/or wherein absence of the increase in the CLDN18.2 level during the therapeutic period is indicative of presence of therapeutic efficacy or positive therapeutic efficacy.

27. The method of claim 26, wherein the method further comprises:

a) increasing the dose of the therapy or discontinuing the therapy when poor therapeutic efficacy is determined; or

b) recommending the subject continuing the therapy when positive therapeutic efficacy is determined.

28. The method of claim 24, wherein the therapy comprises a CLDN18.2 targeted therapy.

29. The method of claim 28, wherein the CLDN18.2 targeted therapy comprises a therapy selected from the group consisting of an anti-CLDN18.2 antibody therapy, a CLDN18.2 targeted compound, a CLDN18.2 targeted nucleic acid therapy, a CLDN18.2 targeted peptide, a CLDN18.2 targeted cell therapy, and a CLDN18.2 targeted gene therapy.

30. The method of claim 28, wherein the method further comprises recommending the subject switching to a therapy other than a CLDN18.2 targeted therapy when post-treatment CLDN18.2 level is below a corresponding reference level or decreased by at least 40% (or at least 50%, 60%, 70%, 80%, 90% or 95%) relative to the pre-treatment CLDN18.2 level.

31. The method of claim 24, wherein the therapy is not a CLDN18.2 targeted therapy.

32. The method of any one of claims 1-31, wherein the diagnostic radionuclide is selected from the group consisting of ^{18}F, ^{32}P, ^{33}P, ^{45}Ti, ^{47}Sc, ^{52}Fe, ^{59}Fe, ^{62}Cu, ^{64}Cu, ^{67}Cu, ^{67}Ga, ^{68}Ga, ^{75}Sc, ^{77}As, ^{86}Y, ^{90}Y, ^{89}Sr, ^{89}Zr, ^{94}Tc, ^{94}Tc, ^{99m}Tc, ^{99}Mo, ^{105}Pd, ^{105}Rh, ^{111}Ag, ^{111} In, ^{123}I, ^{124}I, ^{125}I, ^{131} I, ^{142}Pr, ^{143}Pr, ^{149}Pm, ^{153}Sm, $^{154"1581}Gd$, ^{161}Tb, ^{166}Dy, ^{166}Ho, ^{169}Er, ^{175}Lu, ^{177}Lu, ^{186}Re, ^{188}Re, ^{189}Re, ^{194}Ir, ^{198}Au, ^{199}Au, ^{211} At, ^{211} Pb, ^{212}Bi, ^{212}Pb, ^{213}Bi, ^{223}Ra and ^{225} Ac.

33. The method of claim 32, wherein the diagnostic radionuclide is ^{124}I, ^{123}I, ^{131}I, ^{89}Zr, or ^{177}Lu.

34. The method of claim 33, wherein the anti-CLDN18.2 antibody-radionuclide conjugate is administered at a dose ranging from 0.5mCi to 10mCi (18.5 MBq to 370 MBq).

35. The method of claim 33 or 34, wherein the radionuclide imaging is conducted 2 hours after the administration of the anti-CLDN18.2 antibody-radionuclide conjugate to the subject, or conducted at a time point between 2 hours and 144 hours after the administration of the anti-CLDN18.2 antibody-radionuclide conjugate to the subject.

36. The method of any one of the preceding claims, wherein the anti-CLDN18.2 antibody-radionuclide conjugate comprises heavy chain HCDR1, HCDR2 and HCDR3 and/or light chain LCDR1, LCDR2 and LCDR3 sequences, wherein:

the HCDR1 sequence comprises **GYNMN** (SEQ ID NO: 1), or a homologue sequence of at least 80% sequence identity thereof;

the HCDR2 sequence comprises **X_1IDPYYX_2X_3TX_4YNQKFX_5G** (SEQ ID NO: 32), or a homologue sequence of at least 80% sequence identity thereof;

the HCDR3 sequence comprises **$X_6X_7X_8$GNAFDY** (SEQ ID NO: 33), or a homologue sequence of at least 80% sequence identity thereof;

the LCDR1 sequence comprises **KSSQX$_9$LX_{10}NX_{11}GNX_{12}KNYLT** (SEQ ID NO: 34) or a homologue sequence of at least 80% sequence identity thereof;

the LCDR2 sequence comprises **WASTRX_{13}S** (SEQ ID NO: 35) or a homologue sequence of at least 80% sequence identity thereof;

the LCDR3 sequence comprises **QNDYSX_{15}PX_{16}T** (SEQ ID NO: 36) or a homologue sequence of at least 80% sequence identity thereof;

wherein X_1 is N or Y or H, X_2 is G or V, X_3 is A or G or T, X_4 is R or T or S, X_5 is K or R, X_6 is S or M, X_7 is Y or F, X_8 is Y or H, X_9 is S or N, X_{10} is L or F, X_{11} is S or N, X_{12} is Q or L, X_{13} is E or K, X_{15} is F or Y and X_{16} is F or L.

37. The method of any one of the preceding claims, wherein the CLDN18.2 associated disease is a CLDN18.2 positive tumor or a CLDN18.2 positive non-cancerous lesion (e.g., gastric lesion).

38. The method of claim 20, wherein the tumor is gastric cancer, ovarian cancer, pancreatic cancer, cholangiocarcinoma, colorectal cancer, lung cancer, or esophageal adenocarcinoma.

39. The method of claim 37, wherein the gastric lesion is a gastric ulcer.

40. The method of any one of claims 1-6 and 19, wherein the CLDN18.2 targeted therapy comprises a therapy that specifically targets CLDN18.2 or CLDN18.2-expressing cells.

41. The method of any one of claims 1-6 and 19, wherein the CLDN18.2 targeted therapy comprises a therapy selected from the group consisting of: an anti-CLDN18.2 antibody therapy, a CLDN18.2 targeted compound, a CLDN18.2 targeted nucleic acid therapy, a CLDN18.2 targeted peptide, a CLDN18.2 targeted cell therapy, and a CLDN18.2 targeted gene therapy.

42. The method of claim 41, wherein the anti-CLDN18.2 antibody therapy comprises an anti-CLDN18.2 antibody–therapeutic radionuclide conjugate, wherein the therapeutic radionuclide selected from the group consisting of: ^{111}In, ^{111m}In, ^{177}Lu, ^{212}Bi, ^{213}Bi, ^{211}At, ^{62}Cu, ^{64}Cu, ^{67}Cu, ^{90}Y, ^{124}I, ^{125}I, ^{131}I, ^{32}P, ^{33}P, ^{47}Sc, ^{111}Ag, ^{67}Ga, ^{142}Pr, ^{153}Sm, ^{161}Tb, ^{166}Dy, ^{166}Ho, ^{186}Re, ^{188}Re, ^{189}Re, ^{212}Pb, ^{223}Ra, ^{225}Ac, ^{59}Fe, ^{75}Se, ^{77}As, ^{89}Sr, ^{99}Mo, ^{105}Rh, ^{109}Pd, ^{143}Pr, ^{149}Pm, ^{169}Er, ^{194}Ir, ^{198}Au, ^{199}Au, ^{199}Au, and ^{211}Pb.

43. The method of claim 42, wherein the therapeutic radionuclide is ^{177}Lu or ^{124}I.

44. The method of any one of the preceding claims, wherein the CLDN18.2 targeted cell therapy comprises a CAR T cell, TCR T cell, or CAR NK cell that targets CLDN18.2.

45. The method of any one of the preceding claims, wherein the site of interest has or is suspected of a tumor or a gastric lesion.

46. The method of any one of the preceding claims, wherein the site of interest is whole body.

47. The method of any one of the preceding claims, wherein the radionuclide imaging comprises positron emission tomography (PET) or SPECT.

48. The method of any one of the preceding claims, wherein the radionuclide imaging is combined with CT, MR or ultrasound.

49. A kit for use in the method of any one of the preceding claims, comprising an anti-CLDN18.2 antibody-diagnostic radionuclide conjugate.

50. A kit for 1) diagnosing a subject as having a CLDN18.2 associated disease, 2) identifying a subject in need as likely be responsive to a CLDN18.2 targeted therapy, 3) monitoring progression of a CLDN18.2 associated disease in a subject during a monitoring time period, and/or 4) monitoring therapeutic efficacy in a subject having a CLDN18.2 associated disease and having been treated with a therapy for a therapeutic period, comprising an anti-CLDN18.2 antibody-diagnostic radionuclide conjugate.

51. The kit of claim 49 or 50, further comprising a therapeutically effective amount of an anti-CLDN18.2 antibody-therapeutic radionuclide conjugate.

52. The kit of claim 51, wherein the therapeutic radionuclide is ^{177}Lu or ^{124}I.

53. The kit of claim 51 or 52, wherein the therapeutic radionuclide is the same as the diagnostic radionuclide.

54. The kit of claim 53, wherein both the therapeutic radionuclide and the diagnostic radionuclide are ^{177}Lu or ^{124}I.

55. The kit of any of claims 49-54, wherein the kit further comprises an instruction providing a detectably effective amount of the anti-CLDN18.2 antibody-diagnostic radionuclide conjugate, and a therapeutically effective amount of the anti-CLDN18.2 antibody-therapeutic radionuclide conjugate.

56. The kit of claim 55, wherein the therapeutically effective amount is at least 100%, 150%, 200%, 300%, 400%, 500%, 600%, 700%, 800%, 900%, or 1000% of the detectably effective amount.

57. The method of any one of claims 1-48 or the kit of any one of claims 49-56, wherein the anti-CLDN18.2 antibody-radionuclide conjugate comprises:

a heavy chain variable region comprises a HCDR1 comprising the sequence of SEQ ID NO: 1, a HCDR2 comprising the sequence of SEQ ID NO: 3, and a HCDR3 comprising the sequence of SEQ ID NO: 5; and a light chain variable region comprises a LCDR1 comprising the sequence of SEQ ID NO: 2, a LCDR2 comprising the sequence of SEQ ID NO: 4, and a LCDR3 comprising the sequence of SEQ ID NO: 6;

a heavy chain variable region comprises a HCDR1 comprising the sequence of SEQ ID NO: 1, a HCDR2 comprising the sequence of SEQ ID NO: 7, and a HCDR3 comprising the sequence of SEQ ID NO: 5; and a light chain variable region comprises a LCDR1 comprising the sequence of SEQ ID NO: 2, a LCDR2 comprising the sequence of SEQ ID NO: 4, and a LCDR3 comprising the sequence of SEQ ID NO: 8;

a heavy chain variable region comprises a HCDR1 comprising the sequence of SEQ ID NO: 1, a HCDR2 comprising the sequence of SEQ ID NO: 9, and a HCDR3 comprising the sequence of SEQ ID NO: 11; and a light chain variable region comprises a LCDR1 comprising the sequence of SEQ ID NO: 10, a LCDR2 comprising the sequence of SEQ ID NO: 4, and a LCDR3 comprising the sequence of SEQ ID NO: 6;

a heavy chain variable region comprises a HCDR1 comprising the sequence of SEQ ID NO: 1, a HCDR2 comprising the sequence of SEQ ID NO: 19, and a HCDR3 comprising the sequence of SEQ ID NO: 21; and a light chain variable region comprises a LCDR1 comprising the sequence of SEQ ID NO: 14, a LCDR2 comprising the sequence of SEQ ID NO: 16, and a LCDR3 comprising the sequence of SEQ ID NO: 18; or

a heavy chain variable region comprises a HCDR1 comprising the sequence of SEQ ID NO: 1, a HCDR2 comprising the sequence of SEQ ID NO: 22, and a HCDR3 comprising the sequence of SEQ ID NO: 5; and a light chain variable region comprises a LCDR1 comprising the sequence of SEQ ID NO: 20, a LCDR2 comprising the sequence of SEQ ID NO: 4, and a LCDR3 comprising the sequence of SEQ ID NO: 6.

58. The method of any one of claims 1-48 or the kit of any one of claims 49-56, wherein the heavy chain variable region further comprises one or more of heavy chain HFR1, HFR2, HFR3 and HFR4, and/or the light chain variable region further comprises one or more of light chain LFR1, LFR2, LFR3 and LFR4, wherein:

the HFR1 comprises **QVQLVQSGAEVKKPGASVKVSCKASGYX$_{17}$FT** (SEQ ID NO: 54) or a homologous sequence of at least 80% sequence identity thereof,

the HFR2 comprises **WVX$_{18}$QAPGQGLEWX$_{19}$G** (SEQ ID NO: 55) or a homologous sequence of at least 80% sequence identity thereof,

the HFR3 sequence comprises **RVTX$_{20}$TIDKSTSTVYMELSSLRSEDTAVYYCAR** (SEQ ID NO: 56) or a homologous sequence of at least 80% sequence identity thereof,

the HFR4 comprises **WGQGTTVTVSS** (SEQ ID NO: 57) or a homologous sequence of at least 80% sequence identity thereof,

the LFR1 comprises **DIVMTQSPDSLAVSLGERATX$_{21}$NC** (SEQ ID NO: 58) or a homologous sequence of at least 80% sequence identity thereof,

the LFR2 comprises **WYQQKPGQPPKLLIY** (SEQ ID NO: 59) or a homologous sequence of at least 80% sequence identity thereof,

the LFR3 comprises **GVPDRFX$_{22}$GSGSGTDFTLTISSLQAEDVAVYYC** (SEQ ID NO: 60) or a homologous sequence of at least 80% sequence identity thereof, and

the LFR4 comprises **FGGGTKVEIK** (SEQ ID NO: 61) or a homologous sequence of at least 80% sequence identity thereof,

wherein X_{17} is T or S, X_{18} is R or K, X_{19} is M or I, X_{20} is M or L, X_{21} is I or M, and X_{22} is S or T.

59. The method of claim 58, wherein:

the HFR1 comprises a sequence selected from the group consisting of SEQ ID NOs: 62 and 63,

the HFR2 comprises a sequence selected from the group consisting of SEQ ID NOs: 64 and 65,

the HFR3 comprises the sequence selected from the group consisting of SEQ ID NOs: 66 and 67,

the HFR4 comprises a sequence of SEQ ID NO: 57,

the LFR1 comprises the sequence from the group consisting of SEQ ID NOs: 68 and 69,

the LFR2 comprises a sequence of SEQ ID NO: 59,

the LFR3 comprises a sequence selected from the group consisting of SEQ ID NOs: 70 and 71, and

the LFR4 comprises a sequence of SEQ ID NO: 61.

60. The method of claim 58 or 59, wherein the heavy chain variable region comprises a sequence selected from the group consisting of SEQ ID NO: 25, SEQ ID NO: 27, SEQ ID NO: 29, SEQ ID NO: 37, SEQ ID NO: 39, SEQ ID NO: 41, SEQ ID NO: 45, and SEQ ID NO: 47, and a homologous sequence thereof having at least 80% sequence identity yet retaining specific binding affinity to CLDN18.2.

61. The method of any one of claims 58-60, wherein the light chain variable region comprises a sequence selected from the group consisting of SEQ ID NO: 26, SEQ ID NO: 28, SEQ ID NO: 38, SEQ ID NO: 40, SEQ ID NO: 42, SEQ ID NO: 46, SEQ ID NO: 48, and a homologous sequence thereof having at least 80% sequence identity yet retaining specific binding affinity to CLDN18.2.

62. The method of any one of claims 58-61, wherein:

the heavy chain variable region comprising the sequence of SEQ ID NO: 23 and a light chain variable region comprising the sequence of SEQ ID NO: 24;
the heavy chain variable region comprises a sequence of SEQ ID NO: 25 and the light chain variable region comprises a sequence of SEQ ID NO: 26;
the heavy chain variable region comprises a sequence of SEQ ID NO: 27 and the light chain variable region comprises a sequence of SEQ ID NO: 28;
the heavy chain variable region comprises a sequence of SEQ ID NO: 29 and the light chain variable region comprises a sequence of SEQ ID NO: 26, or 28;
the heavy chain variable region comprises a sequence of SEQ ID NO: 37 and the light chain variable region comprises a sequence of SEQ ID NO: 38;
the heavy chain variable region comprises a sequence of SEQ ID NO: 39 and the light chain variable region comprises a sequence of SEQ ID NO: 40;
the heavy chain variable region comprises a sequence of SEQ ID NO: 41 and the light chain variable region comprises a sequence of SEQ ID NO: 42;
the heavy chain variable region comprises a sequence of SEQ ID NO: 45 and the light chain variable region comprises a sequence of SEQ ID NO: 46; or
the heavy chain variable region comprises a sequence of SEQ ID NO: 47 and the light chain variable region comprises a sequence of SEQ ID NO: 48.

63. The method of any one of claims 58-62, wherein the anti-CLDN18.2 antibody-radionuclide conjugate further comprises an immunoglobulin constant region, optionally a constant region of human Ig, or optionally a constant region of human IgG.

64. The method of any one of claims 58-63, wherein the constant region comprises a constant region of human IgG1, IgG2, IgG3, or IgG4.

65. The method of any one of claims 58-64, wherein the constant region of human IgG1 comprises SEQ ID NO: 49, or a homologous sequence having at least 80% sequence identity thereof.

66. The method of any one of claims 58-65, wherein the anti-CLDN18.2 antibody-radionuclide conjugate is humanized.

67. The method of any one of claims 58-66, wherein the anti-CLDN18.2 antibody-radionuclide conjugate comprises a diabody, a Fab, a Fab', a $F(ab')_2$, a Fd, an Fv fragment, a disulfide stabilized Fv fragment (dsFv), a $(dsFv)_2$, a bispecific dsFv (dsFv-dsFv'), a disulfide

stabilized diabody (ds diabody), a single-chain antibody molecule (scFv), an scFv-Fc antibody, an scFv dimer (bivalent diabody), a multispecific antibody, a camelized single domain antibody, a nanobody, a domain antibody, and a bivalent domain antibody.

68. A composition comprising an anti-CLDN18.2 antibody-radionuclide conjugate defined in any of the preceding claims and one or more pharmaceutically acceptable carriers, wherein the anti-CLDN18.2 antibody-radionuclide conjugate has at least one of the following characteristics:

a) having a radiochemical purity of at least 90% (e.g., at least 91%, at least 92%, at least 93%, at least 94%, at least 95%, at least 96%, at least 97%, at least 98% or at least 99%);

b) having a radiolabeling rate of at least 70% (e.g., at least 75%, at least 80%, at least 85%, at least 90%, at least 92%, at least 94%, at least 95%, at least 96%, at least 97%, at least 98%, or at least 99%,);

c) capable of specifically binding to CLDN18.2 at a Kd value of no more than 15nM (e.g., no more than 14nM, no more than 13nM, no more than 12nM, no more than 10nM, no more than 8nM, no more than 6nM, no more than 4nM, or no more than 4nM) ; and

d) capable of specifically binding to CLDN18.2 at an EC50 value of no more than 1.0 nM (e.g., no more than 0.8 nM, no more than 0.6 nM, no more than 0.5 nM, no more than 0.4 nM, or no more than 0.3 nM) as measured by ELISA.

69. The composition of claim 68, wherein the anti-CLDN18.2 antibody-radionuclide conjugate comprises a therapeutic radionuclide selected from the group consisting of: ^{111}In, ^{111m}In, ^{177}Lu, ^{212}Bi, ^{213}Bi, ^{211}At, ^{62}Cu, ^{64}Cu, ^{67}Cu, ^{90}Y, ^{124}I, ^{125}I, ^{131}I, ^{32}P, ^{33}P, ^{47}Sc, ^{111}Ag, ^{67}Ga, ^{142}Pr, ^{153}Sm, ^{161}Tb, ^{166}Dy, ^{166}Ho, ^{186}Re, ^{188}Re, ^{189}Re, ^{212}Pb, ^{223}Ra, ^{225}Ac, ^{59}Fe, ^{75}Se, ^{77}As, ^{89}Sr, ^{99}Mo, ^{105}Rh, ^{109}Pd, ^{143}Pr, ^{149}Pm, ^{169}Er, ^{194}Ir, ^{198}Au, ^{199}Au, ^{199}Au, and ^{211}Pb, or a diagnostic radionuclide selected from the group consisting of: ^{18}F, ^{32}P, ^{33}P, ^{45}Ti, ^{47}Sc, ^{52}Fe, ^{59}Fe, ^{62}Cu, ^{64}Cu, ^{67}Cu, ^{67}Ga, ^{68}Ga, ^{75}Sc, ^{77}As, ^{86}Y, ^{90}Y, ^{89}Sr, ^{89}Zr, ^{94}Tc, ^{94}Tc, ^{99m}Tc, ^{99}Mo, ^{105}Pd, ^{105}Rh, ^{111}Ag, ^{111} ln, ^{123}l, ^{124}l, ^{125}l, ^{131} l, ^{142}Pr, ^{143}Pr, ^{149}Pm, ^{153}Sm, $^{154"1581}$Gd, ^{161}Tb, ^{166}Dy, ^{166}Ho, ^{169}Er, ^{175}Lu, ^{177}Lu, ^{186}Re, ^{188}Re, ^{189}Re, ^{194}lr, ^{198}Au, ^{199}Au, ^{211} At, ^{211} Pb, ^{212}Bi, ^{212}Pb, ^{213}Bi, ^{223}Ra and ^{225} Ac.

70. The composition of claim 69, wherein the therapeutic radionuclide is ^{177}Lu or ^{124}I.

71. The composition of claim 69, wherein the diagnostic radionuclide is ^{124}I, ^{89}Zr or ^{177}Lu.

72. The composition of any of claims 69-71, wherein the anti-CLDN18.2 antibody-radionuclide conjugate further comprises a chelator.

73. The composition of claim 72, wherein the chelator is DFO or DOTA.

74. The composition of claim 73, wherein the chelator is DFO, and the radionuclide is ^{89}Zr.

75. The composition of claim 73, wherein the chelator is DOTA, and the radionuclide is ^{177}Lu.

76. The composition of claim 74, wherein the anti-CLDN18.2 antibody-radionuclide conjugate comprises a compound of Formula (I):

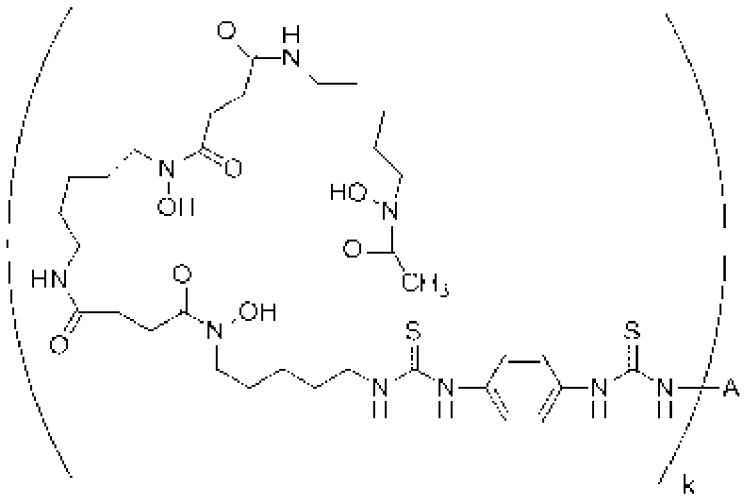

, wherein

A is an anti-CLDN18.2 antibody or antigen-binding fragment thereof defined in any of the preceding claims, k is from 1-40 (e.g., 3-5, 5-35, 10-30, 15-25, or 20).

77. The composition of claim 75, wherein the anti-CLDN18.2 antibody-radionuclide conjugate comprises a compound portion of Formula (II):

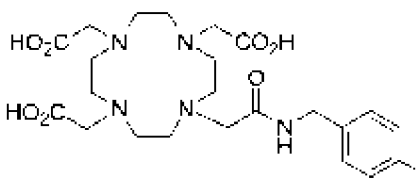

.

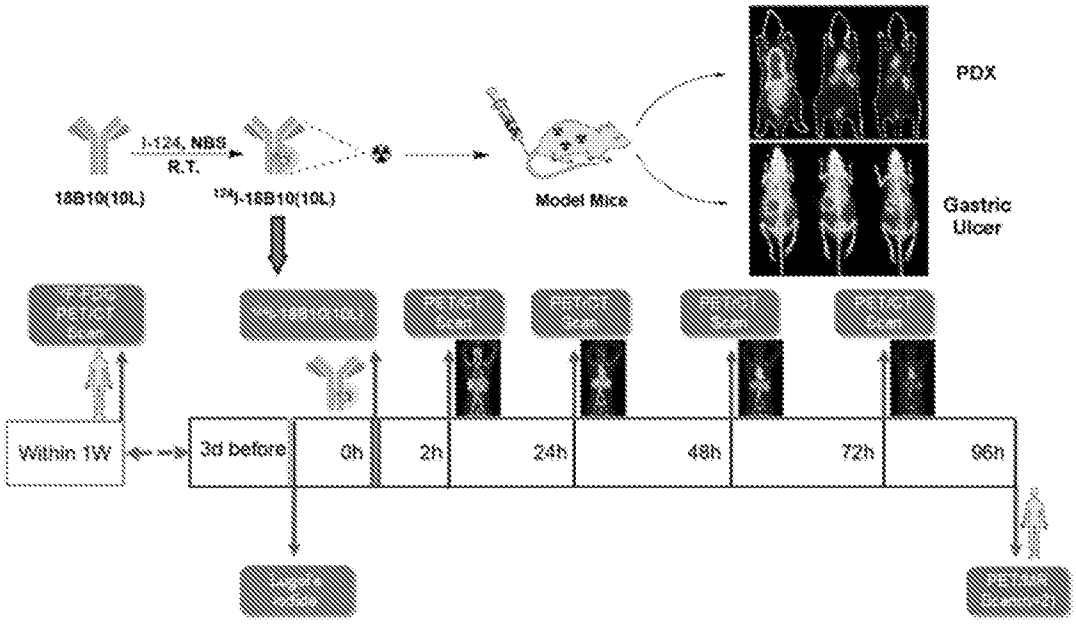

Figure 1

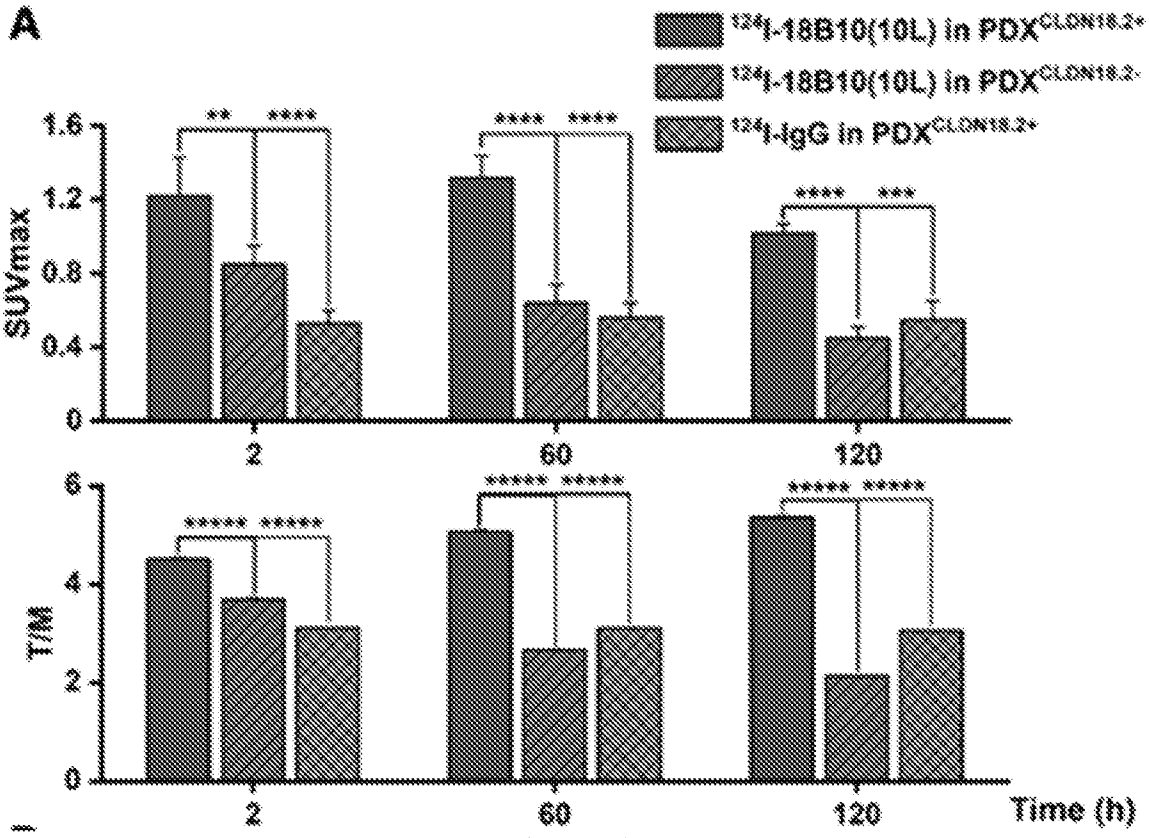

Figure 2A

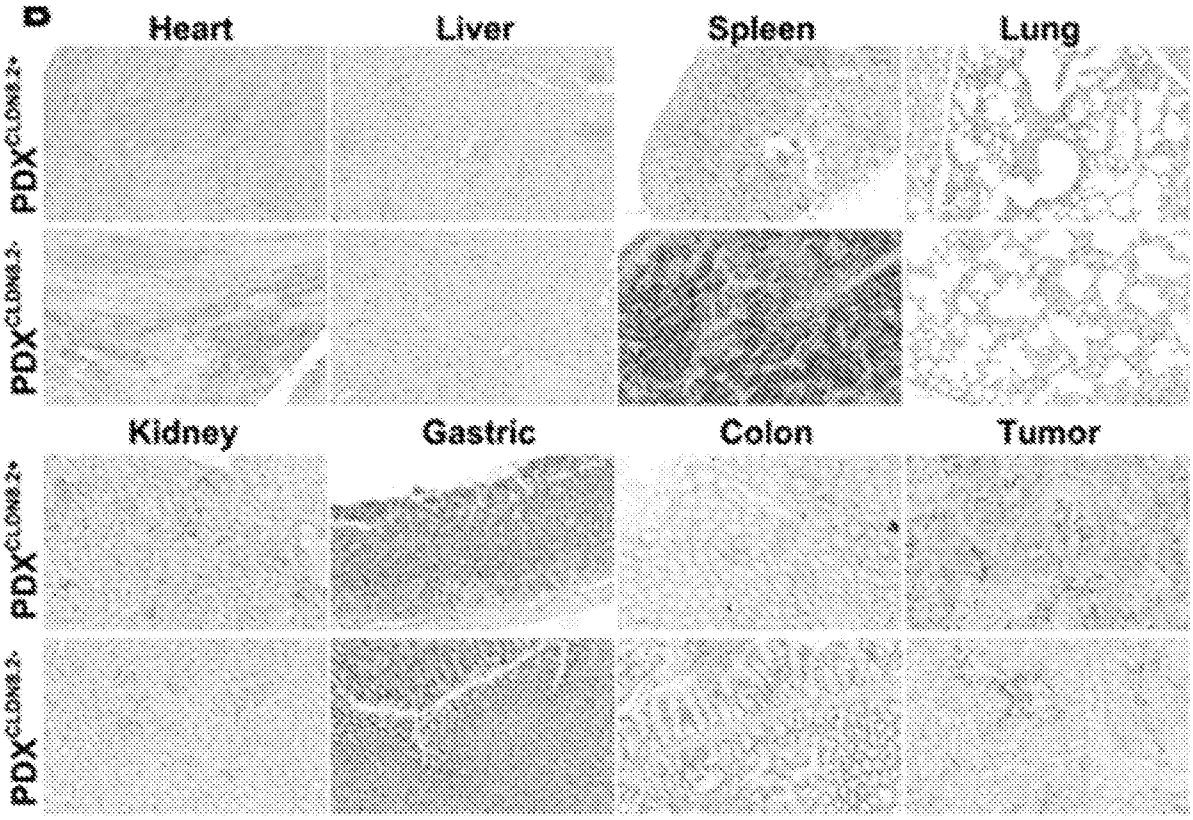

Figure 2B

Figure 2C

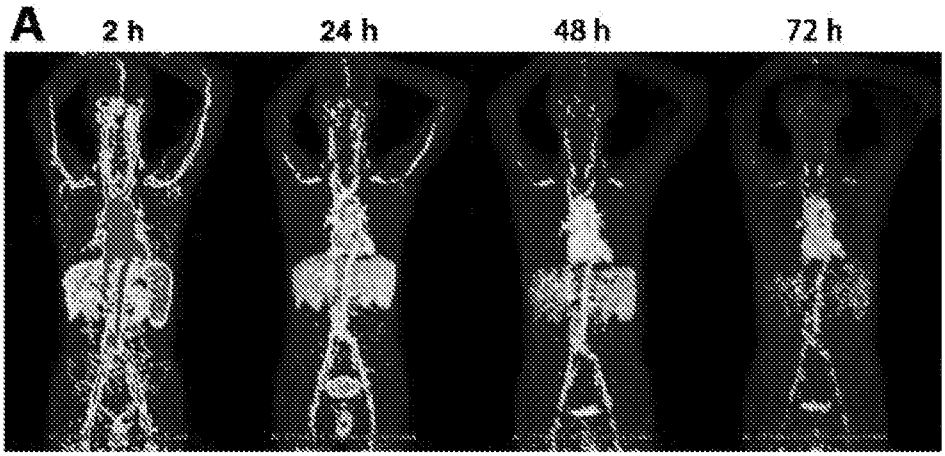

Figure 3A

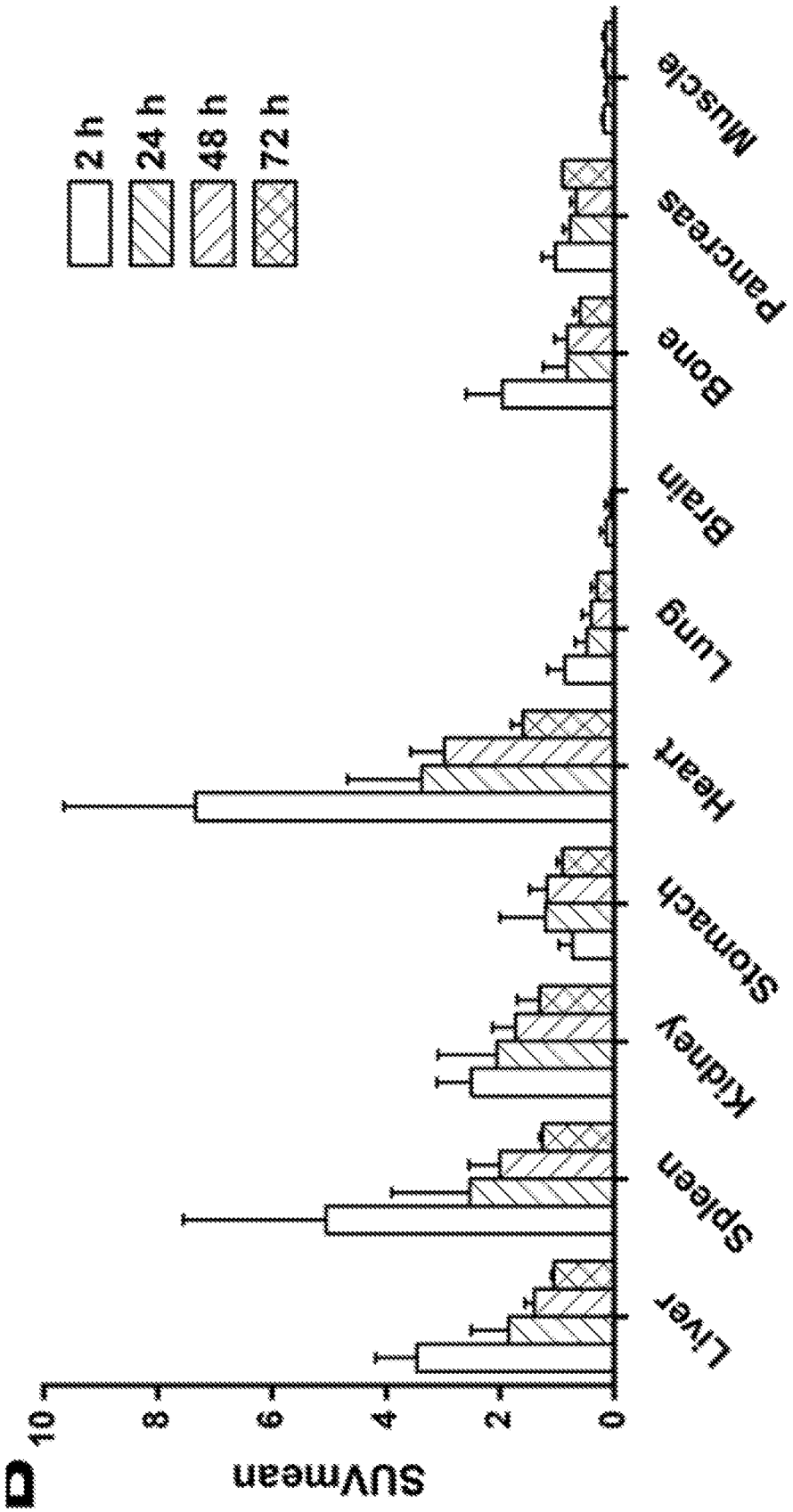
D
SUVmean
0
2
4
6
8
10
2 h
24 h
48 h
72 h
Liver
Spleen
Kidney
Stomach
Heart
Lung
Brain
Bone
Pancreas
Muscle

Figure 3B

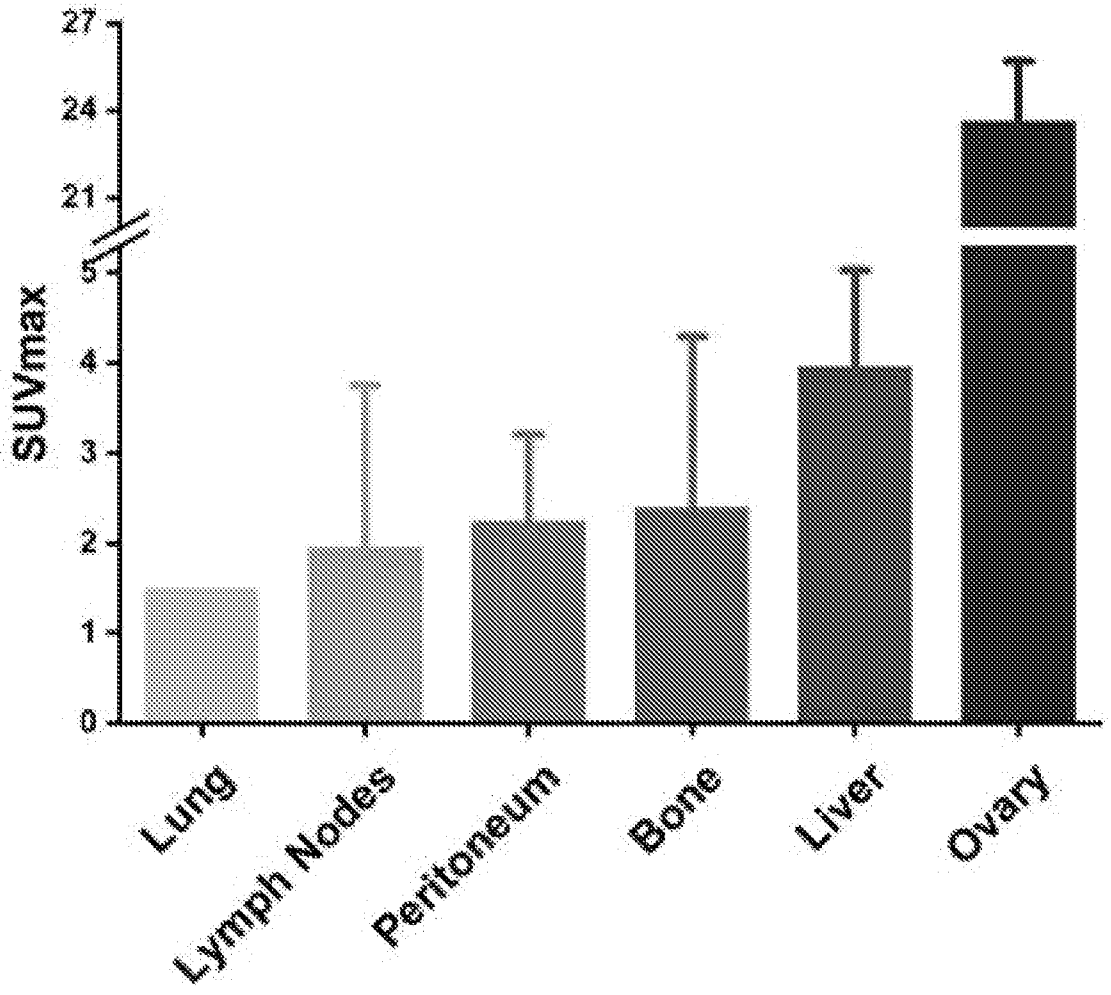
SUVmax
27
24
21
5
4
3
2
1
0
Lung
Lymph Nodes
Peritoneum
Bone
Liver
Ovary

Figure 3C

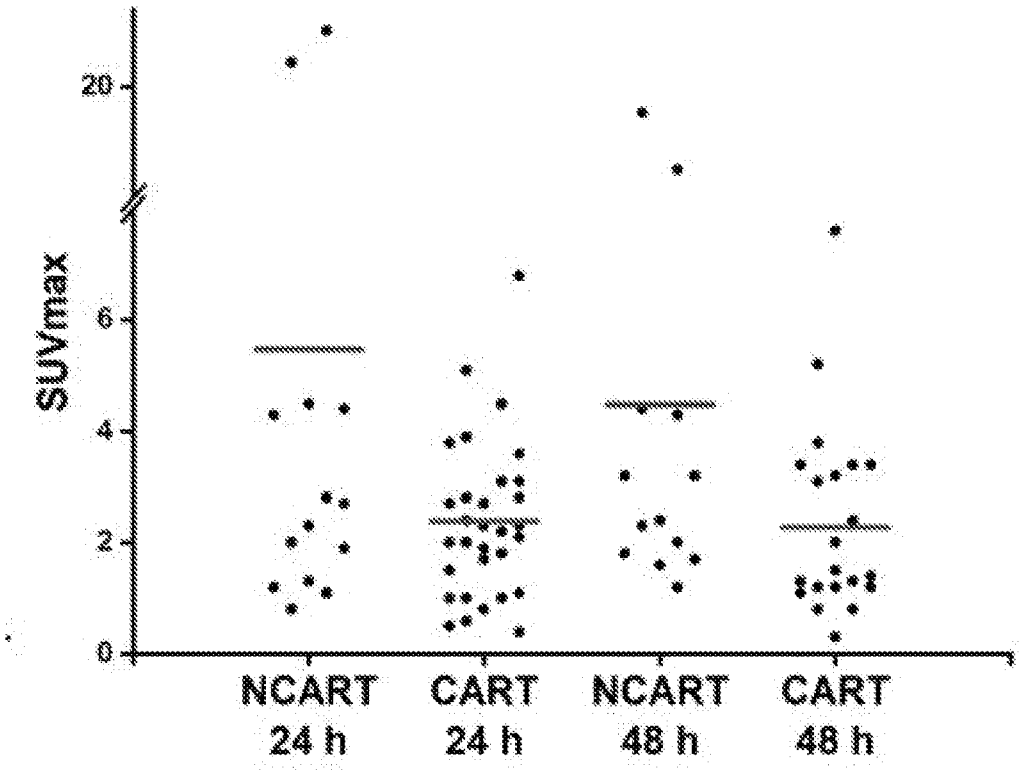

Figure 3D

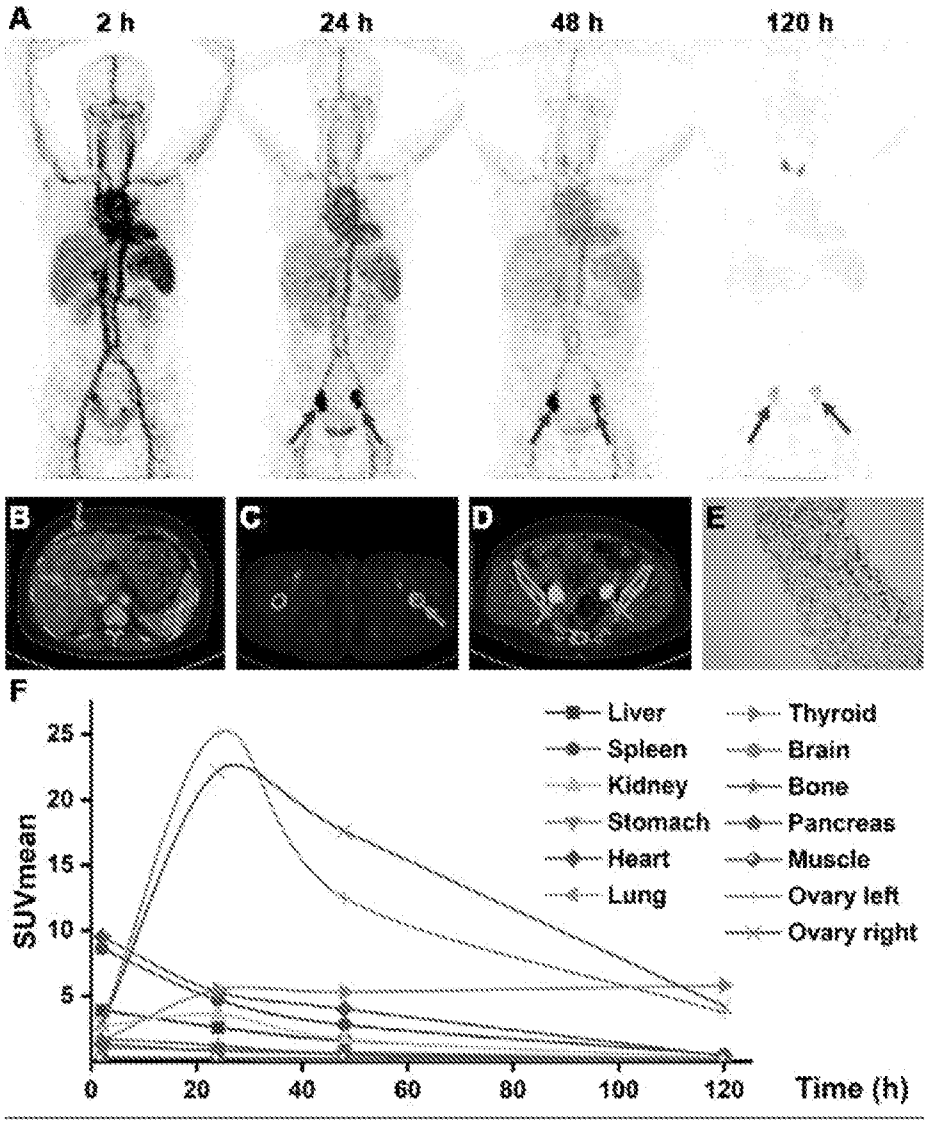

Figure 4

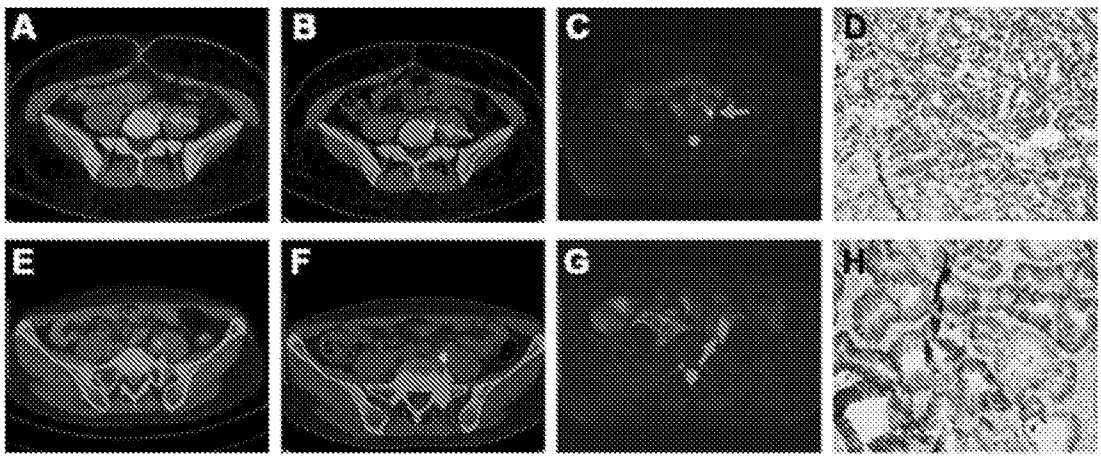

Figure 5

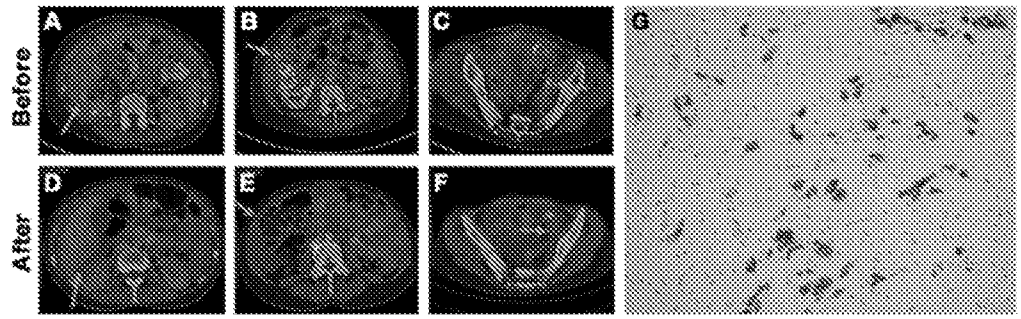

Figure 6

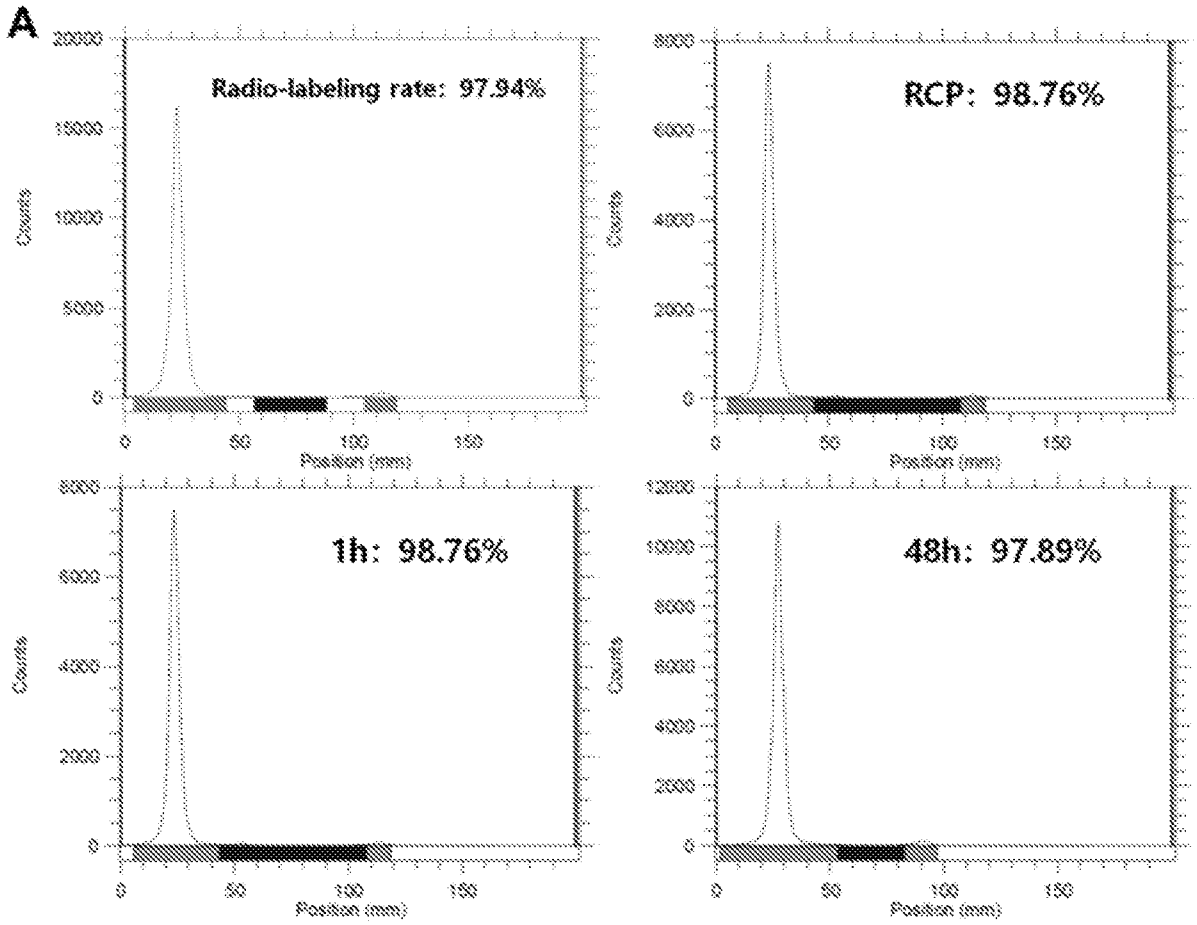

Figure 7A

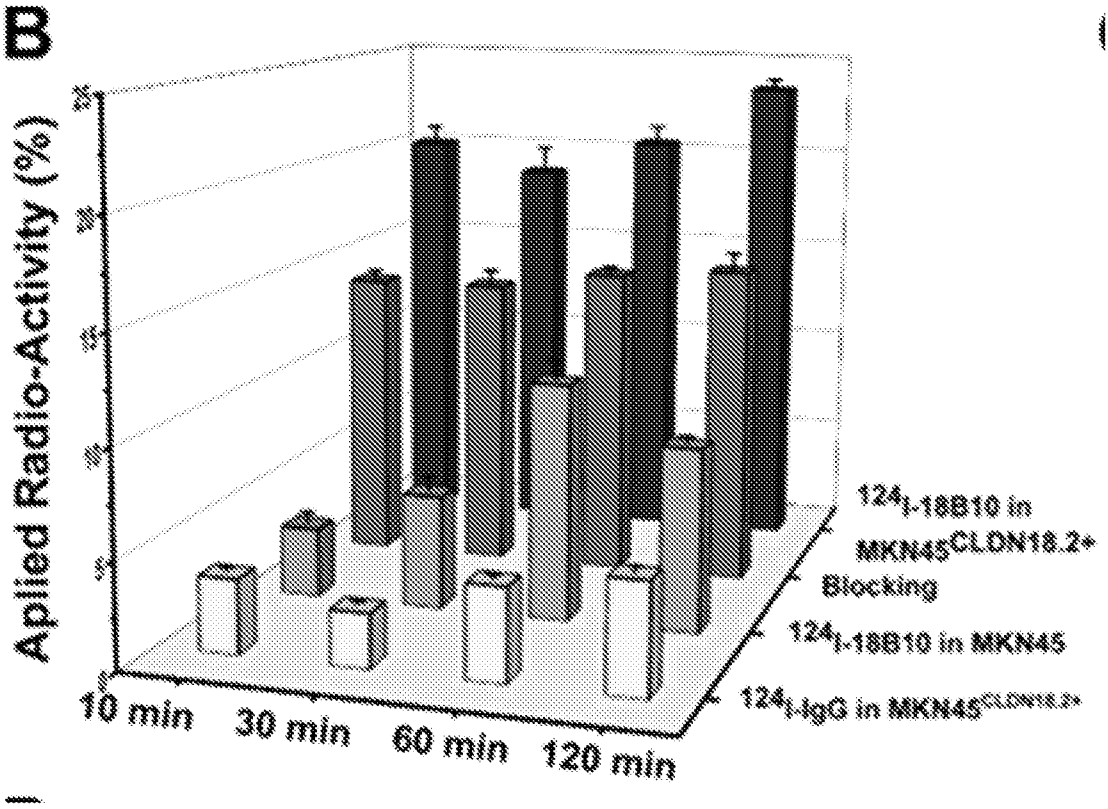
B
Aplied Radio-Activity (%)
10 min
30 min
60 min
120 min
124I-18B10 in MKN45CLDN18.2+ Blocking
124I-18B10 in MKN45
124I-IgG in MKN45CLDN18.2+

Figure 7B

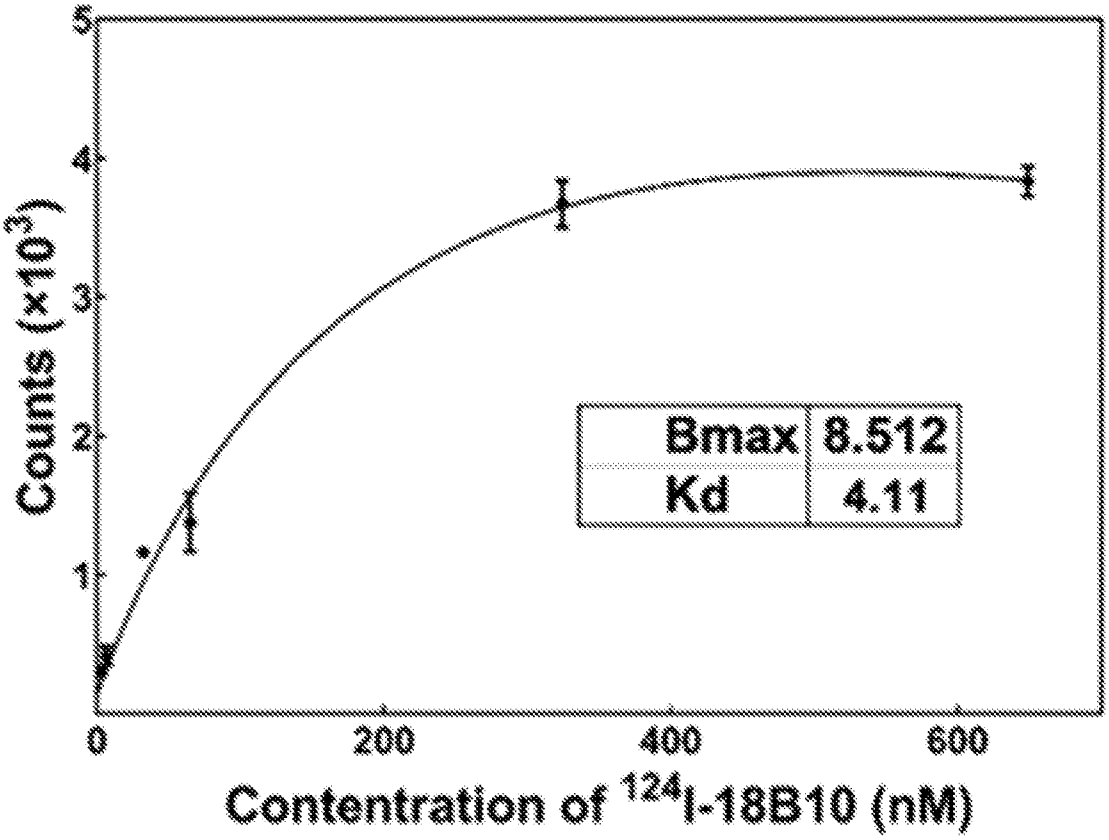
Counts (x10^3)
5
4
3
2
1
0
200
400
600
Contentration of 124I-18B10 (nM)
Bmax 8.512
Kd 4.11

Figure 7C

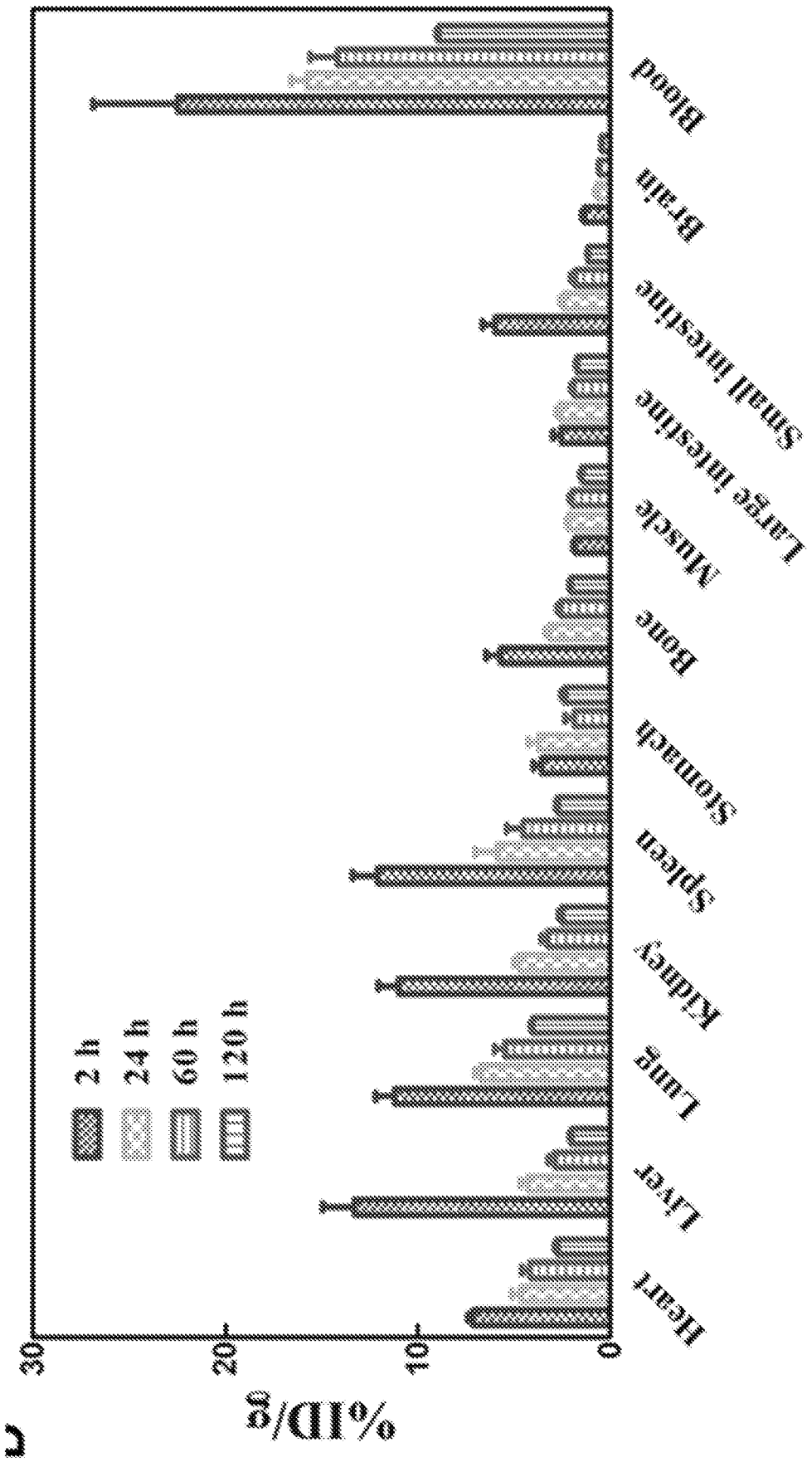
C
%ID/g
30
20
10
0
2 h
24 h
60 h
120 h
Heart
Liver
Lung
Kidney
Spleen
Stomach
Bone
Muscle
Large intestine
Small intestine
Brain
Blood

Figure 7D

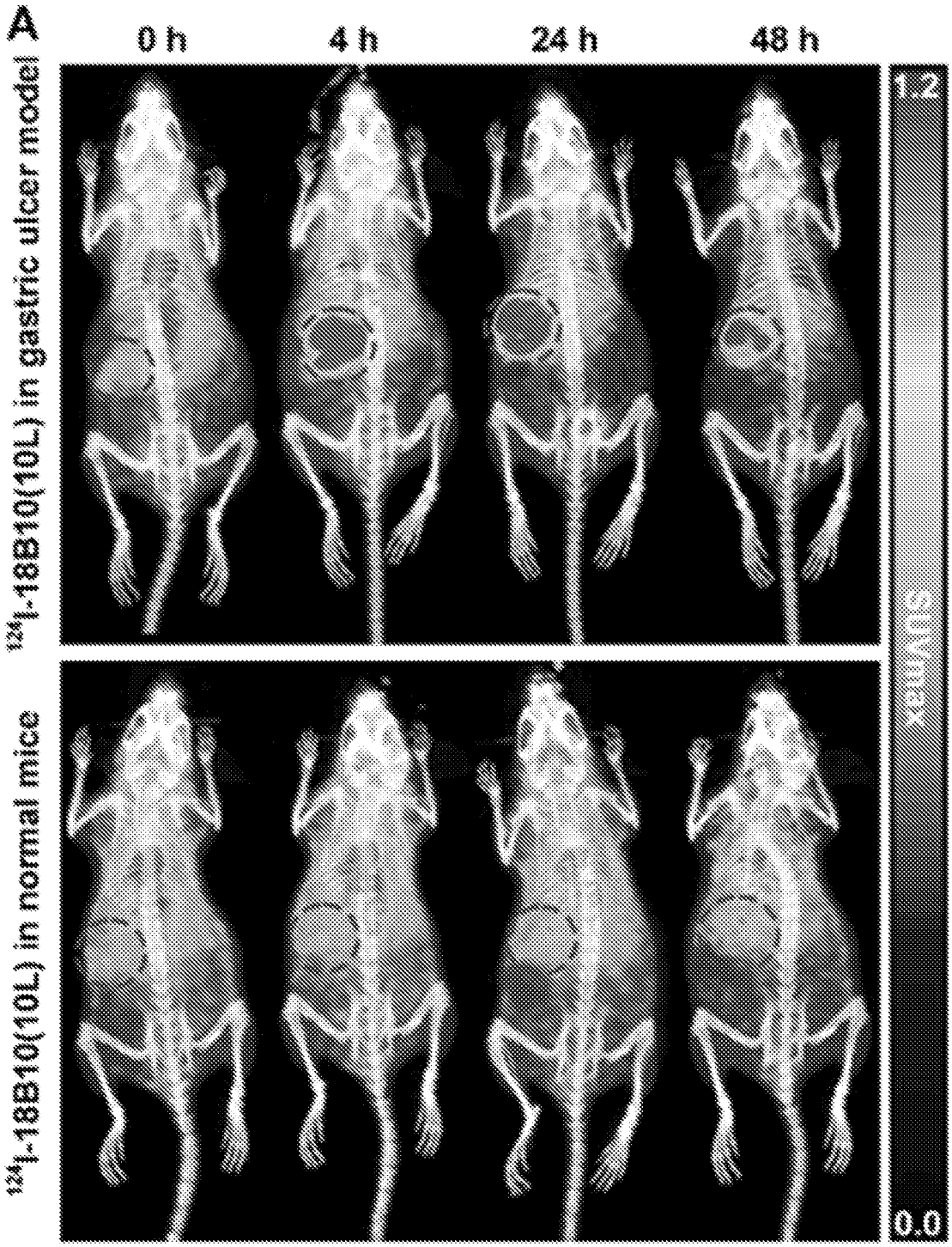
A
0 h
4 h
24 h
48 h
^{124}I-18B10(10L) in gastric ulcer model
^{124}I-18B10(10L) in normal mice
1.2
SUVmax
0.0

Figure 8A

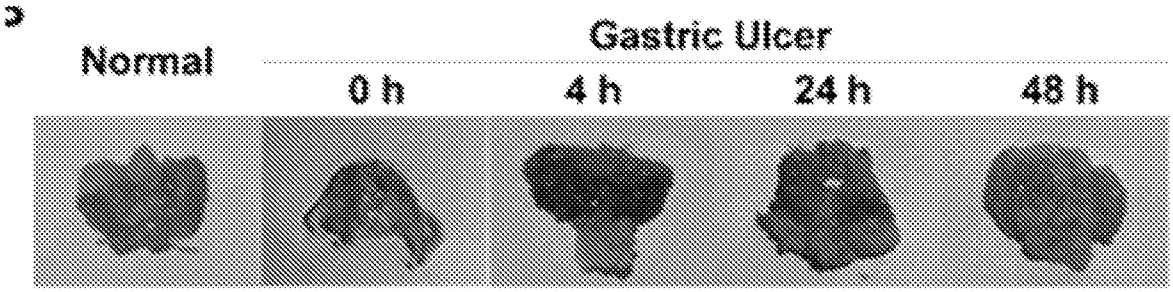

Figure 8B

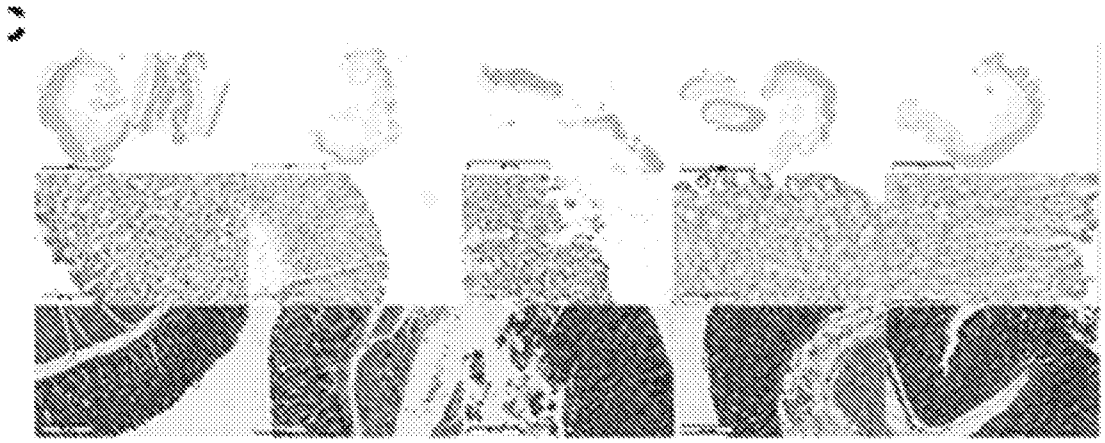

Figure 8C

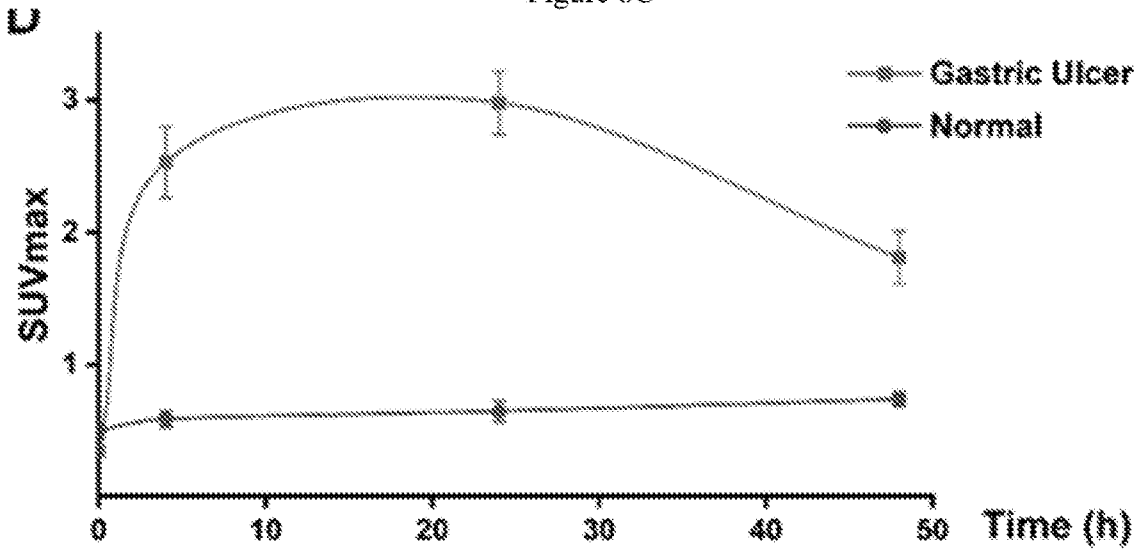

Figure 8D

Quality control of 124I-18B10(10L) used in this study

Parameter	QC Specification	QC Result
Appearance	Clear, Colorless	Pass
Volume	1.0-3.0 mL	2.0 mL
pH	5.0-8.0	7.2
Radio-TLC	>95%	>99%
Radio-HPLC	>95%	>99%
Ethanol	<10%	0%
Endotoxins	<15 EU/mL	Pass
Sterility	Sterile	Pass
Specific Activity	3.0-6.0 GBq/μmol	4.4 GBq/μmol

Figure 9

Patient Characteristics

No.	Gender	Age	Weight (kg)	Injection Dose (mCi)	Tumor Type	CLDN 18.2 Expression	CLDN 18.2 targeted therpay before PET
1[a]	Female	30	54	1.66	gastric cancer	90%, 3+	No
2	Male	55	55	1.99	gastric cancer	0	No
3	Male	61	57	1.81	pancreatic cancer	40%, 2+	No
4	Female	57	57	1.55	cholangiocarcinoma	30%, 3+	No
5	Female	48	32	1.97	gastric cancer	90%, 3+	Yes
6	Male	53	55	1.16	pancreatic cancer	50%, 2+	Yes
7	Female	43	52	1.78	gastric cancer	90%, 3+	Yes
8	Female	36	55	1.26	gastric cancer	90%, 3+	Yes
9	Male	61	51	0.79	gastric cancer	40%, 2+	No
10	Female	43	56	1.24	gastric cancer	90%, 3+	Yes
11	Male	35	56	1.26	gastric cancer	80%, 3+	Yes
12	Female	51	50	1.09	gastric cancer	90%, 3+	Yes
13	Male	62	64	1.25	gastric cancer	80%, 2+	Yes
14	Female	39	32	1.14	gastric cancer	90%, 3+	Yes
15	Female	57	51	1.08	pancreatic cancer	70%, 2+	Yes
16	Female	65	51	1.33	pancreatic cancer	+	No
17	Female	29	60	1.29	gastric cancer	40%，2+	No

Figure 10

Dosemitry

Target Organ	Beta (mGy/MBq)		Total (mSv/MBq)
Adrenals	1.58E+00	0.005333	8.43E-03
Brain	3.76E-02	0.005333	2.01E-04
Breasts	1.60E+00	0.05	8.00E-02
Gallbladder Wall	7.20E-01	0.005333	3.84E-03
LLI Wall	5.49E-02	0.005333	2.93E-04
Small Intestine	1.60E-01	0.12	1.92E-02
Stomach Wall	1.35E+00	0.005333	7.20E-03
ULI Wall	1.85E-01	0.12	2.22E-02
Heart Wall	3.28E+02	0.12	3.94E+01
Kidneys	4.55E-01	0.005333	2.43E-03
Liver	1.23E+00	0.005333	6.56E-03
Lungs	2.32E+00	0.005333	1.24E-02
Muscle	5.27E-01	0.05	2.64E-02
Ovaries	7.19E-02	0.12	8.63E-03
Pancreas	1.84E+00	0.005333	9.81E-03
Red Marrow	6.84E-01	0.12	8.21E-02
Osteogenic Cells	4.52E-01	0.005333	2.41E-03
Skin	2.47E-01	0.12	2.96E-02
Spleen	8.62E-01	0.005333	4.60E-03
Testes	1.27E-02	0.005333	6.77E-05
Thymus	3.80E+00	0.005333	2.03E-02
Thyroid	2.83E-01	0.005333	1.51E-03
Urinary Bladder Wall	2.14E-02	0.05	1.07E-03
Uterus	6.83E-02	0.05	3.42E-03
Total Body	2.03E+00	0.005333	1.08E-02

Figure 11

Amino acid sequence of human CLDN18.2 (SEQ ID NO: 30)

MAVTACQGLGFVVSLIGIAGIIAATCMDQWSTQDLYNNPVTAVFNYQGLWR
SCVRESSGFTECRGYFTLLGLPAMLQAVRALMIVGIVLGAIGLLVSIFALKCIRI
GSMEDSAKANMTLTSGIMFIVSGLCAIAGVSVFANMLVTNFWMSTANMYTG
MGGMVQTVQTRYTFGAALFVGWVAGGLTLIGGVMMCIACRGLAPEETNYK
AVSYHASGHSVAYKPGGFKASTGFGSNTKNKKIYDGGARTEDEVQSYPSKH
DYV

Amino acid sequence of human CLDN18.1 (SEQ ID NO: 31)

MSTTTCQVVAFLLSILGLAGCIAATGMDMWSTQDLYDNPVTSVFQYEGLWR
SCVRQSSGFTECRPYFTILGLPAMLQAVRALMIVGIVLGAIGLLVSIFALKCIRI
GSMEDSAKANMTLTSGIMFIVSGLCAIAGVSVFANMLVTNFWMSTANMYTG
MGGMVQTVQTRYTFGAALFVGWVAGGLTLIGGVMMCIACRGLAPEETNYK
AVSYHASGHSVAYKPGGFKASTGFGSNTKNKKIYDGGARTEDEVQSYPSKH
DYV

Human IgG1 heavy chain constant region (SEQ ID NO: 49):

ASTKGPSVFPLAPSSKSTSGGTAALGCLVKDYFPEPVTVSWNSGALTSGVHTF
PAVLQSSGLYSLSSVVTVPSSSLGTQTYICNVNHKPSNTKVDKKVEPKSCDKT
HTCPPCPAPELLGGPSVFLFPPKPKDTLMISRTPEVTCVVVDVSHEDPEVKFN
WYVDGVEVHNAKTKPREEQYNSTYRVVSVLTVLHQDWLNGKEYKCKVSNK
ALPAPIEKTISKAKGQPREPQVYTLPPSRDELTKNQVSLTCLVKGFYPSDIAVE
WESNGQPENNYKTTPPVLDSDGSFFLYSKLTVDKSRWQQGNVFSCSVMHEA
LHNHYTQKSLSLSPGK

Human Kappa light chain constant region (SEQ ID NO: 50):

RTVAAPSVFIFPPSDEQLKSGTASVVCLLNNFYPREAKVQWKVDNALQSGNS
QESVTEQDSKDSTYSLSSTLTLSKADYEKHKVYACEVTHQGLSSPVTKSFNRG
EC

Figure 12

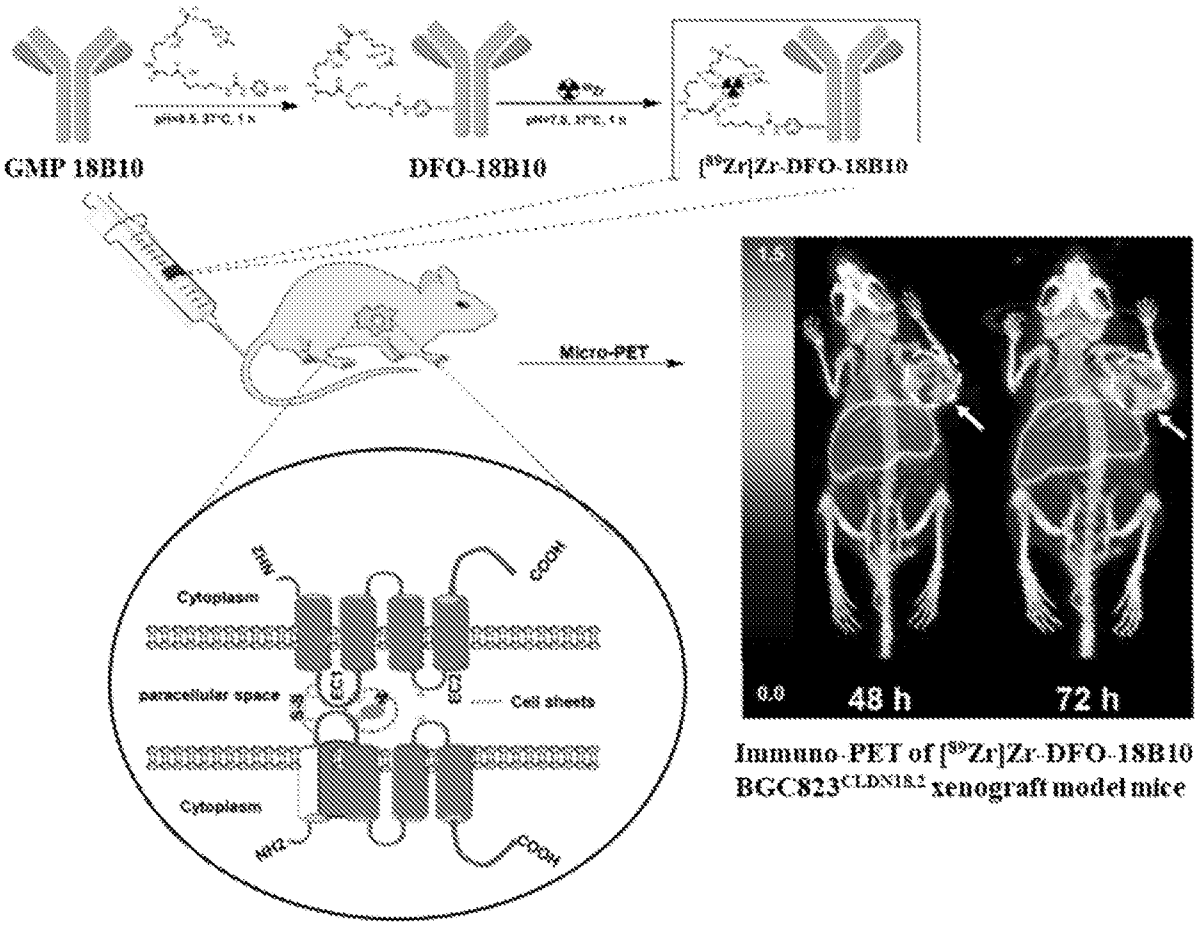

Immuno-PET of [^{89}Zr]Zr-DFO-18B10 BGC823$^{CLDN18.2}$ xenograft model mice

Figure 13

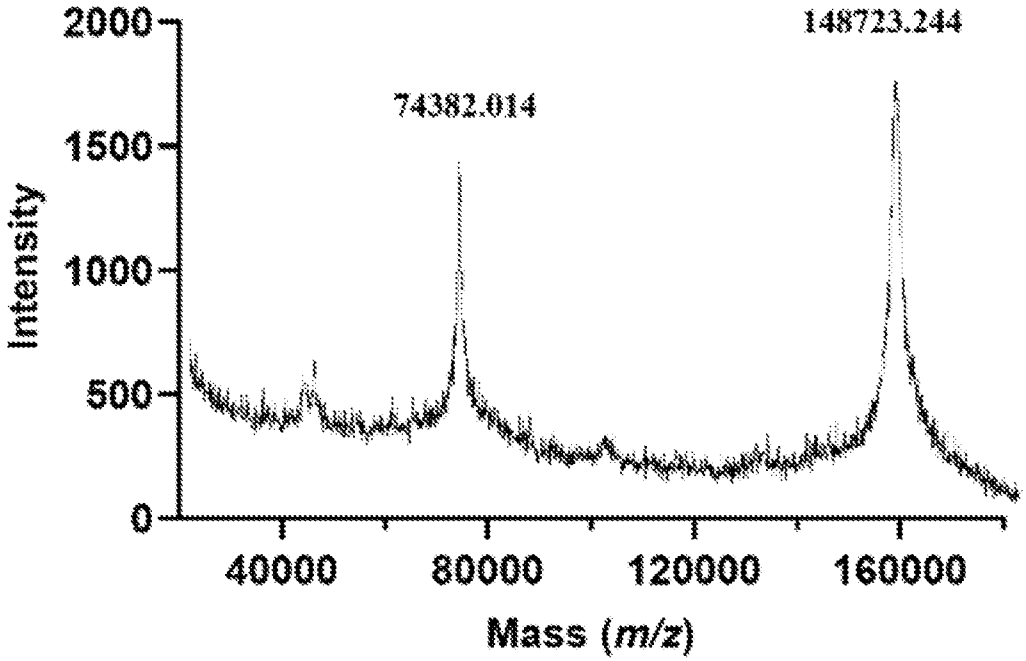
2000
1500
1000
500
0
Intensity
74382.014
148723.244
40000
80000
120000
160000
Mass (m/z)

Figure 14A

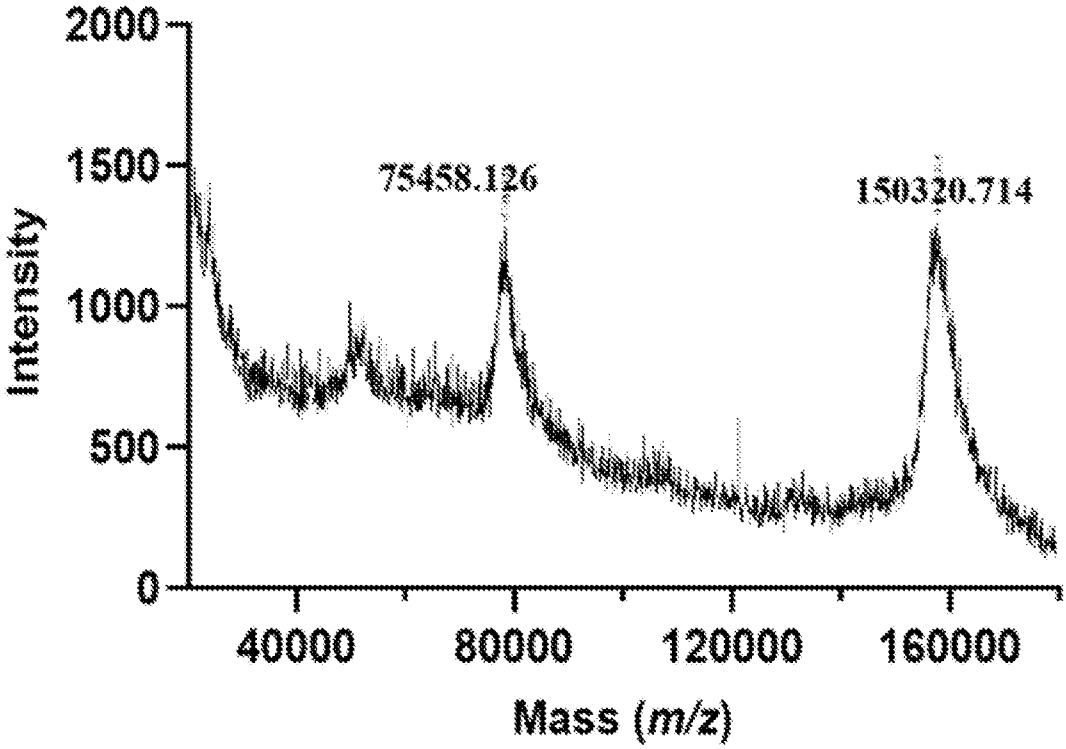

Figure 14B

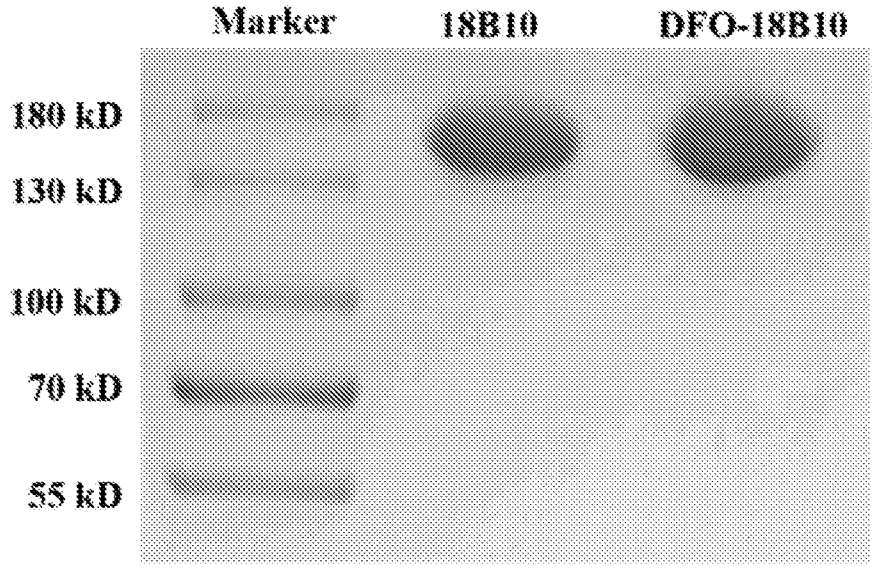

Figure 14C

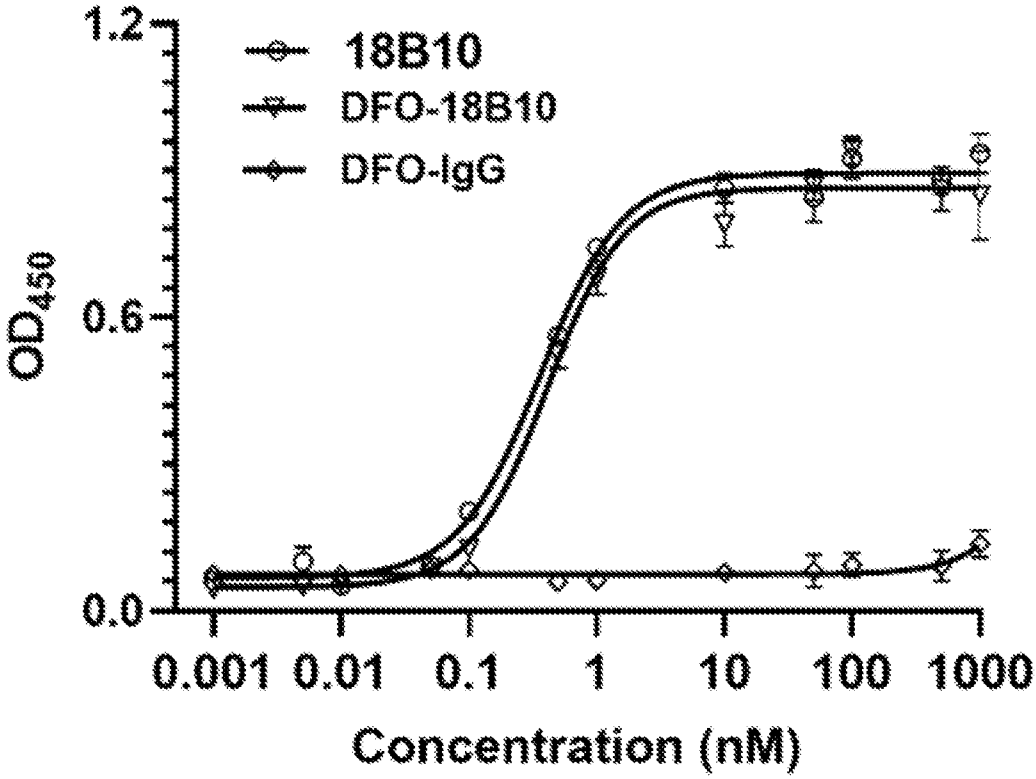
18B10
DFO-18B10
DFO-IgG
OD450
1.2
0.6
0.0
0.001
0.01
0.1
1
10
100
1000
Concentration (nM)

Figure 14D

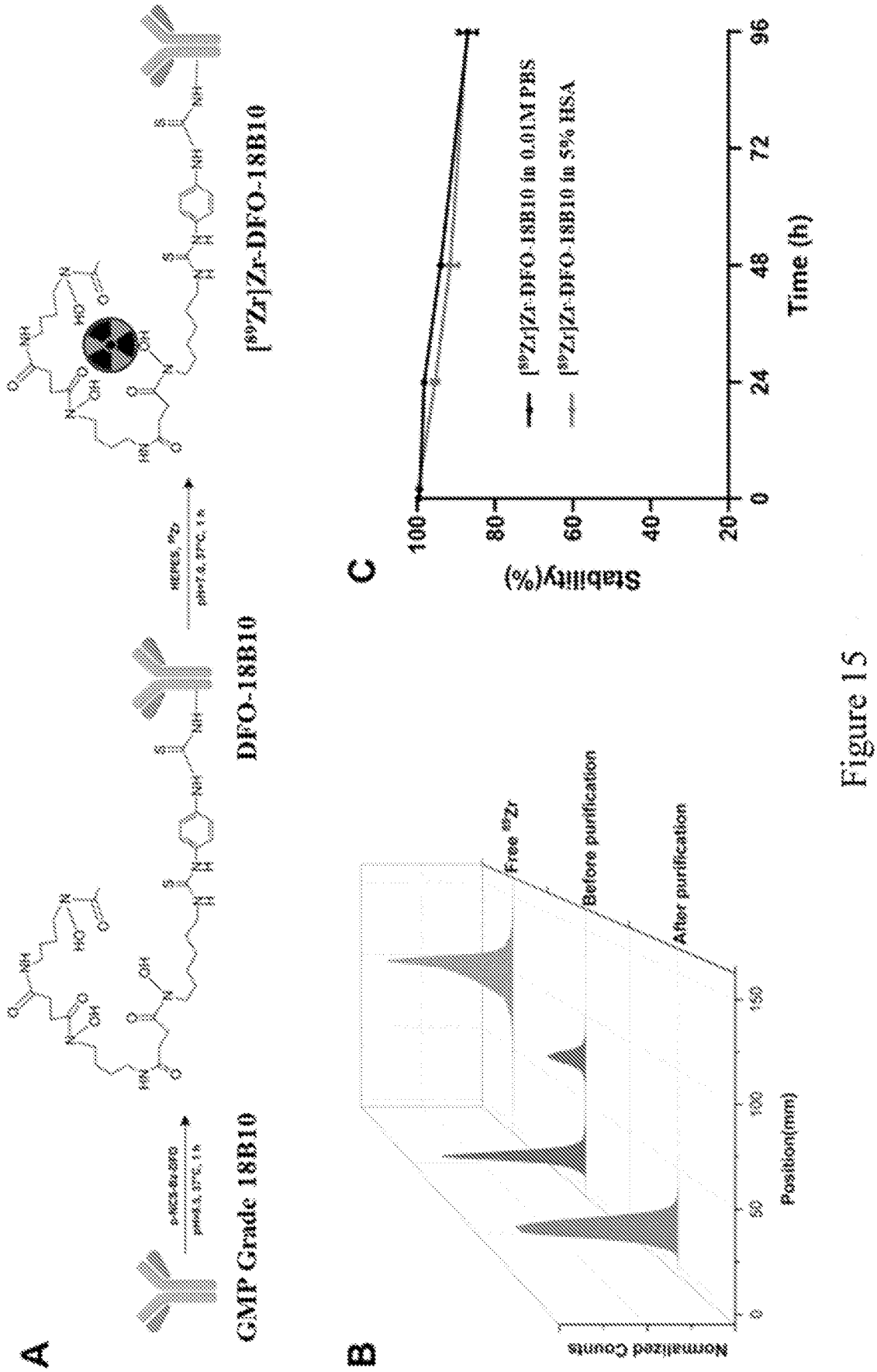
A
GMP Grade 18B10
DFO-18B10
[89Zr]Zr-DFO-18B10
B
Free 89Zr
Before purification
After purification
Normalized Counts
Position(mm)
C
Stability(%)
Time (h)
[89Zr]Zr-DFO-18B10 in 0.01M PBS
[89Zr]Zr-DFO-18B10 in 5% HSA

Figure 15

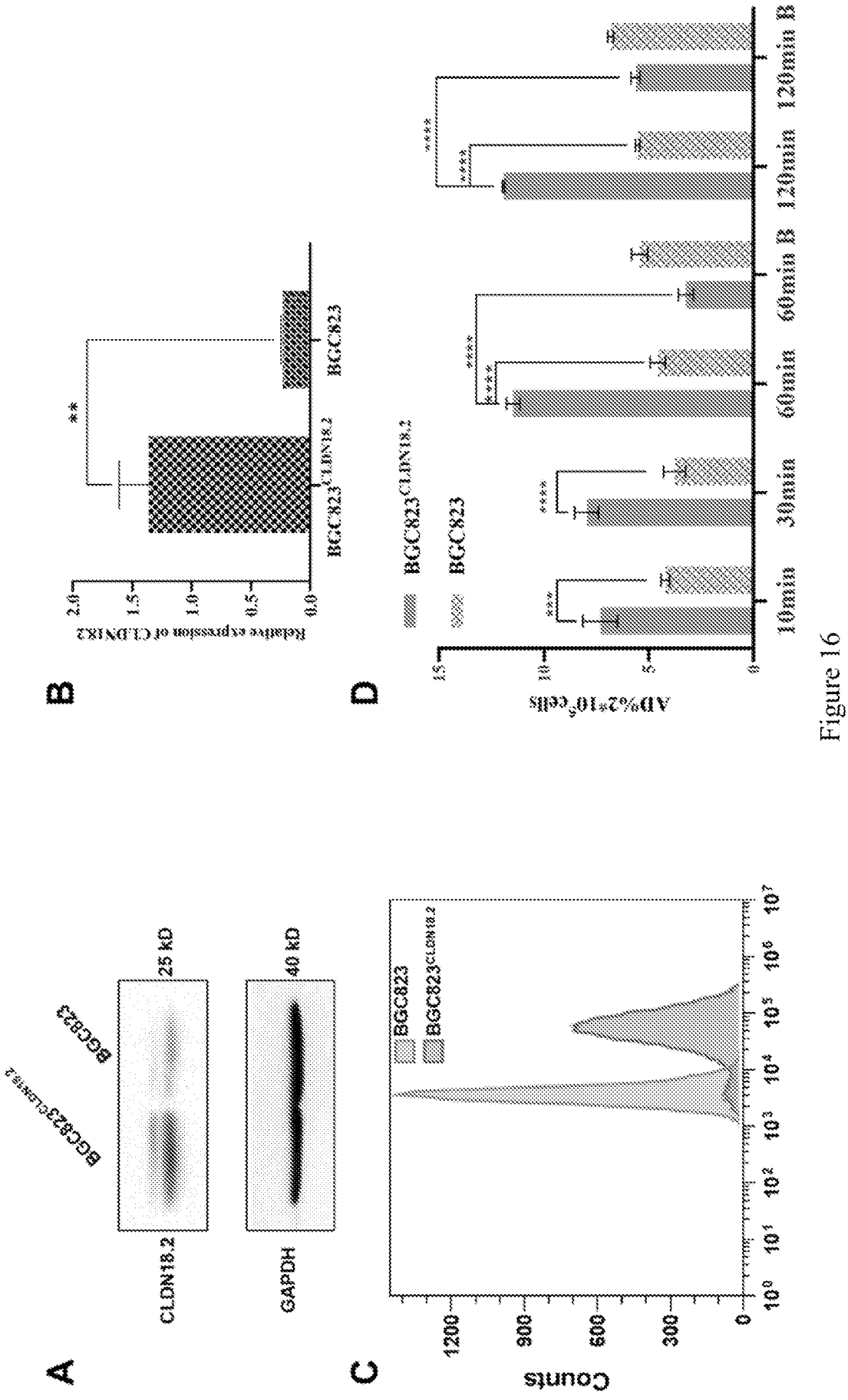
A
25 kD
40 kD
CLDN18.2
GAPDH
B
Relative expression of CLDN18.2
2.0
1.5
1.0
0.5
0.0
**
BGC823
C
Counts
1200
900
600
300
0
D
BGC823
10min
30min
60min
60min B
120min
120min B
***
****

Figure 16

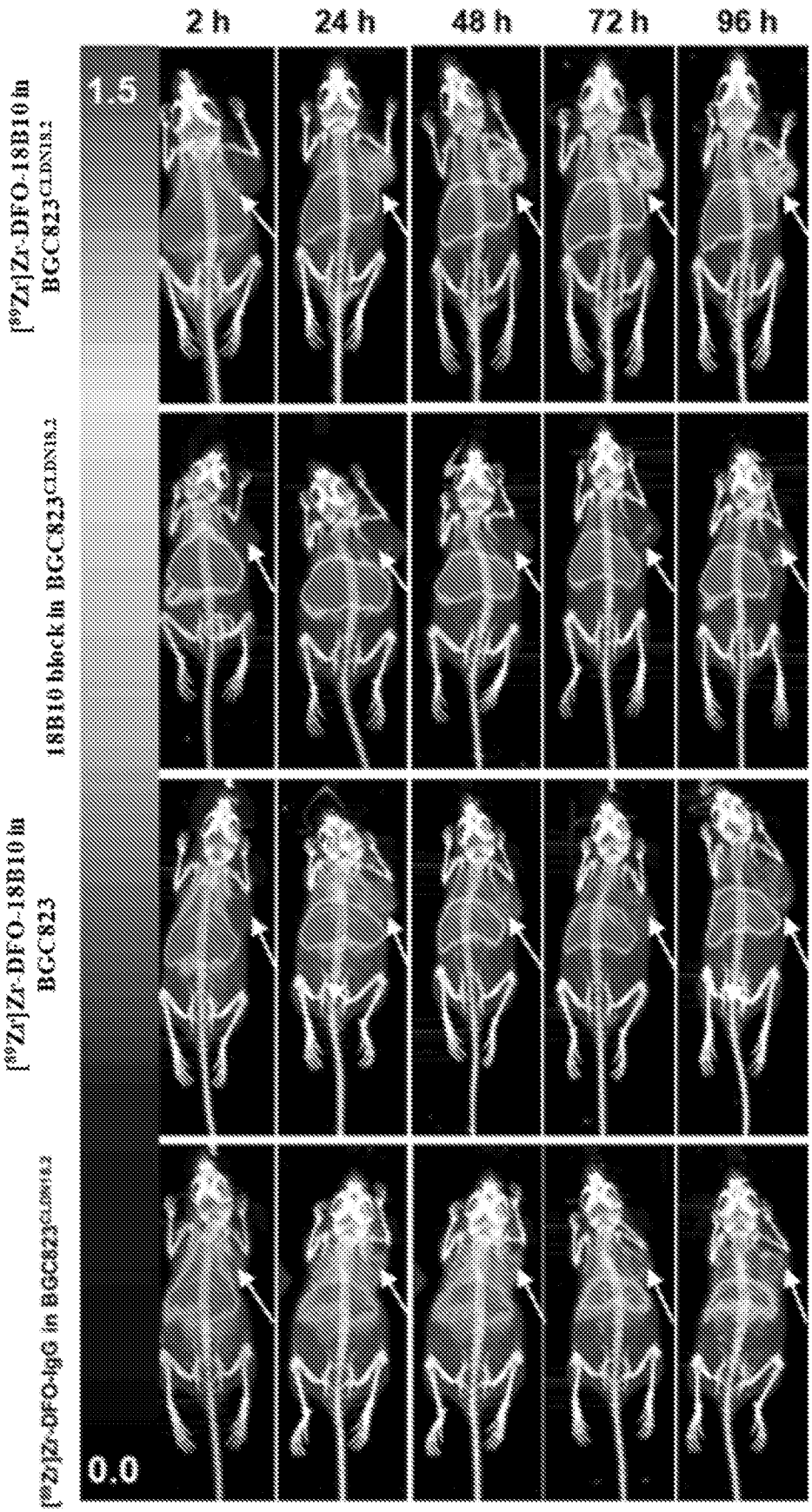
2 h
24 h
48 h
72 h
96 h
1.5
0.0
[89Zr]Zr-DFO-18B10 in BGC823CLDN18.2
18B10 block in BGC823CLDN18.2
[89Zr]Zr-DFO-18B10 in BGC823
[89Zr]Zr-DFO-IgG in BGC823CLDN18.2

Figure 17A

B

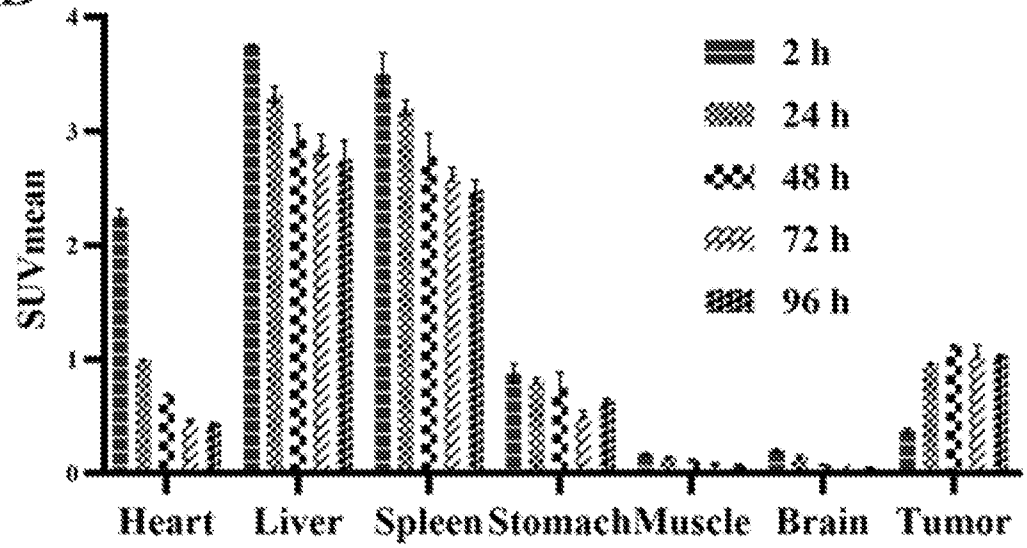

Figure 17B

C

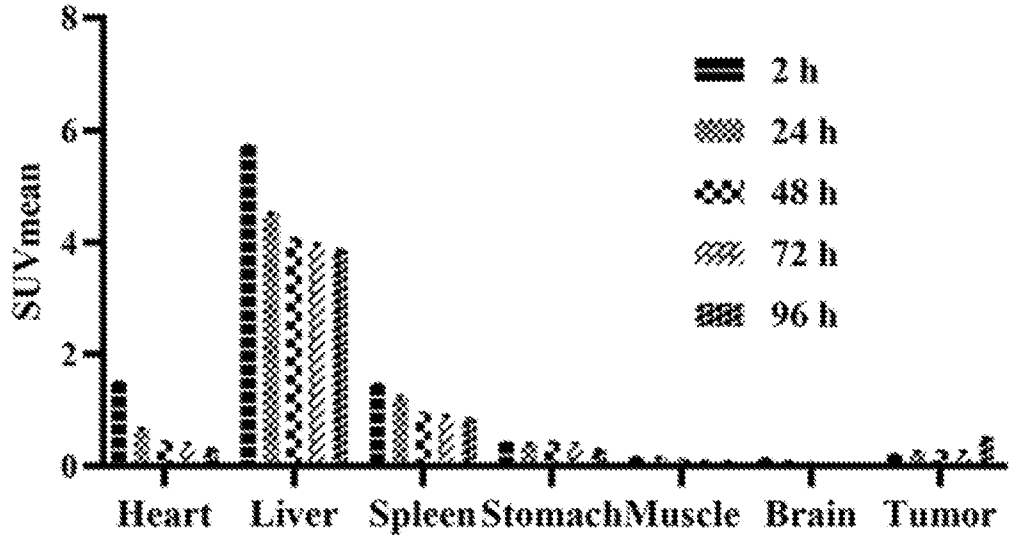

Figure 17C

D

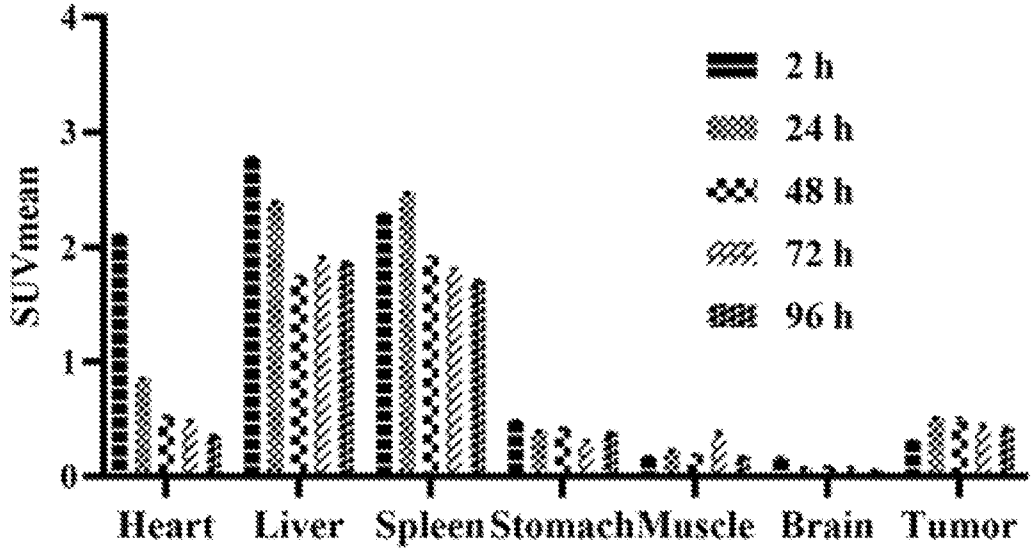

Figure 17D

E

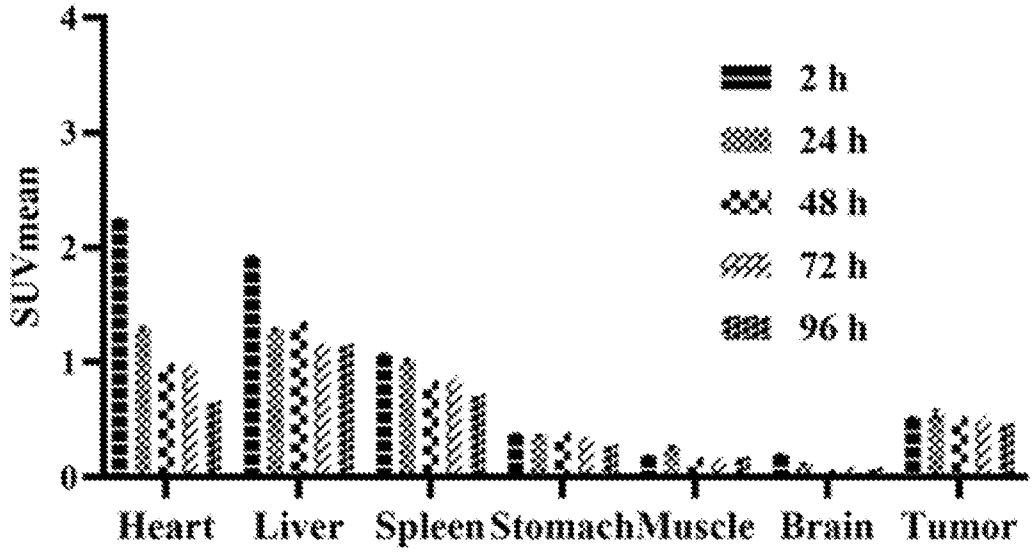

Figure 17E

A

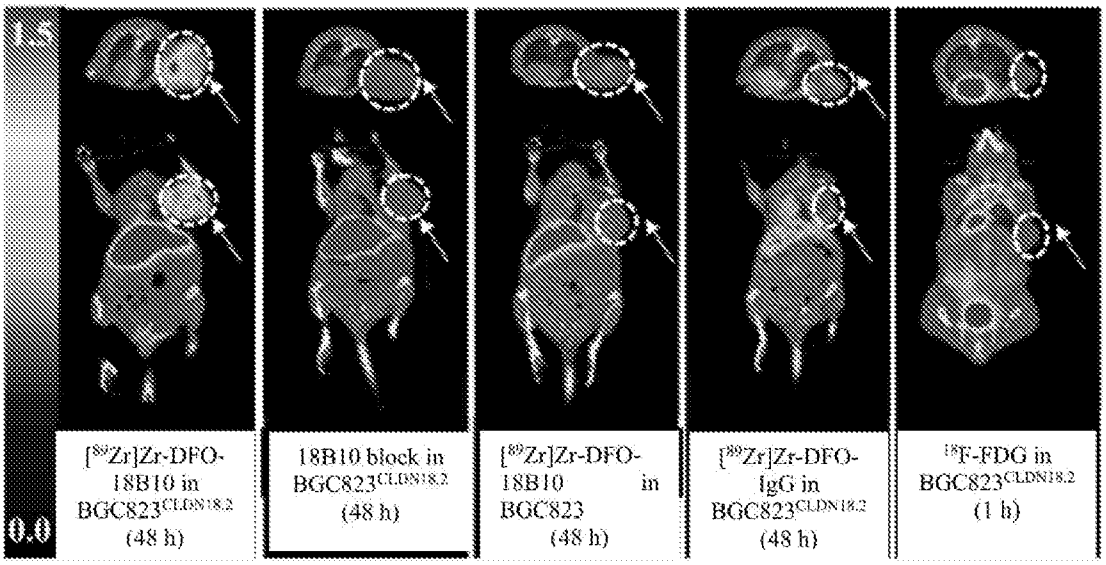

Figure 18A

B

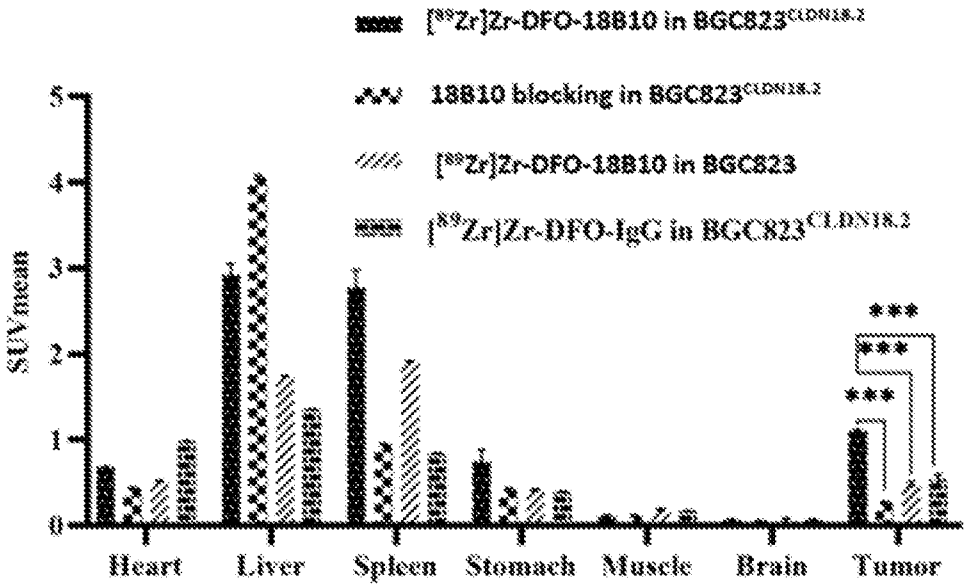

Figure 18B

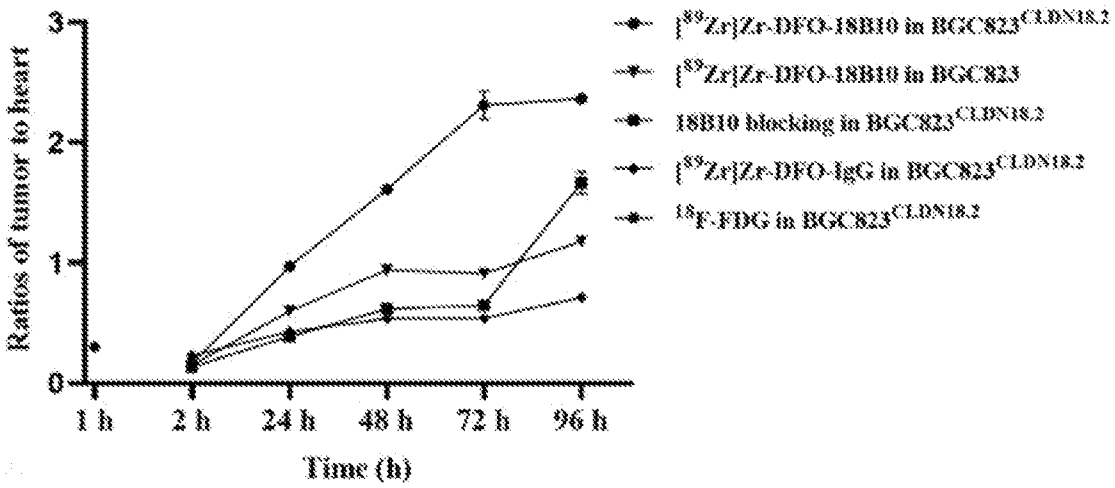

Figure 18C

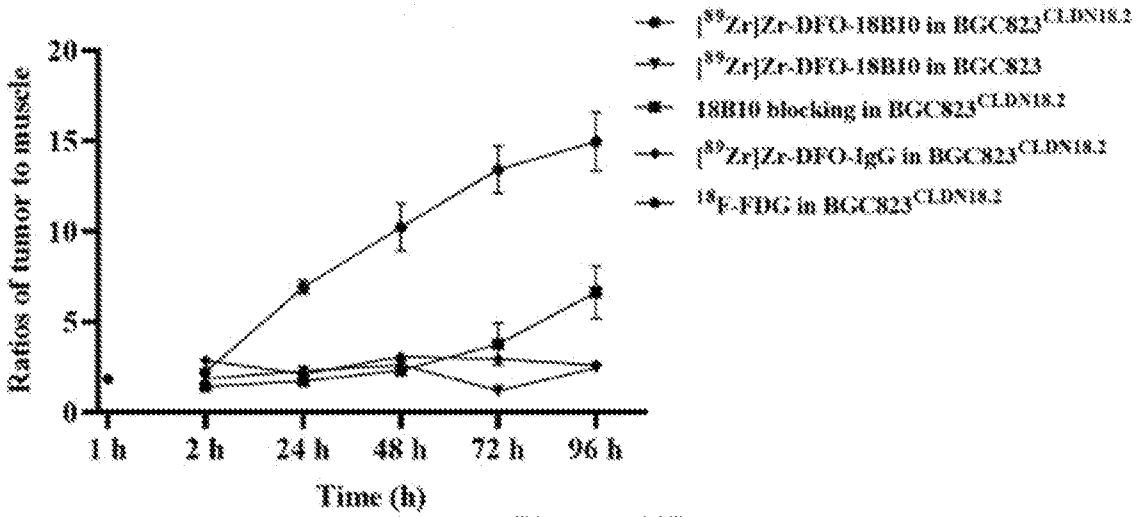

Figure 18D

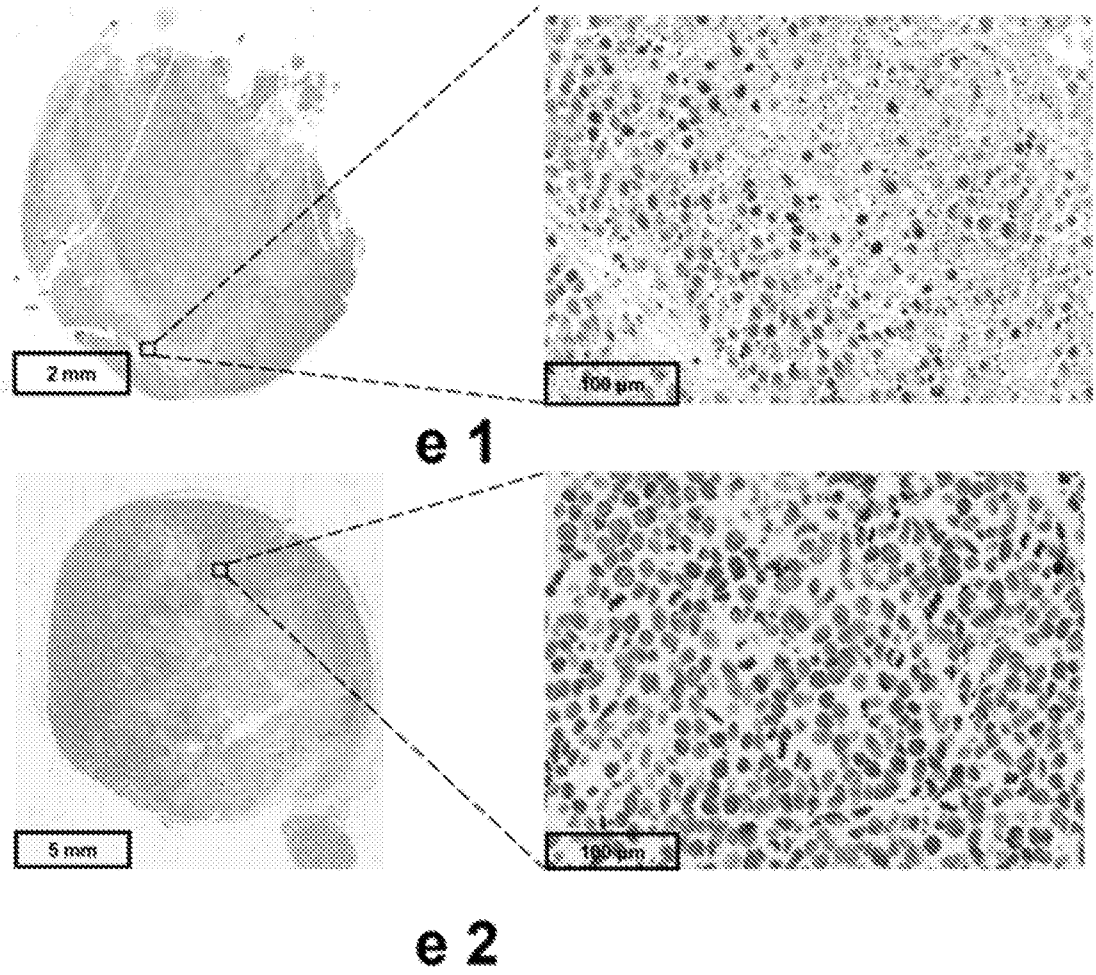

Figure 18E

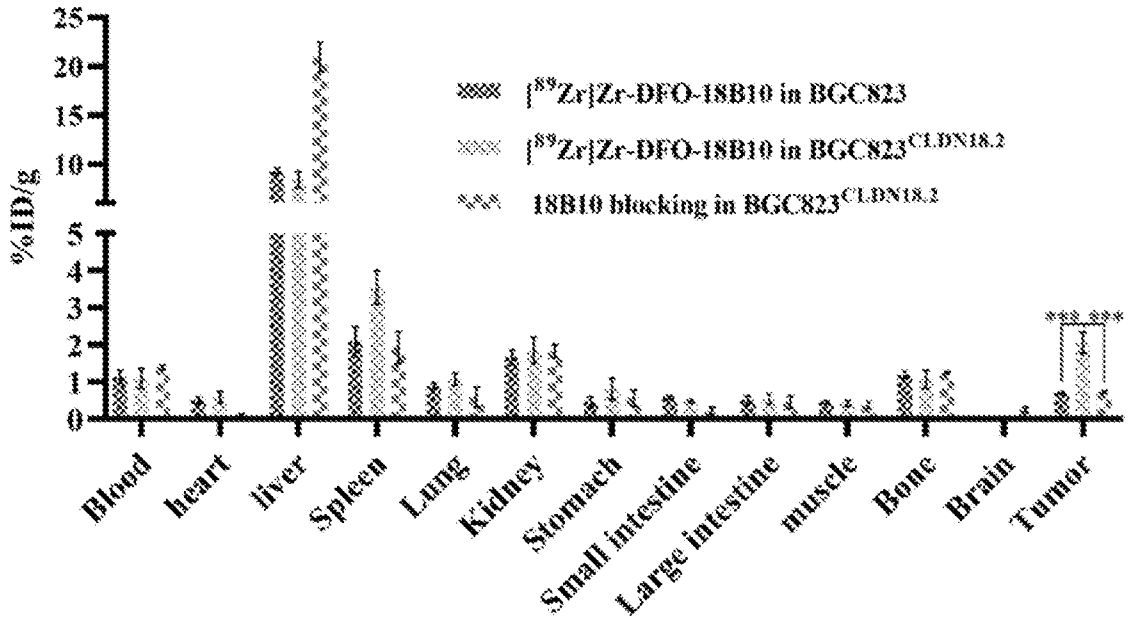

Figure 19A

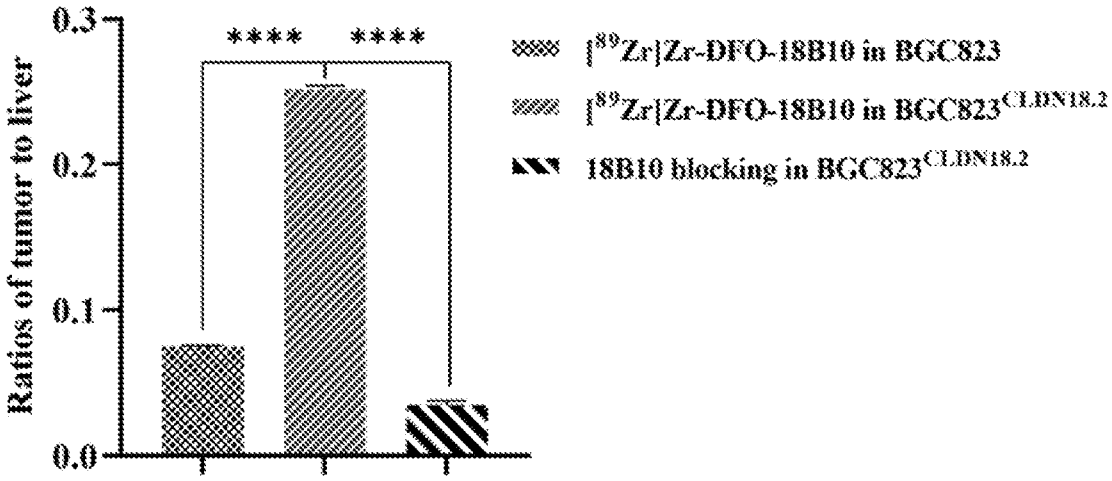

Figure 19B

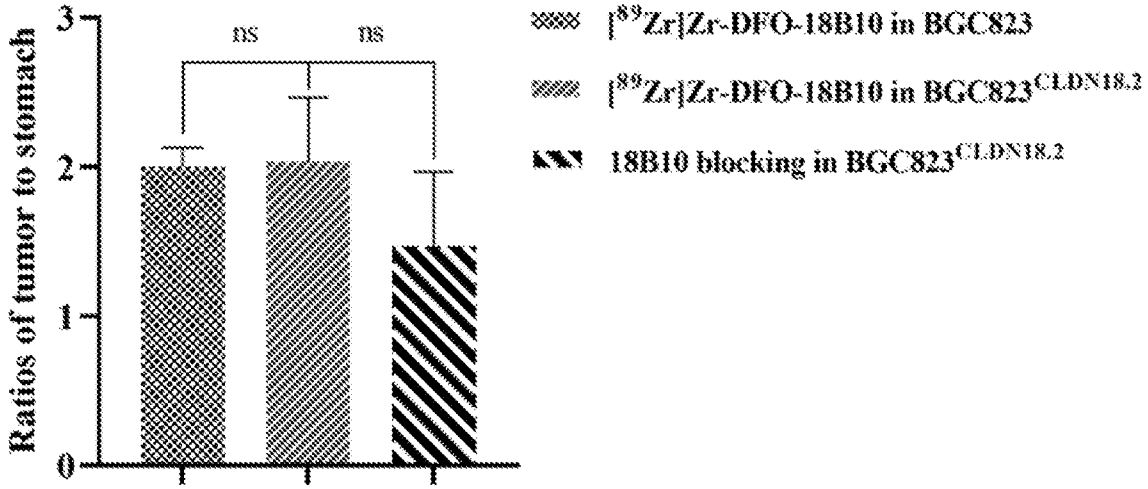

Figure 19C

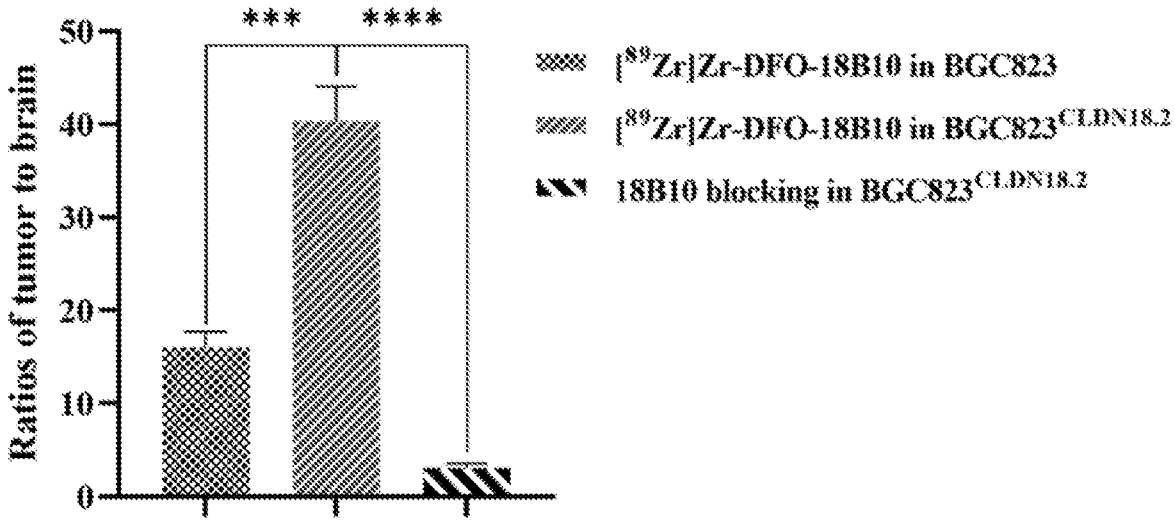

Figure 19D

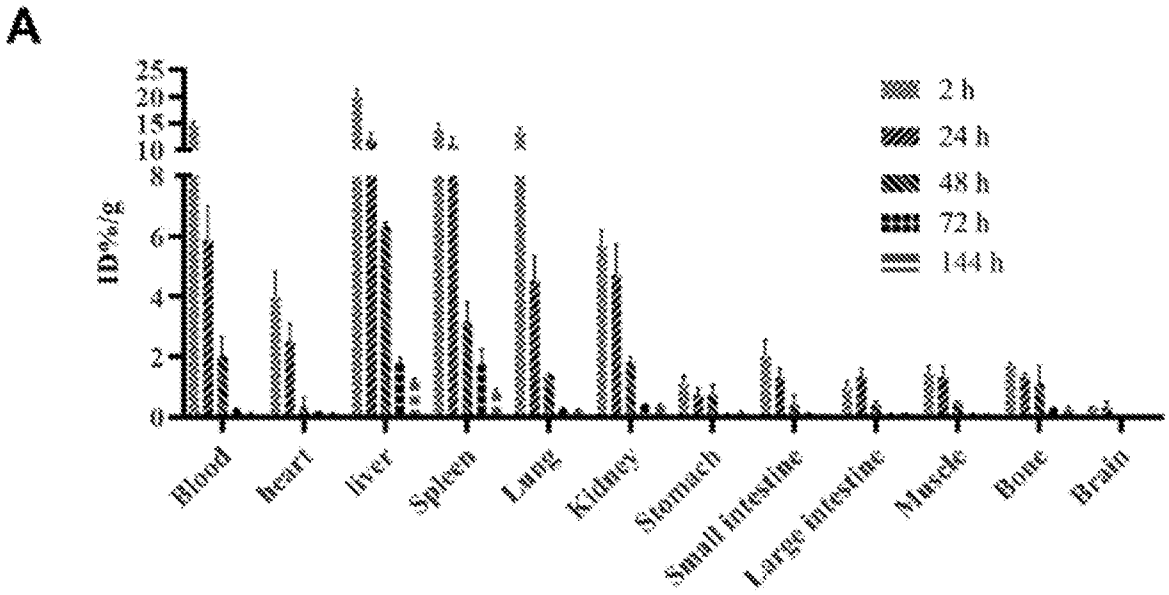

Figure 20A

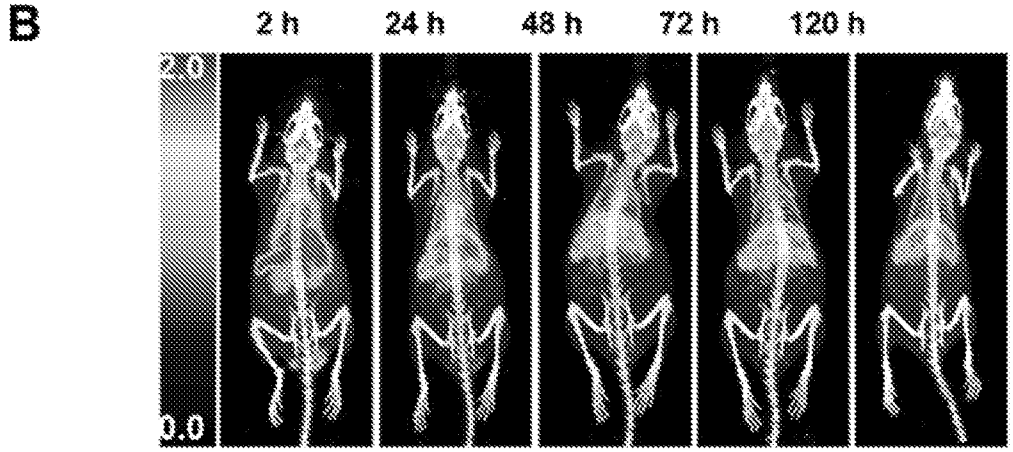

Figure 20B

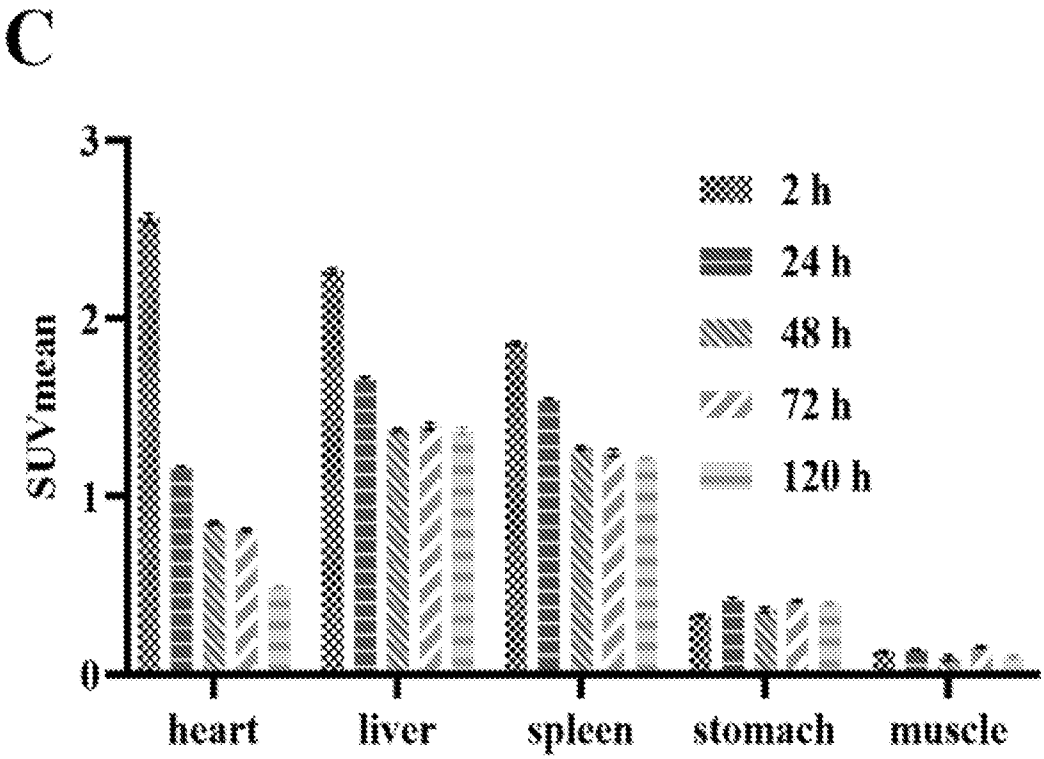

Figure 20C

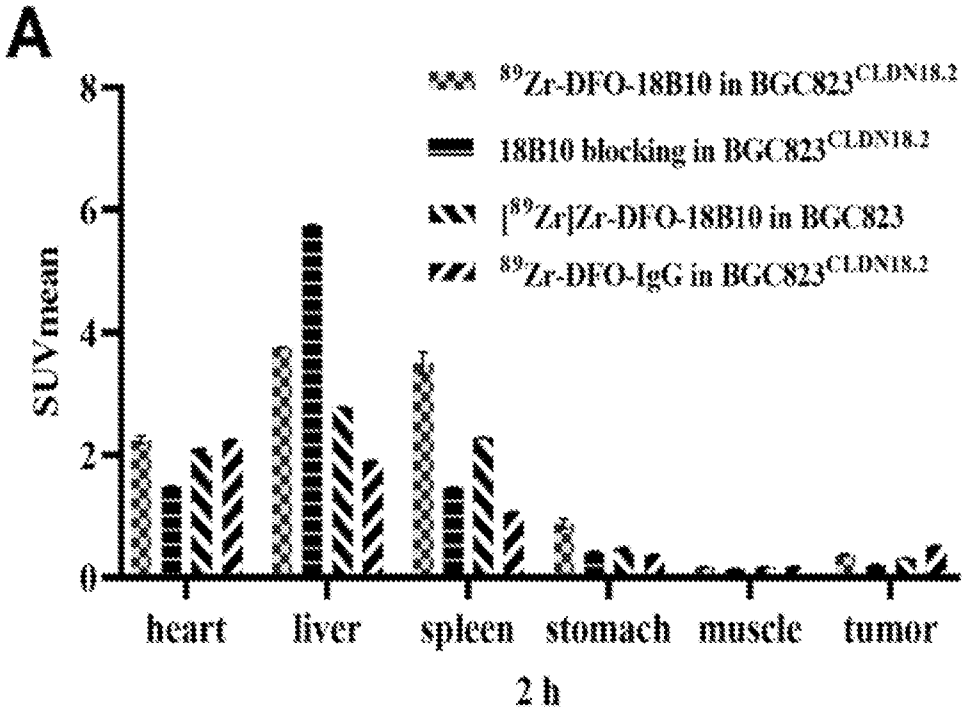

Figure 21A

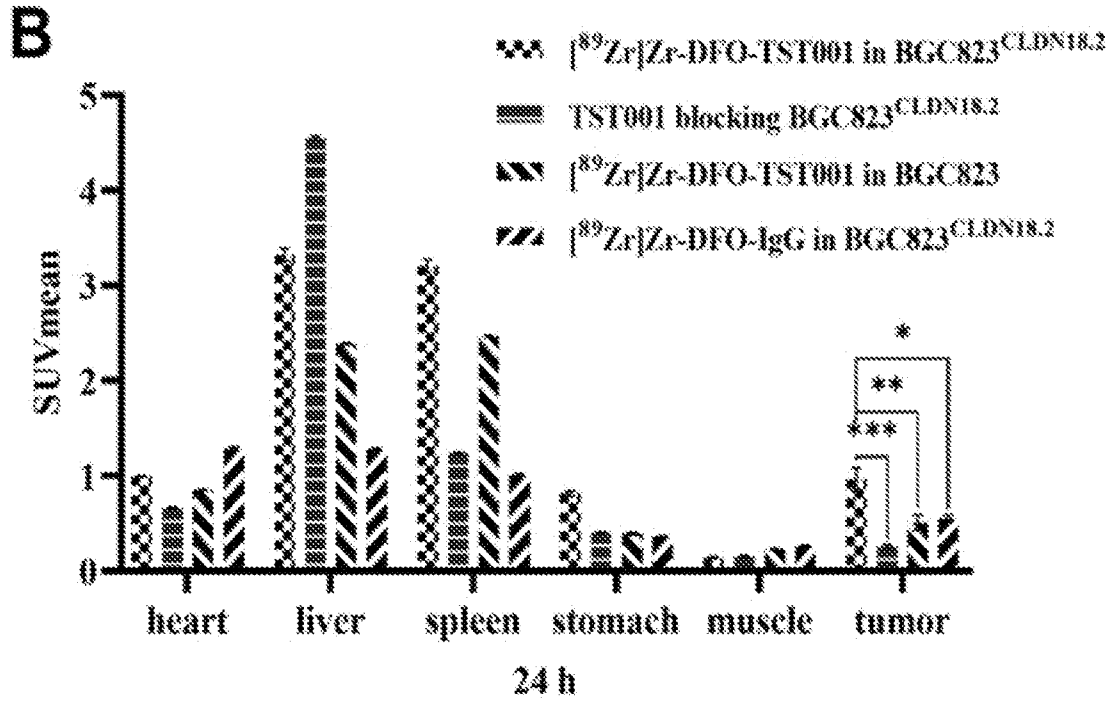

Figure 21B

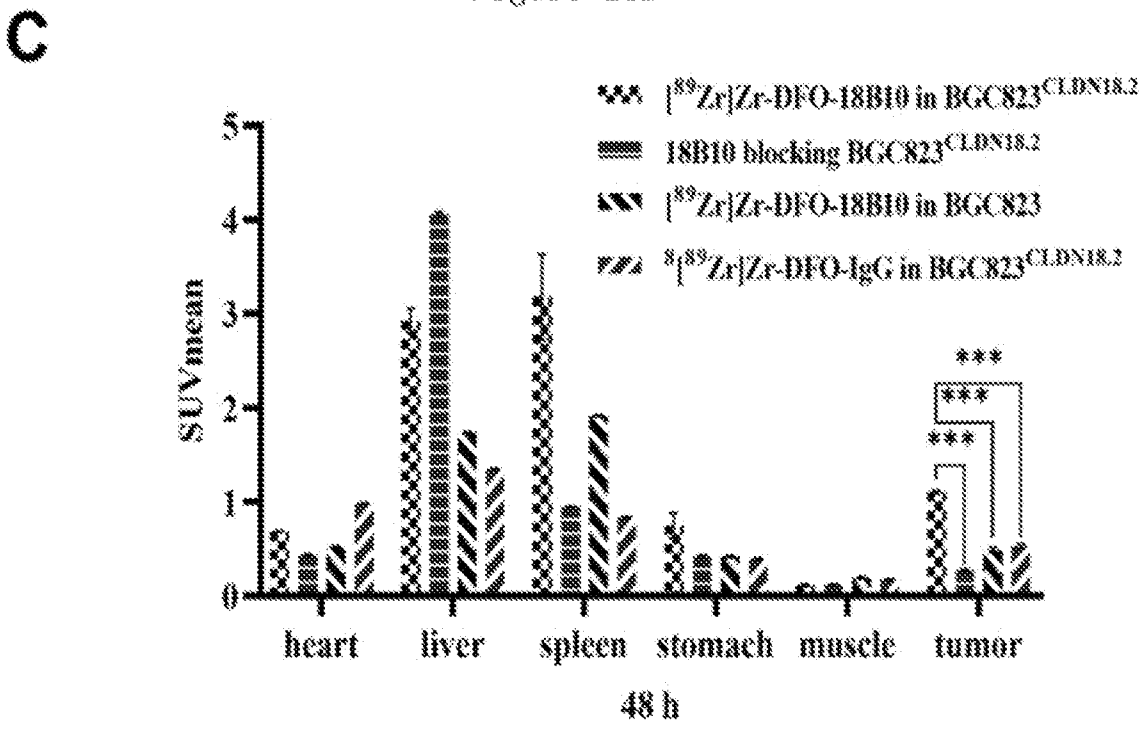

Figure 21C

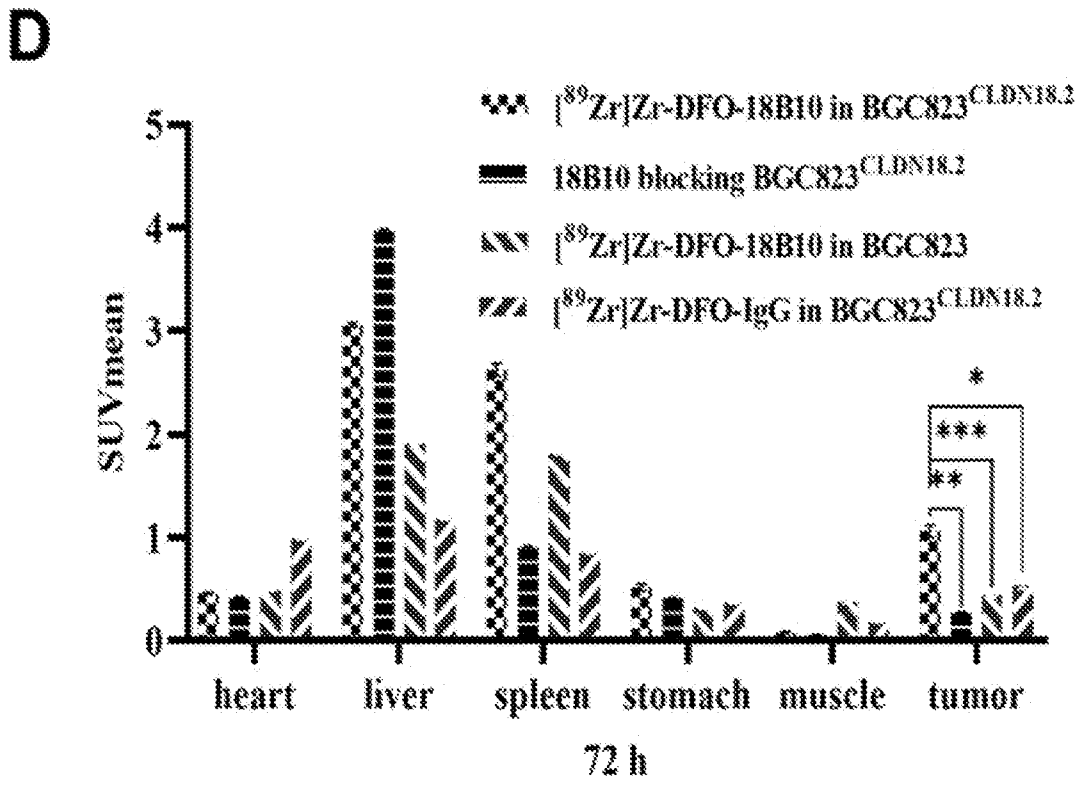

Figure 21D

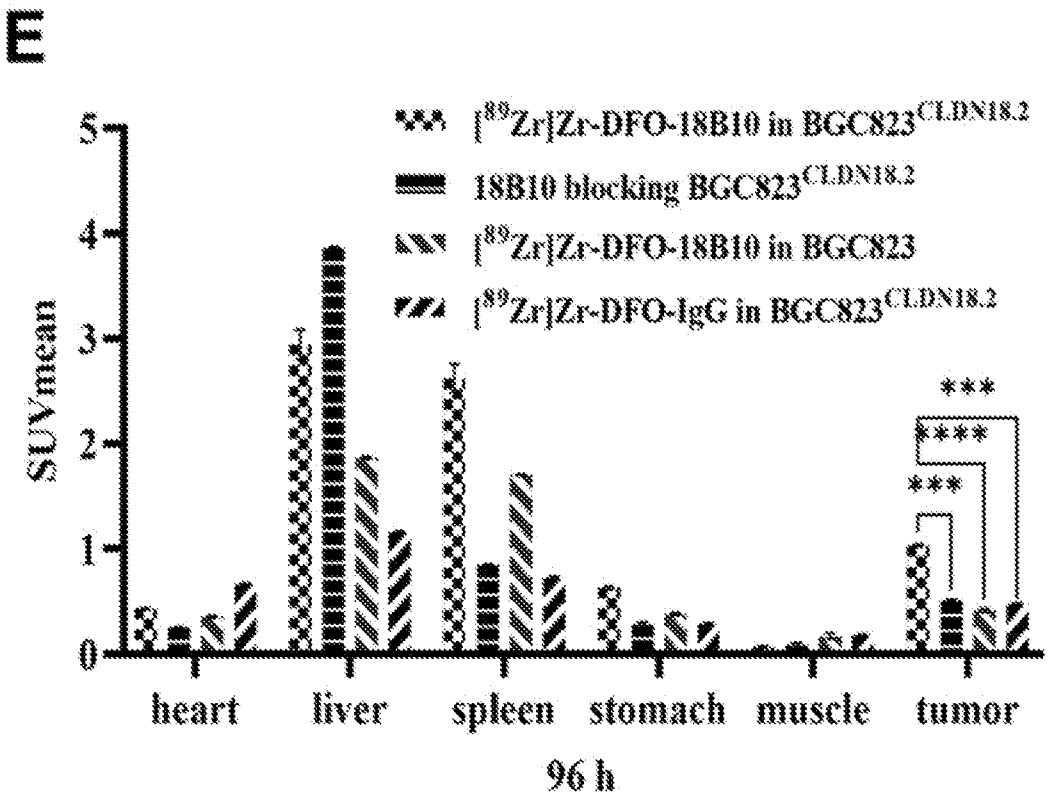

Figure 21E

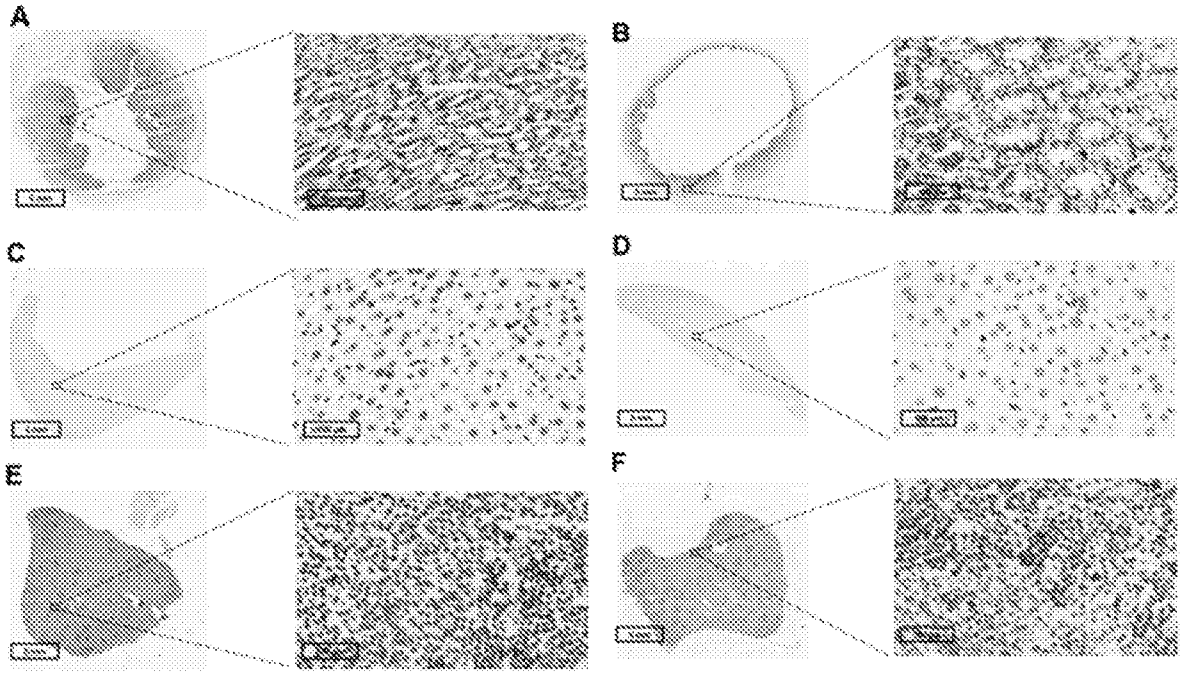

Figure 22

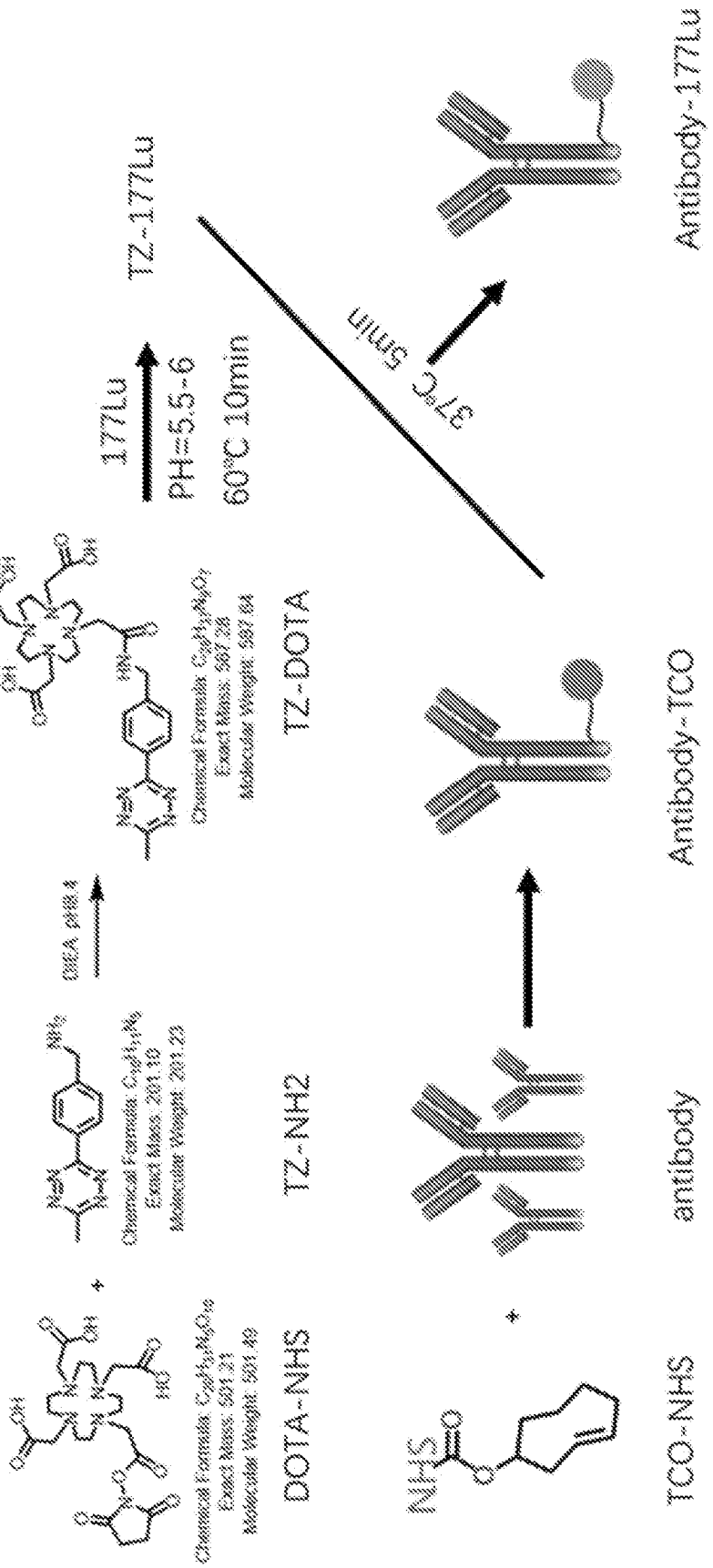
DOTA-NHS
Chemical Formula: C25H39N5O10
Exact Mass: 569.27
Molecular Weight: 569.60
TZ-NH2
Chemical Formula: C19H19N5
Exact Mass: 301.16
Molecular Weight: 301.39
DIEA, pH8.4
TZ-DOTA
Chemical Formula: C44H51N9O11
Exact Mass: 881.37
Molecular Weight: 881.94
177Lu
PH=5.5-6
60℃ 10min
TZ-177Lu
TCO-NHS
antibody
Antibody-TCO
37℃ 5min
Antibody-177Lu

Figure 23

A

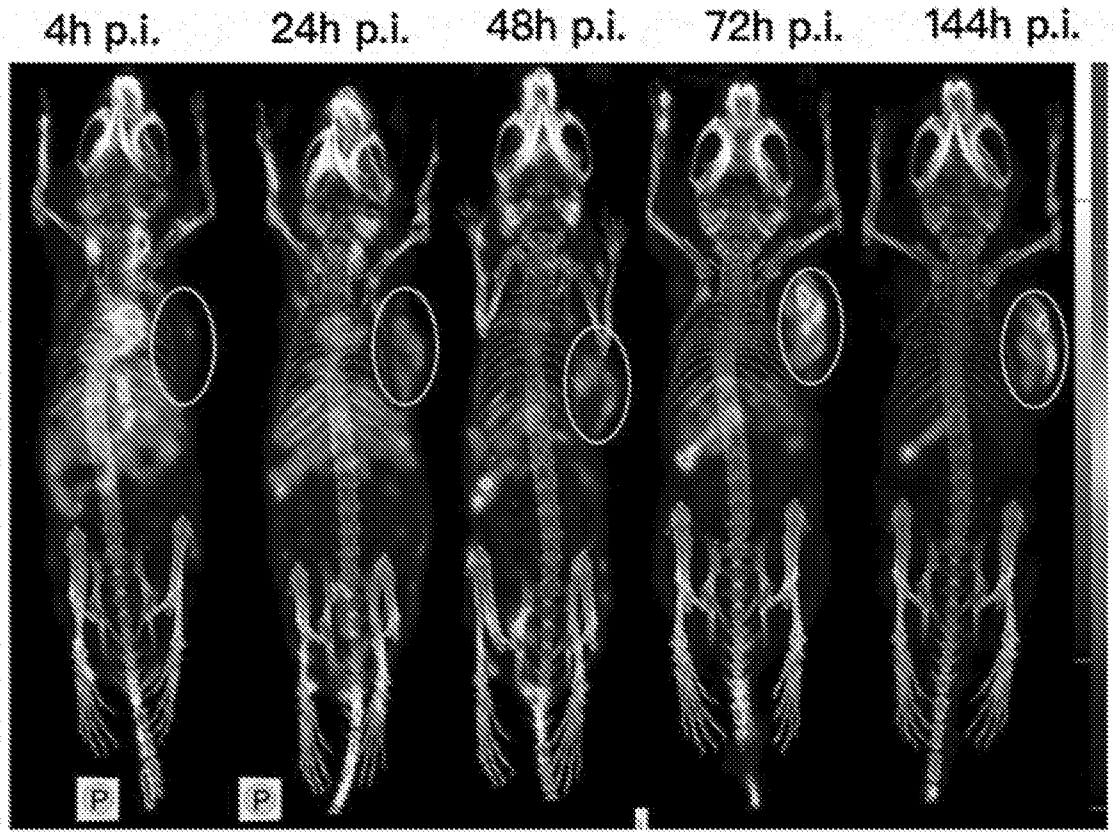

Figure 24A

B

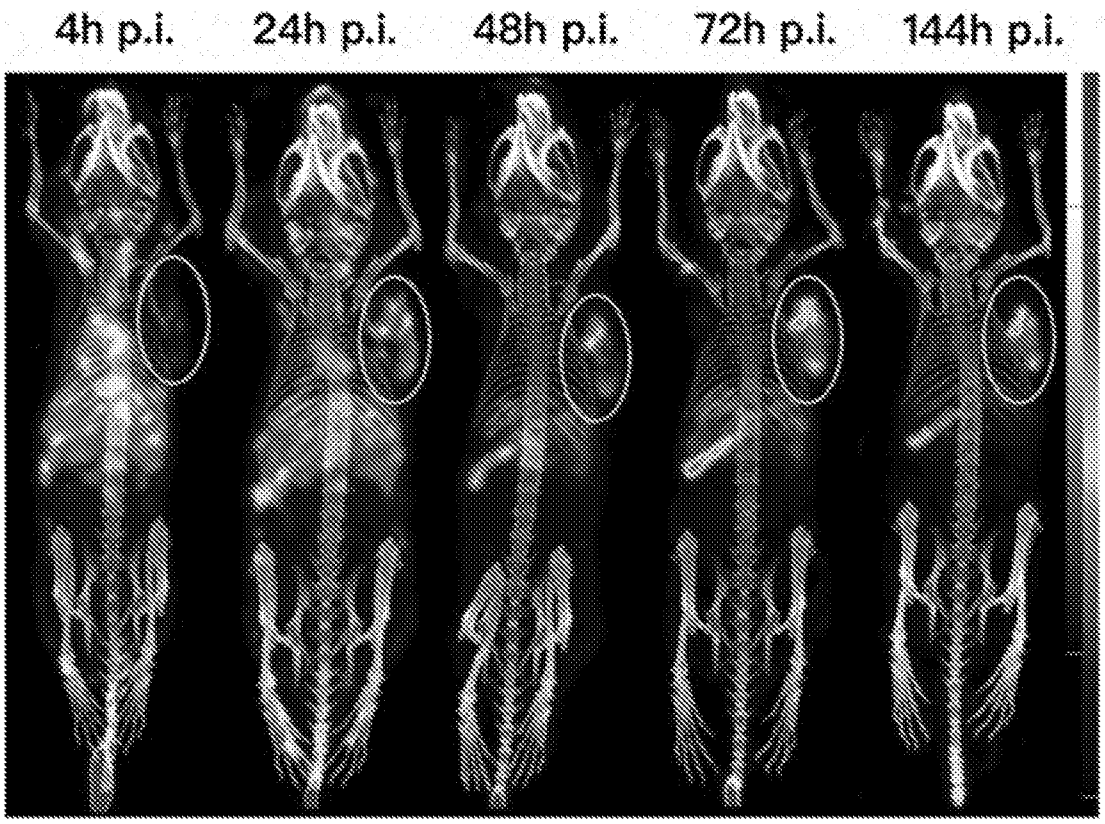

Figure 24B

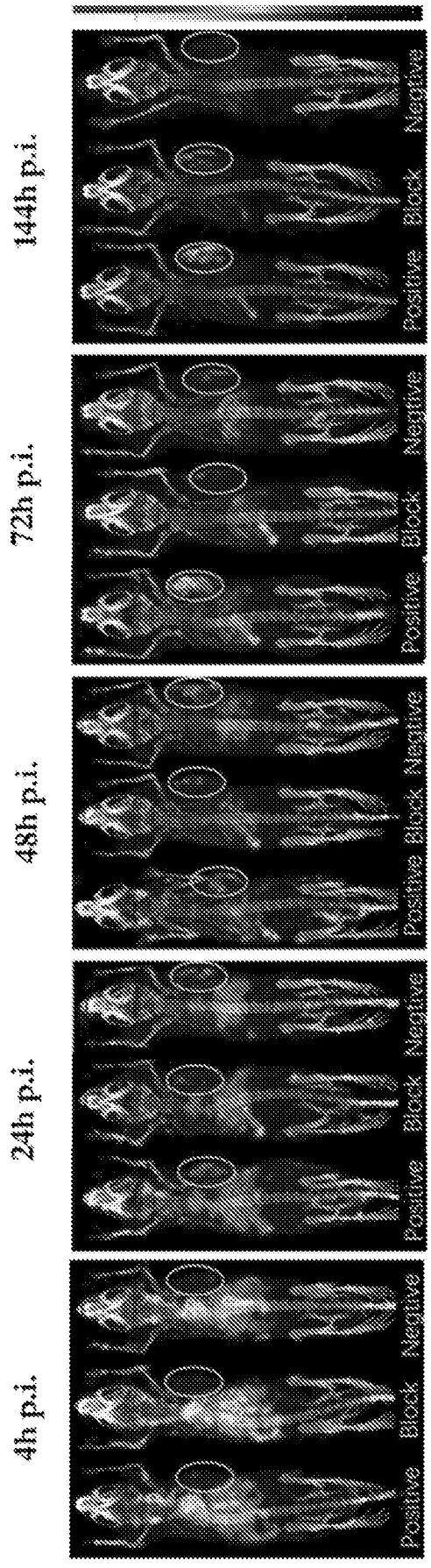

Figure 25

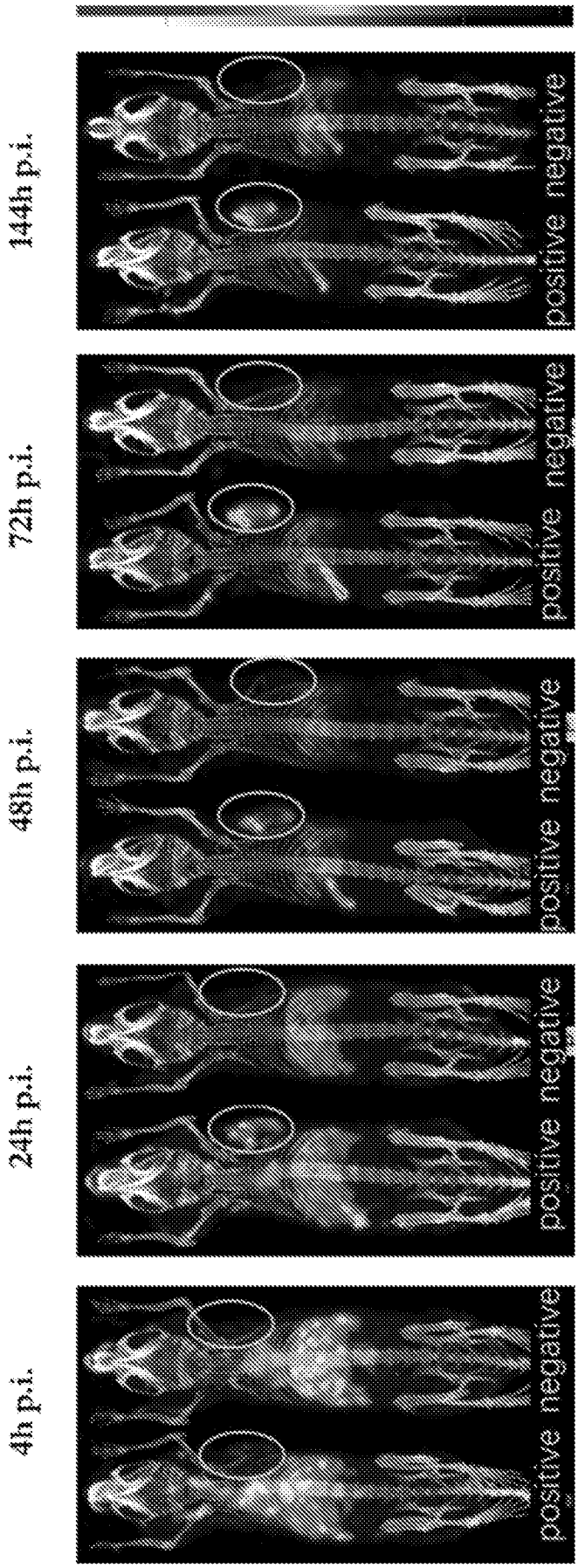
4h p.i.
24h p.i.
48h p.i.
72h p.i.
144h p.i.
positive negative
positive negative
positive negative
positive negative

Figure 26

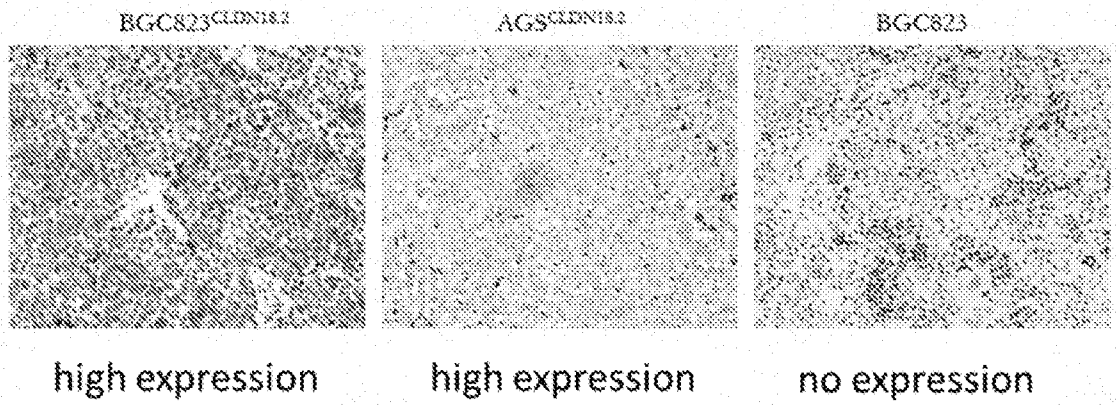

Figure 27

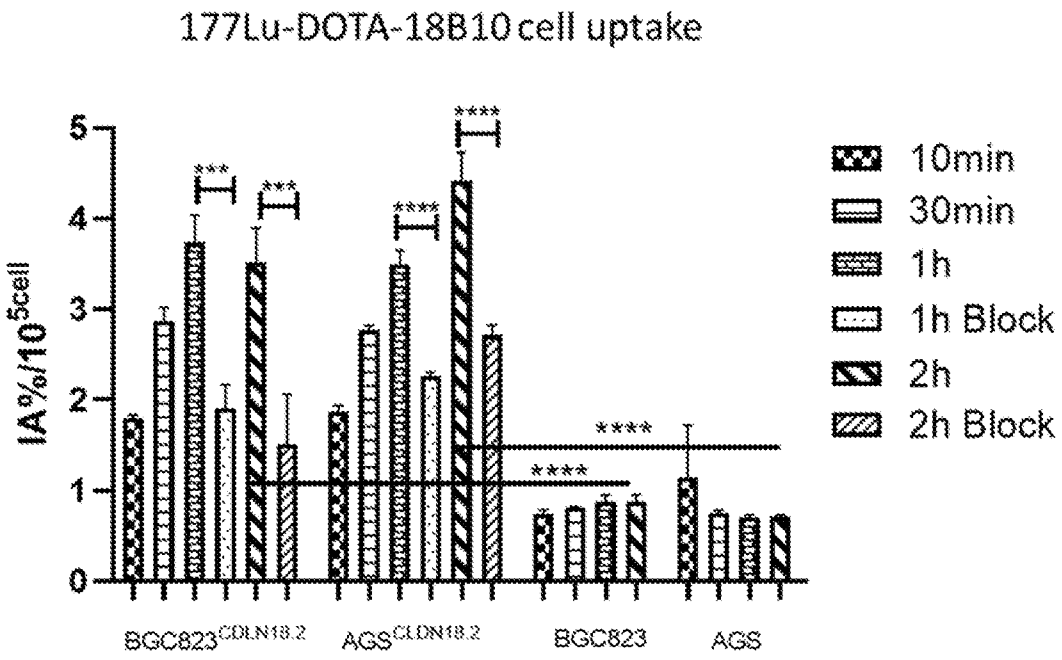

Figure 28

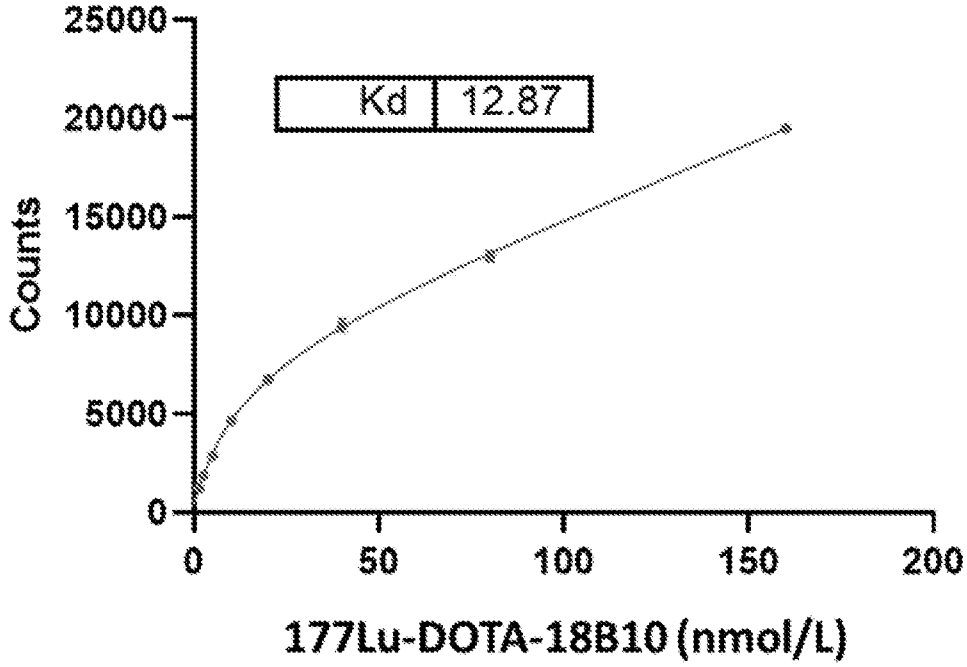

Figure 29A

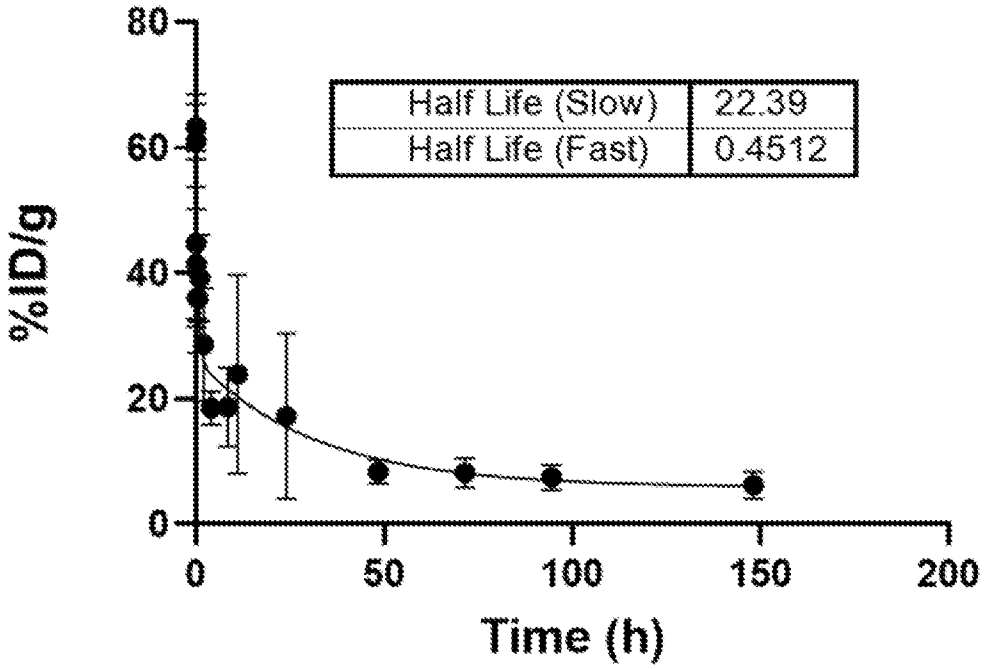

Figure 29B

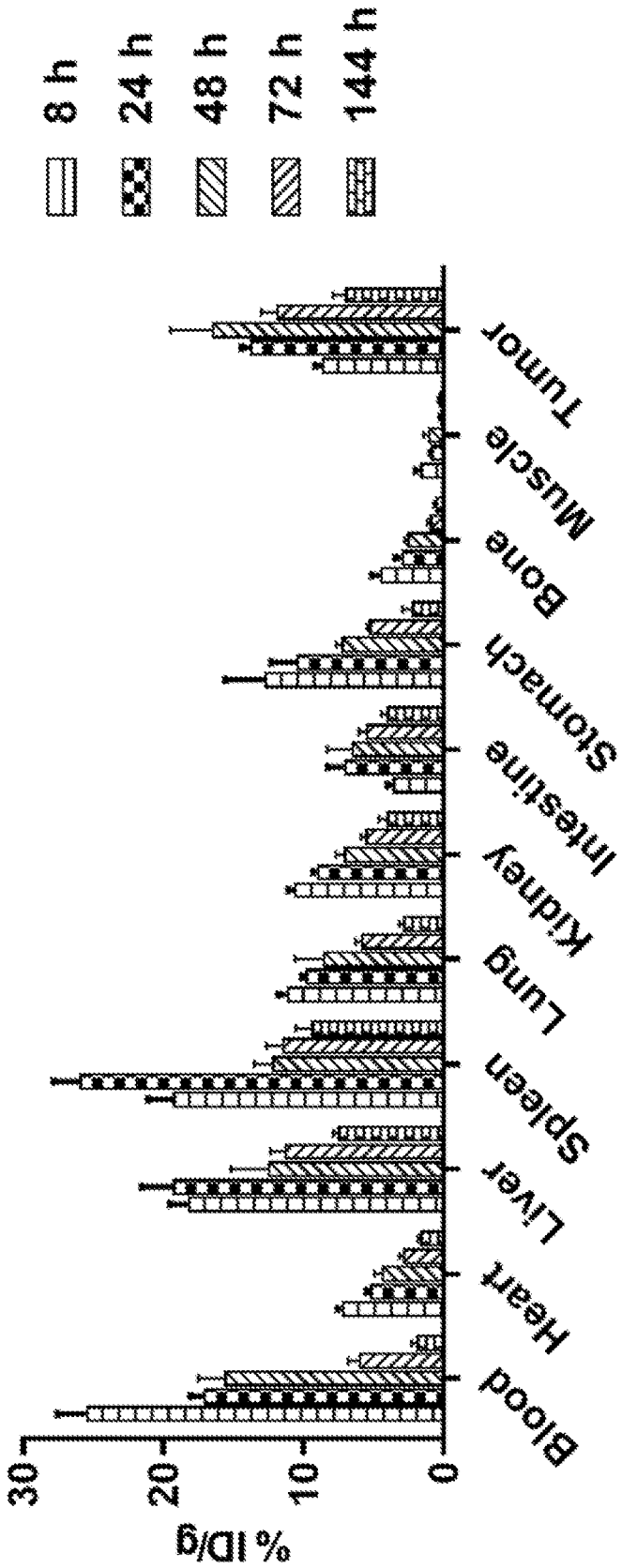
8 h
24 h
48 h
72 h
144 h
% ID/g
0
10
20
30
Blood
Heart
Liver
Spleen
Lung
Kidney
Intestine
Stomach
Bone
Muscle
Tumor

Figure 30

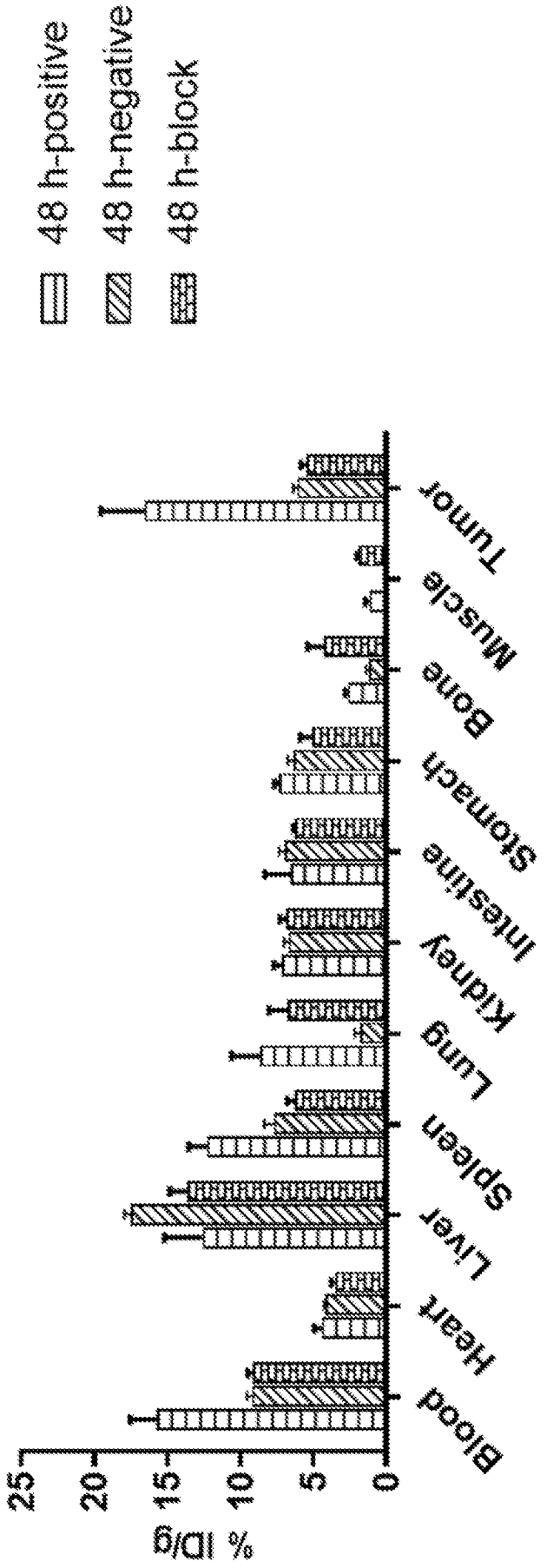
48 h-positive
48 h-negative
48 h-block
% ID/g
25
20
15
10
5
0
Blood
Heart
Liver
Spleen
Lung
Kidney
Intestine
Stomach
Bone
Muscle
Tumor

Figure 31

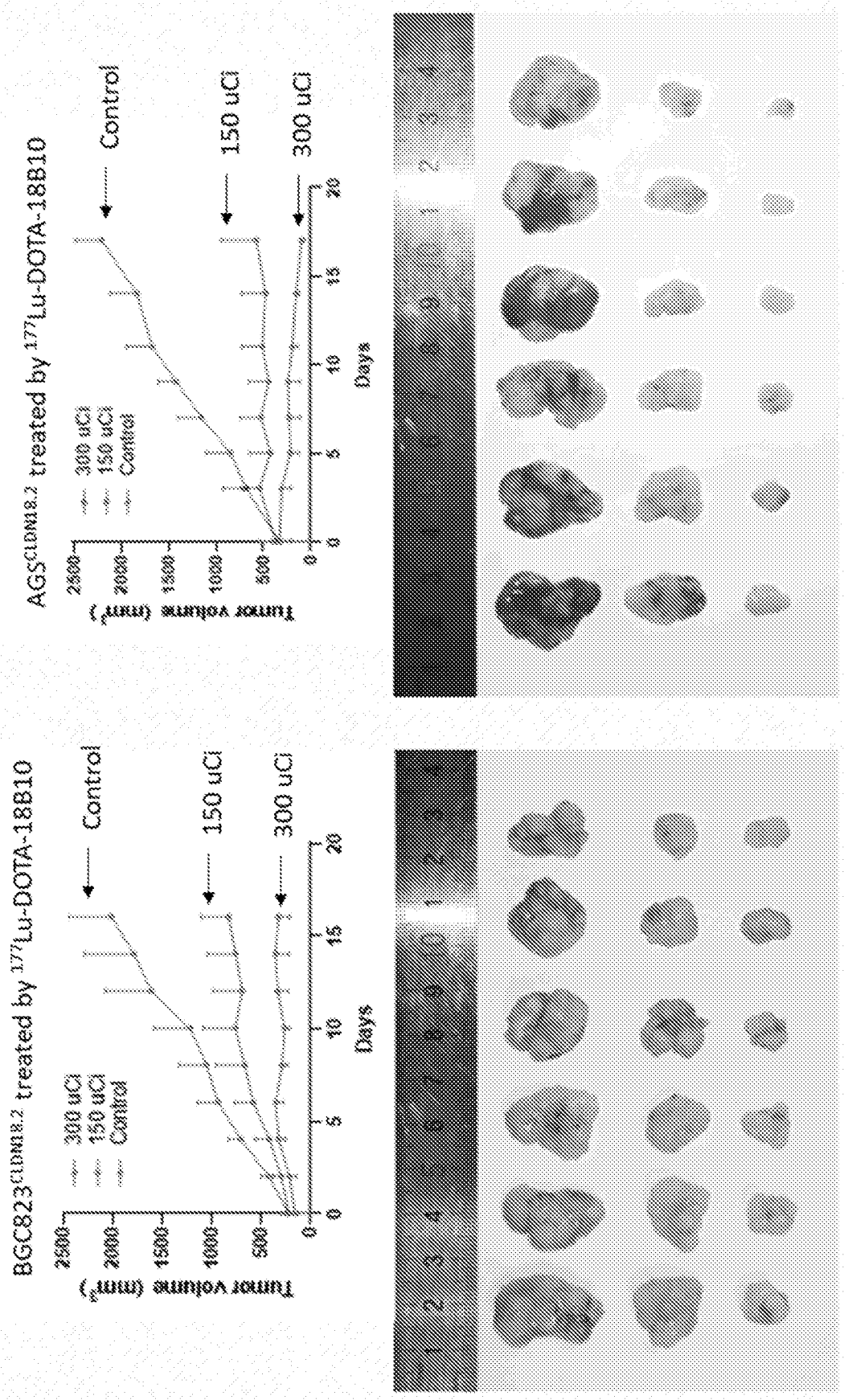
BGC823CLDN18.2 treated by 177Lu-DOTA-18B10
300 uCi
150 uCi
Control
Tumor volume (mm3)
2500
2000
1500
1000
500
0
0
5
10
15
20
Days
Control
150 uCi
300 uCi
AGSCLDN18.2 treated by 177Lu-DOTA-18B10
300 uCi
150 uCi
Control
Tumor volume (mm3)
2500
2000
1500
1000
500
0
0
5
10
15
20
Days
Control
150 uCi
300 uCi

Figure 32

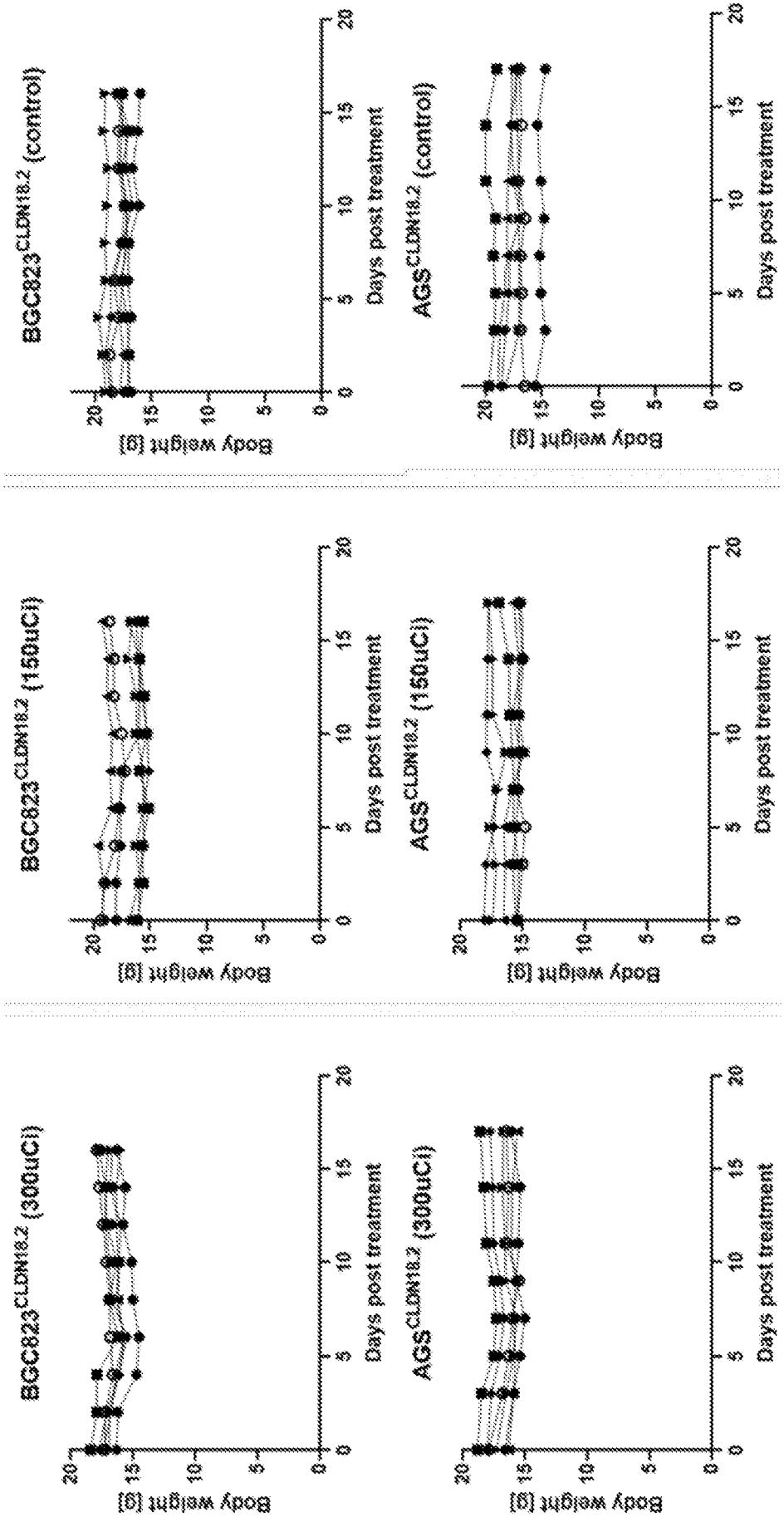
BGC823CLDN18.2 (control)
AGSCLDN18.2 (control)
BGC823CLDN18.2 (150uCi)
AGSCLDN18.2 (150uCi)
BGC823CLDN18.2 (300uCi)
AGSCLDN18.2 (300uCi)
Body weight [g]
Days post treatment
0
5
10
15
20

Figure 33

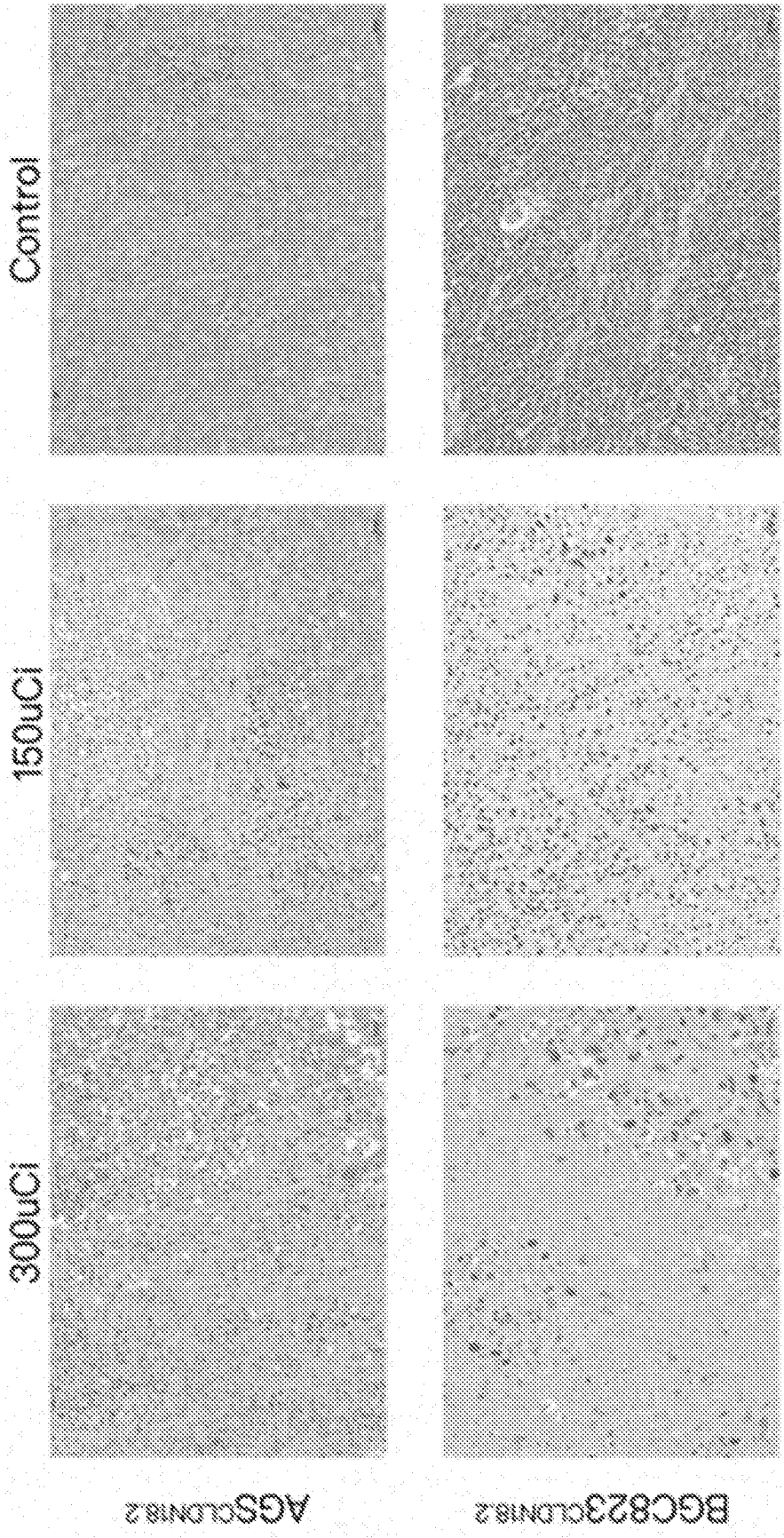

Figure 34

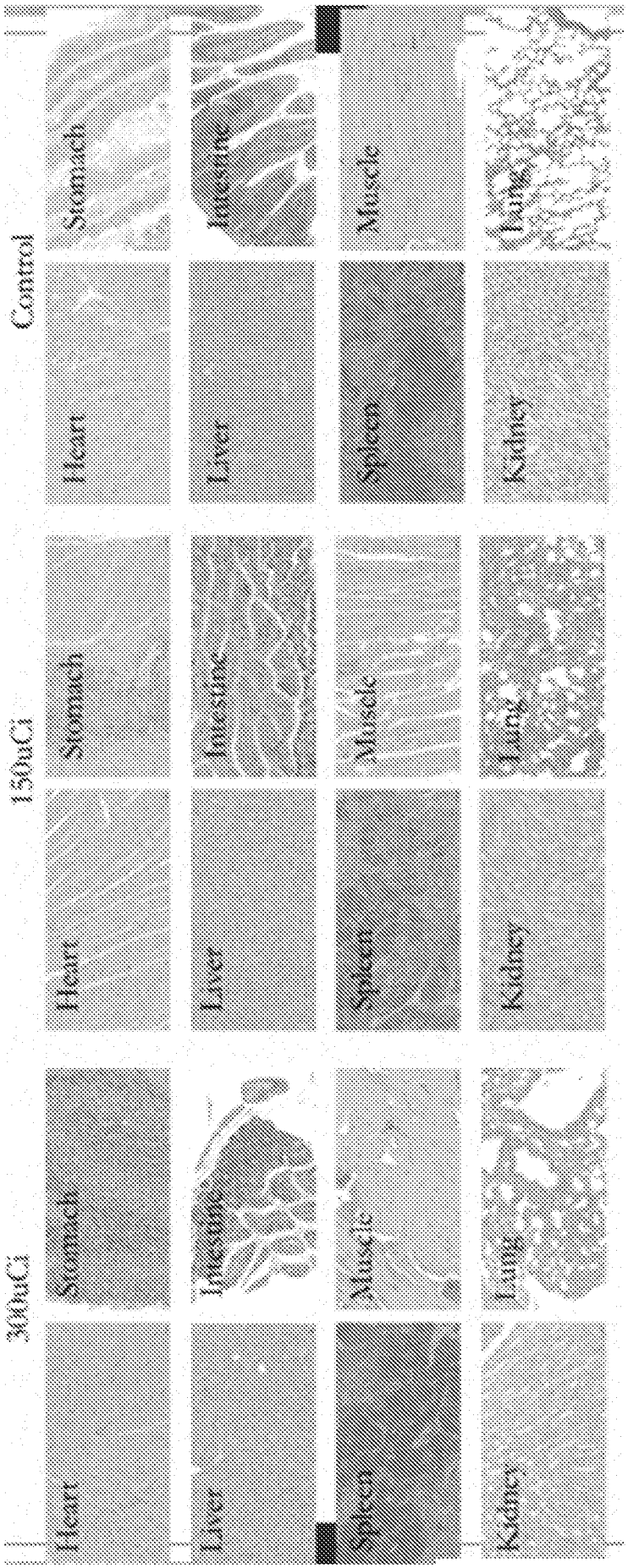
30MuCi
Heart
Stomach
Liver
Intestine
Spleen
Muscle
Kidney
Lung
150uCi
Heart
Stomach
Liver
Intestine
Spleen
Muscle
Kidney
Lung
Control
Heart
Stomach
Liver
Intestine
Spleen
Muscle
Kidney
Lung

Figure 35

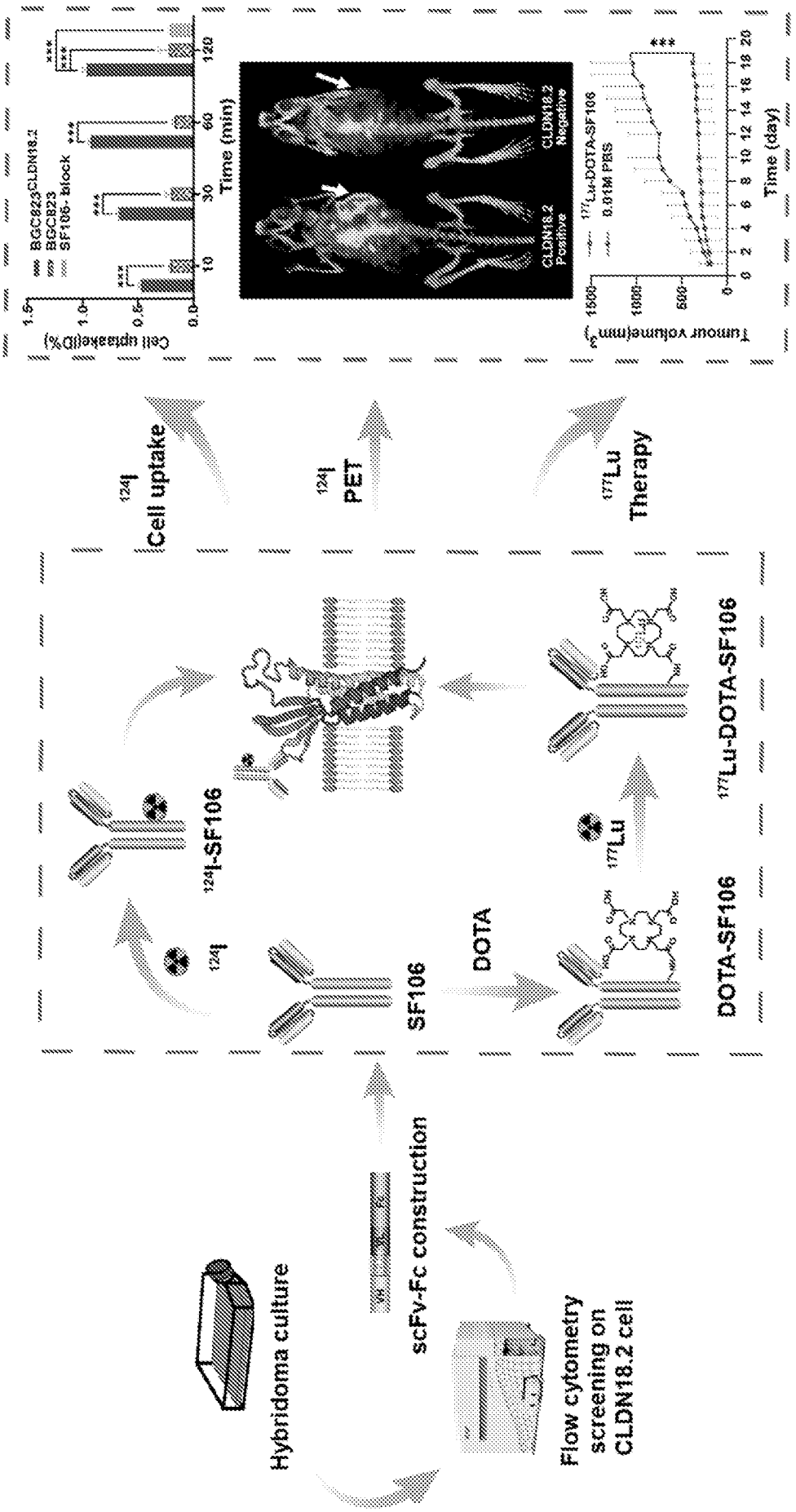
Hybridoma culture
scFv-Fc construction
Flow cytometry screening on CLDN18.2 cell
SF106
DOTA
DOTA-SF106
^{124}I
^{124}I-SF106
^{177}Lu
^{177}Lu-DOTA-SF106
^{124}I Cell uptake
^{124}I PET
^{177}Lu Therapy
Cell uptake(%)
BGC823-CLDN18.2
BGC823
SF106- block
Time (min)
CLDN18.2 Positive
CLDN18.2 Negative
Tumour volume(mm^3)
^{177}Lu-DOTA-SF106
0.01M PBS
Time (day)

Figure 36

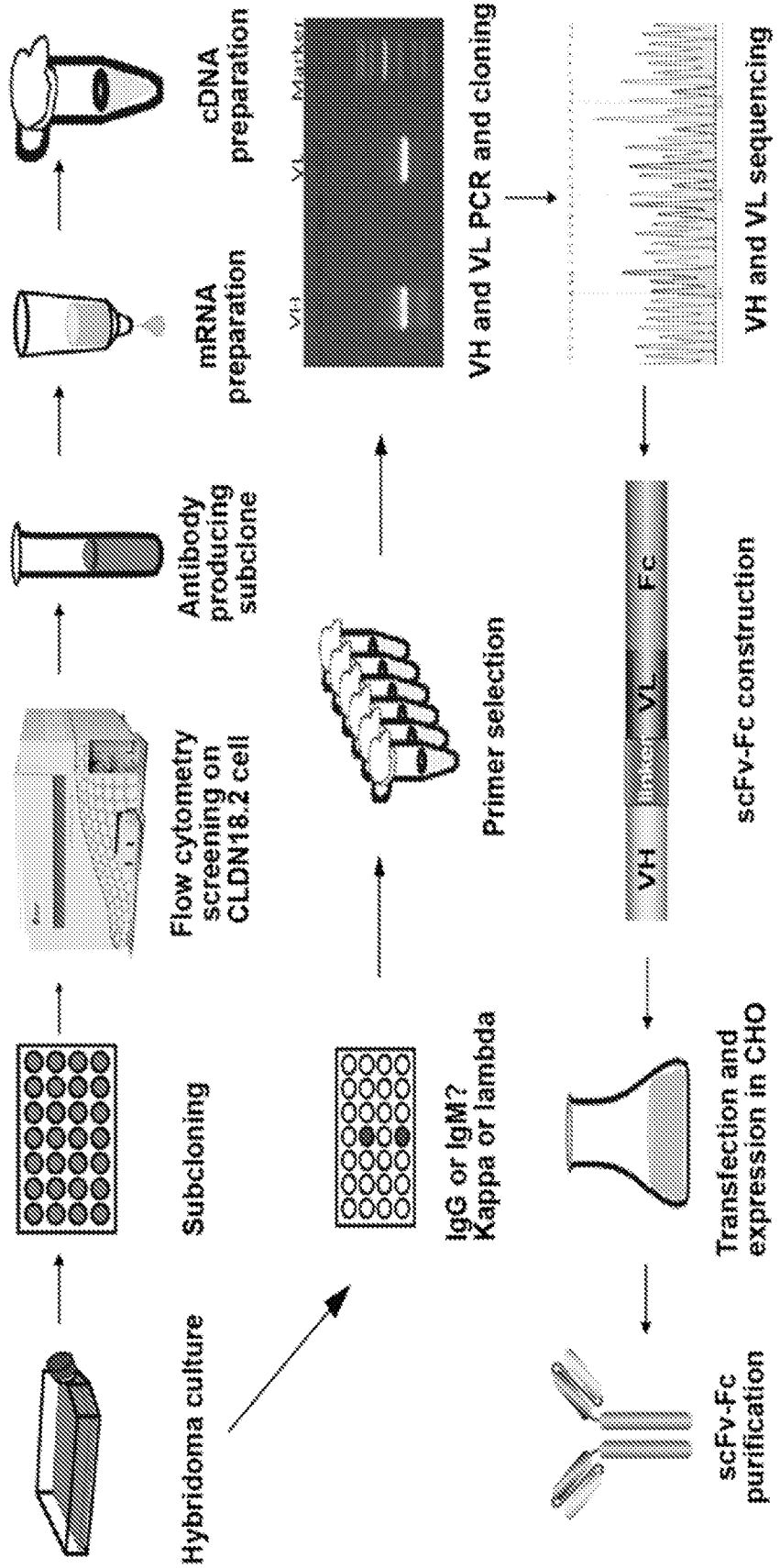
Hybridoma culture
Subcloning
Flow cytometry screening on CLDN18.2 cell
Antibody producing subclone
mRNA preparation
cDNA preparation
IgG or IgM? Kappa or lambda
Primer selection
VH and VL PCR and cloning
VH
VL
Marker
VH and VL sequencing
scFv-Fc construction
VH
linker
VL
Fc
Transfection and expression in CHO
scFv-Fc purification

Figure 37A

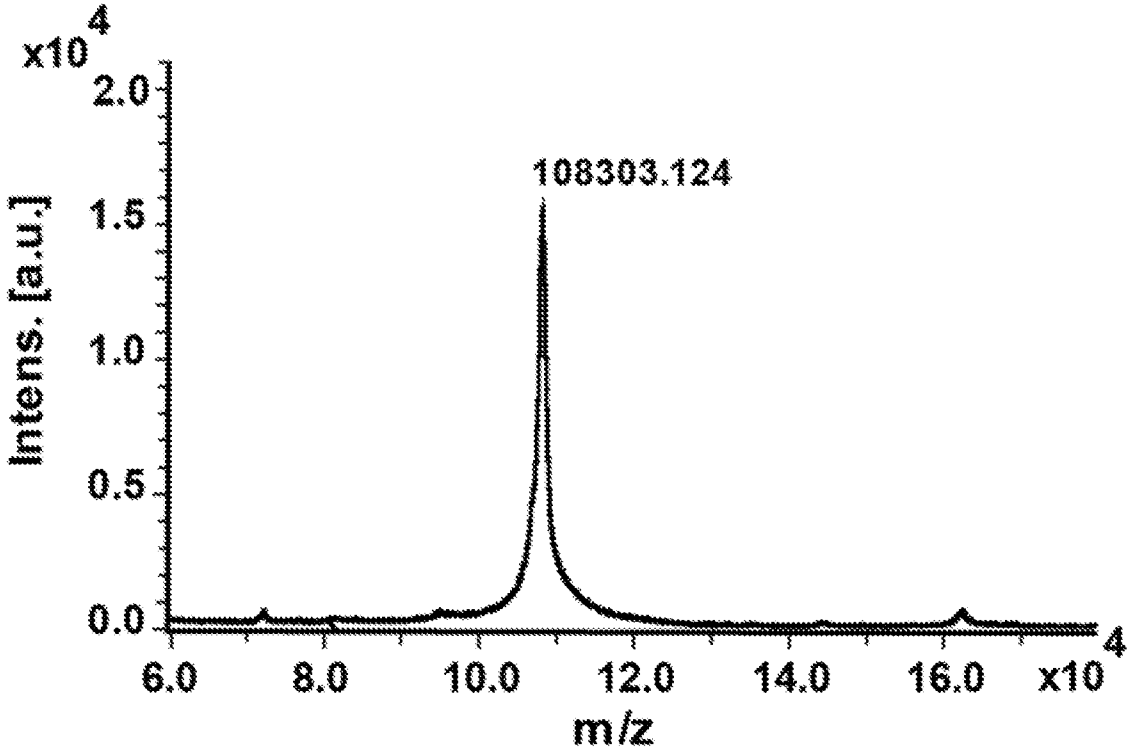
x10^4
2.0
1.5
1.0
0.5
0.0
Intens. [a.u.]
108303.124
6.0
8.0
10.0
12.0
14.0
16.0
x10^4
m/z

Figure 37B

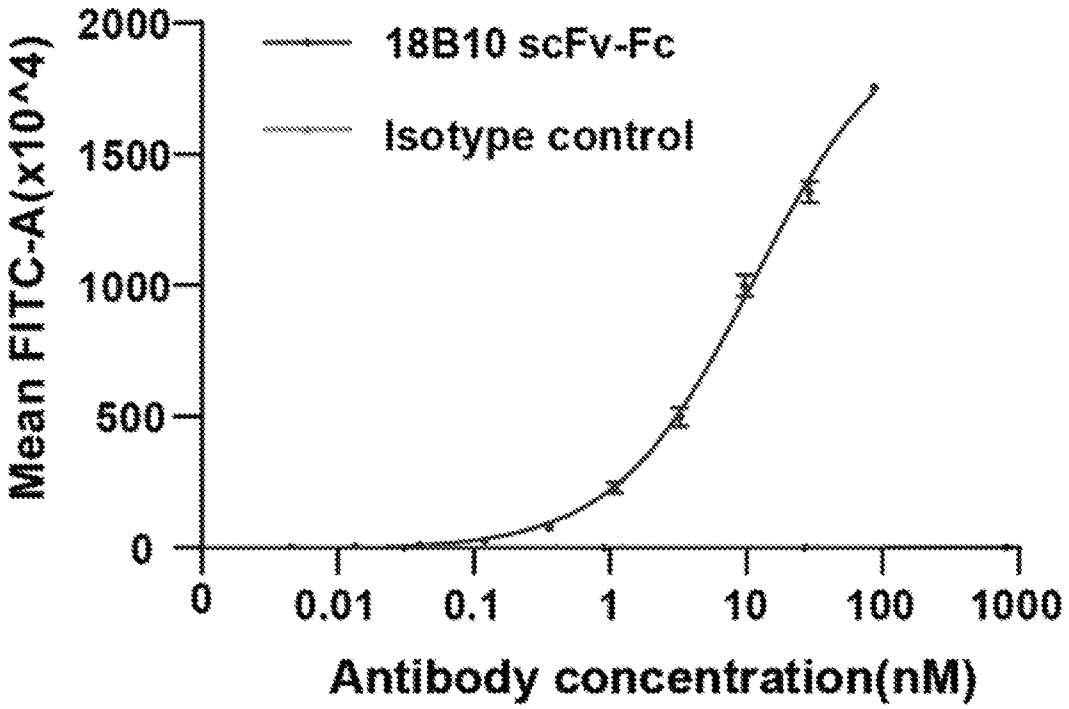
18B10 scFv-Fc
Isotype control
Mean FITC-A(x10^4)
2000
1500
1000
500
0
0
0.01
0.1
1
10
100
1000
Antibody concentration(nM)

Figure 37C

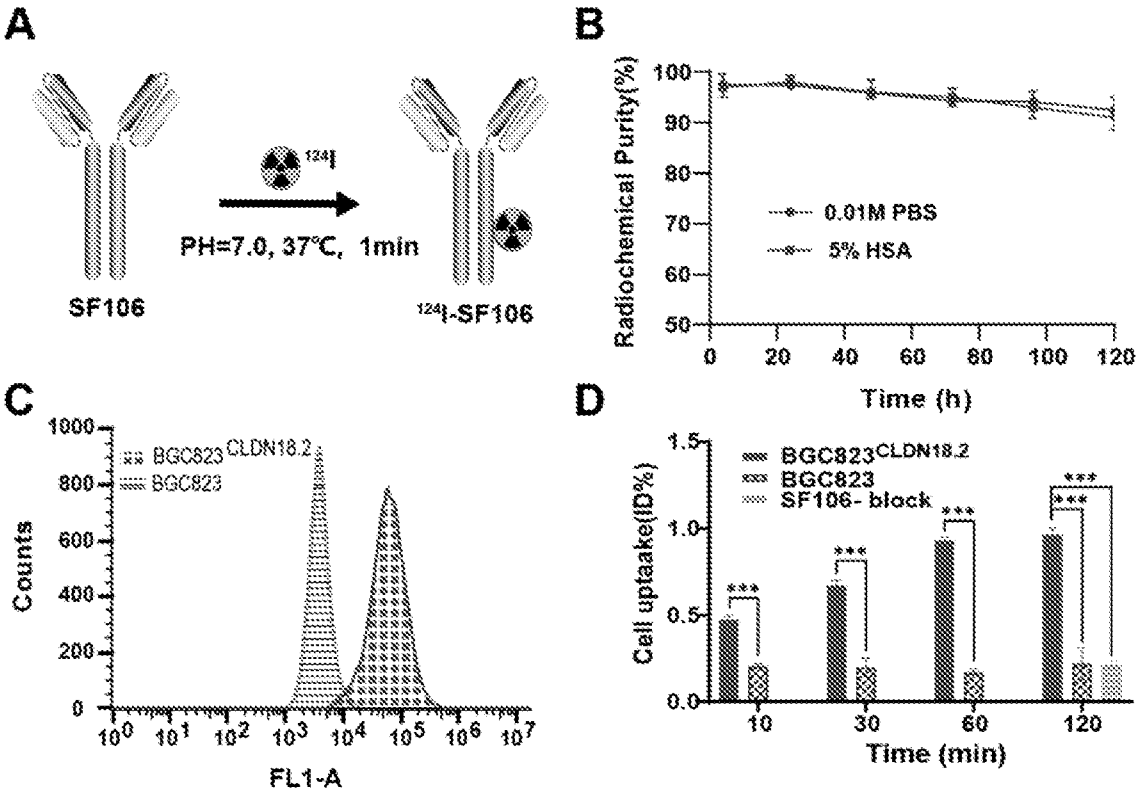
A
SF106
124I
PH=7.0, 37℃, 1min
124I-SF106
B
Radiochemical Purity(%)
0.01M PBS
5% HSA
Time (h)
C
Counts
BGC823CLDN18.2
BGC823
FL1-A
D
Cell uptaake(ID%)
BGC823CLDN18.2
BGC823
SF106- black
Time (min)

Figure 38

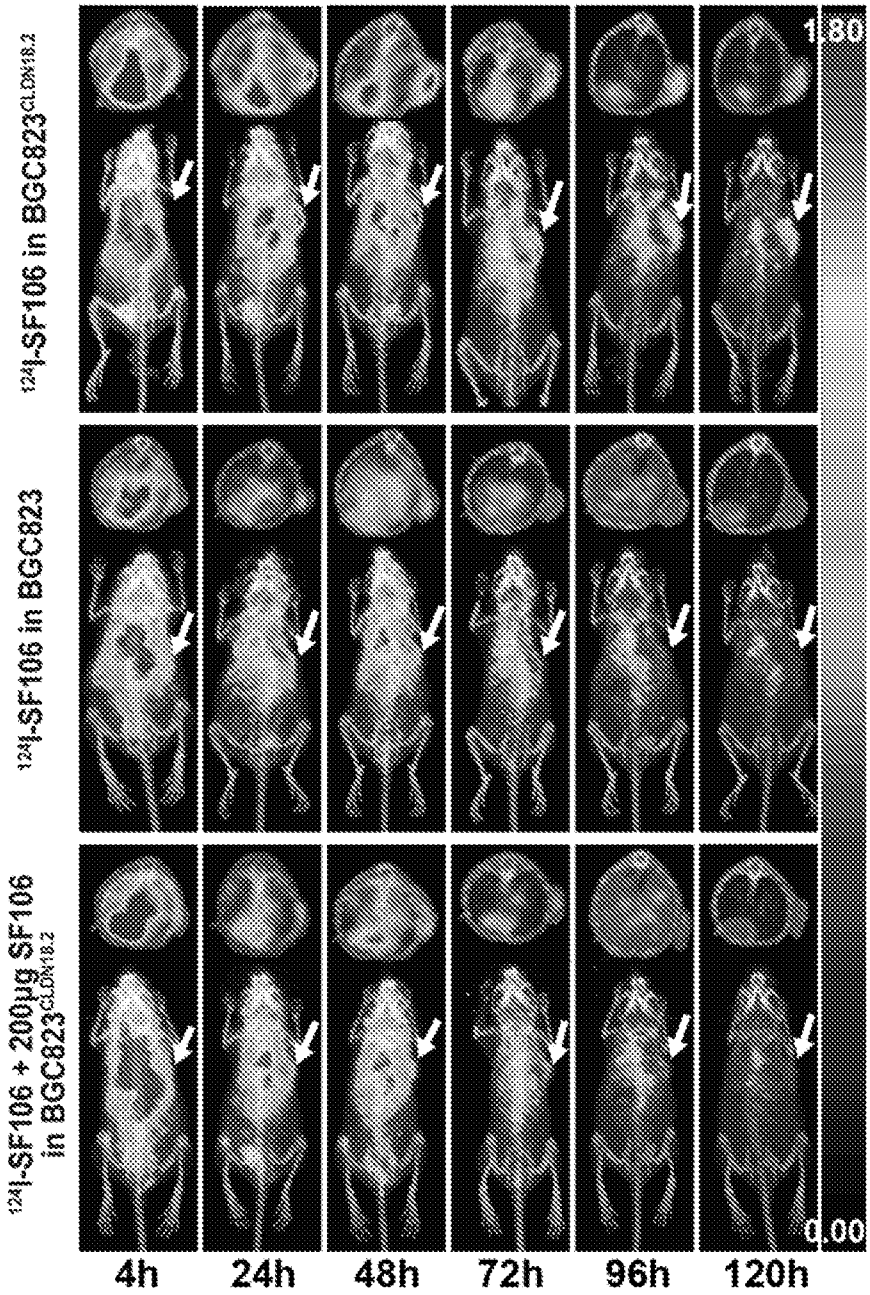
^{124}I-SF106 in BGC823$^{CLDN18.2}$
^{124}I-SF106 in BGC823
^{124}I-SF106 + 200μg SF106 in BGC823$^{CLDN18.2}$
1.80
0.00
4h
24h
48h
72h
96h
120h

Figure 39

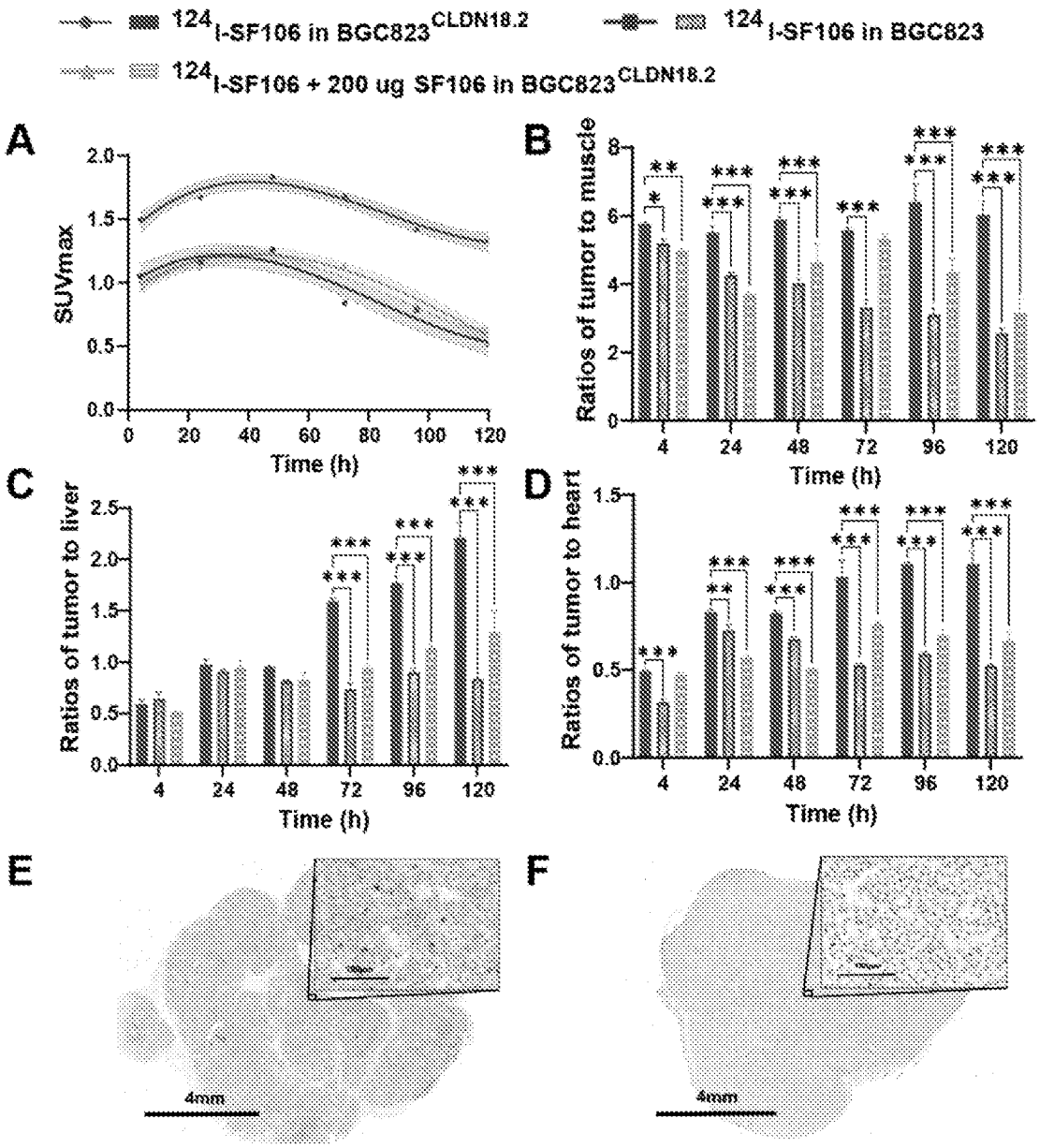
124I-SF106 in BGC823CLDN18.2
124I-SF106 in BGC823
124I-SF106 + 200 ug SF106 in BGC823CLDN18.2
A
SUVmax
Time (h)
B
Ratios of tumor to muscle
Time (h)
C
Ratios of tumor to liver
Time (h)
D
Ratios of tumor to heart
Time (h)
E
4mm
F
4mm

Figure 40

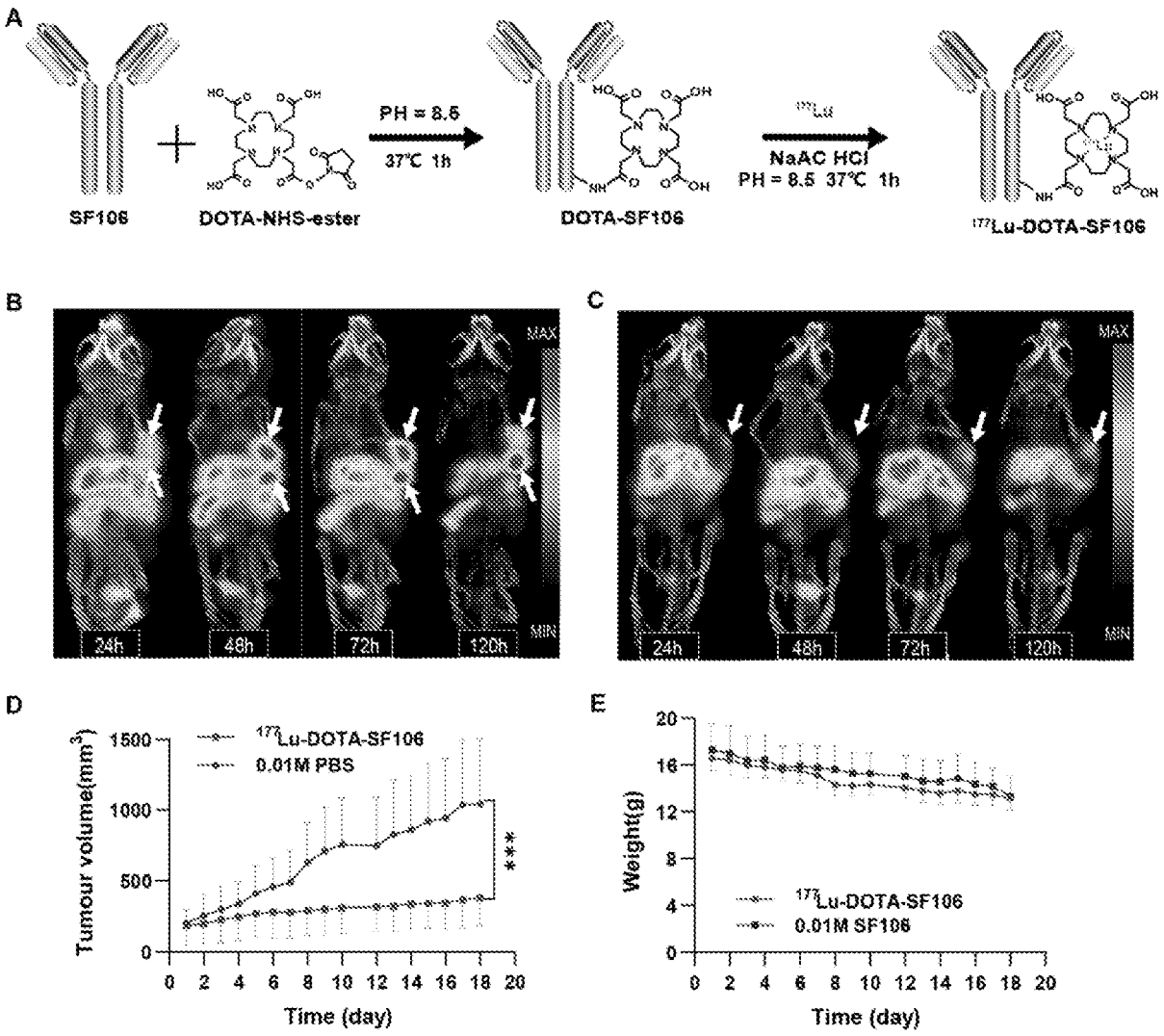
A
SF106
DOTA-NHS-ester
PH = 8.5
37℃ 1h
DOTA-SF106
NaAC HCl
PH = 8.5 37℃ 1h
177Lu-DOTA-SF106
B
C
MAX
MIN
24h
48h
72h
120h
D
Tumour volume(mm3)
177Lu-DOTA-SF106
0.01M PBS
***
Time (day)
E
Weight(g)
177Lu-DOTA-SF106
0.01M SF106
Time (day)

Figure 41

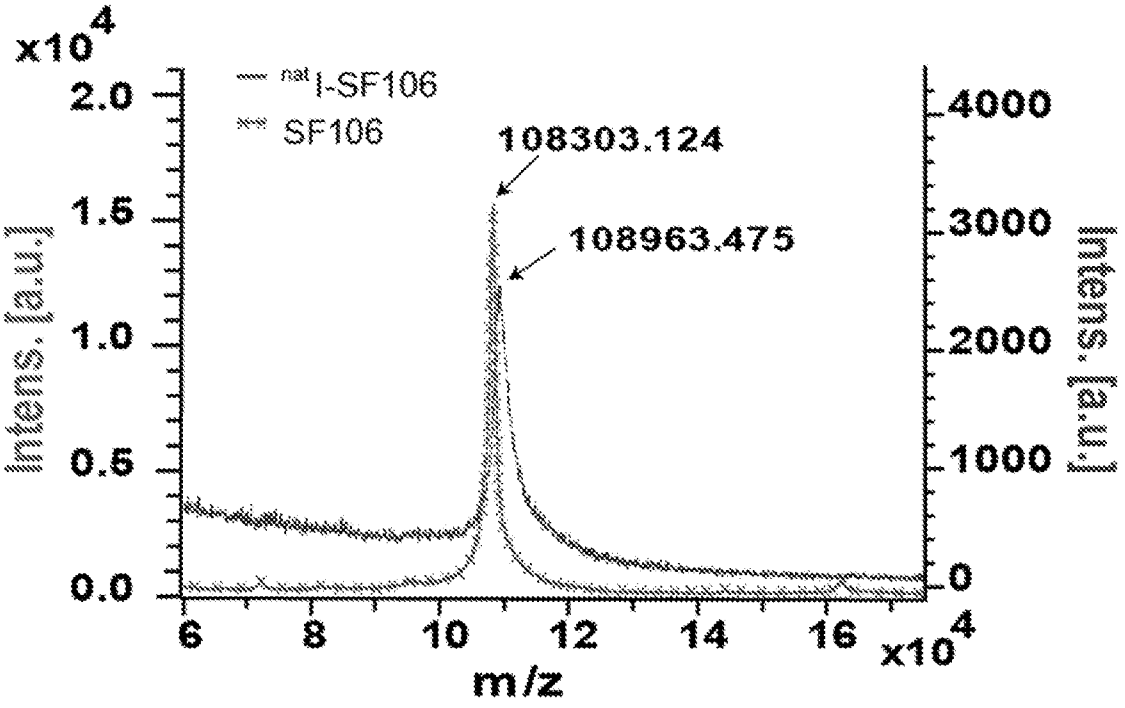

Figure 42A

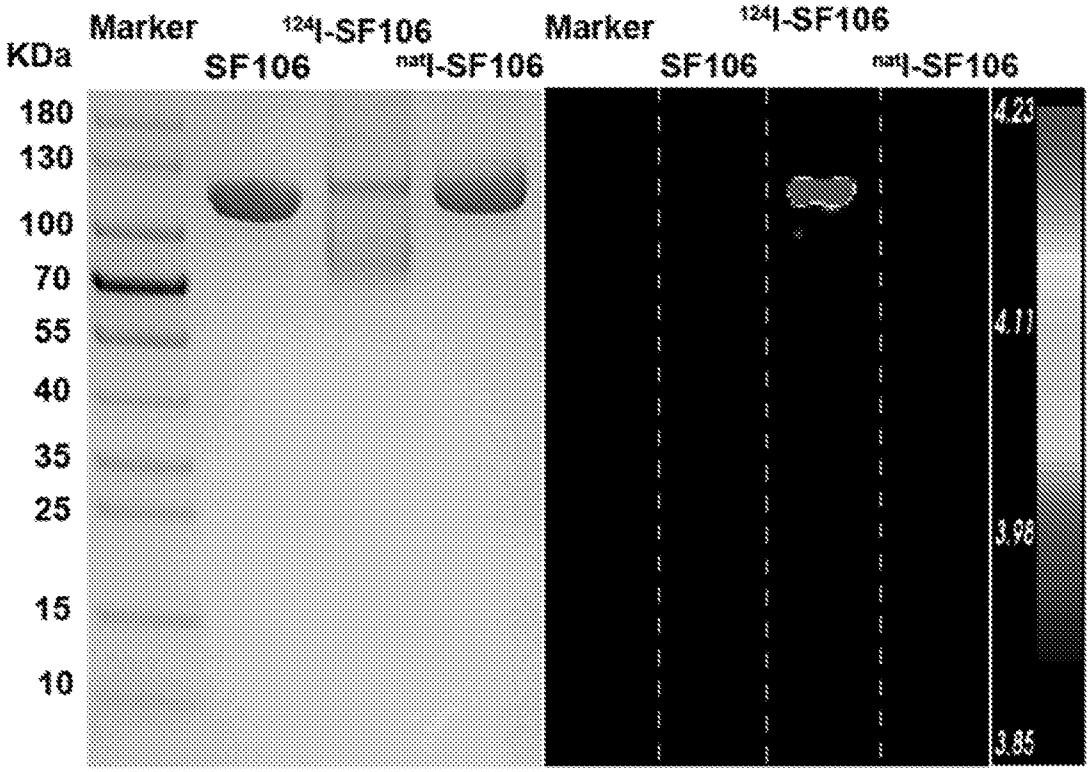

Figure 42B

C

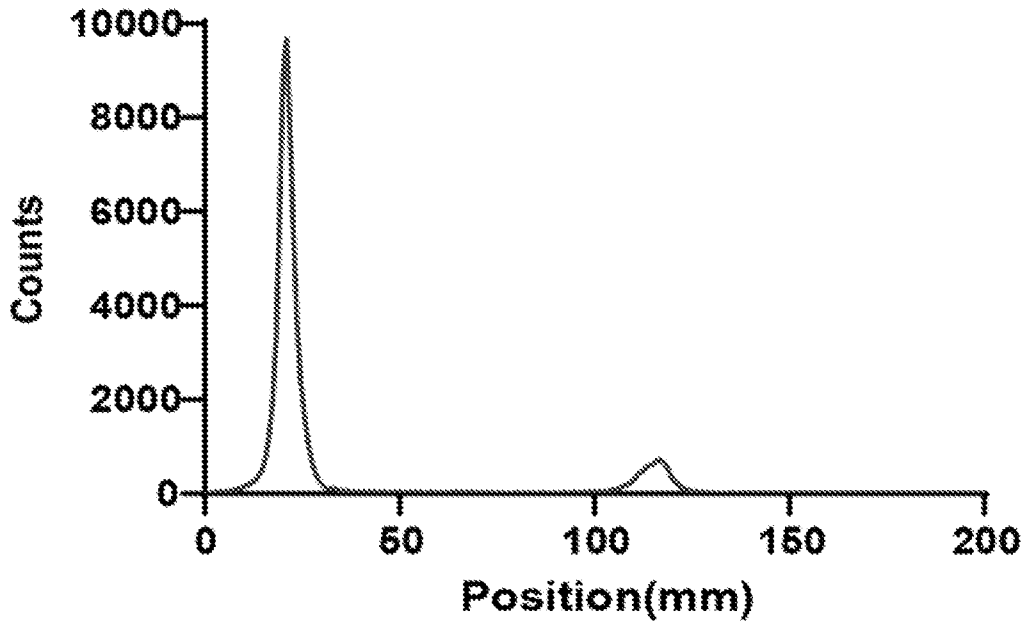

Figure 42C

D

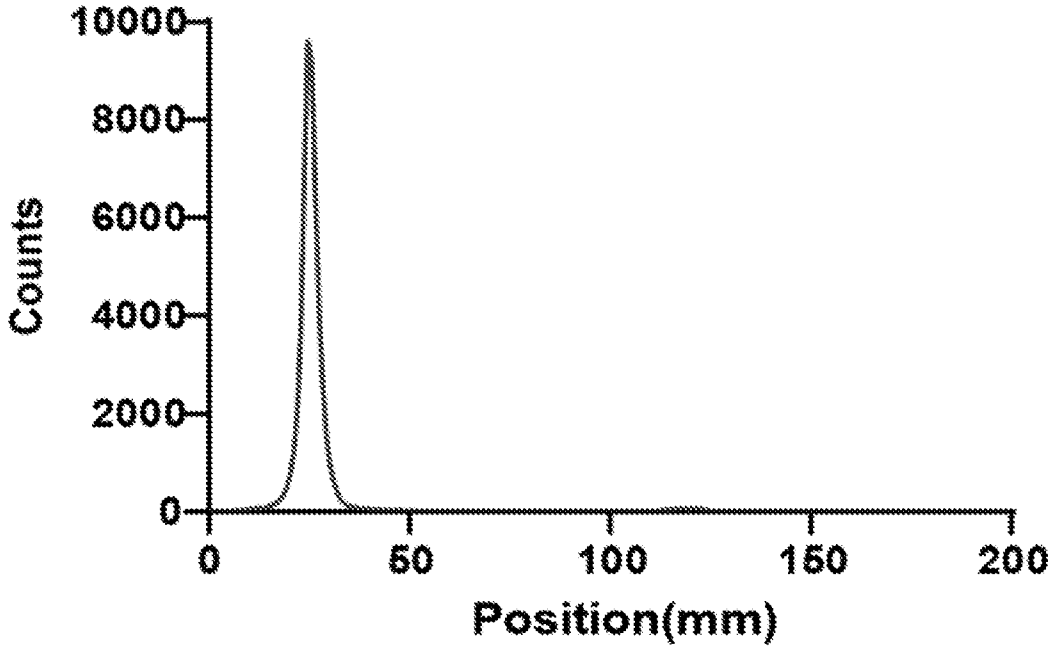

Figure 42D

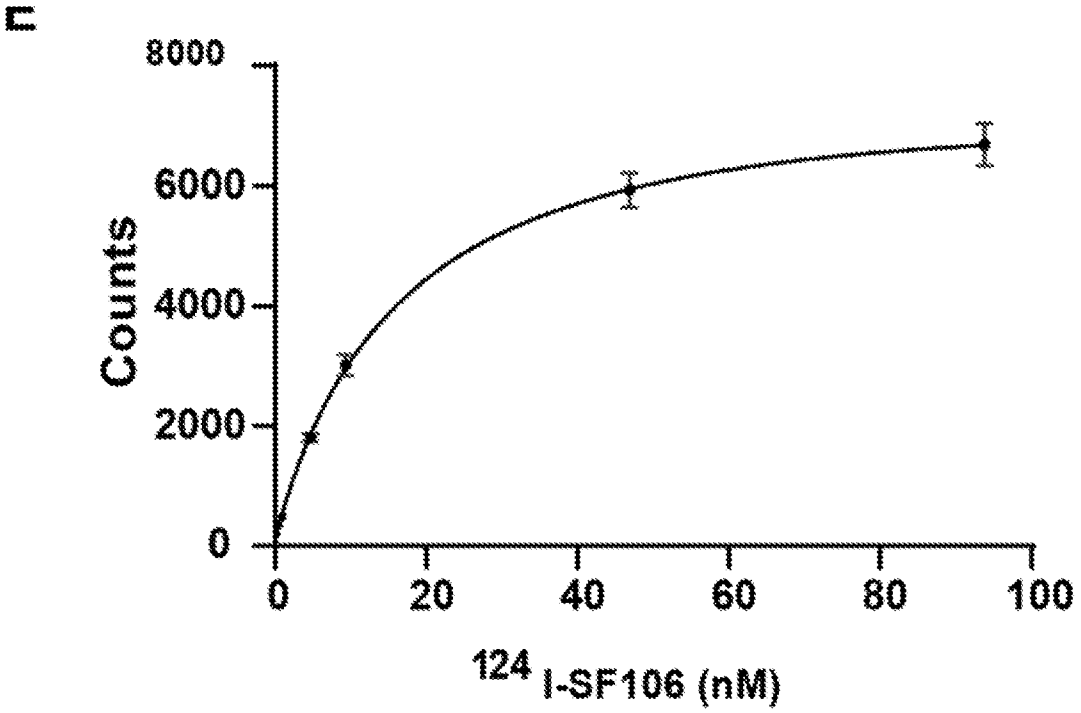

Figure 42E

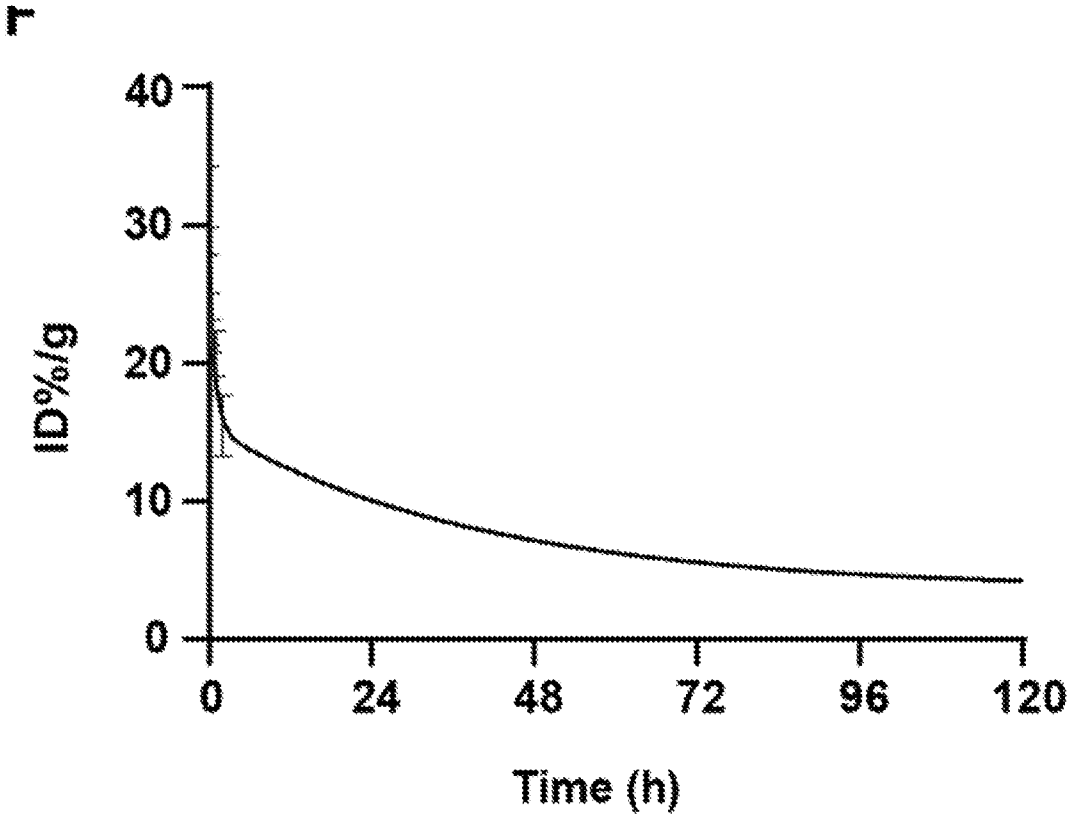

Figure 42F

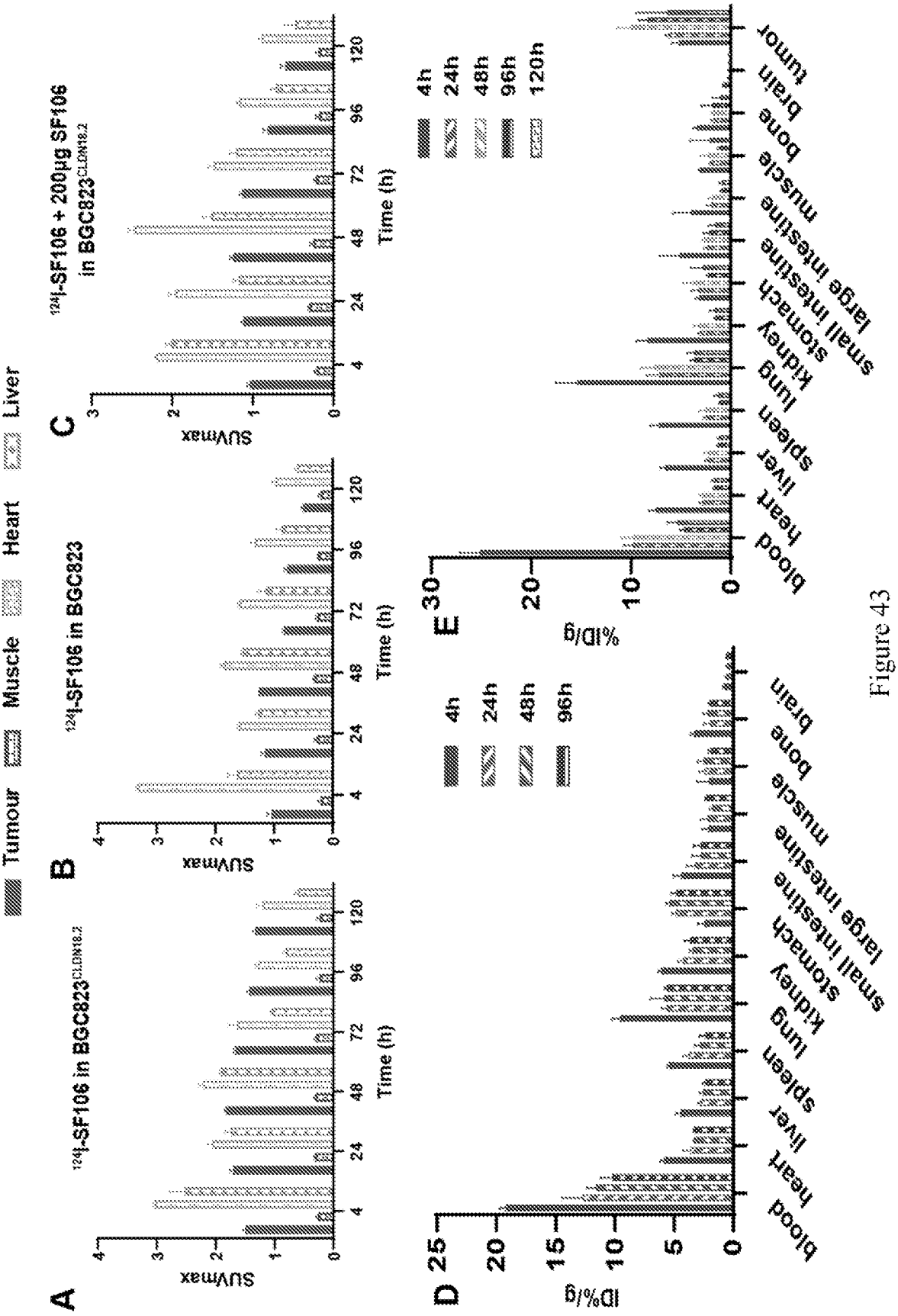
Tumour
Muscle
Heart
Liver
A
124I-SF106 in BGC823CLDN18.2
B
124I-SF106 in BGC823
C
124I-SF106 + 200μg SF106 in BGC823CLDN18.2
SUVmax
Time (h)
D
E
4h
24h
48h
96h
120h
%ID/g
blood
heart
liver
spleen
lung
kidney
stomach
small intestine
large intestine
muscle
bone
brain
tumor

Figure 43

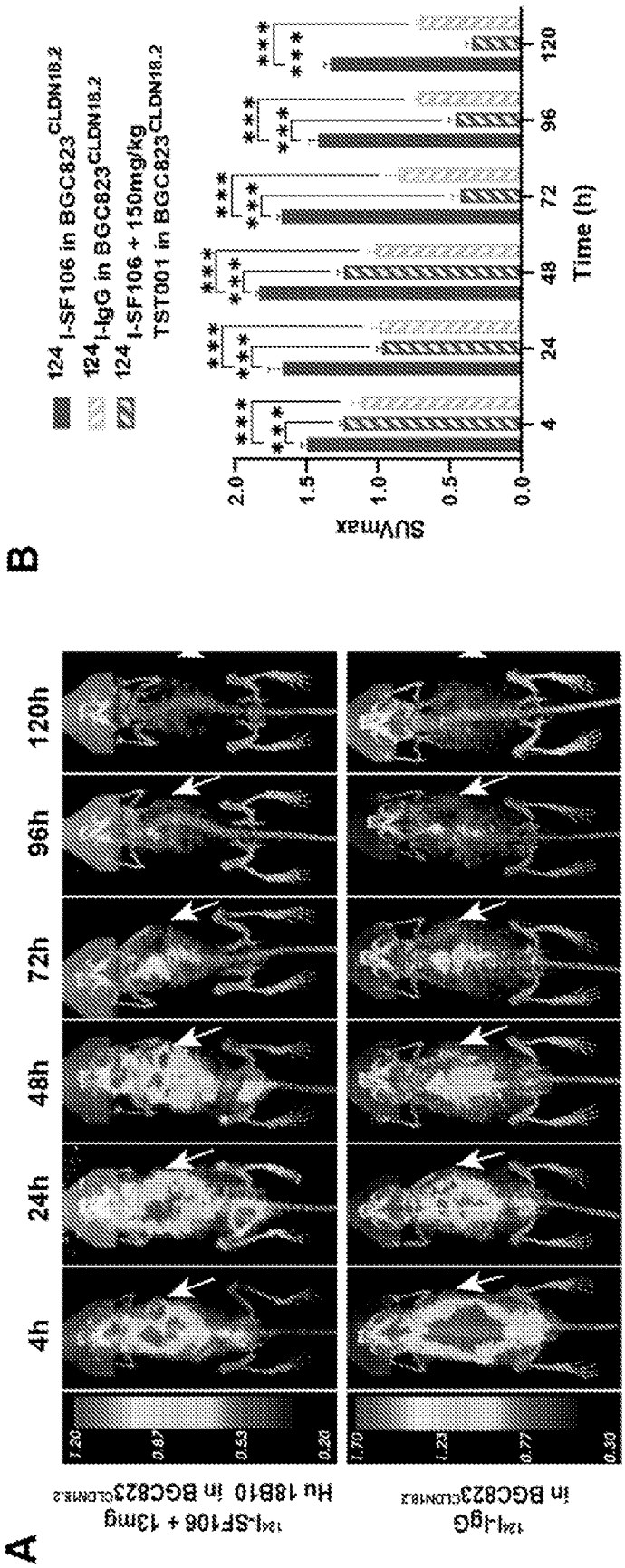
A
4h
24h
48h
72h
96h
120h
124I-SF106 + 13mg
Hu 18B10 in BGC823CLDN18.2
124I-IgG
in BGC823CLDN18.2
B
124I-SF106 in BGC823CLDN18.2
124I-IgG in BGC823CLDN18.2
124I-SF106 + 150mg/kg
TST001 in BGC823CLDN18.2
SUVmax
Time (h)

Figure 44

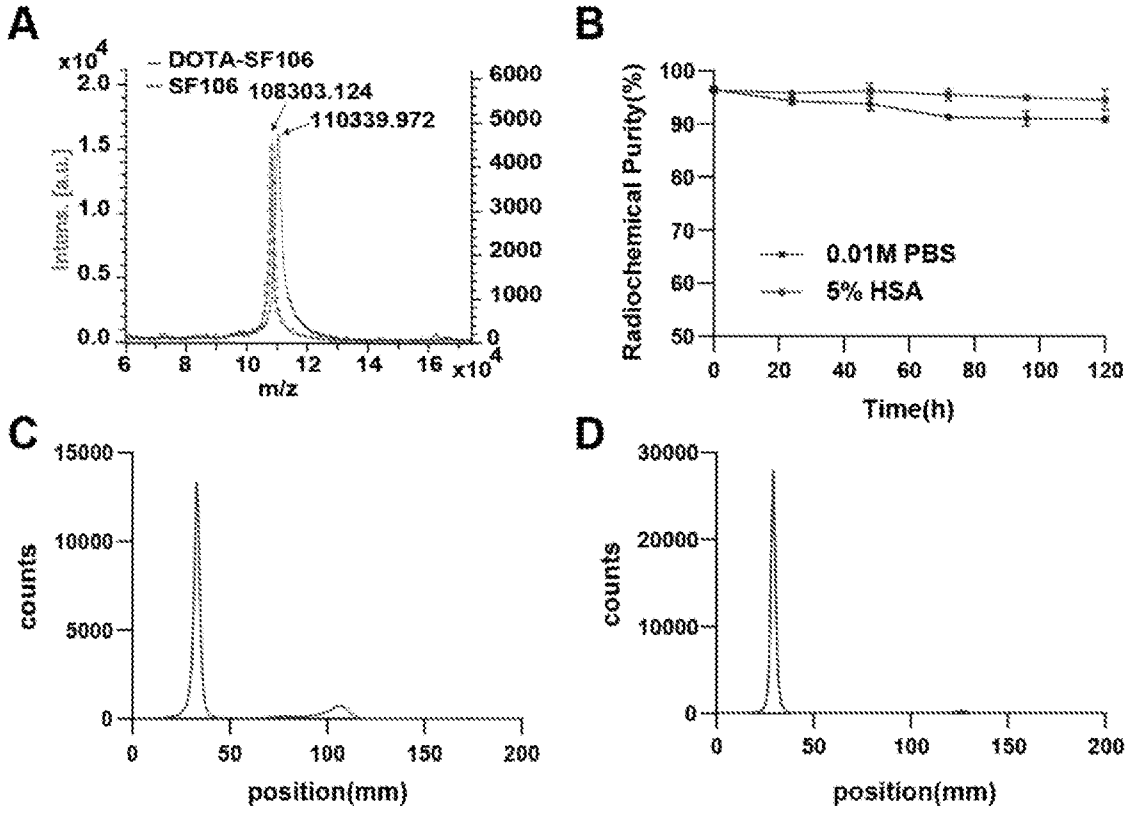
A
x10^4
2.0
1.5
1.0
0.5
0.0
Intens. [a.u.]
DOTA-SF106
SF106
108303.124
110339.972
6000
5000
4000
3000
2000
1000
0
6
8
10
12
14
16
x10^4
m/z
B
Radiochemical Purity(%)
100
90
80
70
60
50
0.01M PBS
5% HSA
0
20
40
60
80
100
120
Time(h)
C
counts
15000
10000
5000
0
0
50
100
150
200
position(mm)
D
counts
30000
20000
10000
0
0
50
100
150
200
position(mm)

Figure 45

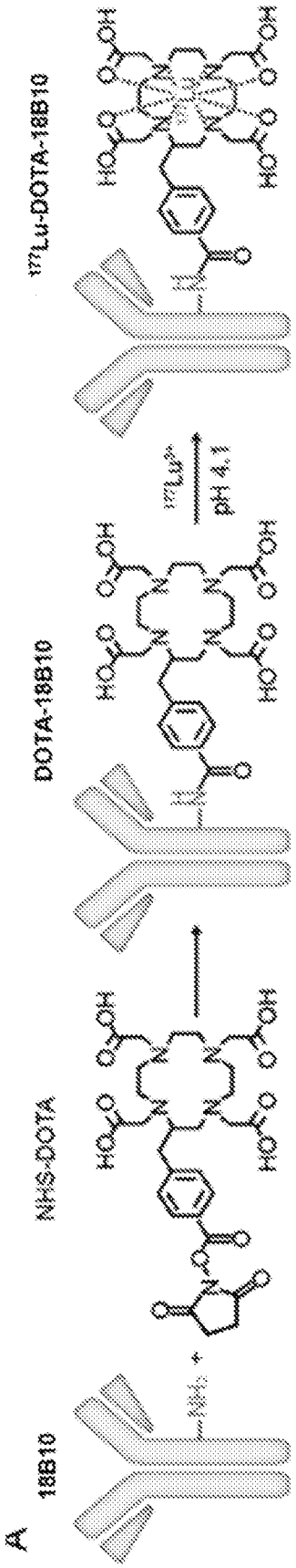

Figure 46A

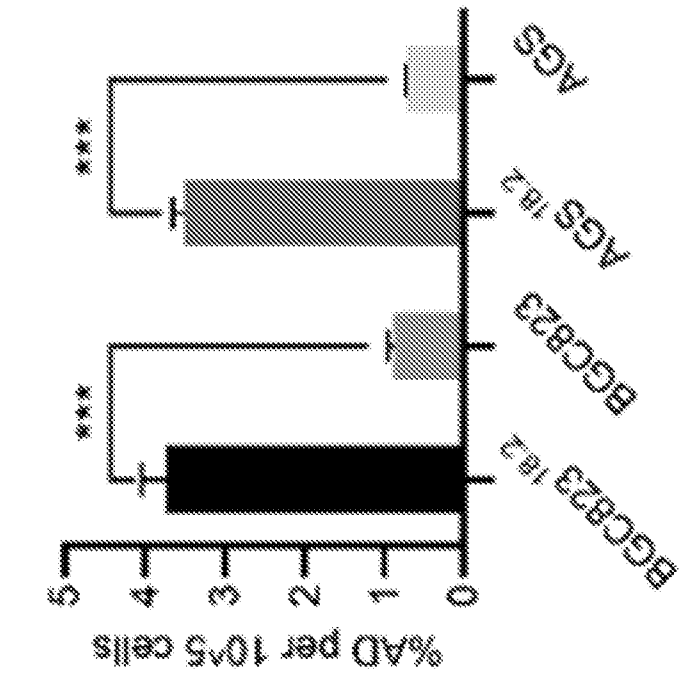
%AD per 10^5 cells
0
1
2
3
4
5
AGS
AGS 1a2
BGC823
BGC823 1a2
***
***

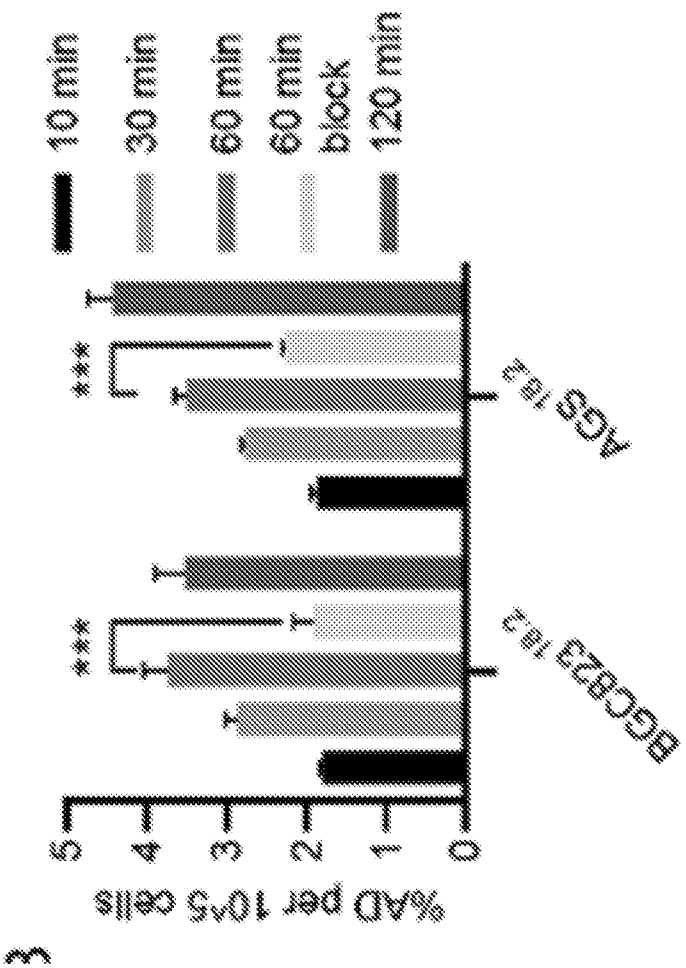
10 min
30 min
60 min
60 min block
120 min
%AD per 10^5 cells
0
1
2
3
4
5
AGS
AGS 1a2
BGC823
BGC823 1a2
***
***

Figure 46B

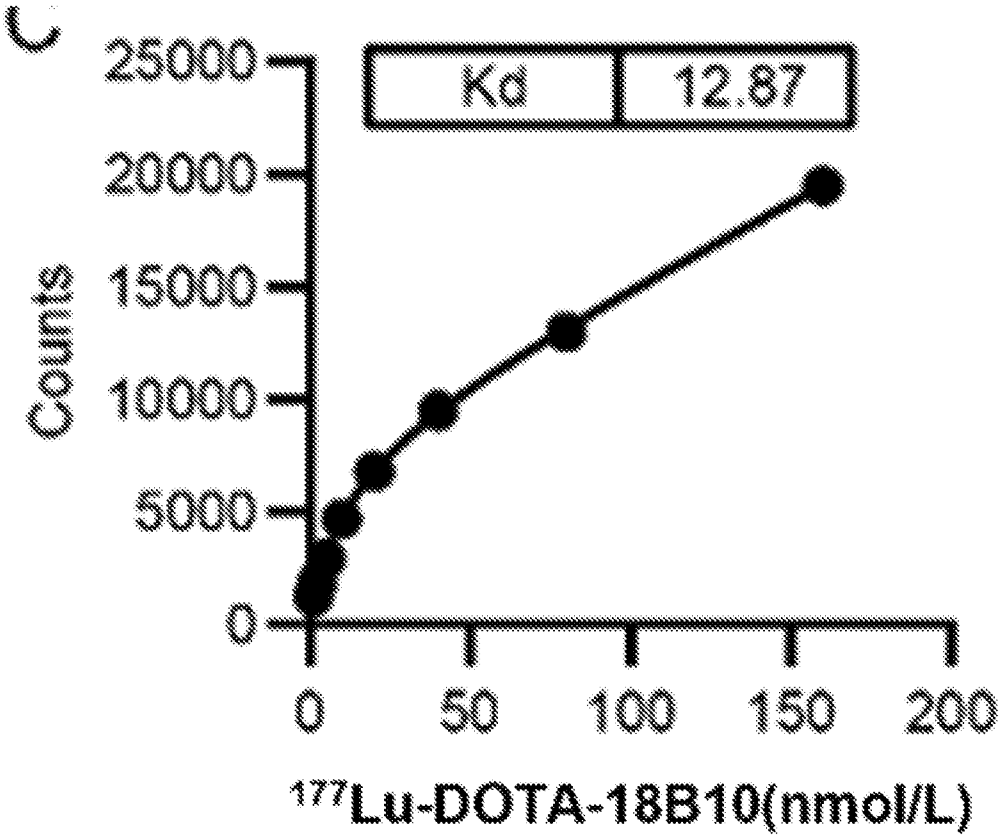
C
25000
20000
15000
10000
5000
0
Counts
Kd
12.87
0
50
100
150
200
177Lu-DOTA-18B10(nmol/L)

Figure 46C


A
BGC823CLDN18.2 xenografts
@4 h
@24 h
@48 h
@72 h
@144 h
AGSCLDN18.2 xenografts
@4 h
@24 h
@48 h
@72 h
@144 h
max
%ID/cc
min

Figure 47A

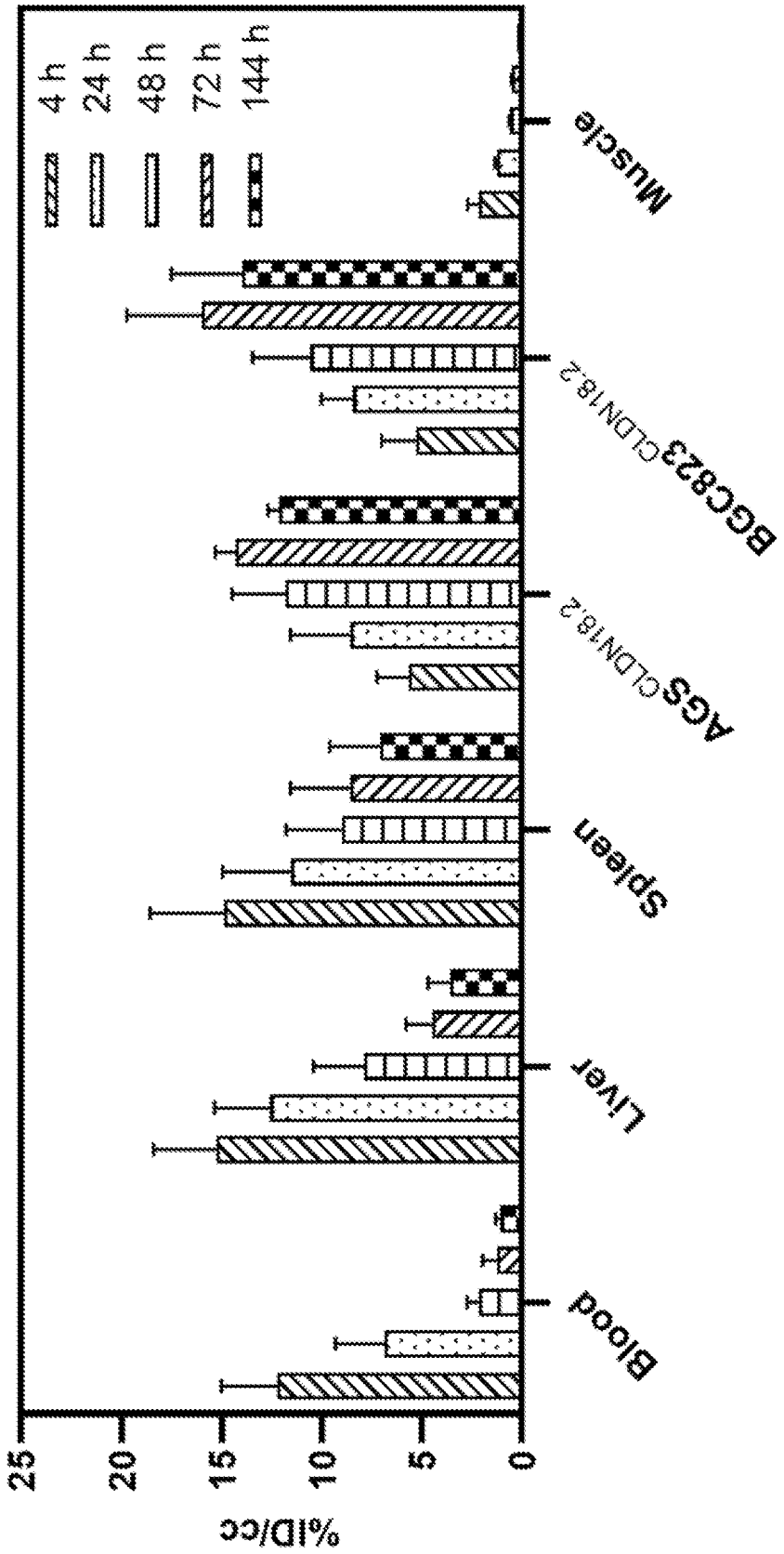
4 h
24 h
48 h
72 h
144 h
%ID/cc
25
20
15
10
5
0
Blood
Liver
Spleen
AGS CLDN18.2
BGC823 CLDN18.2
Muscle

Figure 47B

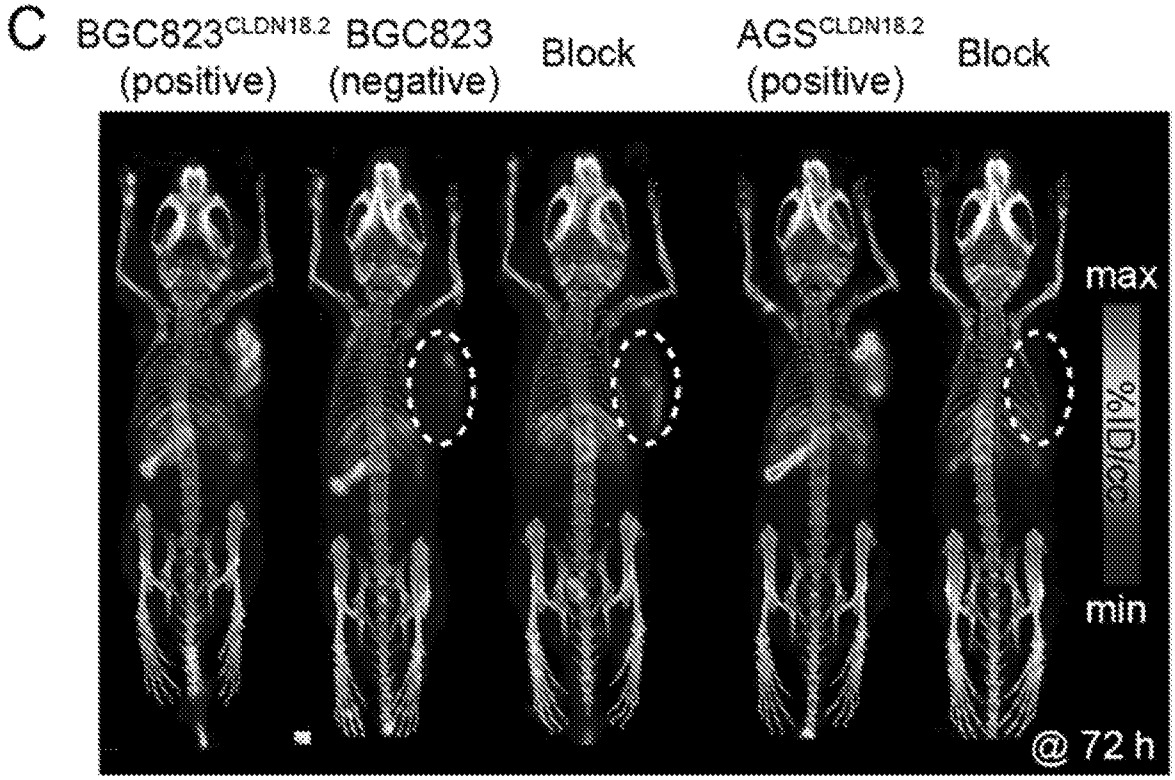

Figure 47C

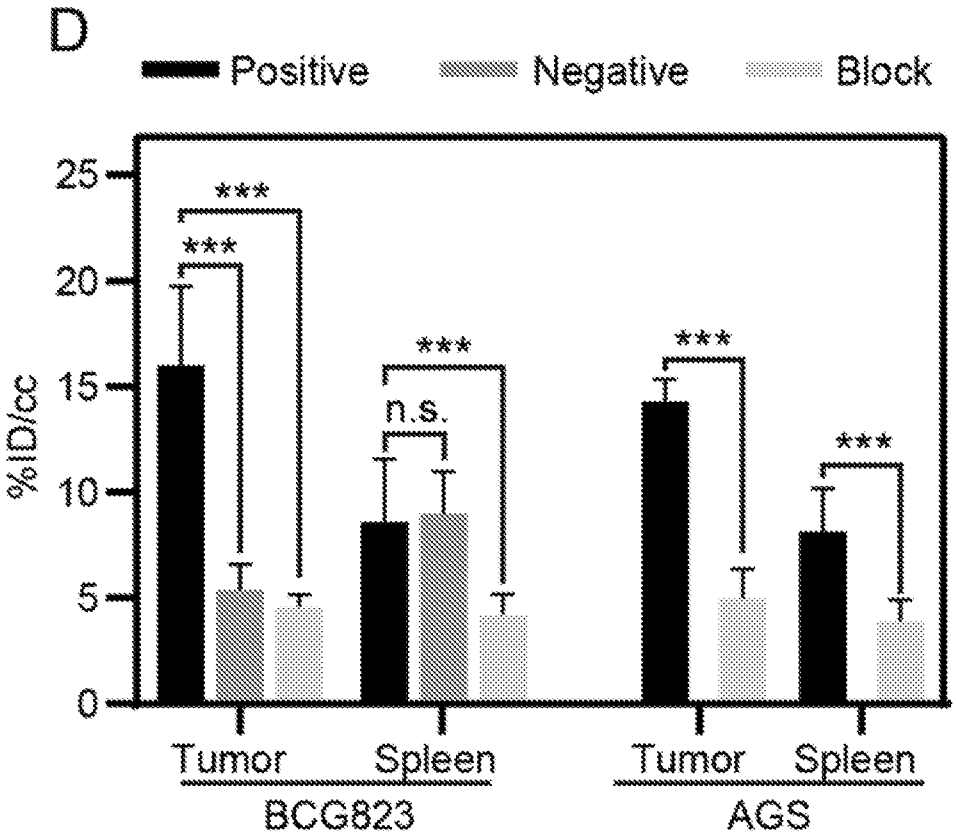

Figure 47D

E

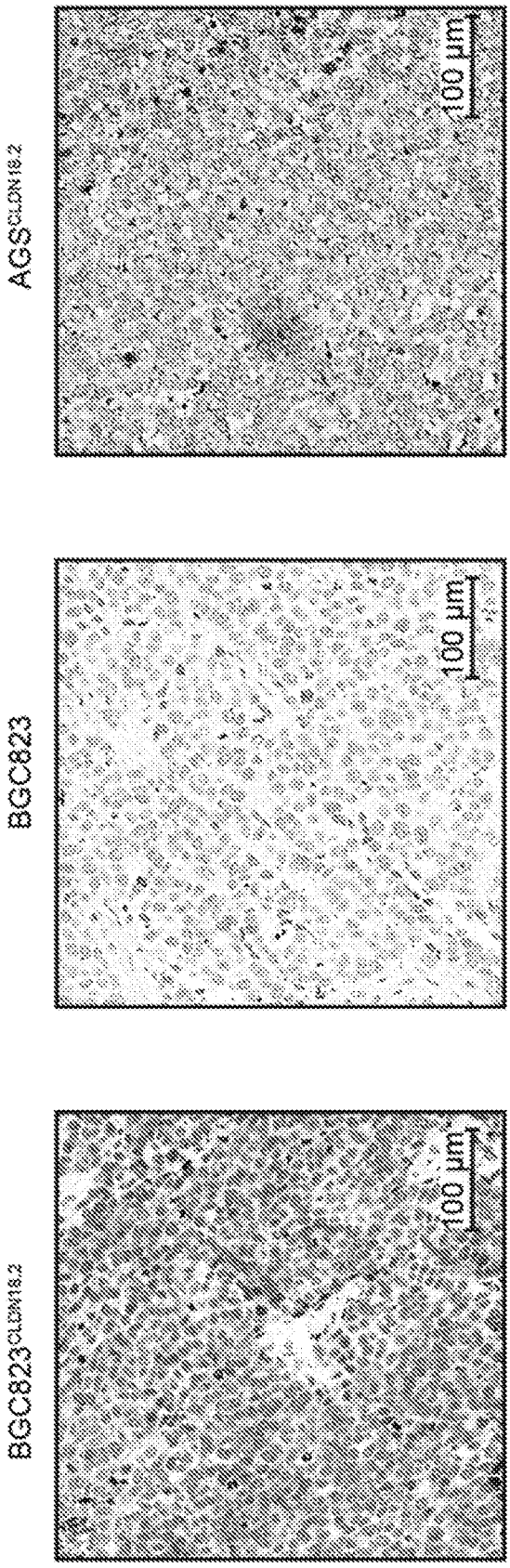

Figure 47E

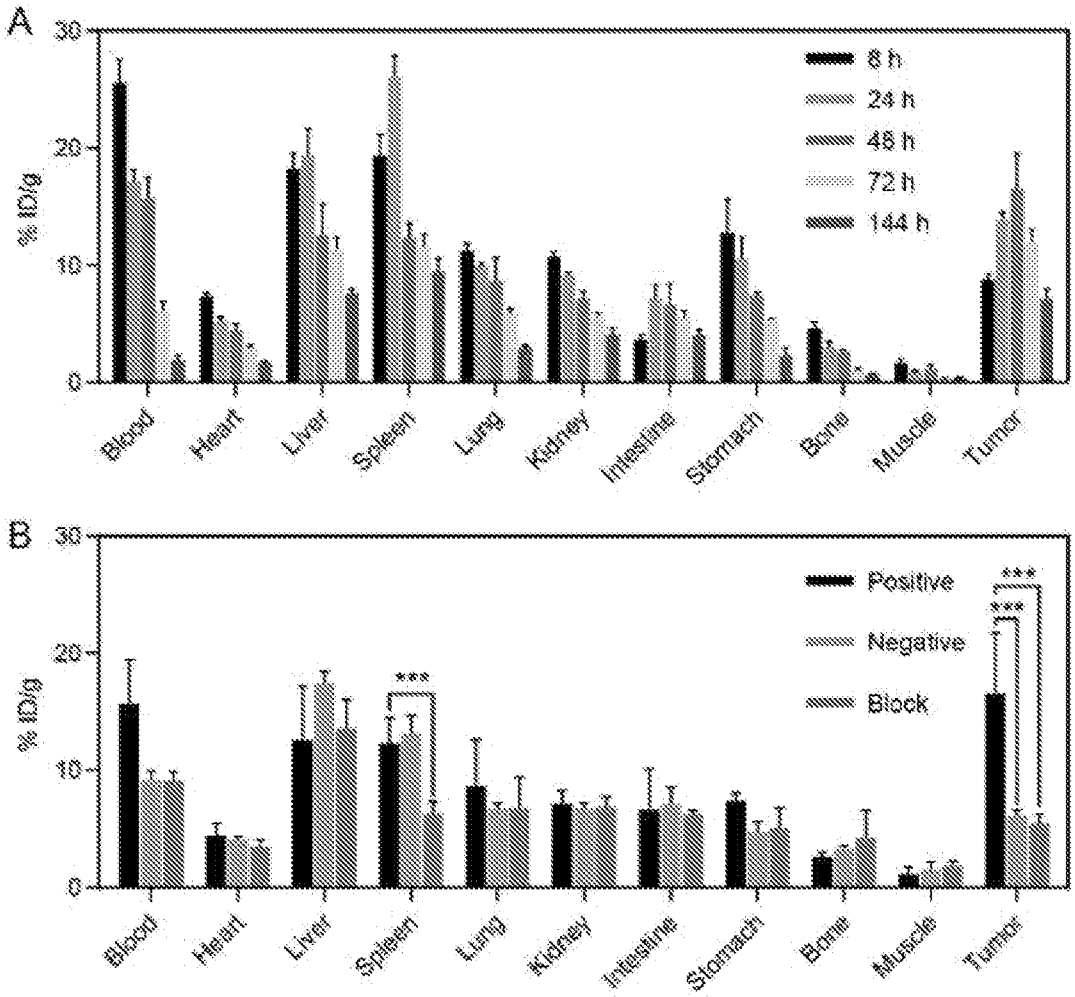
A
30
20
10
0
%ID/g
8 h
24 h
48 h
72 h
144 h
Blood
Heart
Liver
Spleen
Lung
Kidney
Intestine
Stomach
Bone
Muscle
Tumor
B
30
20
10
0
%ID/g
Positive
Negative
Block
***
***
***
Blood
Heart
Liver
Spleen
Lung
Kidney
Intestine
Stomach
Bone
Muscle
Tumor

Figure 48

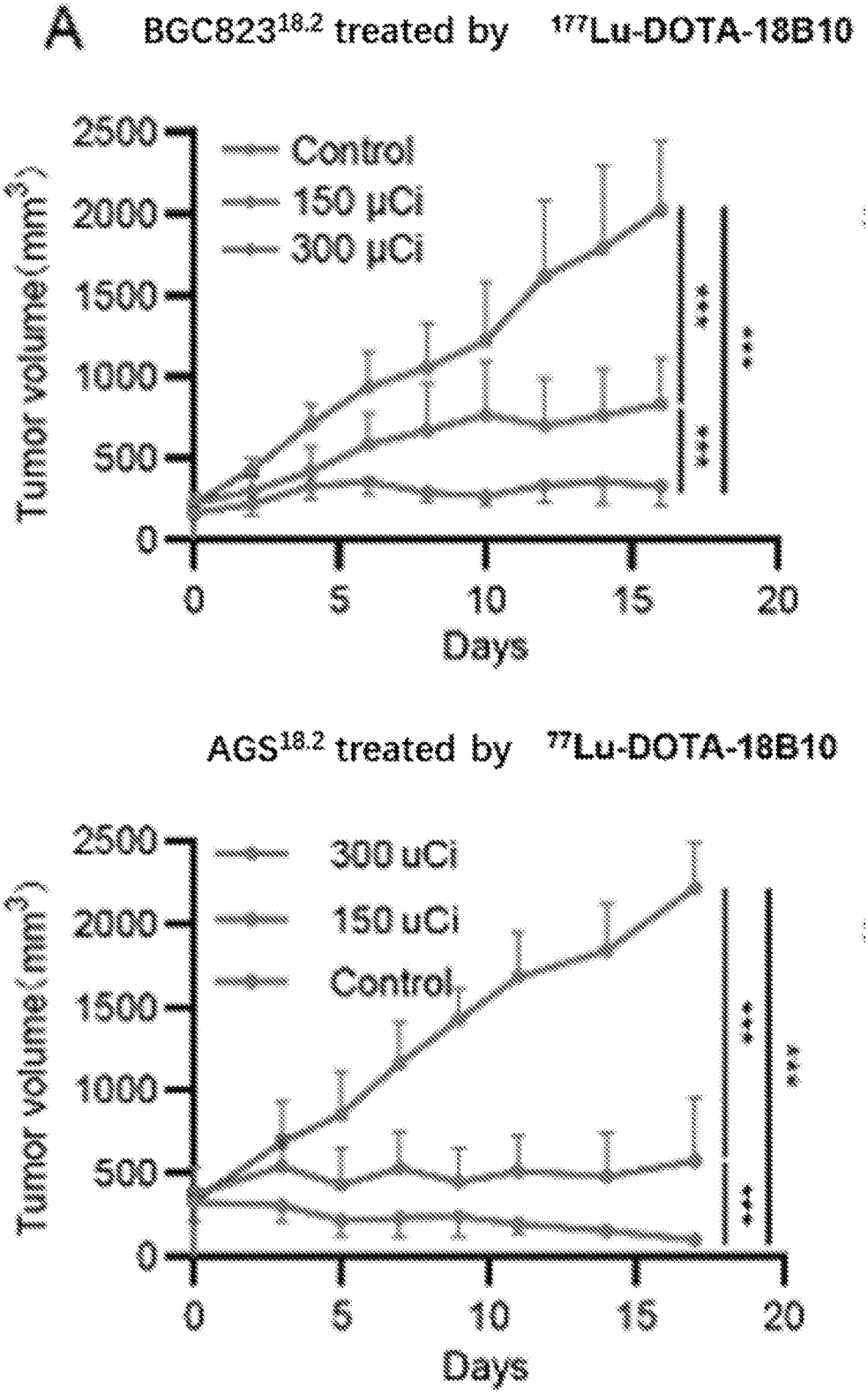
A
BGC823^18.2 treated by ^177Lu-DOTA-18B10
Tumor volume(mm^3)
2500
2000
1500
1000
500
0
Control
150 μCi
300 μCi
***
***
0
5
10
15
20
Days
AGS^18.2 treated by ^77Lu-DOTA-18B10
Tumor volume(mm^3)
2500
2000
1500
1000
500
0
300 uCi
150 uCi
Control
***
***
0
5
10
15
20
Days

Figure 49A

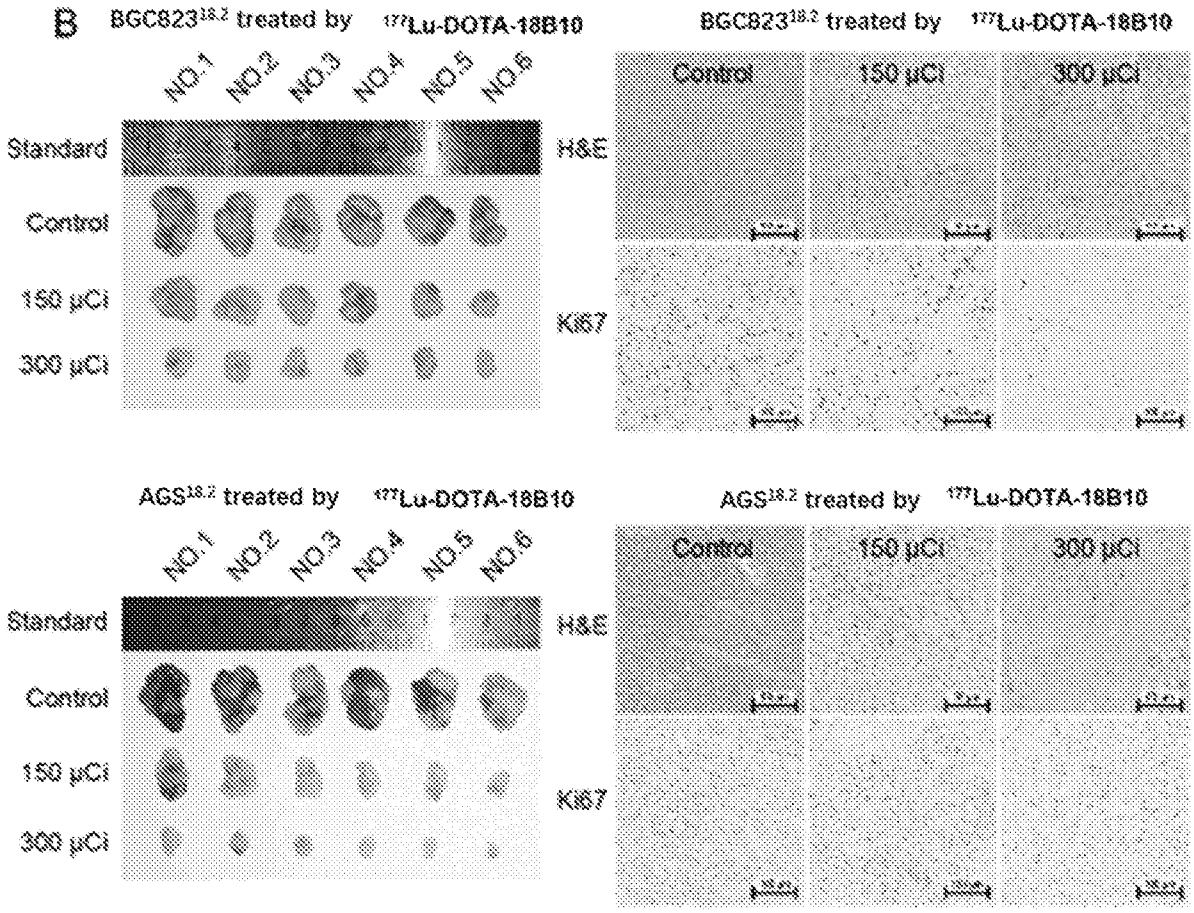
B
BGC823$^{18.2}$ treated by ^{177}Lu-DOTA-18B10
NO.1
NO.2
NO.3
NO.4
NO.5
NO.6
Standard
Control
150 μCi
300 μCi
H&E
Ki67
BGC823$^{18.2}$ treated by ^{177}Lu-DOTA-18B10
Control
150 μCi
300 μCi
AGS$^{18.2}$ treated by ^{177}Lu-DOTA-18B10
NO.1
NO.2
NO.3
NO.4
NO.5
NO.6
Standard
Control
150 μCi
300 μCi
H&E
Ki67
AGS$^{18.2}$ treated by ^{177}Lu-DOTA-18B10
Control
150 μCi
300 μCi

Figure 49B

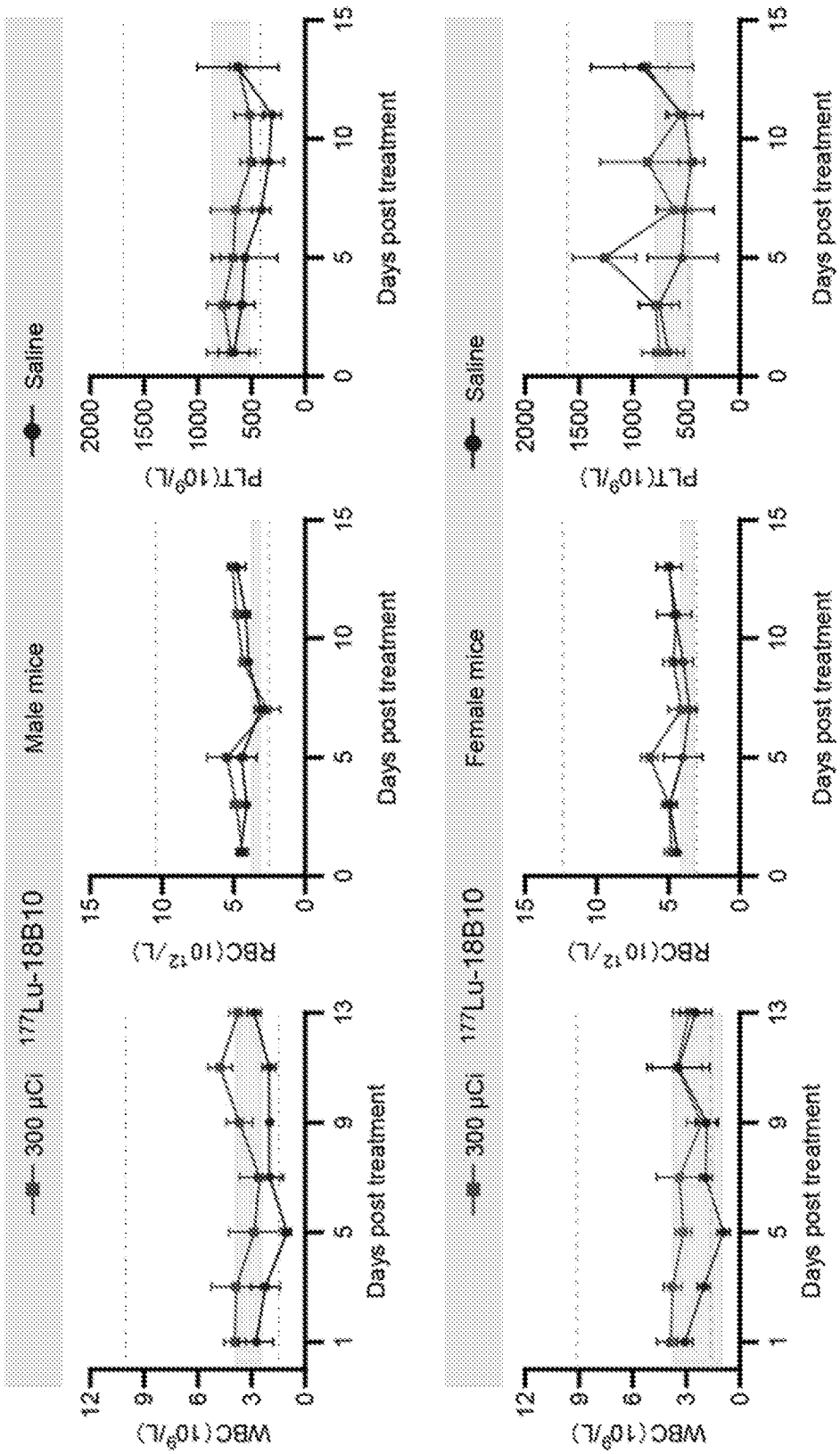
300 μCi 177Lu-18B10
Male mice
Saline
Female mice
WBC(10^9/L)
RBC(10^12/L)
PLT(10^9/L)
Days post treatment

Figure 50

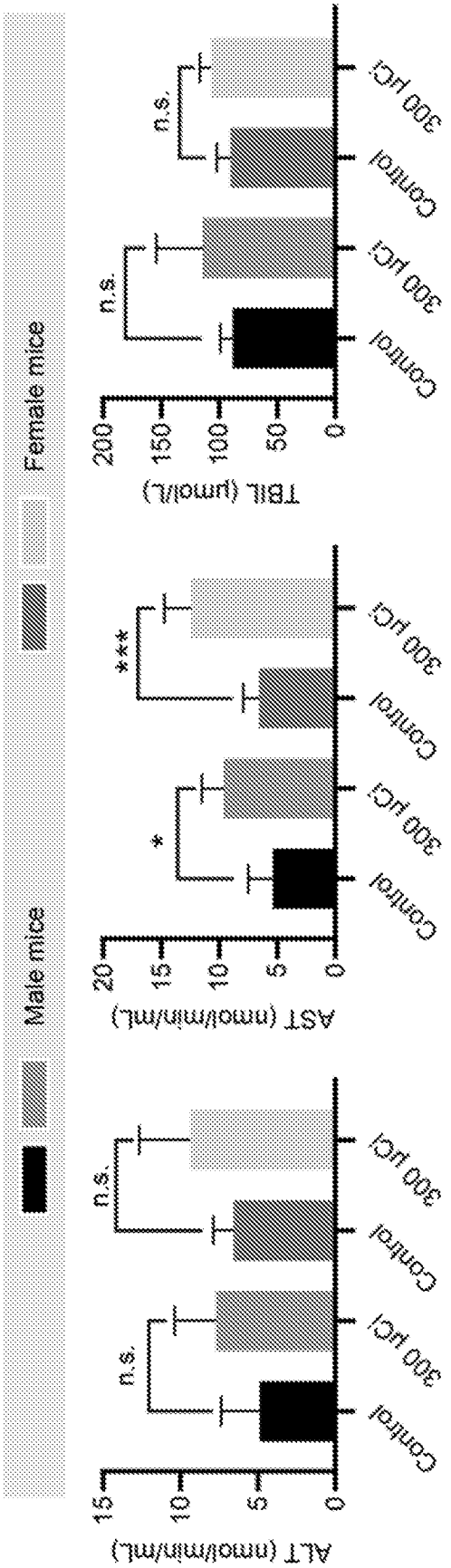

Figure 50 (Continued)

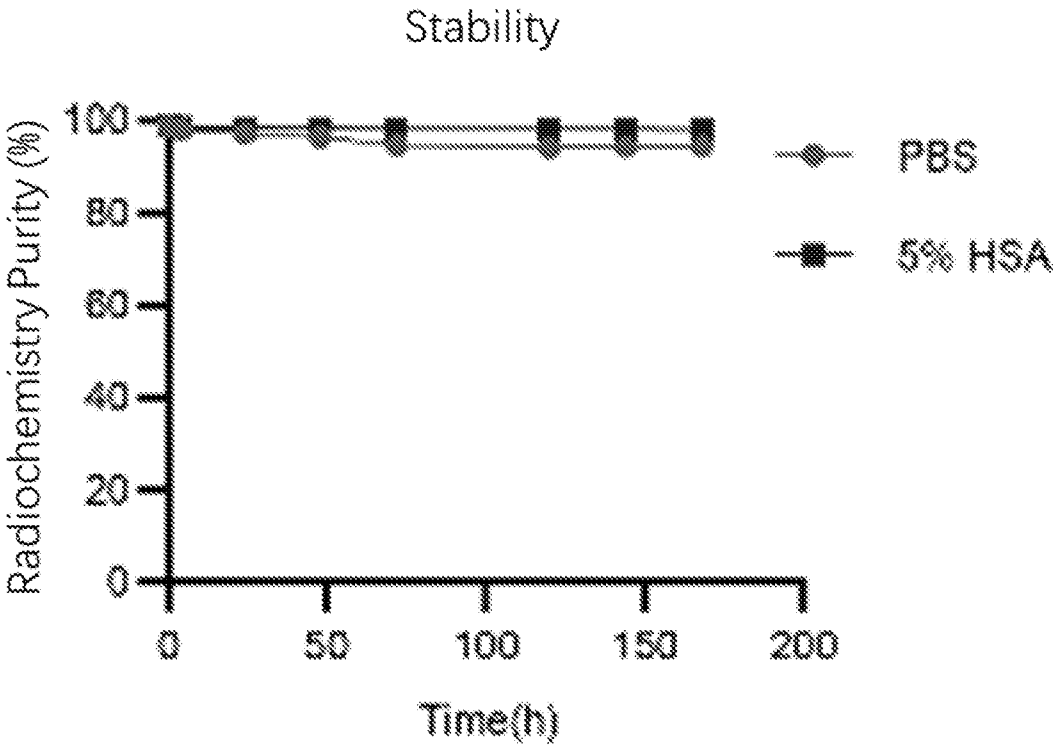
Stability
Radiochemistry Purity (%)
100
80
60
40
20
0
0
50
100
150
200
Time(h)
PBS
5% HSA

Figure 51

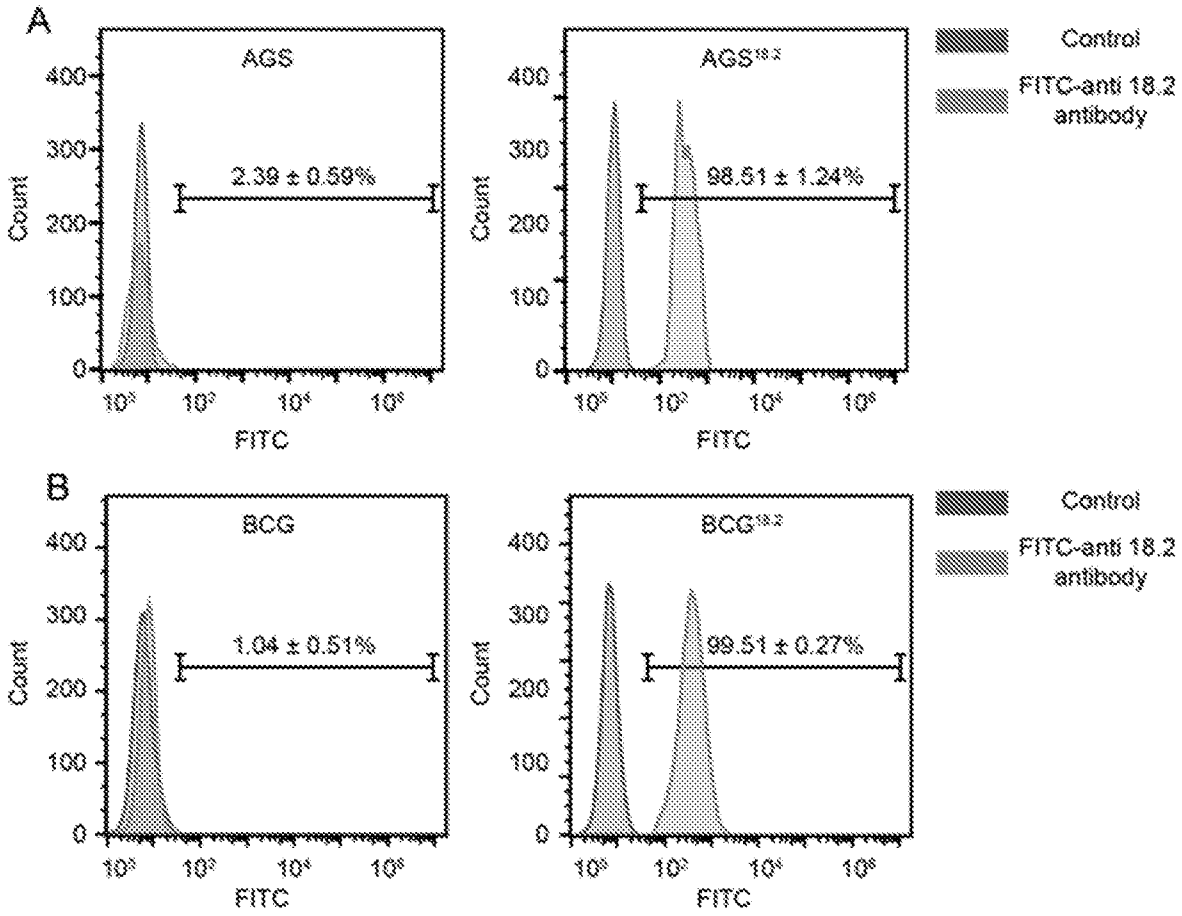

Figure 52

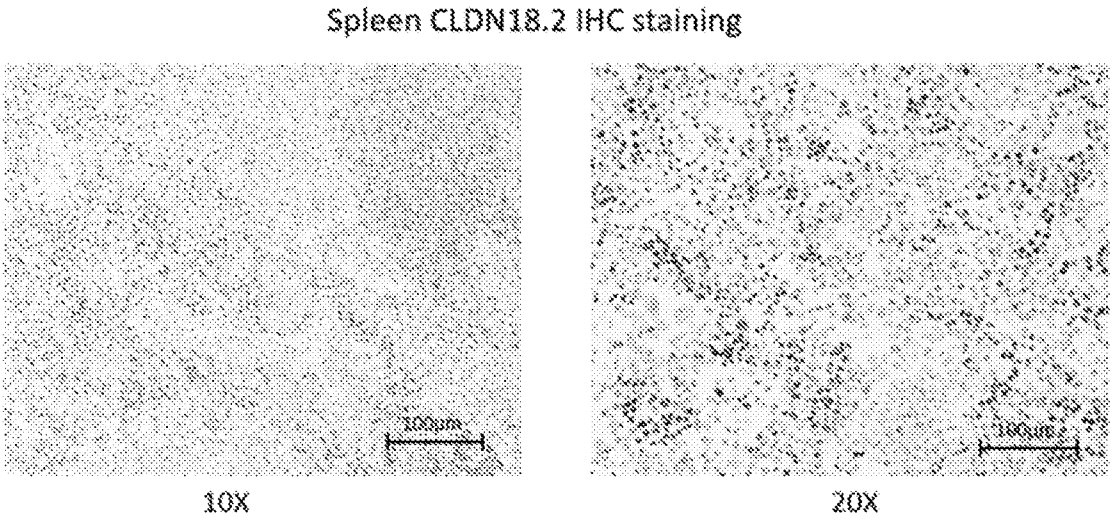

Figure 53

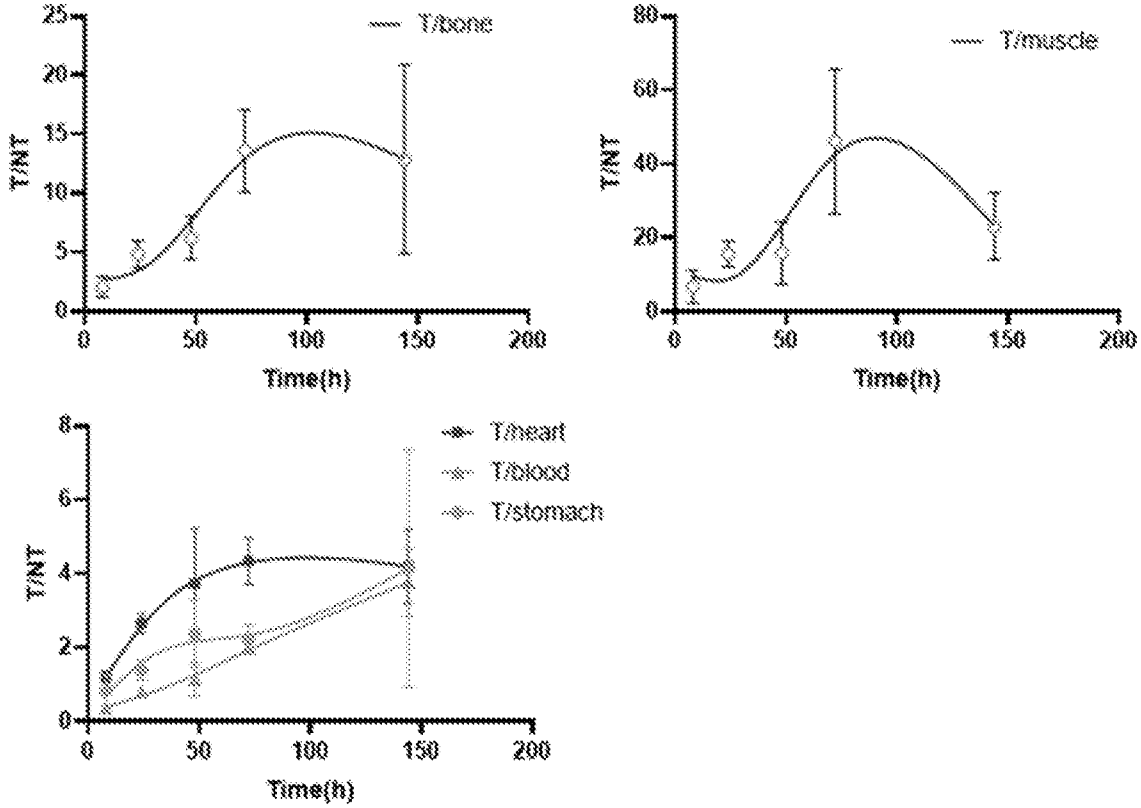
T/bone
T/NT
Time(h)
T/muscle
T/NT
Time(h)
T/heart
T/blood
T/stomach
T/NT
Time(h)

Figure 54

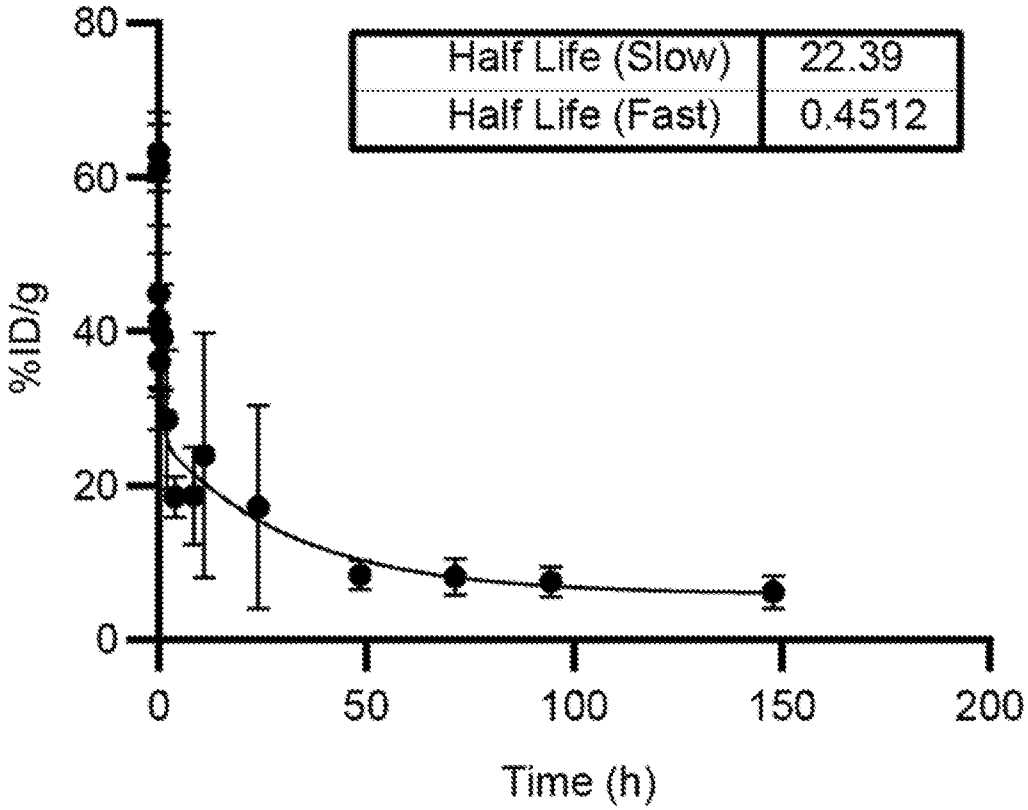
Half Life (Slow) 22.39
Half Life (Fast) 0.4512
%ID/g
80
60
40
20
0
0
50
100
150
200
Time (h)

Figure 55

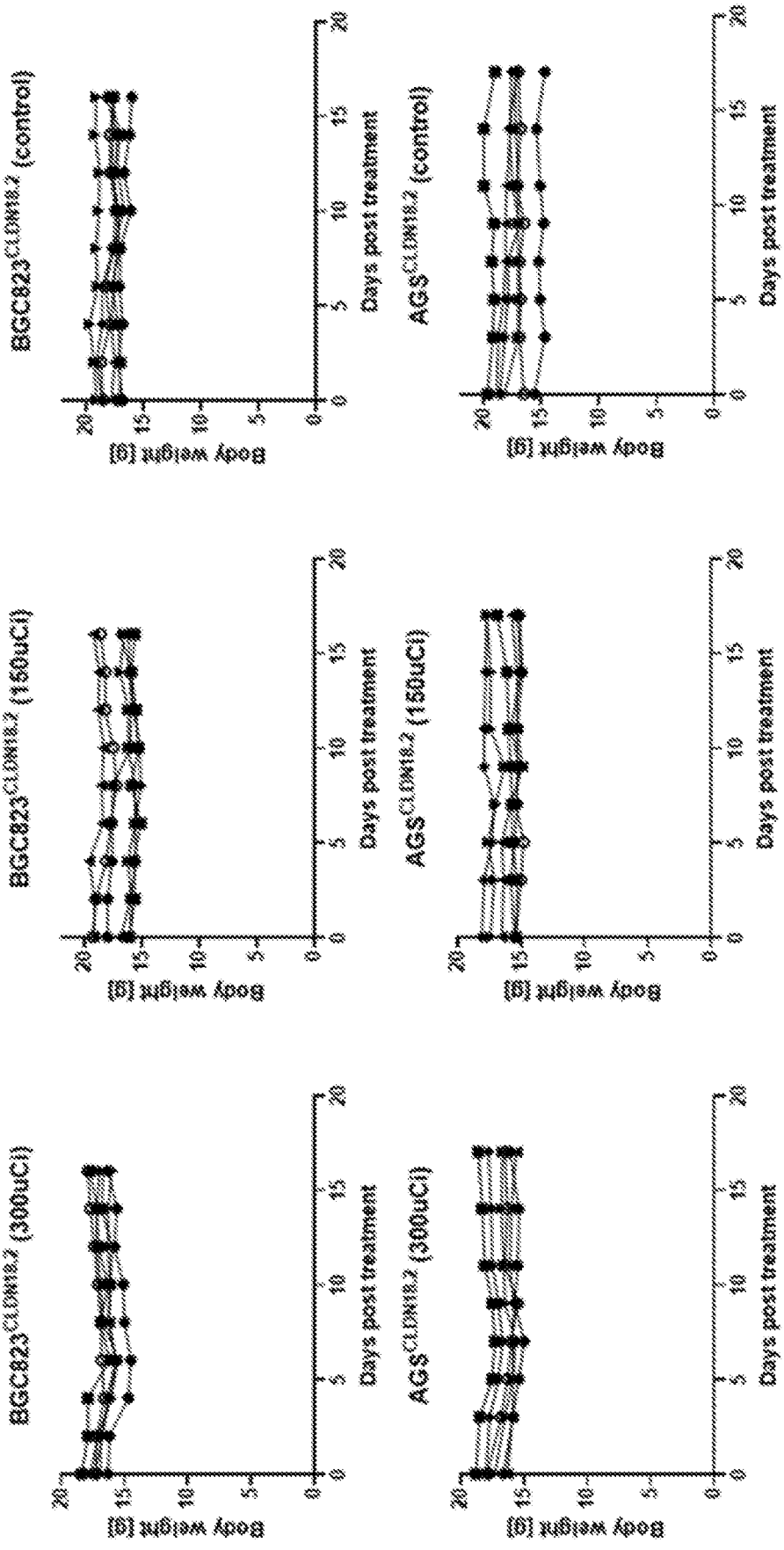
BGC823CLDN18.2 (control)
AGSCLDN18.2 (control)
BGC823CLDN18.2 (150uCi)
AGSCLDN18.2 (150uCi)
BGC823CLDN18.2 (300uCi)
AGSCLDN18.2 (300uCi)
Body weight [g]
Days post treatment
0
5
10
15
20

Figure 56

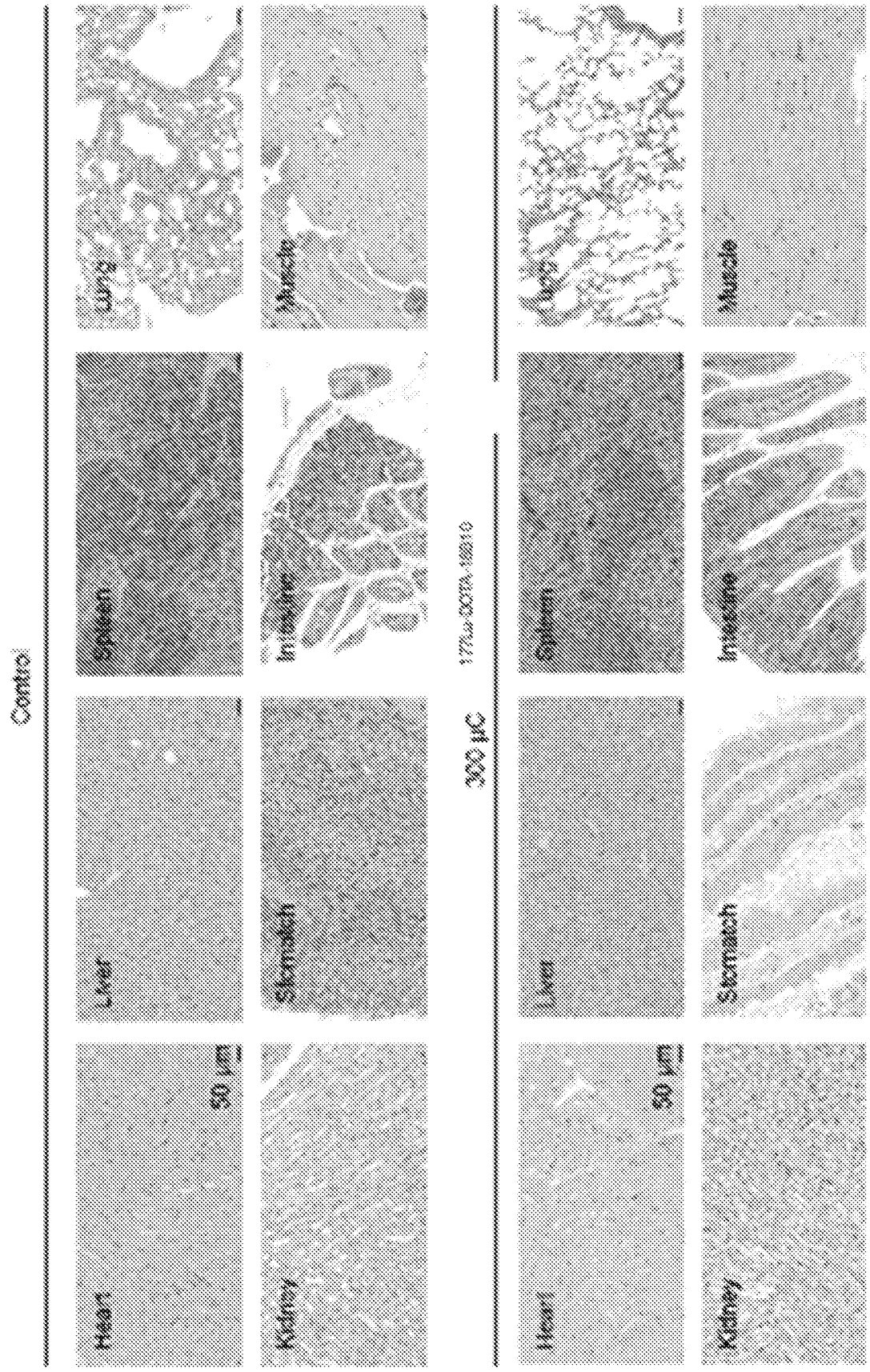
Control
300 μC
177Lu-SCTA 16210
Heart
Liver
Spleen
Lung
Kidney
Stomach
Intestine
Muscle
50 μm
Heart
Liver
Spleen
Lung
Kidney
Stomach
Intestine
Muscle
50 μm

Figure 57

INTERNATIONAL SEARCH REPORT

International application No.
PCT/CN2023/114497

Box No. I Nucleotide and/or amino acid sequence(s) (Continuation of item 1.c of the first sheet)

1. With regard to any nucleotide and/or amino acid sequence disclosed in the international application, the international search was carried out on the basis of a sequence listing:
   a. ☑ forming part of the international application as filed.
   b. ☐ furnished subsequent to the international filing date for the purposes of international search (Rule 13*ter*.1(a)),
      ☐ accompanied by a statement to the effect that the sequence listing does not go beyond the disclosure in the international application as filed.

2. ☐ With regard to any nucleotide and/or amino acid sequence disclosed in the international application, this report has been established to the extent that a meaningful search could be carried out without a WIPO Standard ST.26 compliant sequence listing.

3. Additional comments:

INTERNATIONAL SEARCH REPORT

International application No.
PCT/CN2023/114497

Box No. II Observations where certain claims were found unsearchable (Continuation of item 2 of first sheet)

This international search report has not been established in respect of certain claims under Article 17(2)(a) for the following reasons:

1. ☑ Claims Nos.: **1-48, 57-58(part), 59-67**
because they relate to subject matter not required to be searched by this Authority, namely:

Claims 1-48, 57-58(part), 59-67 relate to detecting, diagnosing or monitoring methods of CLDN18.2 related diseases in a subject and do not meet the criteria set out in PCT Rules 39.1(iv).

2. ☐ Claims Nos.:
because they relate to parts of the international application that do not comply with the prescribed requirements to such an extent that no meaningful international search can be carried out, specifically:

3. ☐ Claims Nos.:
because they are dependent claims and are not drafted in accordance with the second and third sentences of Rule 6.4(a).

INTERNATIONAL SEARCH REPORT

International application No.
PCT/CN2023/114497

A. CLASSIFICATION OF SUBJECT MATTER

A61K 39/395(2006.01)i; C07K16/30(2006.01)i; A61K47/50(2017.01)i; C12Q1/6886(2018.01)i; A61P35/00(2006.01)i

According to International Patent Classification (IPC) or to both national classification and IPC

B. FIELDS SEARCHED

Minimum documentation searched (classification system followed by classification symbols)

IPC: A61K C07K C12Q A61P

Documentation searched other than minimum documentation to the extent that such documents are included in the fields searched

Electronic data base consulted during the international search (name of data base and, where practicable, search terms used)

DWPI,ENTXT,ENTXTC,CNTXT,CNABS,GENBANK,NCBI,elsevier science,ISI Web of Science,CNKI,EMBL,Chinese Patnet Biological Sequence Retrieval System,STNext Registry,STNext Caplus:ADC,antibody drug conjugate,CLDN18.2, Claudin18.2,radionuclide,SUZHOU TRANSCENTA,QIAN Xueming

C. DOCUMENTS CONSIDERED TO BE RELEVANT

Category*	Citation of document, with indication, where appropriate, of the relevant passages	Relevant to claim No.
PX	WO 2022174809 A1 (SUZHOU TRANSCENTA THERAPEUTICS CO., LTD. et al.) 25 August 2022 (2022-08-25) claims 1-50	49-58,68-77
X	WO 2022007808 A1 (KEYMED BIOSCIENCES CO., LTD. et al.) 13 January 2022 (2022-01-13) claims 1-13, page 7 lines 20-24	49-56
Y	WO 2022007808 A1 (KEYMED BIOSCIENCES CO., LTD. et al.) 13 January 2022 (2022-01-13) claims 1-13, page 7 lines 20-24	57-58, 68-77
Y	WO 2021032157 A1 (MABSPACE BIOSCIENCES (SUZHOU) CO., LTD.) 25 February 2021 (2021-02-25) claims 16-25	57-58, 68-77
A	WO 2020025792 A1 (AMGEN RESEARCH (MUNICH) GMBH et al.) 06 February 2020 (2020-02-06) the whole document	49-58, 68-77

☑ Further documents are listed in the continuation of Box C. ☑ See patent family annex.

* Special categories of cited documents:
"A" document defining the general state of the art which is not considered to be of particular relevance
"D" document cited by the applicant in the international application
"E" earlier application or patent but published on or after the international filing date
"L" document which may throw doubts on priority claim(s) or which is cited to establish the publication date of another citation or other special reason (as specified)
"O" document referring to an oral disclosure, use, exhibition or other means
"P" document published prior to the international filing date but later than the priority date claimed
"T" later document published after the international filing date or priority date and not in conflict with the application but cited to understand the principle or theory underlying the invention
"X" document of particular relevance; the claimed invention cannot be considered novel or cannot be considered to involve an inventive step when the document is taken alone
"Y" document of particular relevance; the claimed invention cannot be considered to involve an inventive step when the document is combined with one or more other such documents, such combination being obvious to a person skilled in the art
"&" document member of the same patent family

Date of the actual completion of the international search	Date of mailing of the international search report
23 November 2023	**30 November 2023**

Name and mailing address of the ISA/CN	Authorized officer
CHINA NATIONAL INTELLECTUAL PROPERTY ADMINISTRATION **6, Xitucheng Rd., Jimen Bridge, Haidian District, Beijing 100088, China**	**WU,TieSheng** Telephone No. **(+86) 010-53961870**

C. DOCUMENTS CONSIDERED TO BE RELEVANT

Category*	Citation of document, with indication, where appropriate, of the relevant passages	Relevant to claim No.
A	WO 2020238730 A1 (SANYOU BIOPHARMACEUTICALS CO., LTD.) 03 December 2020 (2020-12-03) the whole document	49-58, 68-77
A	WO 2022115778 A1 (RAYZEBIO, INC.) 02 June 2022 (2022-06-02) the whole document	49-58, 68-77

INTERNATIONAL SEARCH REPORT
Information on patent family members

International application No.
PCT/CN2023/114497

Patent document cited in search report			Publication date (day/month/year)	Patent family member(s)			Publication date (day/month/year)
WO	2022174809	A1	25 August 2022	CA	3211403	A1	25 August 2022
				AU	2022223150	A1	21 September 2023
				TW	202302153	A	16 January 2023
WO	2022007808	A1	13 January 2022		None		
WO	2021032157	A1	25 February 2021		None		
WO	2020025792	A1	06 February 2020	CR	20210120	A	21 May 2021
				EA	202190435	A1	30 June 2021
				AU	2019314999	A1	11 February 2021
				KR	20210042117	A	16 April 2021
				AR	114541	A1	16 September 2020
				MA	53330	A	09 June 2021
				TW	202023611	A	01 July 2020
				MX	2021001353	A	13 April 2021
				CA	3107192	A1	06 February 2020
				PH	12021550224	A1	06 December 2021
				JP	2020018298	A	06 February 2020
				SG	11202100987	RA	25 February 2021
				CO	2021002907	A2	31 May 2021
				EP	3829633	A1	09 June 2021
				CL	2021000291	A1	13 August 2021
				JOP	20210022	A1	28 January 2021
				UY	38326	A	31 January 2020
				PE	20211400	A1	27 July 2021
				IL	280467	A	01 March 2021
				BR	112021002032	A2	20 July 2021
				US	2020055932	A1	20 February 2020
				US	11692031	B2	04 July 2023
WO	2020238730	A1	03 December 2020	JP	2022533804	A	25 July 2022
				US	2022396616	A1	15 December 2022
				EP	3978532	A1	06 April 2022
				EP	3978532	A4	18 October 2023
				CA	3141504	A1	03 December 2020
				TW	202108627	A	01 March 2021
				KR	20220012262	A	03 February 2022
WO	2022115778	A1	02 June 2022	EP	4251639	A1	04 October 2023
				US	2023158179	A1	25 May 2023